The University of Hull

On-line Estimation Approaches to Fault-Tolerant Control of Uncertain Systems

Being a thesis submitted for the Degree of PhD

in the University of Hull

by

SUPAT KLINKHIEO

MSc Electronics (Hull)

June 2009

Acknowledgements

First of all, I would like to express my sincere gratitude to my academic supervisor, Professor Ron J Patton, who has guided and helped me in every aspect of the thesis, which is deeply appreciated through my three-year PhD research. He has always supported me understand the essence of engineering research and find the real potential of my self. He always give me opportunities to explore myself and also created an environment which gave me the flexibility to explore new ideas, while helping me to make critical decisions whenever the project was at a crossroads. I admire him for his broad knowledge, creative thinking, and deep insight in the subject of control systems. I personally feel so proud and fortunate to have had him as my research and academic supervisor.

I also thank to Dr. Ming Hou for his useful lecture notes on basic control systems. It has been a privilege to work together with the intelligent and friendly people in the Control and Intelligent Systems Engineering (Control Group), the University of Hull. Thanks also go to Dr. Chandra Kambhampati, Dr. Cahit Perkgoz and Lam Aun Cheah my fellow researchers and students, for their valuable suggestions and good friendship. I have completely enjoyed and enormously benefited from the interaction and collaboration with them.

I gratefully acknowledge the financial support of my PhD. study from the Loyal Thai Government and Synchrotron Light Research Institute (SLRI), Thailand.

Finally, special acknowledgment to my loving wife, Bang-Oen Klinkhieo for her understanding, patience, love and support during all these years.

Abstract

This thesis is concerned with fault estimation in Fault-Tolerant Control (FTC) and as such involves the joint problem of on-line estimation within an adaptive control system. The faults that are considered are significant uncertainties affecting the control variables of the process and their estimates are used in an adaptive control compensation mechanism. The approach taken involves the active FTC, as the faults can be considered as uncertainties affecting the control system. The engineering (application domain) challenges that are addressed are:

(1) On-line model-based fault estimation and compensation as an FTC problem, for systems with large but bounded fault magnitudes and for which the faults can be considered as a special form of dynamic uncertainty.
(2) Fault-tolerance in the distributed control of uncertain inter-connected systems

The thesis also describes how challenge (1) can be used in the distributed control problem of challenge (2). The basic principle adopted throughout the work is that the controller has two components, one involving the nominal control action and the second acting as an adaptive compensation for significant uncertainties and fault effects. The fault effects are a form of uncertainty which is considered too large for the application of passive FTC methods. The thesis considers several approaches to robust control and estimation: augmented state observer (ASO); sliding mode control (SMC); sliding mode fault estimation via Sliding Mode Observer (SMO); linear parameter-varying (LPV) control; two-level distributed control with learning coordination.

Table of Contents

List of Figures

List of Tables

List of Symbols and Abbreviation

Symbols

$\|.\|$	Euclidean norm (vectors) or induced spectral norm (matrices)
$\|a\|$	The absolute value of the real number a
$\lambda_{\max}, \lambda_{\min}$	Largest and smallest eigenvalues
$\Re, \Re_+$	Field of real numbers and the set of strictly positive real numbers
$\mathbf{N}(A)$	Null space of the matrix A
$\mathbf{R}(A)$	Range space of the matrix A
$\mathcal{L}\{\cdot\}$	Denotes the Laplace Transform of the continuous-time signal $\{\cdot\}$

Abbreviations

ACSS	Autonomous Coordination and Supervision Scheme
AFTCS	Active Fault-Tolerant Control Systems
ASO	Augmented State Observer
FD	Fault Diagnosis
FDD	Fault Detection and Identification
FDI	Fault Detection and Isolation
FTC	Fault-Tolerant Control
GARTEUR	Group for Aeronautical Research and Technology in Europe
GLR	Generalised Likelihood Ratio
IPP	Interaction Prediction Principle
IMM	Interactive Multiple Model
LMI	Linear Matrix Inequality
LPV	Linear Parameter Varying
LQR	Linear Quadratic Regulator
MBPC	Model Based Predictive Control
MIC	Methyl Isocyanate
MMST	Multiple Model Switching and Tuning
NASB	Nederland Aviation Safety Board
NCS	Networked Control System

NeCST	Networked Control Systems Tolerant to faults
PFTCS	Passive Fault-Tolerant Control Systems
RHC	Receding Horizon Control
RMS	Root Mean Square
RNN	Recurrent Neural Network
S.P.D	Symmetric Positive Definite
SMC	Sliding Mode Control
SMO	Sliding Mode Observer
SPR	Sequential Probability Ration
SVD	Singular Value Decomposition
UIO	Unknown Input Observer
USSR	Union of Soviet Socialist Republics
VSC	Variable Structure Control

List of Publications

Within the period of this research the following works were accepted and submitted for publication:

- Patton R J and Klinkhieo S (2009), Robust Estimation and Compensation using Augmented State Observer, *48th IEEE Conference on Decision and Control and 28th Chinese Conference*, December 16th -18th, (accepted).
- Patton R J, Putra D and Klinkhieo S (2009), Friction Compensation as a Fault-Tolerant Control Problem, *International Journal of Systems Science*, (under review).
- Patton R J and Klinkhieo S (2009), Robust Estimation and Compensation using Augmented State Observer, S*pecial issue on Modelling, Monitoring and Fault-Tolerant Control for Complex Systems*, *The Open Automation and control System Journal*, (accepted).
- Patton R J, Klinkhieo S and Putra D (2009), A Fault-tolerant Control Approach to Friction Compensation, *European Conference on Control 2009 (ECC'09*), August 23rd -26th , Budapest, Hungary.
- Klinkhieo S and Patton R J (2009), A Two-Level Approach to Fault-Tolerant Control of Large Scale Systems based on the Sliding Mode, *Safeprocess'09*, June 30th – July 3rd, Barcelona.
- Patton R J, Putra D and Klinkhieo S (2008), Friction Compensation as a Fault-Tolerant Control Problem, *23rd IAR Workshop on Advanced Control and Diagnosis*, November 27th -28th, Coventry University, UK.
- Klinkhieo S and Patton R J (2008), A De-convolution Approach to Robust De-coupling for FTC in Distributed Systems, *23rd IAR Workshop on Advanced Control and Diagnosis,* November 27th -28th, Coventry University, UK.
- Klinkhieo S and Patton R J (2008), Robust Fault Isolation for Autonomous Coordination in NCS, *International Conference on Control 2008 (UKACC)*, September 2nd -4th, Manchester, UK.

- Klinkhieo S, Patton R J and Kambhampati C (2008), Robust FDI for FTC Coordination in a Distributed Network System, *18th IFAC World Congress*, July 6th -11th, Seoul, Korea.

Chapter 1. Introduction

1.1 Introduction

As modern technological systems increase in complexity, their corresponding control systems become more and more sophisticated. Control system methodologies have evolved from simple mechanical feedback structures, into advanced electronic devices for controlling high performance and highly unstable systems which optimize the cost and control effort (Franklin *et al*., 2002). Some of the control methods that have received good attention in the last two decades are predictive control (Pachter *et al*., 1995, Monaco *et al*. 1997; Huzmezan and Maciejowski, 1998; Kale and Chipperfield, 2005), robust control (Morari *et al*., 1989; Grimble, 2001) and adaptive control (Ahmed-Zaid *et al*. 1991; Bodson and Groszkiewicz, 1997; Wise *et al*., 1999; Tao *et al*., 2001; Tao, Chen, and Joshi, 2002; Kim *et al*., 2003). So far only predictive control has been well applied to industry problems (e.g. process industry). However, very few applied or theory-based control systems methods involve fault signal estimation of fault detection in their designs.

The performance of many control systems and especially for safety-critical applications e.g. aircraft, chemical and nuclear power plants must be optimised to handle wide changes in system operation and still maintain reliability, dependability and integrity in terms of stability, robustness and performance.

Some unexpected scenarios or unusual system events mean the performance and even the stability of the designed closed-loop system can be degraded. These unexpected scenarios may be faults, failures or system damage, which are usually not considered in the controller design process. The need to account for faults in a closed-loop system has been the main motivation for this research, providing some new concepts in *fault-tolerant control* (FTC) of uncertain systems.

1.2 Faults, Failures and Fault Diagnosis Terminology

In order to develop this subject further the terms *fault* and *failure* need to be defined in the context of uncertain systems. A '*Fault*' is an unexpected change in the system function. Isermann (1984) defined a fault as '*… a non-permitted deviation of a characteristic property, which leads to the inability to fulfill the intended purpose…*'

Faults in the components of controlled systems may lead to total system failure, depending on the precise conditions, the criticality of the fault, etc and if appropriate action is not taken [Definitions established by the Technical Committee for IFAC (International Federation of Automatic Control) Symposium SAFEPROCESS (Fault Detection Supervision and Safety for Technical Processes), Isermann and Ballé, 1997].

On the other hand, a '*Failure*' describes the condition when the system is no longer performing the required function i.e. the system function involving the faulty component may have failed.

A wide range of different process control variables, e.g. temperatures, flow-rates, liquid levels, pressures, voltages, currents, etc., can be constantly monitored on-line and the required control effort may be calculated on the basis of any or all of these measurements, either directly or via transformation. In general, faults in the control system may be seen to arise in input/output signals from: (i), actuators, (ii) sensors, (iii) the controller or within the system being controlled (see Figure 1-1).

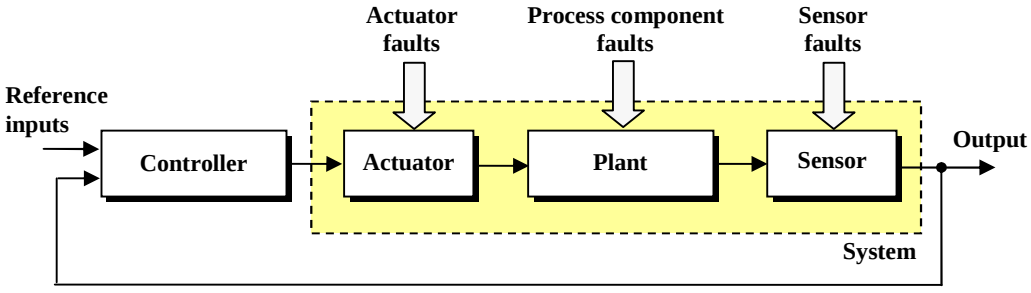

Figure 1-1: Types of faults in a control system

Faults within the system itself (i.e. arising from the system components) are often termed *component faults*, arising as variations from the structure or parameters used during system modelling, and as such cover a wide class of possible faults e.g. dirty water having a different heat transfer coefficient compared to when it is clean, changes in a liquids viscosity or components slowly degrading over time through wear and tear, aging or environmental effects, etc.

Structural changes, due to hard failures of equipment or external obstacles, can include anything from leaks due to fractures or cracks in pipes, stuck valves, short circuits, or simply from parts which become loose. These lead to changes in the interaction between variables and can sometimes result in what may be considered a new process operating as the physical laws of the system, such as conservation of mass or flow, may be fundamentally altered. These types of faults may be simple to detect but can be difficult or expensive to locate, estimate and compensate for through an active FTC system (Zhang and Jiang, 2006; Isermann, 2006).

Actuator faults: In equipment such as motors, valves, solenoids, relays, etc., faults may be the result of a jam, the actuator may become 'stuck' at a constant level, damage to bearings or gears, changes from the design characteristics or complete failure. For example this may occur due to increased resistance through friction and, as actuators usually require a separate power source, a fall in a supply voltage or current.

Sensor faults: The sensors are any equipment that takes a measurement or observation from the system, e.g. potentiometers, ammeters, voltmeters, accelerometers, tachometers, thermocouples, pressure gauges, strain gauges, etc., and faults are often due to poor calibration or bias, scaling errors or a change in the sensors dynamic characteristics however many signals also need a power source and some conditioning or amplification and these too can raise potential faults.

'*Fault Diagnosis*' (FD) is the name given that used to determine the presence and characteristics of faults. FD also comprises '*Fault Detection*', '*Isolation*' and '*Identification*' of faults. *Fault Detection* is the determination of the presence of faults in a system and the time of detection. *Fault Isolation* is used to discriminate the location of fault and the time of detection while *Fault Identification* gives information of size and the nature of the fault (Chen and Patton, 1999).

The subject Fault detection and isolation (FDI) has developed as a field of research and application in control systems, that is particularly important when dependability is required, especially since faults in sensors, actuators and components are associated

with increasing operating costs, off-specification production and can even lead to system failure or shut-down. In the FDI problem, faults are detected and isolated, principally using model-based methods although data-driven FDI methods are also important in real applications, especially when system models are ill-defined.

The procedures of Fault Detection and Identification (FDD) offer an extension to those of FDI by providing an additional "diagnosis" of faults in terms of fault identification or fault estimation and sometimes an assessment of the degree of severity of the fault(s) (Blanke *et al*., 2003).

This thesis describes methods for Fault-Tolerant Control (FTC) that are based on the fault estimation and fault accommodation aspects arising from FDD. As a consequence, issues concerning residual generation and fault isolation of FDI are not central to the theme. However, there are similarities between fault estimation and the residual generation problem and these are discussed in Chapter 2.

From a practical point of view, the topics of FDI and FDD raise very interesting and challenging directions for applied research. For example: the detection of faults, to be useful in practice, should be achieved early by detecting "incipient" effects associated with the fault before its effect becomes serious.

Incipiency in this context means that the fault is difficult to detect because of its small effect on the system. The detection and isolation of incipient faults leads to a robustness problem as the effects of the faults become comparable with the effects of modelling uncertainties (Patton *et al*, 1989). It is important to detect and isolate incipient faults with high reliability in terms of low false-alarm and missed-alarm rates, in order to avoid the consequences of (a) system breakdown (b) mission abortion and (c) catastrophes (Beard 1971; Willsky 1976; Patton *et al*., 1989).

1.3 Practical Requirements for Fault Tolerant Control

The context of FD includes the terms *monitoring* and *supervision*. '*Monitoring*' is an on-line task for determining the "condition" or "health" of a system, by recording necessary information, recognising and indicating anomalies in the behaviour, whereas '*Supervision*' can be classified as on-line monitoring a physical system and taking suitable actions to maintain the operation and system performance in the presence of a fault (Blanke *et al*., 2003). These challenges have motivated a control strategy widely

known in the literature as *Fault Tolerant Control* (FTC) (Patton, 1997; Blanke *et al*., 2003).

As the complexity of modern systems increases, the high numbers of variables that are involved in the dynamical system structure of these systems make it difficult for even the most experienced human operator to notice that a fault has occurred. S/he may not understand the fault development and its possible propagation through the system and may not be able to respond correctly and promptly. This is particularly the case for fast modern systems, requiring fast decision speeds (Blanke *et al*., 2003; Zhang and Jiang, 2003). The authorities of roles that the human operator can perform have therefore decreased in many complex applications with a noticeable trend towards full automation.

Even in aircraft flight systems, modern pilots have limited authority surrounded by complex avionics systems with quadruplex fly-by-wire redundancy. The dissimilar redundancy flight computer hardware and software systems are able to maintain the safety and integrity of the flight for many fault scenarios. However, when there are structural faults, the pilot's experience and decisions are required. It is well known that the majority of accidents that correspond to these flight systems faults are caused by pilot error (Burcham and Burken, 1997; Burcham *et al*., 1998 and 1999; Jones, 2005).

It is a valid generalisation that in all safety-critical systems, e.g. for those found on aircraft, spacecraft and automobiles or within the nuclear, petro-chemical and chemical process industries, etc. a small malfunction or fault that is uncompensated by the control system or redundancy (involving reconfiguration etc) may lead to serious failure and even catastrophe. An example of this is the military aircraft which is designed to be unstable without the control system (referred to as static instability), to enhance the agility and manoeuvrability of the aircraft. The flight control system not only makes the aircraft stable but also provides important handling qualities for flight. If the control system malfunctions there is a real danger that the controllability and stability of the aircraft will be lost and an accident will follow. The robustness and integrity of the flight control system are thus of high importance and a very large percentage of the cost of the development of a modern aircraft reflects the cost of the high integrity avionics and flight systems (Ganguli *et al*., 2002; Alwi and Edwards, 2005, 2006; Boskovic, Bergström, and Mehra, 2005; Boskovic, Prasanth, and Mehra 2007). The quadruplex level of redundancy of a fly-by-wire aircraft can, under certain circumstances, be reduced to a triplex level of redundancy by using FDI or FDD systems, by replacing the

hardware redundancy by analytical redundancy using system model information (Patton *et al*., 2000a).

The detection, isolation and diagnosis of faults in a safety-critical system can be used in several ways to enhance the system integrity. Once the faults are detected and isolated the unhealthy part(s) of the system can be replaced by using either analytical estimation methods (soft redundancy) or by using control system reconfiguration. Alternatively, the fault can be estimated on-line and compensated by an adaptive control scheme.

(a) (b) (c)

Figure 1-2: Accidents show that fault information is important

Figure 1-2 shows some examples that faults can lead to serious accidents: (a) an actuator fault caused an airplane to crash, (b) a sensor fault caused a rollercoaster to stop in mid-air, and (c) a component fault caused another aircraft to crash (www.cnn.com).

In case of the aviation accidents, e.g. ELAL Flight 1862 Bijlmermeer Incident, on 4 October 1992, a Boeing 747, ELAL Flight 1862, cargo plane of the Israeli airline ELAL, crashed into an apartment building in Bijlmermeer, Amsterdam, Netherlands (see Figure 1-3). 43 people were killed, plus 39 persons on the ground. Many more were injured. [Nederland Aviation Safety Board: (NASB)].

Figure 1-3: ELAL flight 1862: the aircraft the and the Bijlmermeer apartment building

NASB indicated that: '…*the plane had only managed to maintain level flight at first due to its high air speed (280 knots). The damage to the right wing, resulting in reduced lift, had made it much more difficult to keep the plane level. At 280 knots (520 km/h),*

there was nevertheless sufficient lift on the right wing to keep the plane aloft. Once the plane had to reduce speed for landing, however, it was doomed; there was too little lift on the right wing to enable stable flight, and the plane banked sharply to the right without any chance of recovery…'

However, according to many incidents, where pilots successfully landed crippled aircraft, Burcham *et al* (2004) and Gero (2006) show that in many cases, the damaged/faulty aircraft is still flyable, controllable and some level of performance can still be achieved, to allow the pilot to safely land the aircraft. An independent investigation by Smaili and Mulder (2000) on the ELAL flight 1862, suggested that there was still some control and flying capability associated with the crippled aircraft, where pilots successfully landed crippled aircraft. Maciejowski and Jones (2003) demonstrated in simulation, using a model-based predictive control approach that the ELAL 1862 disaster could have been avoided and it may have been possible to control the crippled aircraft using a form of FTC in the flight control system to maintain the required controllability for the purpose of a quick landing back at Schiphol airport, Amsterdam.

In 2004, the Group for Aeronautical Research and Technology in Europe (GARTEUR) organization initiated the Flight Mechanics Action Group 16 to study this accident further. The AG16 group developed further research on fault-tolerant flight control and demonstrated the value of using FTC methods to reduce the probability of accident for cases such as the ELAL 1862 Amsterdam flight disaster. The goal was to apply a number of FDD and FTC algorithms within a realistic failure scenario, based on the earlier study provided by Smaili and Mulder (2000).

Although the aircraft of the ELAL 1862 flight was a Boeing 747 some modern aircraft (e.g. Boeing 777 and Airbus 320, 330, 340, 350, 360, 370, and 380) are equipped with fly-by-wire flight control computers which can increase the safety of aircraft operations by guarding the safe flight envelope and easing manual flight control. With a forward-looking interest the AG16 study developed and tested several types of fault-tolerant flight control systems that could be used not only for systems such as the Boeing 747 but mainly for modern fly by wire aircraft systems. The controllers employed techniques ranging from H_∞ (Cieslak *et al*., 2009), sliding mode control allocation (Alwi and Edwards, 2009), and model-predictive control (Joosten *et al*., 2009) to parameter estimation and nonlinear dynamic inversion (Lombaerts *et al*., 2009). The use

of these FTC algorithms in a high fidelity flight simulator can further increase safety in the case of actuator, aerodynamic or even structural failures in the aircraft.

Amongst industrial accidents, the Bhopal disaster in December 1984 shows an important example. The release of toxic methyl isocyanate (MIC) gas from the Union Carbide chemical plant in Bhopal, India, has been referred to as the worst industrial accident in history i.e. 2000 fatalities, 10,000 permanent disabilities, and 200,000 injuries (Chisti, 1986). [see Figure 1-4 (a)]

Leveson (2002) states '…*The Indian government said the accident on human error the improper cleaning of a pipe at the plant. A relatively new worker was assigned to wash out some pipes and filters, which were clogged [i.e. worker ignored the early warning signs which were available on temperature measurement gauges]. MIC produces large amounts of heat when in contact with water, and the worker properly closed the valves to isolate the MIC tanks from the pipes and filters being washed. However, without inserting a required safety disk (a slip blind) to back up the valves in case they leaked...*'

(a) (b) (c)

Figure 1-4: Some serious industrial accidents

In March 23, 2005, at the BP oil refinery in Texas City, the second-largest oil refinery in the state and the third-largest in the United States, a major explosion occurred in an isomerization unit at the site, killing 15 workers and injuring more than 170 others. According to a report issued after the accident, the disaster was caused by aging process control techniques and the liquid level in the tower being 20 times normal [see Figure 1-4 (b)].

At the Buncefield oil refinery, the fifth largest oil depot in the UK, in December 2005, a combination of a faulty sensor indicating that fuel had stopped being pumped and human error resulted in the largest fire in Europe since World War 2 [see Figure 1-4 (c)]. An ongoing 10 billion pound compensation claim and prosecutions for 5 companies, including those responsible for the control system design. The poor

maintenance procedures and incorrect results arising from the FDI procedure were also of major significance (Buncefield Major Incident Investigation Board, 2006. http://www.buncefieldinvestigation.gov.uk/reports/initialreport.pdf).

Recently, improvements in production and quality control techniques have greatly improved reliability however this has been offset by higher performance specifications and increasing complexity in both control algorithms and the hardware used. These mean that such systems strongly require some coordination of supervision for both control and diagnosis for possible faults, with the level of FTC dependent on the probability of a fault occurring, how critical it is within the overall process and the possible consequences of missing a problem or not identifying a problem in a timely manner (Patton, 1997; Sharif and Grosvenor, 1998).

1.4 Classification and Review of FTC Methods

Modern technological systems rely heavily on sophisticated control systems to meet increased safety and performance requirements. This is particularly true in safety critical applications e.g. aircraft, spacecraft, power plants, and chemical plants processing hazardous materials, where a minor fault could potentially develop into catastrophic events if left unattended or incorrectly responded to. To prevent fault induced losses and to minimize the potential risks, new control techniques and design approaches need to be developed to handle system component malfunctions whilst maintaining the desirable degree of overall system stability and performance levels. A control system that possesses such a capability is often known as an FTC system (Patton, 1997; Blanke *et al*., 2003). Historically, from the point of view of practical application, a significant amount of research on FTC systems has been motivated by aircraft flight control system designs (Steinberg, 2005).

Patton (1997) stated in his survey that, '*. . . Research into fault tolerant control is largely motivated by the control problems encountered in aircraft system design. The goal is to provide a self-repairing capability to enable the pilots to land the aircraft safely in the event of serious fault ….'*

During the last two decades, there have been various approaches to active FTC. Most of these belong to the following categories: pseudo-inverse modelling (Gao and Antsaklis, 1991), adaptive control systems (Bodson and Groszkiewicz, 1997; Diao and Passino, 2001; Tao *et al*., 2002), eigenstructure assignment (Jiang, 1994), multiple-model

methods (Maybeck and Stevens 1991; Rauch, 1995; Maybeck, 1999; Boskovic and Mehra, 2000, 2002; Yen and Ho 2003; Jiang and Zhang, 2006), reliable control (Veillette *et al*., 1992; Veillette, 1995) H_∞ control (Yang and Stoustrup, 2000; Yang *et al*., 2001), model-matching (Huang and Stengel, 1990; Gao and Antsaklis, 1992), compensation via additive input design (Noura *et al*., 2000; Theilliol *et al*., 2000 and 2002), sliding mode control (Utkin 1992; Edwards and Spurgeon, 1998; Hess and Wells; 2003; Vetter *et al*., 2003; Edwards, 2004; Alwi and Edwards, 2005, 2006, 2007, 2009).

During the last two decades there has been a substantial literature on the subject of FTC according to reviews, survey papers and books (Patton *et al*., 1997; Blanke *et al*., 2001, 2003, 2006; Zhang and Jiang, 2003, 2006), which give the state of the art and perspectives in the field of control reconfiguration in FTC. As discussed above, approaches to FTC are motivated only by a particular application. For example, safety in flight control, efficiency and quality improvements in industrial processes, etc.

The main challenges to be faced in the design of FTC systems are:

(1) It is difficult to compensate a number of possible faults acting within or on the system.

(2) The control system or control system parameters must be changed in some way using available redundancy (hardware or analytical forms), either by accommodating the fault(s) (e.g. using fault estimation methods) or by a reconfiguration mechanism (either based on the use of FDI/FDD procedures or fault estimation).

(3) The stability of the FTC system must be maintained. The occurrence of a fault can make the system deviate far from its normal operation and can lead to a severe change in system behaviour. Even bounded faults can cause the closed-loop system to deviate rapidly from its required operation and hence the fault accommodation time is a critical parameter. The requirement for rapid reaction to faults can mean that the FDI or FDD procedure, if used, may slow down the accommodation process. The accommodation ability of a control system depends on several factors, for instance, the magnitude of the fault, the robustness of the system, etc. Therefore, to overcome such problems, new controllers must be developed with accommodation capabilities and tolerance to faults.

Generally, there exist two approaches to FTC: (a) *passive fault tolerant control systems* (PFTCS) and (b) *active fault tolerant control systems* (AFTCS) (Beard, 1971; Patton, 1997; Chen and Patton, 1999).

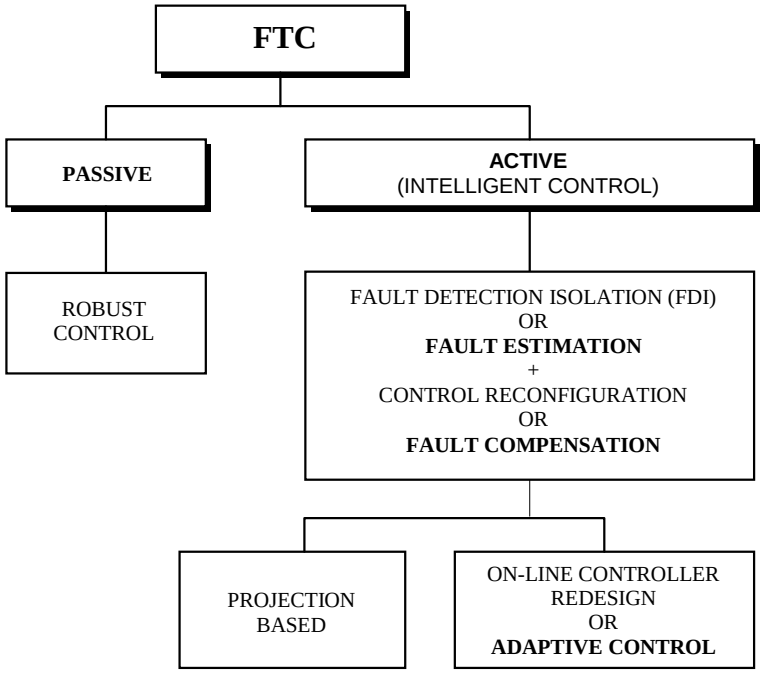

Figure 1-5: Fault-tolerant control methods (adapted from Patton, 1997)

Figure 1-5 shows the generally accepted taxonomy of active and passive FTC methods.

(a) In the *passive approach*, robust control techniques are used to make sure that the control loop system remains insensitive to faults. The effectiveness of this strategy, that usually assumes a very restrictive repertory of faults, depends upon the robustness of the nominal closed-loop system. It is interesting to note that PFTCS does not require FDI and controller reconfiguration/adaptation (Patton, 1997).

(b) In the *active approach*, a new control system is re-designed according to the estimation of the fault performed by the FDI unit and according to the specification to be met for the faulty system. The control law(s) is/are reconfigured/restructured to achieve performance requirements, subsequent to faults. Therefore most AFTCS require FDI to provide the fault or failure information so that reconfiguration can be achieved (Patton, 1997).

Active approaches are divided into two main types of methods: (1) *projection-based methods* and (2) *on-line automatic controller redesign methods*. In projection-based methods, a new pre-computed control law is selected according to the required

controller structure (i.e. depending upon the type of malfunction which has been isolated). The latter calculates for new controller parameters in response to control impairment. This is often referred to as *reconfigurable control* (Patton, 1997 and 2007; Chen and Patton, 1999).

Figure 1-6 shows the architecture of FTC consisting of two blocks: (1) fault diagnosis and (2) controller re-design, these tasks will carry out the two steps of FTC:

(1) *The diagnosis block* uses the measured inputs and outputs and tests their consistency with the plant model. Its result is a characterisation of the fault with sufficient accuracy for the controller re-designs.

(2) *The re-design block* uses the fault information and adjusts the controller to the faulty situation.

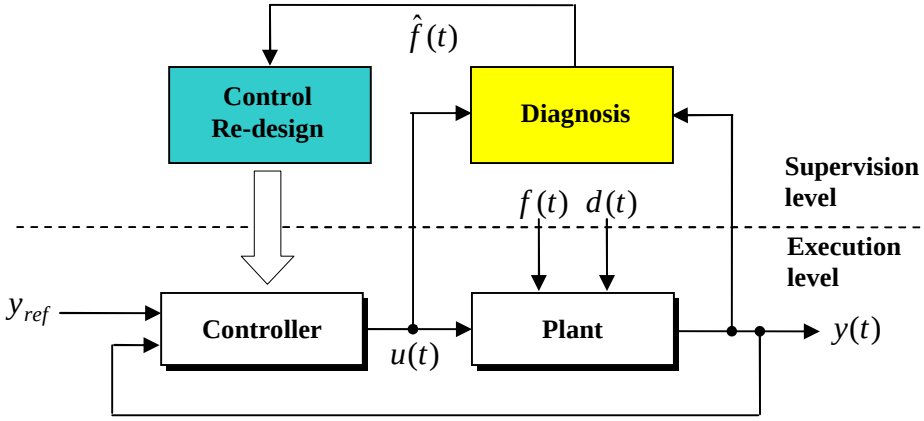

Figure 1-6: The architecture of FTC (Blanke *et al*., 2003)

Figure 1-6 illustrates that FTC extends the usual feedback controller by a *supervisor*, which includes the diagnostic function and the controller re-design blocks. In the absence of a fault, the system works as before, i.e. on the *execution level*. The nominal controller (sometimes referred to as the "baseline" controller, see Patton, 1997), which is designed for the fault-free system, attenuates the disturbance $d(t)$ and ensures good set-point/reference following and other requirements on the closed-loop system. In this situation, the diagnostic block recognizes that the closed-loop system is faultless (fault-free) and no change of the control law is necessary.

If a fault $f(t)$ occurs, the *supervision level* makes the control loop fault-tolerant. The diagnostic block identifies the fault and the controller re-design block adjusts the controller to the new situation. Following this, the execution level alone continues to satisfy the control target.

However, fault tolerance can also be achieved without the structure given in Figure 1-6 by means of well established control methods. As this is possible only for a restricted class of faults, these methods will not be described in more detail in this Chapter. However, they require brief outline as follows:

(i) *Robust control*: a fixed controller is designed that tolerates changes of the plant dynamics. The controlled system satisfies its goals under all faulty conditions. Fault tolerance is obtained without changing the controller parameters. It is, therefore relates closely to *passive fault tolerance*. However, the theory of robust control has shown that robust controllers exist only for a restricted class of changes that may be caused by faults. Further, a robust control works suboptimally for a given nominal plant because its parameters are obtained as a trade-off between performance and robustness; this is the classical Pareto-optimal optimization result. The controller is not adjusted to the nominal process behaviour but is chosen to satisfy the performance specifications for the plant subject to all faults, and

(ii) *Adaptive control*: the controller parameters are adapted to changes of the plant parameters. If these changes are caused by some fault, the adaptive control may provide *active fault tolerance*. However, the theory of adaptive control shows that this principle is particularly efficient only for plants that are described by linear models with slowly varying parameters. These restrictions are usually not met by systems under the influence of faults, which typically have a nonlinear behaviour with sudden parameter changes. The faults cause nonlinear effects as the system moves away from its known equilibrium point.

Patton (1997) proposed the complex combination of *three* major research fields in FTC; i.e. FDI/FDD, robust control, and reconfigurable control (see Figure 2.2).

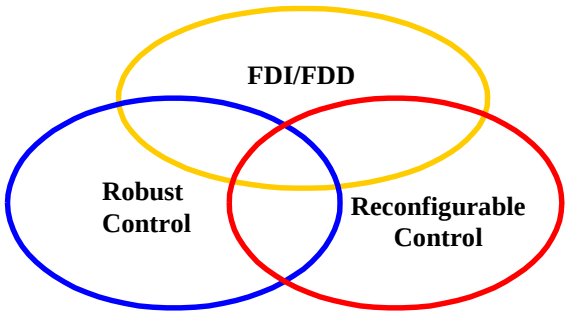

Figure 1-7: The three disciplines of FTC (Patton, 1997)

Patton (1997) also discussed the relationship between these fields of research. For a typical FTC scheme, when a fault occurs, the *FDI/FDD* scheme will detect and locate the source of the fault. It is important to note that FDI is concerned with the decision problem (fault detection and isolation), whist FDD is concerned with a little more than FDI in the sense of possible fault causes, including fault estimation and diagnosis of the fault severity etc. This information is then passed to the mechanism unit to initiate reconfiguration. The *Reconfigurable Controller* will try to adapt to the fault, and provide stability and some level of performance. Both the FDI/FDD and reconfigurable controller also need to be robust against uncertainty and disturbance. *Robust control* is designed to be robust against disturbances and uncertainty during the design stage. This enables the controller to counteract the effect of a fault without requiring reconfiguration or FDI/FDD. For some robust methodologies, its fault tolerant capability is limited, i.e. total actuator failure cannot be handled directly.

Some widely referred to survey materials on FTC and FDI are: (Patton, 1997; Blanke *et al*., 1997, 2000, 2001; Zhang and Jiang, 2003, 2006), and (Isermann and Ballé, 1997; Chen and Patton, 1999) and more recent publications (books and edited monographs) such as (Blanke *et al*. 2001, 2003, 2006; Caccavale and Villani, 2003; Mahmoud *et al*., 2003; Tao *et al*., 2004) in the field of FTC and (Chen and Patton, 1999; Patton *et al*., 2000a; Isermann, 2006; Simani *et al*., 2003) for FDI.

Some studies describe the integration and combination of FDI and FTC schemes (Polycarpou and Vemuri, 1995; Demetriou and Polycarpou, 1998; Wu, 2000). Some papers discuss the fault accommodation problem based on the integration of control and FDI (Napolitano *et al*. 1995; Niemann and Stoustrup, 1997; Belcastro, 2001; Theilliol *et al*., 2002; Yen and Ho, 2003). Zhang and Jiang (2003, 2006) give a good bibliographical review of reconfigurable FTC systems. Their work proposes a classification of reconfiguration methods which is based on the mathematical tools used, the design methodologies used, the way of achieving reconfiguration, etc. They also address a bibliographical classification based on the design methods with emphasis on the different practical applications, discussing open problems, an overall picture of historical, current, and future development in this area.

The combination of both FDI/FDD and reconfigurable controllers within the overall system structure is the main feature distinguishing *active* from *passive* FTC. Therefore the main issues in active FTC are how to design; (i) a controller which can be easily reconfigured, (ii) a FDI/FDD unit with high sensitivity to faults and robustness to model

uncertainties and external disturbances, and (iii) a reconfiguration mechanism which is able to recover the pre-fault system performance within the constraints of control inputs and system states.

It should be noted that for some FTC schemes, the detection and isolation of faults is not sufficient. Some FTC schemes require further information about the nature and behaviour of each fault. In active FTC, the information obtained from the diagnostic algorithm should be used in the controller re-design. Hence, process diagnosis should not only indicate that some fault has occurred but it has to identify the fault location and fault magnitude with sufficient precision. This information will make it possible to set up a model of the fault system, which can be used in the controller re-design. Therefore, FDI and FDD (including fault estimation/identification) are essential features of an active FTC system (Blanke *et al*., 2003).

1.5 The Fault Estimation Approach to FTC

This research focuses on the development of methods to estimate the magnitude variations of the fault rather than to detect the presence of a fault via the use of a residual signal. The residual signal is suitable for the combined problem of fault detection and isolation, when the structure of the fault effect on the system is not completely known. Whenever it is necessary to isolate a fault, beyond the use of one residual signal, a bank of dissimilar residual signals can be used to indicate the location of the fault in the system (Patton *et al*, 1989; Chen and Patton, 1999; Edwards *et al*., 1998, 2000).

In other words, fault estimation is a direct way to provide fault information e.g. the fault estimation technique provides an estimate of the size and severity of the fault. This can be important in many on-line applications. Furthermore, when compared with other fault estimation signals within the same system, these can be used to isolate all faults in the same system.

This thesis is thus concerned with the active approach to FTC and in particular the use of on-line fault estimation embedded within an adaptive control problem. In this approach the fault isolation decision process is obviated, as the accommodation to the fault(s) is automatic within the adaptive scheme. Hence, in this work the residual generation problem of fault detection is replaced by one of fault estimation. It is important to note, as pointed out by Chen and Patton (1999) that an ideal residual signal

for FDI, even in an uncertain system application, can be defined as a robust estimator of the fault to be detected. If this ideal residual generator remains insensitive to uncertainty and modelling errors it can be further defined to be robust '…*The fault estimator and ideal residual signal are thus equivalent when true robustness is achieved...*' It is important to note that the fault estimation algorithms developed in this research are essentially ideal residual generators corresponding to the particular fault. The link between fault estimation and residual generation has interesting potential for future research and is not pursued further in this thesis.

The challenges for fault estimation in FTC that are investigated by this thesis can be summarised as follows:

(i) The need to develop new methods for rapid and accurate estimation of actuator faults. The work focuses on the estimation of actuator faults as a specific part of an adaptive control system within FTC.

(ii) The challenge to develop adaptive/autonomous control schemes for FTC based on fault estimation that is simple to implement in real applications.

(iii) The need to consider robustness in the active FTC designs. This is achieved as the disturbance and uncertainty signals are considered implicitly in the fault estimation and accommodation, once again making the proposed general approach attractive for real application studies.

1.6 Thesis Structure and Contributions

The remainder of the thesis is arranged in the following manner:

Chapter 2 introduces the definition of the terms fault and failure and briefly discusses the different types of faults and failures which can occur on actuators and sensors examples, a description of the residual generator structure in model-based FDI is presented and an example mathematical model of a general faulty system is also given. Chapter 2 also reviews the robust FDI methods that can be achieved using disturbance-decoupling techniques via the Unknown Input Observer (UIO). The main issue of the FDI based on analytical redundancy is the sensitivity of the FDI algorithm to modelling uncertainties, parameter variation, and disturbance. Chapter 2 also introduces the background concepts of quantitative model-based FDI and FDD as well as an outline of the taxonomy of FTC methods, based on either active or passive methods. The main

concepts and strategies behind some of the FTC and FDD schemes in the literature, as well as their advantages and drawbacks, are also discussed.

Chapter 3 proposes a new approach to fault compensation for FTC using fault estimation by which the faults acting in a dynamical system are estimated and compensated within an adaptive control scheme with required stability and performance robustness. The proposed FTC scheme includes an augmented state observer (ASO) in the control system, which has an intrinsic robustness in terms of the stability and performance of the estimation error. The ASO includes a compensation gain matrix which is designed using a Lyapunov LMI-pole-placement approach, based on knowledge of the fault bounds. This stability concept is developed via a theorem and a corresponding proof. Additionally, the novel adaptive compensation FTC concept is illustrated by considering friction force as a special type of input or actuator fault in a mechatronic system. The example given is an illustration based on the friction compensation problem via a nonlinear inverted pendulum with Stribeck friction. It is very reasonable to consider the friction as a fault in the system as it is a bounded but unwanted effect which causes the performance of the system to change.

This Chapter also shows that the friction (fault) estimation and compensation is handled and the results demonstrate excellent performance of the adaptive controller in removing the effect of the friction force to yield very precise positioning control. It is also important to note that combined fault estimation and fault compensation control problem provides a powerful method of loop-transfer recovery, enabling the *Separation Principle* to be reached as the bounded faults and/or uncertainties are estimated and compensated in the observer feedback control system. The theory and approach have wide application to more complex problems in which actuator, sensor faults as well as multiplicative faults and unknown input signals can all be compensated together using the system description and proposed stability conditions.

Chapter 4 focuses on an alternative approach to the one described in Chapter 3, using sliding mode theory for estimation and control. The bounded estimation problem is defined along with the stability and control performance requirements for the FTC system, corresponding to a combination of the well known sliding mode observer (SMO) and sliding mode control (SMC) structures. Chapter 4 also develops a design method for on-line FTC, based on fault estimation. The interconnection of the SMO and

SMC structures is made via a bounded fault estimate signal is illustrated using the friction compensation example discussed in Chapter 3.

As discussed in Chapter 3, the key idea behind this example is that the friction force can be considered as an actuator fault acting on the system. The estimates of the friction force generated via the SMO theory are then directly used in an adaptive SMC scheme. The main contribution of this Chapter is the development of an adaptive gain for the nonlinear unit vector term which 'compensates' for the effects of friction force. The approach is illustrated using a nonlinear inverted pendulum with Stribeck friction. Necessary and sufficient conditions for SMO estimation (as a matched uncertainty) and SMC stability are from (Edwards *et al*., 1998 and 2000). The new ideas and contributions are thus two-fold; (a) the concept of viewing friction as a fault-effect and (b) the combined use of the sliding mode friction estimation and sliding mode control. The friction compensation problem is merely one example of an adaptive FTC system and the principles are applicable to a wide range of application systems.

Chapter 5 addresses the robust fault estimation problem of linear parameter-varying (LPV) systems where the state-space equation depends on the time-varying system parameters as an alternative to robust residual generation for FDD as discussed in Chapter 2. This Chapter describes the development of a robust fault estimator which can be characterized via a set of linear matrix inequalities (LMIs) with the robustness property to exogenous disturbance. First, the LPV feedback controller for the fault-free case is designed. To demonstrate the proposed method, an illustrative example of a two-link manipulator is provided and the polytopic LPV model of this system is also presented. Finally, the active FTC mechanism is illustrated by an on-line combination of the polytopic feedback controller and polytopic LPV estimator [using the introduced fault-effect factor estimation] for achieving actuator fault estimation and compensation.

Chapter 6 provides a novel approach associated with a distributed control system that is designed to be tolerant to faults. The key to the formulation of the basic control problem is one of being able to decompose the global level task and associate each subsystem with its own goals and performance requirements. Chapter 6 focuses on the development of the global controller, its structure and optimisation under the action of the *Autonomous Coordination and Supervision Scheme* (ACSS). The global controller is developed as an intelligent learning coordinator from the knowledge base of the ACSS. This Chapter also proposes learning control systems methods which can be used

together with on-line constrained optimisation strategies. The solutions are achieved using two different combinations of neural networks and learning paradigms: (i) at a local level, a Recurrent Neural Network (RNN) is used to identify the subsystem dynamics in a suitable structure for the purpose of FDI, and (ii) at the higher, global level, a feed-forward network is used along with Hebbian learning to learn the coordinating function. The first illustration of these concepts is made in Chapter 6 using a simple example of two interconnected sub-systems. Chapter 6 forms the basis for further work on FTC of distributed control systems in Chapter 7.

Chapter 7 provides the estimation strategies for both fault(s) and interconnection disturbance. The work is linked with the use of compensation via the design of a distributed system two-level control scheme. The estimation methods are based on the use of the ASO approach described in Chapter 3. This new adaptive approach to compensating control in FTC is computed using the fault/interconnection estimation. A tutorial study is given of estimation and compensating control in the presence of faults within an example of a nonlinear Three-Tank interconnected system. The system comprises both faults and interconnection disturbances. Finally, the proposed FTC concept is applied via the ASO approach dealing with the problem of interconnection/local fault estimation and compensation, whereas the two-level control approach (as described in Chapter 6) is used to handle the interconnection disturbances acting on each subsystem, via the Interaction Prediction Principle.

Chapter 8: summarises and concludes the overall work described by the thesis and makes suggestions and recommendations as to how the research can be further developed in the future.

Chapter 2.
Outline Review of Model-based FDI and FDD Methods

2.1 Introduction

This Chapter provides an overview of the main research topics and published work on *quantitative* model-based FDI and FDD. Section 2.2 provides a classification of FDI/FDD methods and Section 2.3 and 2.4 discuss is some detail the main mathematical properties of residual generation approaches for FDI and FDD, respectively. Section 2.5 provides a specific study of the literature and the main concepts involved in the use of fault estimation for different forms of control reconfiguration in active FTC. This Section also discusses a potential correspondence between residual generation and fault estimation concepts and their importance in robust FTC.

2.2 Classification of Fault Diagnosis Approaches

Research developments in the field of analytical redundancy methods for FD started in the 1970's (Beard, 1971; Willsky, 1976). Many approaches in the context of robust model-based fault diagnosis have been proposed (Clark, 1978; Himmelblau, 1978;

Chow and Willsky, 1984; Isermann, 1984; Gertler, 1988; Patton *et al*, 1989, 1994; Chen and Patton, 1999; Patton *et al*., 2000a; Simani *et al*, 2003; Blanke *et al*, 2003; Isermann, 2006; Ding, 2007).

Since the 1970s many monitoring methods and procedures have become available through developments in computer technology. Fault diagnosis techniques have also gained interest and have been engineered into many practical and industrial systems. Fault diagnosis requirements followed the trend in increased automation in science and engineering applications (e.g. industry, medicine, defence, transportation) [ref???].

In the field of flight systems, aircraft dynamics are well studied and hence model-based FDI methods can be quite easily applied in flight control systems (Deckert *et al*., 1977; Chandler 1984; Ioannou *et al* 1989; Patton 1991a, 1991b; Rauch *et al*., 1995; Polycarpou and Heilmicki, 1995; Smaili and Mulder, 2000; Alwi and Edwards, 2005, 2006; Cieslak *et al*., 2009). The challenges here are mainly of reliability of FDI methods (for safety-critical application) and verification and certification for flight air worthiness.

The development of real time/on-line FDI systems is becoming an issue of primary significance in the design of intelligent and autonomous control systems. However, the imprecise measurements and uncertain dynamical behaviour of the process, together with unknown disturbances, make the '*early fault detection*' problem difficult to achieve (Patton, 1997; Chen and Patton, 1999; Simani *et al*, 2003).

On-line monitoring tools not only provide early warning of plant malfunction (including loss of safety, environmental degradation, poor economy, etc.) but also information as to how to minimize maintenance schedule costs. Precise diagnostic information must be generated quickly to protect the plant/system from shut down and provide human operators with appropriate process status information to help them take correct decisive actions not only when faults become serious but also when faults are developing and difficult to detect (also called incipient faults). It is clear that the application of supervised on-line diagnosis schemes can be profitable in terms of a decrease in service costs (Patton, 1997; Chen and Patton, 1999, Isermann, 2006).

The main idea of the model-based approach to FDI/FDD is to generate signals that reflect inconsistencies between nominal and faulty system operation. Such signals, termed "residuals", are usually generated using analytical approaches, such as observers (Chen and Patton, 1999; Patton *et al*., 2000a), parameter estimation (Isermann, 1994) or parity equations (Gertler, 1998) based on analytical (or functional) redundancy.

Considerable attention has been given to both research and application studies of real processes, using *analytical redundancy* as this is a powerful alternative to the use of repeated hardware (hardware redundancy).

As discussed in Chapter 1 the terms *monitoring* and *supervision* are sometimes used in FDI. Many mathematical model-based methods for FDI have been developed (See, e.g., Willsky, 1976; Isermann, 1984; Gertler, 1988; Patton and Frank, 1989; Chen and Patton, 1999).

However, a fault diagnosis system should have the same following characteristics:

- Low detection delay
- Low rate of false alarms
- Fault isolability (the ability to find the correct location of the fault)
- Robustness to noise, uncertainty and parameter variation

One of the main challenges lies in finding the fault when it is just developing. This may give more time to take the necessary measures to avoid breakdown or malfunction of the system.

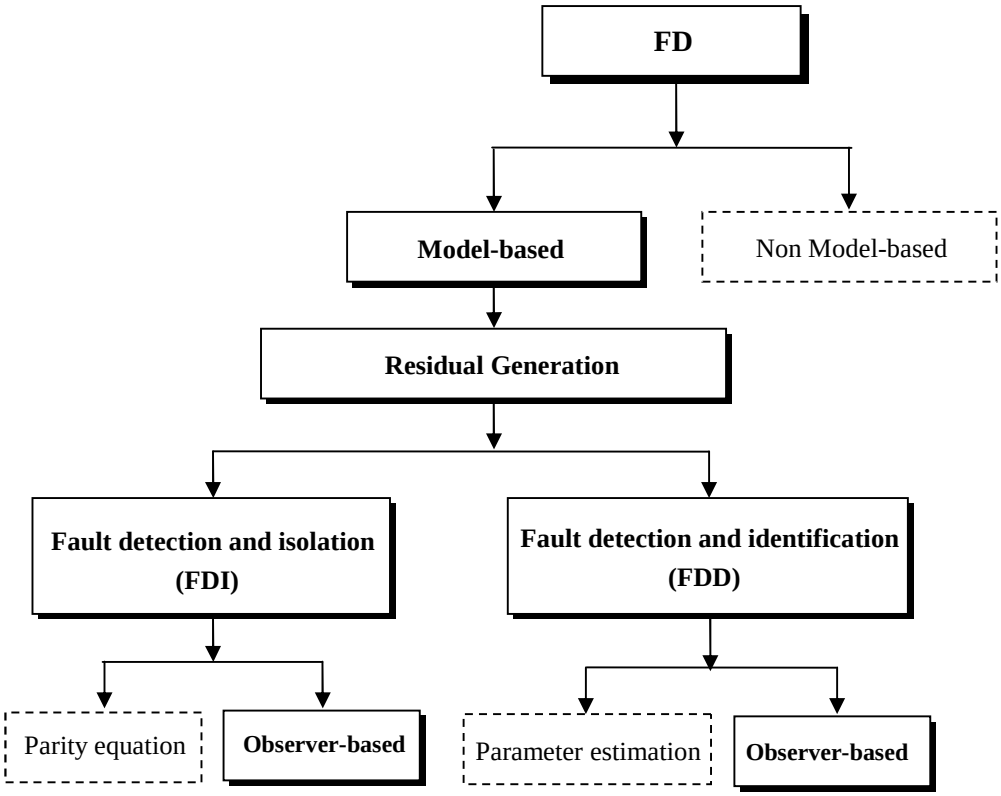

Figure 2-1: Fault diagnosis (FD) classification (from Chen and Patton, 1999)

There are many classifications of FD in the literature (Chen and Patton, 1999; Isermann and Ballé, 1997). The obvious classification is model and non-model-based fault diagnosis. However, in this thesis the emphasis will be only on model-based fault diagnosis. In view of the overall fault tolerant strategy, model-based schemes are grouped based on their capabilities into *two* major categories; (i) FD using residual schemes (residual generation) and, (ii) FD which has the capability to estimate the faults (fault estimation) [see Figure 2-1]

The following Sections, review the basic theoretical concepts of model-based fault detection and isolation first, followed by a classification based on *residual generation* and *fault estimation*.

2.3 Residual Generation Approaches to FDI

2.3.1 The idea behind model-based FDI

The main idea behind model-based FDI is to compare the system's available measurements, with a *priori* information represented by the system's mathematical model as illustrated in Figure 2-2.

The main advantage of the model-based approach is that no redundant hardware components are required to implement the FDI scheme. The model-based information is used to create a form of analytical or functional redundancy, rather than hardware redundancy. In this work only the quantitative form of mathematical model is used. Other model forms can be qualitative or a combination of qualitative and quantitative, based for example on fuzzy reasoning, neural networks or neuro-fuzzy modelling strategies (Patton *et al*., 2000b; Calado *et al*., 2001; Uppal and Patton, 2005).

A model-based FDI algorithm can be achieved in software on the process control computer and in many cases the measurements needed for control are sufficient for the FDI algorithm so that no additional hardware is required (Chen and Patton, 1999).

Figure 2-2 shows the conceptual structure model-based fault diagnosis comprising residual generation and decision making: (i) *the residual generation* providing a residual signal that carries information on the time and location of the faults. The residual signal should be close to zero in the fault-free case and deviate from zero when a fault has occurred, whereas (ii) *the decision making* evaluates the residuals and

monitors if and where a fault has occurred. This two-stage structure was first suggested by Chow and Willsky (1980) and is now widely accepted by the fault diagnosis community.

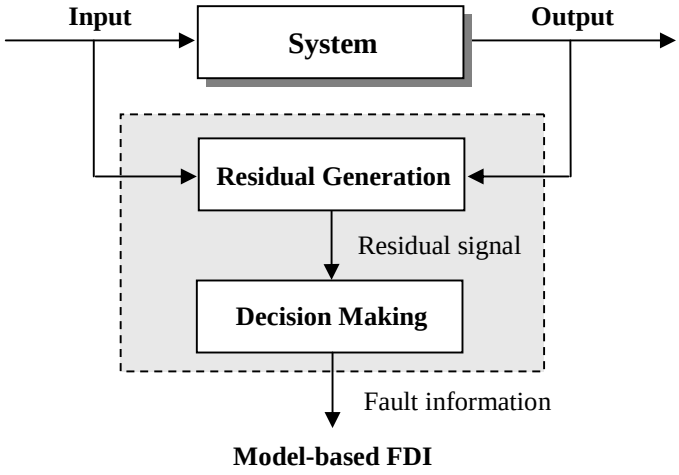

Figure 2-2: Conceptual structure of model-based fault diagnosis

(Chen and Patton, 1999)

The most important issue in model-based fault diagnosis is robustness against modelling uncertainty which arises from incomplete or inaccurate modelling of the monitored process. Robust fault diagnosis has become an interesting research issue over recent years (Chen and Patton, 1999).

FDI used the measured outputs $y(t)$ from sensors {normally needed in the feedback control} and the control inputs $u(t)$ as the control actuation generated by the controller and demanded reference signals. Model-based FDI is mainly concerned with on-line fault diagnosis, which is carried out during system operation. This is because the system inputs and outputs required by model-based FDI are only available when the system is in operation.

The relationship between the FDI role and the control loop is shown in Figure 2-3. It can be seen that the system model needed in the model-based FDI is an ideal replica of the open-loop system dynamics, although the system is considered to be operating in closed-loop. This is because both the inputs and outputs needed for the FDI algorithm are related to the open-loop system. '…*Therefore, it is not necessary to consider the controller in the design of a fault diagnosis scheme. Once the inputs to the actuators are available, the fault diagnosis problem is the same no matter how the system is working in open-loop or in the closed-loop*…' (Chen and Patton, 1999)

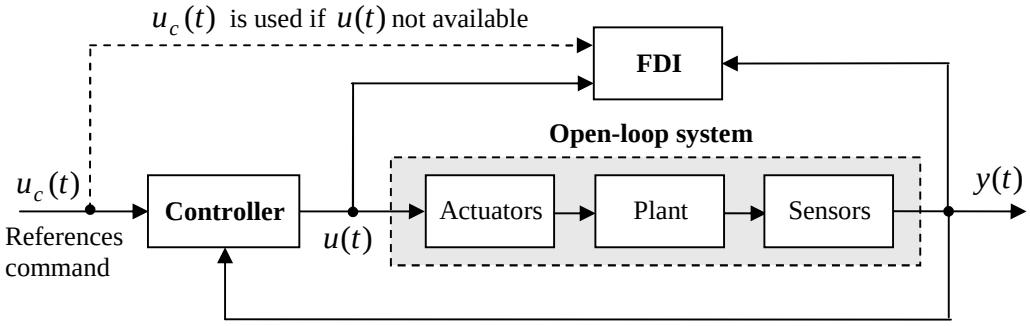

Figure 2-3: Fault diagnosis and control-loop

However, in cases when the inputs $u(t)$ to the actuator are not available, the reference command $u_c(t)$ is used in FDI. Therefore, the model depends on the relationship between the reference command $u_c(t)$ and the measured output $y(t)$. In this case the controller plays an important role in the design of the FDI scheme.

In the presence of modelling uncertainty the controller may desensitise the residual signals to the fault effects and possibly weaken the robustness of the FDI system with the potential for lower reliability in both fault detection and fault isolation. To attempt to overcome this problem the controller and FDI system can be designed simultaneously (Jacobson and Nett, 1991; Wu, 1992; Stoustrup *et al*., 1997; Chen and Patton, 1999; Weng *et al*., 2008). The connection between fault diagnosis and robust control design is an on-going topic of research and is not considered further in this thesis.

The first step in the model-based approach to FDI is to make a mathematical model of the system to be monitored. In the case of a nonlinear system, this implies a model linearization around an operating point.

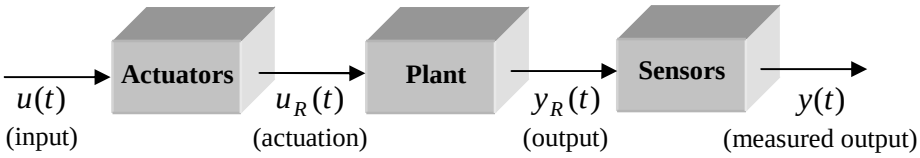

Figure 2-4: The open-loop system

We can consider the open-loop system to be represented in Figure 2-4 by a time-invariant, linear dynamic system in state-space form as follows:

$$\begin{aligned} \dot{x}(t) &= Ax(t) + Bu_R(t) \\ y_R(t) &= Cx(t) \end{aligned} \qquad (2\text{-}1)$$

where $x \in \Re^n$ is the system state vector, $u_R \in \Re^m$ is the real actuator input vector to the actuator and $y_R \in \Re^p$ is the real system output vector. A, B and C are the system matrices with appropriate dimensions.

2.3.2 Modeling of system with faults

Consider when the component faults $f_c(t)$ occurring in the system of Figure 2-4 the dynamic model of the faulty system can then be presented as: (see Figure 2-5)

$$\dot{x}(t) = Ax(t) + Bu_R(t) + f_c(t) \qquad (2-2)$$

The component fault represents some change in the system, for example, a leak in a water tank in the three tank system, etc. In some circumstances, the fault could be described as a parameter change in a system e.g. in i^{th} row and j^{th} column element of the system matrix A, the open-loop dynamics of the system can then be described as:

$$\dot{x}(t) = Ax(t) + Bu_R(t) + I_i \Delta a_{ij} x_j(t) \qquad (2-3)$$

where: x_j is the j^{th} element of the vector x, $I_i \in \Re^n$ is the vector with all zero elements except '1' in the i^{th} element and Δa_{ij} the parameter change.

However, the actual "output states" y_R of the system are not accessible and sensors must be used to measure the system output that also introduce additional dynamics. Ignoring the sensor dynamics, the measured outputs $y(t)$ can be described as:

$$y(t) = y_R(t) + f_s(t) \qquad (2-4)$$

where: $f_s \in \Re^p$ is a vector of additive output sensor faults. When there is a variation in the sensor scalar factors (multiplicative faults), a particular system measurement becomes $y(t) = (1 \pm \Delta) y_R(t)$ and the fault vector can then be written as $f_s(t) = \pm \Delta y_R(t)$. Figure 2-5 illustrates the open-loop system with actuator, component and sensor faults, respectively.

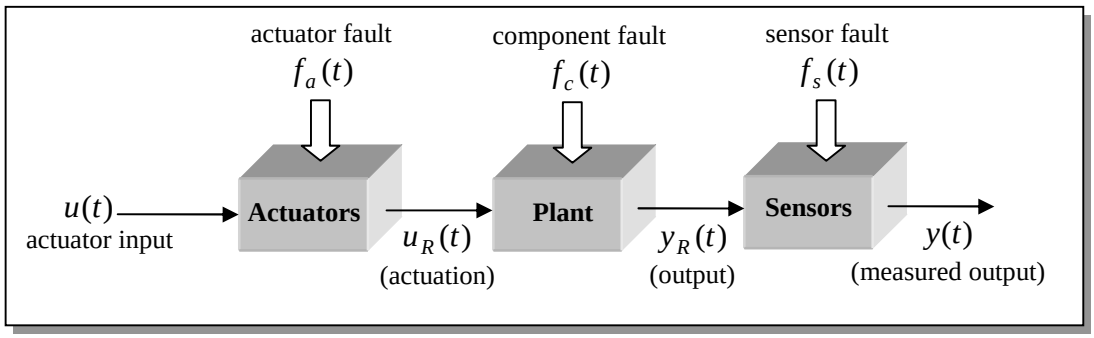

Figure 2-5: Open-loop system with faults

Consider the case when the actuator control input vector $u \in \Re^m$ is a known control command. The input sensors are not considered in this case and the actuator response $u_R(t)$ is not directly accessible. For a controlled system (if the actuator dynamics can be neglecting) $u_R(t)$ can be described as:

$$u_R(t) = u(t) + f_a(t) \qquad (2\text{-}5)$$

where: $f_a(t) \in \Re^m$ is the actuator fault vector.

The open-loop linear system model with all *actuator*, *component* and *sensor* faults can be described as:

$$\begin{aligned} \dot{x}(t) &= Ax(t) + Bu(t) + Bf_a(t) + f_c(t) \\ y(t) &= Cx(t) + f_s(t) \end{aligned} \qquad (2\text{-}6)$$

Considering the general case with all faults, the system may be described as:

$$\begin{aligned} \dot{x}(t) &= Ax(t) + Bu(t) + F_1 f(t) \\ y(t) &= Cx(t) + F_2 f(t) \end{aligned} \qquad (2\text{-}7)$$

The system is *strictly proper* (for $F_2 \neq 0$) with respect to the fault vector $f(t) \in \Re^g$. Each element $f_i(t)\,[i = 1, 2, \ldots g]$ of $f(t)$ corresponds to a specific fault. F_1 and F_2 are matrices with appropriate dimensions and represent the signal effect of faults on the system. These are called '*the fault entry matrices*'. Vectors $u(t)$ and $y(t)$ are the measured input and output vectors called '*the input-output vectors of the monitored system*' and are assumed to be known for the FDI purpose (Chen and Patton, 1999).

The system with faults (Figure 2-5) can also be represented by an input-output transfer matrix representation:

$$y(s) = G_u(s)u(s) + G_f(s)f(s) \qquad (2\text{-}8)$$

where:

$$G_u(s) = C(sI - A)^{-1}B \qquad (2-9)$$

$$G_f(s) = C(sI - A)^{-1}F_1 + F_2 \qquad (2-10)$$

Eqs.(2 - 7) or Eq. (2 - 8) are a generalised and widely accepted framework for linear model-based FDI in either the time-domain or the frequency domain (see more details in Patton and Chen, 1999; Ding, 2007).

The FDI methods use prior knowledge about some signal characteristics e.g. the dynamic range of the signal, the frequency spectrum etc, that is not always available. Moreover, these characteristics strongly depend on the operating point of the system. Indeed, the introduction of "residuals" is one of the most significant contributions in model-based FDI methodology. *These residuals can be designed to be sensitive to faults and insensitive to model uncertainties and operating point chang*es (Chen and Patton, 1999).

'*…Residuals are quantities that represent the inconsistency between the actual system variables and the mathematical model. Based on the mathematical model, many invariant relations (dynamic or static) among different system variables can be derived, and any violation of these relations can be used as residuals…*' (Chen and Patton, 1999).

A general structure of the residual generator (Patton and Chen, 1991a, 1991b) shown in Figure 2-6 can be expressed as:

$$\begin{aligned} r(s) &= [H_u(s) \quad H_y(s)]\begin{bmatrix} u(s) \\ y(s) \end{bmatrix} \\ &= H_u(s)u(s) + H_y(s)y(s) \end{aligned} \qquad (2-11)$$

In fault-free conditions the residual should be zero therefore from Eq. (2-11) it is clear that the transfer matrices $H_u(s)$ and $H_y(s)$ must satisfy the condition:

$$H_u(s) + H_y(s)G_u(s) = 0 \qquad (2-12)$$

The fault detection is performed by the comparing the residual evaluation function with a threshold function $T(t)$ as follows:

$$\begin{cases} J_{ev}(r(t)) \leq T(t) & \text{for} \quad f(t) = 0 \\ J_{ev}(r(t)) \geq T(t) & \text{for} \quad f(t) \neq 0 \end{cases} \qquad (2-13)$$

A simple and most frequently used method is to compare the residual with a *fixed threshold*.

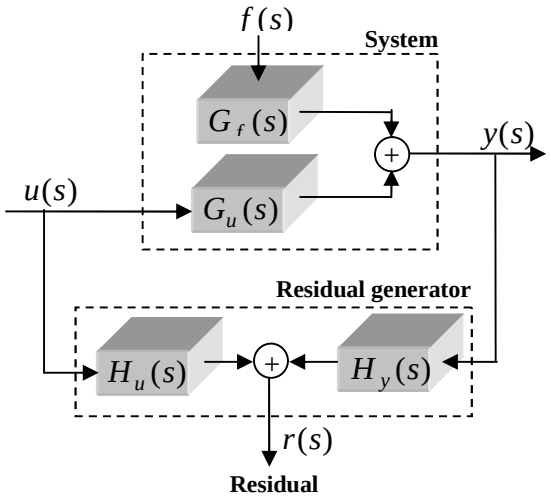

Figure 2-6: General structure of a residual generator (from Chen and Patton, 1999)

This method works well if the system is in steady state and either the faults to be diagnosed are not very small or the model used for the residual generator is a faithful replica of the process dynamic behaviour. In order to make the fixed threshold approach work well many investigations use robust systems principles to ensure that the residual is robust to model mismatch (modelling uncertainty, unknown disturbances, etc). This strategy is known as '*active robustness*' in FDI. In this approach there is an active attempt to make the residual robust.

The alternative strategy of scheduling the threshold in a dynamic way (perhaps as a function of the controls signal variation) is known as '*passive robustness*'. Here there is little or no attempt to make the residual robust to uncertainty but the effect of robustness is taken up in the adaptive behaviour of the threshold (Chen and Patton 1999 and the references therein).

2.3.3 Fault detectability and isolability

The concept of fault detectability and isolability are introduced here as they are used in Section 7.3. By using the transfer matrix representation of the system with faults in Eq. (2 - 8) and the general residual structure Eq. (2 - 1 1) the residual in the presence of faults can be described as:

$$r(s) = \underbrace{[H_u(s) + H_y(s)G_u(s)]}_{\text{"0"}} u(s) + H_y(s)G_f(s)f(s) \qquad (2\text{-}14)$$

From the constraint condition of the residual (2-12), now have:

$$\begin{aligned} r(s) &= \underbrace{H_y(s)G_f(s)}\, f(s) \\ &= G_{rf}(s) f(s) \\ &= \sum_{i=1}^{g} [G_{rf}(s)]_i f_i(s) \end{aligned} \qquad (2\text{-}15)$$

where $G_{rf}(s) = H_y(s)G_f(s)$ is the fault transfer matrix representing the relationship between the residuals and faults (see Figure 2-7), $[G_{rf}(s)]_i$ is the i^{th} column of the transfer matrix $G_{rf}(s)$ and $f_i(s)$ is the i^{th} element of $f(s)$ (Chen and Patton 1999).

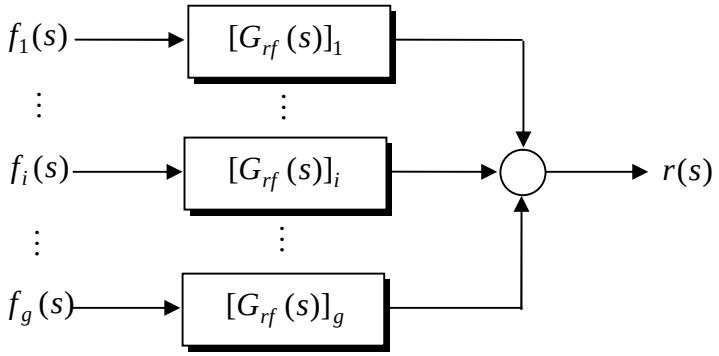

Figure 2-7: The relationship between fault and the residual

In order to detect the i^{th} fault $f_i(s)$, $[G_{rf}(s)]_i$ should be (designed to be) non-zero:

$$[G_{rf}(s)]_i \neq 0 \qquad (2\text{-}16)$$

If the condition in Eq. (2-16) is satisfied, the i^{th} fault f_i is *detectable* in the residual $r(s)$. '*…This can be defined as 'Fault Detectability Condition' for the residual* $r(s)$ *to the* i^{th} *fault* f_i *…*' (Chen and Patton, 1999).

The condition:

$$[G_{rf}(0)]_i \neq 0$$

follows by application of the *final value theorem*, as a '*Strong Fault Detectability Condition*', which holds as time $t \to \infty$.

For fault isolation a residual set is needed. If the residual set can isolate all the faults, it can be said that it has the required '*isolability*' property. There are <u>*two*</u> main approaches to achieve the fault isolation task:

- **Structured residual approach**

  In the structured residual approach, each residual must be designed to be sensitive to a subset of faults. In a '*Structured residual set*' each residual in the set of residuals has a required sensitivity to specific faults whilst insensitivity to others (Gertler, 1991), so that individual faults can easily be isolated. To generate a structured set of residuals:

  (i). The first step is to specify the sensitivity and insensitivity relationship between residuals and faults.

  (ii). The second step is to design a set of residual generators, based on the relationships specified in step one.

  There are various kinds of structured residuals. The '*Dedicated Residual Set*' is a set of residuals where each one is sensitive to only one fault [inspired by the Dedicated Observer Scheme proposed by Clark (1978)]. The '*Generalized Residual Set*' is a set of residuals, with each residual sensitive to all but one fault [based on the Generalized Observer Scheme by Frank, (1990)].

- **Directional residual approach**

  Another approach for fault isolation is to design a directional residual vector, which lies in a fixed and fault-specified direction in the residual space (Chen and Patton, 1999). The generated residual vector is compared with known fault signature directions. However, for reliable fault isolation, each fault signature has to be uniquely related to one fault (See more details in Section 2.7 of Chen and Patton, 1999).

2.3.4 Residual generation methodologies

It is clear that the generation of residual signals is the main issue in model-based FDI. There are a variety of methods available for residual generation both for continuous and discrete system models. This Section outlines the commonly used model-based residual generation techniques. If robust residual generation is achieved then the residual evaluation is easily achievable, e.g. through the use of any well-developed statistical

approaches of ‘Generalised Likelihood Ratio’ (GLR) testing (Willsky and Jones, 1974; Tanaka and Müller, 1993; Peng *et al*., 1997) and the ‘Sequential Probability Ratio’ (SPR) test (Willsky, 1976; Basseville, 1988), can be utilised.

However, it is well known that model-reality mismatches always exist in practice. Disturbances as well as model uncertainty are inevitable in real application problems, which imply the need for robustness in the FDI design. Consider the following FDI approaches:

- **Parameter estimation approach**

  In this approach, the parameters of the model of the system are estimated using the input-output measurements of the system (Isermann, 1984, 2006). The main idea is that by detecting a change in the system parameters residuals can be generated. These residuals can then be used to detect and isolate faults. The main drawback of this approach is that the model parameters should have a physical meaning and they should correspond to the actual physical parameters of the system (FDI is straightforward if this is true). If this condition is not true it is difficult to distinguish fault effects on the residual from causal effects of parametric variation, uncertainty or other time-varying system properties (e.g. changing disturbance or even system structure changes). As a result, the fault isolation task becomes difficult. Moreover, if the model structure is nonlinear in its parameters, non-linear modelling methods or non-linear feedback structures should be applied and these may cause serious difficulties in the case of complex (difficult to model) systems. Robust parameter estimation techniques may be applied to account for system-model mismatch. However, Patton *et al* (2000) pointed out that the detection of faults in sensors and actuators is possible but complicated using the parameter estimation.

- **Parity relation approach**

  Parity relations (equations) can be used in a systematic approach, based on analytical redundancy, to design structured residuals for fault isolation. The basic idea of this approach is to provide a check of consistency of the measurements. However, this approach is more suitable for linear systems as discussed in more detail in (Chen and Patton, 1999). Patton and Chen showed that the parity equation approach has a strict mathematical equivalence with the observer –based approach, under certain conditions (Patton and Chen, 1991).

- **Observer approach**

  The observer approach to FDI can be used to generate residuals via the difference between the estimated actual system outputs. The main advantage of this approach over the parity equation approach is more suitable for tolerating some degree of nonlinearity and uncertainty. For this reason the observer approach is given more attention in the literature (Patton and Chen, 1997). The observer-based approach, particularly the unknown input observer or UIO, is described in Section 2.3.5 and applied to a distributed and interconnected system example in Section 7.3.

Clark *et al*. (1975) first applied the Luenberger observer to the problem of fault detection. The main concept of observer-based FDI is that the estimates of certain measured or unmeasured signals can be obtained via a state estimator in either Luenberger observer or Kalman filter forms. The estimates of measured signals can then be compared with the original signals to generate the residuals. Another focus on observer-based FDI arises from the popularity of using state space models and the wide applicability of observers (especially for linear systems) in control. A brief history of observer-based FDI can be found in Patton (1994), Patton and Chen (1997) and Chen and Patton, (1999). The problem of model mismatch is usually addressed by using the concept of "*the unknown input*". Using the observer-based approach the residuals are generated as the difference between the estimated and the actual output. Consider a state observer (see Figure 2-8) for the system described by Eq. (2 - 7) .

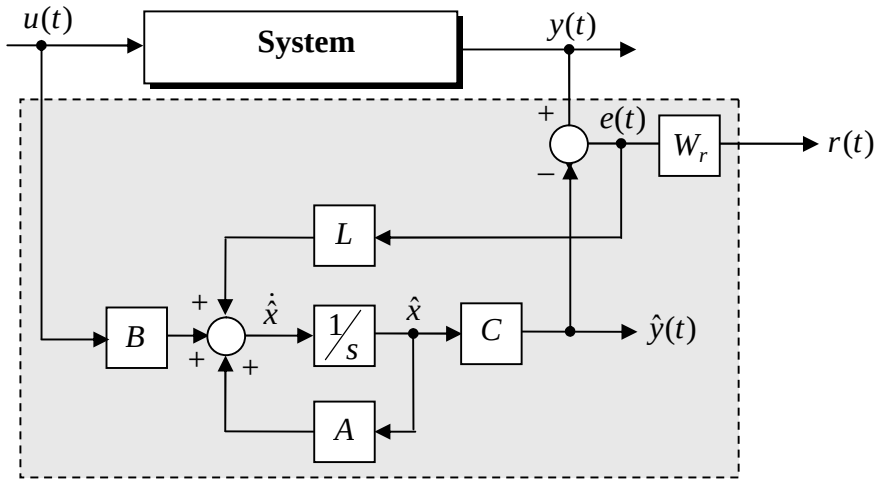

Figure 2-8: State observer for FDI (from Chen and Patton, 1999)

The observer shown in Figure (2-10) can be described by the following equations:

$$\begin{aligned} \dot{\hat{x}}(t) &= A\hat{x}(t) + Bu(t) + Le(t) \\ \hat{y}(t) &= C\hat{x}(t) \\ e(t) &= y(t) - C\hat{x}(t) \end{aligned} \qquad (2\text{-}17)$$

where $L \in \Re^{nxn}$ is a designed observer gain, $\hat{x}(t)$ is the estimated state, $\hat{y}(t)$ is the estimated output and $e(t)$ is the output estimation error. The state estimation error can be expressed as: $e_x(t) = x(t) - \hat{x}(t)$, thus:

$$\begin{aligned} \dot{e}_x(t) &= A[x(t) - \hat{x}(t)] - Le(t) \\ &= Ae_x(t) - LCe_x(t) \\ &= (A - LC)e_x(t) \end{aligned} \qquad (2\text{-}18)$$

Applying this observer to the system in Eq. (2 - 7) with actuator, component and sensor faults, and the *output estimation error* $e(t)$ can be expressed as:

$$\begin{aligned} e(t) &= y(t) - \hat{y}(t) \\ &= Ce_x(t) + F_2 f(t) \end{aligned} \qquad (2\text{-}19)$$

The state estimation error can be written as:

$$\begin{aligned} \dot{e}_x(t) &= Ax(t) + Bu(t) + F_1 f(t) - A\hat{x}(t) - Bu(t) - Le(t) \\ &= (A - LC)e_x(t) + F_1 f(t) - LF_2 f(t) \end{aligned} \qquad (2\text{-}20)$$

The residual can then be generated as:

$$r(t) = W_r e(t) \qquad (2\text{-}21)$$

The matrices $W_r \in \Re^{pxn}$ can be designed to generate residuals with desired characteristics e.g. time response and directional property, e.g. using eigenstructure assignment (Patton and Chen, 1991b; Patton and Chen, 2000) or via multi-objective optimisation (Chen, Patton and Liu, 1996; Liu and Patton, 1996).

2.3.5 The unknown input observer (UIO)

The Unknown Input Observer (UIO) has been known in the control literature since 1975 (Wang, Davison and Dorato, 1975). However, the concept was introduced to FDI applications to achieve robust FDI by Watanabe and Himmelblau (1982). Since that work many studies have proposed a wide range of robust FDI design tools (Patton, Frank and Clark, 1989; Frank and Ding, 1997; Chen and Patton, 1999; Patton *et al.*,

2000; Ding, 2007). The UIO can tolerate some extent of model uncertainty and hence increase the degree of fault diagnosis reliability. The UIO can be represented by the linear time-invariant state space model [the following continuous-time deterministic description has been adopted from (Chen and Patton, 1999; Patton *et al*., 2000)]:

$$\begin{aligned} \dot{x}(t) &= Ax(t) + Bu(t) + Ed(t) \\ y(t) &= Cx(t) \end{aligned} \qquad (2\text{-}22)$$

where $d(t) \in \Re^q$ is the unknown input or disturbance and $E \in \Re^{nxq}$ is disturbance distribution direction. Consider the UIO shown in (Figure 2-9). The effect of unknown disturbance $d(t)$ is de-coupled using:

$$\begin{aligned} \dot{z}_{uio}(t) &= F_{uio} z(t) + T_{uio} Bu(t) + K_{uio} y(t) \\ \hat{x}(t) &= z_{uio}(t) + H_{uio} y(t) \end{aligned} \qquad (2\text{-}23)$$

where $z_{uio}(t)$ is the state of the observer, $F_{uio}, T_{uio}, K_{uio}$ and H_{uio} are the matrices to be designed to achieve disturbance decoupling and $\hat{x}(t)$ is the estimated state vector (Chen and Patton, 1999).

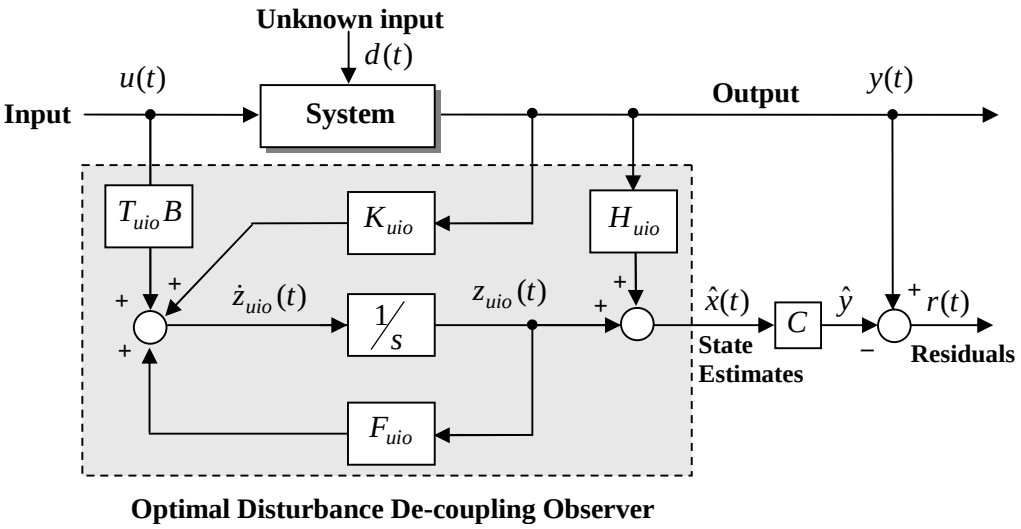

Figure 2-9: The Unknown Input Observer [Chen and Patton, 1999]

The state estimation error $e_x(t) = x(t) - \hat{x}(t)$ can be described by the following equation (Chen and Patton, 1999):

$$\begin{aligned} \dot{e}_x(t) = (A - H_{uio}CA - K^1_{uio}C)e_x(t) + [F_{uio} - (A - H_{uio}CA - K^1_{uio}C]z_{uio}(t) \\ + [K^2_{uio} - (A - H_{uio}CA - K^1_{uio}C)H_{uio}]y(t) + [T_{uio} - (I - H_{uio}C)]Bu(t) \\ + (H_{uio}C - I)Ed(t) \end{aligned} \qquad (2\text{-}24)$$

where:

$$K_{uio} = K_{uio}^1 + K_{uio}^2 \qquad (2\text{-}25)$$

Along with the UIO observer design the decoupling of the effects of the unknown input signals acting on the estimation error system dynamics is achieved if the following conditions are satisfied:

$$\begin{aligned} (H_{uio}C - I)E &= 0 \\ T_{uio} &= I - H_{uio}C \\ F_{uio} &= A - H_{uio}CA - K_{uio}^1 C \\ K_{uio}^2 &= F_{uio}H_{uio} \end{aligned} \qquad (2\text{-}26)$$

The matrix K_{uio}^1 contains free design parameters that should be chosen to stabilise the observer dynamics matrix F_{uio} (e.g. the design can be achieved using multivariable pole placement). The choice of matrix K_{uio}^1 is not unique due to the multivariable degrees of design freedom. The remaining design freedom could, in principle be used e.g. to structure the design of the residual equation. The gain matrix K_{uio}^2 is used to de-couple the unknown input signal in the observer feedback. Once the unknown input distribution matrix E is known, then the matrix H_{uio} is determined from Eq. (2-26). Note that for $E = 0$, the observer design is identical to that of the standard Luenberger Observer with $K_{uio} = K_{uio}^1$ and with $K_{uio}^2 = 0$.

Hence, the state estimation error $e_x(t)$ becomes:

$$\dot{e}_x(t) = F_{uio}e_x(t) \qquad (2\text{-}27)$$

It can be seen that the state estimate $e_x(t)$ will approach zero asymptotically, i.e. $\hat{x}(t) \to x(t)$ if all eigenvalues of the matrix F_{uio} are stable. The necessary and sufficient conditions of UIO are given by: (Chen and Patton, 1999)

(i) $rank(CE) = rank(E)$

This means that the number of disturbances to de-couple cannot be greater than the number of measurements.

(ii) (C, A_1) is a detectable pair

where $A_1 = A - E(CE)^+ CA$ and $(CE)^+ = [(CE)^T CE]^{-1}(CE)^T$ denotes the pseudo-inverse of (CE).

If the condition (i) holds true the first relation in Eq. (2-26) is solvable and $H_{uio}^{*} = E(CE)^{+}$ is a special solution for the matrix H_{uio}. If there are no unknown inputs in the system i.e. $E = 0, T_{uio} = I,$ and $H_{uio} = 0$, the UIO becomes a simple full-order Identity Observer.

2.3.6 Robust FDI scheme based on UIO

The system in Eq. (2-22) with the presence of sensor and actuator faults can be described as:

$$\begin{aligned} \dot{x}(t) &= Ax(t) + Bu(t) + Ed(t) + Bf_a(t) \\ y(t) &= Cx(t) + f_s(t) \end{aligned} \qquad (2\text{-}28)$$

where $f_a \in \Re^m$ and $f_s \in \Re^p$ are sensor and actuator faults respectively. When state estimation is available, the UIO residual signal can be generated as:

$$\begin{aligned} r(t) &= y(t) - C\hat{x}(t) \\ &= (I - CH_{uio})y(t) - Cz_{uio}(t) \end{aligned} \qquad (2\text{-}29)$$

When this UIO is applied to the system of Eq. (2-28), the state estimation and residual signal become:

$$\dot{e}_x(t) = (A_1 - K_{uio}^1)e_x(t) + T_{uio}Bf_a(t) - K_{uio}^1 f_s(t) - H_{uio}\dot{f}_s(t) \qquad (2\text{-}30)$$

$$r(t) = Ce_x(t) + f_s(t) \qquad (2\text{-}31)$$

It should be noted that in the above equation that <u>*the disturbance effects are de-coupled*</u>. To detect actuator faults, it is necessary that $T_{uio}B \neq 0$. A fault in the i^{th} actuator will affect the residual if we make, $T_{uio}b_i \neq 0$ where b_i is the i^{th} column of input matrix B. However, the sensor faults have a direct effect on the residual.

To achieve fault isolation, a structured residual set can be used, as mentioned in Section 2.3.3.

For <u>*sensor fault isolation*</u> the Generalized Observer Scheme (Chen and Patton, 1999) is as shown in Figure 2-10. Each *Observer*$_j$, $j = 1, 2, \ldots, p$, is driven by all inputs and all outputs except the j^{th} output. Hence, the fault appearing on the j^{th} sensor will have no effect on *Observer*$_j$. In this scheme it is assumed that all actuators are fault-free.

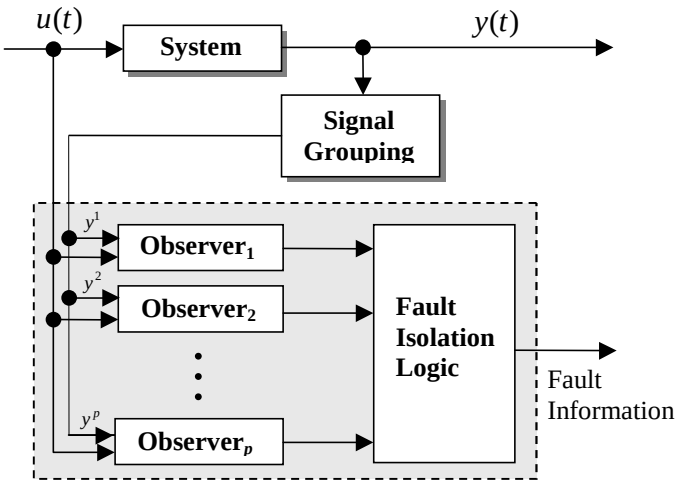

Figure 2-10: Sensor fault isolation scheme using UIO (Chen and Patton, 1999)

The system can be described by (Chen and Patton, 1999):

$$\begin{aligned} \dot{x}(t) &= Ax(t) + Bu(t) + Ed(t) \\ y^j(t) &= C^j x(t) + f_s^j(t) \\ y_j(t) &= c^j x(t) + f_{sj}(t) \end{aligned} \qquad (2\text{-}32)$$

where $c_j \in \Re^{1\times n}$ is j^{th} row of matrix C, $C^j \in \Re^{(p-1)\times n}$ is j^{th} row deleted from matrix C, y_j is j^{th} component of $y(t)$ and $y^j(t) \in \Re^{p-1}$ is the component deleted from the vector $y(t)$. A set of m UIOs can be constructed as:

$$\dot{z}_{uio}^j(t) = F_{uio}^j z_{uio}^j(t) + T_{uio}^j Bu(t) + K_{uio}^j y^j(t) \qquad \text{for} \quad j = 1, 2, \ldots, p \qquad (2\text{-}33)$$

and a set of residuals can be generated as:

$$r^j(t) = (I - C^j H_{uio}^j) y^j(t) - C^j z_{uio}^j(t) \qquad (2\text{-}34)$$

The parameter vectors must satisfy the following:

$$\begin{aligned} (H_{uio}^j C^j - I)E &= 0 \\ T_{uio}^j &= I - H_{uio}^j C^j \\ F_{uio}^j &= A - H_{uio}^j C^j A - K_{uio}^{1j} C^j \end{aligned} \qquad (2\text{-}35)$$

F_{uio}^j is designed to have stable eigenvalues and:

$$K_{uio}^{2j} = F_{uio}^j H_{uio}^j \qquad (2\text{-}36)$$

$$K_{uio}^j = K_{uio}^{1j} + K_{uio}^{2j} \qquad (2\text{-}37)$$

If the above conditions hold true, each residual r^j is driven by all inputs and all outputs but the j^{th} output, and it is insensitive to j^{th} sensor fault.

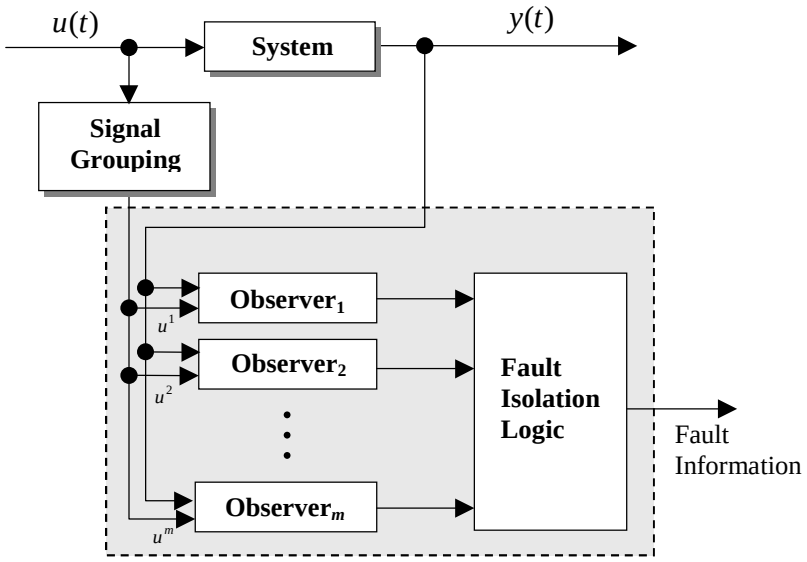

Figure 2-11: Actuator fault isolation scheme using UIO
[Chen and Patton, 1999]

For *actuator fault isolation*, the Generalized Observer Scheme (Chen and Patton, 1999) is as shown in (Figure 2-11).

As shown in the Figure 2-11, each *Observer*$_i$, $i = 1, 2, \ldots, m$, is driven by all outputs and all the inputs but the i^{th} input. All sensors are supposed to be fault-free and the system can be represented by the following equations:

$$\begin{aligned} \dot{x}(t) &= Ax(t) + B^i u^i + B^i f_a^i + b_i[u_i + f_{ai}(t)] + Ed(t) \\ &= Ax(t) + B^i u^i + B^i f_a^i + E^i d^i(t) \\ y(t) &= Cx(t) \end{aligned} \qquad (2\text{-}38)$$

where $i = 1, 2, \ldots, m$, u_i and $f_{ai}(t)$ and are the i^{th} components of control input u and actuator faults, respectively. $u^i \in \Re^{m-1}$ is obtained from control input u by deleting the i^{th} component of u_i, and $B^i \in \Re^{nx(m-1)}$ is obtained by deleting the i^{th} column of B and taking $b_i \in \Re^n$ as the i^{th} column of B.

The disturbance terms can be written as:

$$E^i = \begin{bmatrix} E & b_i \end{bmatrix}, \quad d^i(t) = \begin{bmatrix} d(t) \\ u_i(t) + f_{ai}(t) \end{bmatrix} \tag{2-39}$$

For the above system, a set of m unknown input observers can be constructed as:

$$\dot{z}^i_{uio}(t) = F^i_{uio} z^i_{uio}(t) + T^i_{uio} B^i u^i(t) + K^i_{uio} y(t) \qquad \text{for} \quad i = 1, 2, \ldots, m \tag{2-40}$$

and residuals can be generated as:

$$r^i(t) = (I - CH^i_{uio}) y(t) - C z^i_{uio}(t) \tag{2-41}$$

The parameter vectors must satisfy the following:

$$\begin{aligned} (H^i_{uio} C - I) E^i &= 0 \\ T^i_{uio} &= I - H^i_{uio} C \\ F^i_{uio} &= A - H^i_{uio} CA - K^{1i}_{uio} C \end{aligned} \tag{2-42}$$

The matrix F^i_{uio} is designed to have stable eigenvalues and:

$$K^{2i}_{uio} = F^i_{uio} H^i_{uio} \tag{2-43}$$

$$K^i_{uio} = K^{1i}_{uio} + K^{2i}_{uio} \tag{2-44}$$

If the above conditions hold true, each residual r^i is driven by all outputs and all inputs but the i^{th} input, and it is insensitive to i^{th} actuator fault. Other fault information e.g. frequency response data may be used to isolate such faults (Bogh, 1995).

Many good research studies have been done on residual based FDI using different methods for various applications. In particular, Chen and Patton (1999) provide a discussion on model-based residual FDI schemes, covering all aspects including basic principles and robustness issues. Note that in the residual generation problem, a fault is detected and its location identified, but there is no further information on the fault (e.g. its magnitude, fault type or characteristics, or the fault severity in the system).

2.4 Residual Generation Approaches to Fault Estimation

Figure 2-12 seeks to illustrate an idea from Blanke *et al* (2003) showing that the residual signal $r(t)$ can be processed further to develop an estimator of the fault $\hat{f}(t)$. Blanke *et al* (2003) refer to this operation as "residual evaluation" but the term *Residual Post-Processor* is preferred here as the term residual evaluation is usually reserved for

the decision-making process applied to detect that a fault has occurred (i.e. using a constant or variable *threshold* evaluation function).

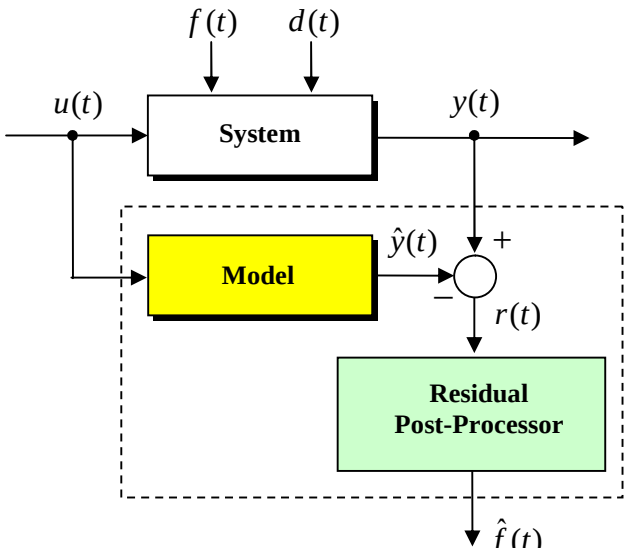

Figure 2-12: The structure of fault estimation (adapted from Blanke *et al*, 2003)

In the *ideal case* i.e. when the residual generator model is a perfect replica of the system dynamics, and when there are no exogenous disturbances acting on the system of Figure 2-12, [i.e. $d(t) = 0$] the generalized residual is expressed as [see Eq. (2-12)]:

$$\begin{aligned} r(s) &= \underbrace{[H_u(s) + H_y(s)G_u(s)]}_{\text{"0"}}u(s) + H_y(s)G_f(s)f(s) \\ &\approx H_y(s)G_f(s)f(s) \end{aligned} \qquad (2\text{-}45)$$

A "post-processing" operation may be applied to Eq. (2-45) to generate an estimate of $\hat{f}(t)$, corresponding to the ideal case.

The *non-ideal case*, when the term $[H_u(s) + H_y(s)G_u(s)] \neq 0$, corresponds to the fact that the residual $r(s)$ is also a function of a control-induced uncertainty $[H_y(s)\Delta_u(s)G_u(s)]u(s) \neq 0$ term and an exogenous disturbance term $[H_y(s)\Delta_d(s)G_d(s)]d(s) \neq 0$, where $d(s) = \mathcal{L}\{d(t)\}$ and $\mathcal{L}\{\}$ denotes the Laplace Transform of the continuous-time signal $\{.\}$ as follows (modified from Section 8.3.4 in Chen and Patton, 1999):

$$\begin{aligned} r(s) = {} & H_y(s)G_d(s)d(s) + H_y(s)G_f(s)f(s) \\ & + H_y(s)\Delta_d(s)G_d(s)d(s) + H_y(s)\Delta_f(s)G_f(s)f(s) \\ & + H_y(s)\Delta_u(s)G_u(s)u(s) \end{aligned} \qquad (2\text{-}46)$$

Following the above, the fault estimation problem then becomes one of de-convolution to remove from $r(s)$ the effects of: (a) the control signal-induced uncertainty and (b) the exogenous disturbances $d(s)$. These effects act together on the state estimation error $e_x(s)$.

This is, in principle, a starting point for generating a robust estimate $\hat{f}(t)$ of $f(t)$. Chen and Patton (1999) provide a detailed discussion of the significance of this potential approach in their Chapter 8 which is a development of using the residual generation of FDI.

2.5 Overview of Fault Estimation in Reconfigurable FTC

FDI approaches have an intrinsic capability to detect the presence or occurrence of fault (i.e. select one among two hypotheses of "normal system" or "faulty operation") and to distinguish the faulty component (i.e. select one among several hypotheses). This facilitates the development of the concept of reconfiguration in FTC e.g. to turn off the faulty component(s), and turn on some redundant non-faulty ones, so that the system can continue with acceptable operation. However, in some cases, fault accommodation mechanisms (based on fault estimation) are necessary, i.e. the control function is adapted based on the FDI in order to recover acceptable control of the system subject to bounded faults (Patton 1997, Blanke *et al*. 2000, Staroswiecki and Gehin 2000; Blanke *et al*, 2003).

When fault estimation is used, it is important to consider the FDD rather than the FDI problem (see definitions in Section 1.2) since the FDD problem includes fault estimation as a sub-task. However, it is still interesting to bear in mind the approach to fault estimation based on residual generation as described in Section 2.4.

Research on '*reconfigurable FTC systems*' has increased progressively since the initial research on restructurable control and self-repairing flight control systems of the early 1980s (Chandler, 1984; Eterno *et al*., 1985; Montoya, 1983). Reconfigurable FTC has attracted more and more attention in both industry and academic communities due to increased demands for safety, high system performance, productivity and operating efficiency in a wider engineering application, not limited to traditional safety-critical systems.

2.5.1 Linear Parameter Varying (LPV) approaches to fault estimation and control reconfiguration

In recent years, LPV modelling methods have become popular in the FDI and FTC community, especially for applications related to vehicle and aerospace control (Bokor and Balas, 2004).This approach is very valuable whenever nonlinear plants can be modelled as LPV systems with on-line measurable state-dependent parameters. The resulting system is known as "quasi-LPV" because the time-varying parameters are not exogenous independent variables but depend on the state space system see (Packard and Kantner, 1992; Rugh, 1991; Shamma and Athans, 1992); and surveys (Rugh and Shamma 2000; Leith and Leithead, 2000) for more details.

The first solution to the FDI design problem based on LPV systems was given in (Bokor, Szabó and Stikkel, 2002) and (Bokor and Balas, 2004). Recently, FDI and FTC for LPV systems have attracted many investigators (Bokor and Balas, 2004; Henry and Zolghadri, 2004; Casavola *et al*., 2005a, 2005ab, 2007; Weng *et al*., 2008; Zolghadri *et al* ., 2008; Issury and Henry, 2009; Henry *et al*., 2009; Cieslak *et al*., 2009).

Casavola *et al* (2007, 2008) in their work on LPV filter-design methods for FDI showed that the fault detection filter of Beard (1971) is essentially an H_∞ Luenberger observer synthesized by minimizing frequency conditions that ensure guaranteed levels of disturbance rejection and fault detection. They used the bounded real lemma (BRL) of Apkarian (1995) and the Separation Principle to formulate the fault detection filter problem as a convex LMI obtimization problem.

In another research direction, time-delay problems have received attention for more than two decades. It is well known that time delays are sometimes present in systems due to measurement or state variable transport delays, computational delays, or transmission lags, etc. Although the stability and control analysis of such systems has been investigated extensively in the control literature, there have also been several important studies on the application of robust FDI methods to systems with time-delay (Wu and Grigoriadis, 2001; Zhang P *et al*., 2002; Zhong *et al*., 2003, 2005; Mahmoud, 2004, Mohammadpour and Grigoriadis, 2006; Sun *et al*., 2007). Recent work by Weng *et al* (2008) considers the robust fault detection of LPV time-delay systems where the time-delay is unknown but with bounded variation rates. An LPV residual generator is

generated in terms of LMIs which can be obtained via efficient interior-point algorithms.

Returning to the active FTC problem posed in terms of sensor faults, the availability of a fault reconstruction signal means that if the sensor faults can be estimated/reconstructed, this information can be used directly to correct the sensor faults before they are used by the controller. The system can be tolerant to sensor faults without the need for controller reconfiguration or restructure. The severity of an actuator fault (actuator effectiveness) can be estimated, which is beneficial for controller reconfiguration (Zhang and Jiang, 1999 and 2002; Wu *et al*., 2000). This is one step further than the use of the residual-generation based FDI, but is applicable only to specific types of reconfigurable/FTC controllers. Some FTC controllers such as the methods proposed in (Wu *et al*., 2000; Zhang and Jiang, 1999, 2002) require estimates of the actuator efficiency to allow the FTC controller to tolerate the faults/failures. Rodrigues *et al*., (2005) proposed the design of an active FTC and polytopic UIO for system represented by a multi-model representation in which a polytopic UIO is synthesized for providing actuator fault estimation, and this estimation is used in a FTC strategy which schedule some predefined state feedback gains. The design of a static output feedback is later synthesized and developed through LMIs (Rodrigures *et al*., 2007).

Weng, Patton and Cui (2007) proposed an active FTC scheme based on a gain-scheduled form of H_∞ design under the assumption that the effects of faults on the system can be of affine parameter dependence. They developed a reconfigurable robust H_∞ controller using this approach and demonstrated the concepts on an interesting component fault in the double inverted pendulum. The controller is a function of the "fault effect factors" (as defined in Chen *et al* 1999 and Chen and Patton 2001). The fault effect factors are estimated on-line from the FDI residual vector. The effectiveness of the proposed method is demonstrated through the nonlinear double inverted pendulum system with a fault in the motor tachometer loop (Weng, Patton and Cui, 2007).

Later, a joint design of robust controller and fault estimator for LPV systems is presented which relates to earlier work by Jacobson and Nett (1991) [see also discussion in Section 2.3]. An LPV controller is also developed to generate both control signals and fault estimates. The proposed method is illustrated through an uncertain system with actuator faults (Weng, Patton and Cui, 2008).

2.5.2 Sliding mode approaches to fault estimation and control reconfiguration

Based on sliding mode theory there have been some interesting threads of development on the use of SMO designs for reconfigurable FTC systems. The first sliding mode observer designs used typical residual-based FDI ideas (Sreedhar *et al*., 1993; Yang and Saif, 1995; Hermans and Zarrop, 1996). The idea is to ensure that the sliding motion is broken when faults/failures occur in the system and a residual is generated containing information about the fault.

Edwards *et al* (1998, 2000) provided an alternative way of using variable structure and sliding mode theory to eliminate some of the restrictions in the design methods of fault estimation that found in the literature. Their work considered the application of a special SMO to the problem of FDI. Edwards and Spurgeon (1998) proposed the so-called *equivalent output injection* concept to reconstruct fault signals. However, in their early work they did not include and analysis of modelling uncertainty. The effects of uncertainty were taken account in Tan and Edwards (2003) and Jiang *et al*. (2004) demonstrating good capability for reconstructing/identifying faults. Not only do these design approaches have the ability to detect and isolate the source of the fault they also provide further information about the fault which can be used especially for controller reconfiguration.

The fault detection and identification based sliding mode approaches are developed later and several studies by Yan, Edwards and Spurgeon in the field of interconnected large-scale system are published [see the references therein e.g. Yan *et al*., 2003, 2004, 2006, and 2008]. Furthermore, the interesting papers in the field of fault tolerant flight control can be found in work by Alwi and Edwards (2005, 2006, and 2007) and Alwi *et al* (2009).

2.5.3 Alternative approaches to fault estimation and control reconfiguration

Although extensive individual research studies on FTC have been carried out, systematic concepts, design methods, and even terminology are still not yet standardized. During the last decade efforts have been made to unify some terminology (Isermann and Ballé, 1997; Blanke *et al*., 2000, 2001, 2003, 2006; Staroswiecki and

Gehin, 2001; Isermann, 2006; Mahmoud *et al*., 2003; Simani *et al*., 2003). However, in some cases further confusion has been caused by even introducing redundant terminology!

For historical reasons and problem complexity, most research studies on FDD and reconfigurable control have been carried out as two *separate* entities. These two subjects are investigated mostly by separate fields or groups of researchers. More specifically, most of the FDI/FDD techniques are developed as a diagnostic or monitoring tool, rather than as an integral part of FTC. As a result, some existing FDD methods may not satisfy the requirement for controller reconfiguration.

On the other hand, most of the research on reconfigurable control is carried out assuming the availability of a perfect FDD. Little attention has been paid to the analysis and design with the overall system structure and interaction between FDD and reconfigurable control. For example, from the viewpoint of reconfigurable controls design (Zhang, 2003, 2006); *"… (a) What are the needs and requirements for FDD? (b) What information can be provided by the existing FDD techniques for overall FTC designs? (c) How to analyze systematically the interaction between FDD and reconfigurable controls? (d) How to design the FDD and reconfigurable controls in an integrated manner for on-line and real-time applications? ..."*

Many other challenging issues concerning the integration of FDD and reconfigurable control still remain open for further research and development and some of these are considered in later chapters of this thesis.

2.6 Conclusion

This Chapter summarises briefly the types of faults and failures acting on actuators and sensors and its importance to FTC and FDI and reviews the model-based FDI approaches that rely on the concept of analytical redundancy. The main advantage of analytical redundancy based FDI as compared with the use of hardware redundancy is that extra hardware components are not required. However, there is always a model-reality mismatch between the process and the assumed model of the system dynamics. The Chapter also reviews the robust FDI methods that can be achieved using disturbance-decoupling techniques. The Chapter outlines the main issues of FDI based on analytical redundancy are the sensitivity of the FDI algorithm to model uncertainties and exogenous disturbance and the resulting robustness problem.

The Chapter focuses on the UIO as a special form of traditional state observer for FDI, applicable to uncertain systems. The treatment of this subject is useful in Chapter 7 which deals with the problem of FTC for nonlinear distributed systems.

The Chapter ends by outlining different methods of FTC and the mechanisms of achieving fault tolerance, ranging from robust control to control signal redistribution. The existing approaches to FDD and reconfigurable control are outlined.

Chapter 3.
Fault Estimation and Compensation based on Augmented State Approach

3.1 Introduction

With reference to the classification of FTC systems given in Figure 1-5 of Chapter 1, this Chapter is concerned with the *active* approach to FTC, involving *fault estimation*, *fault compensation* and *adaptive control*. The work of this Chapter only considers actuator faults since if the sensor fault can be estimated, this information can be used directly to correct the fault from sensor measurements before using by the controller. This avoids reconfiguring or restructuring the controller to be tolerant to sensor faults.

As stated in Chapter 2, there have been a number of studies on FTC based on fault estimation methods [see Wang and Daley, 1996; Wang *et al*., 1997; Wu *et al*., 2000; Zhang and Jiang, 1999 and 2002; Rodrigues *et al*., 2005, 2007]. Some of these studies deal with tolerance to sensor faults and others deal with the FTC problem for actuator faults (Jiang and Staroswiecki, 2002; Zhang, Jiang and Cocquempot, 2002).

Of these studies, the most relevant to the work of this thesis and which fit to the scheme of Figure 1-6 is that of Wang and Daley (1996, 1997). Wang *et al* (1997) proposed an FDD algorithm where an observer is constructed to diagnose the faults via the augmented error technique from *Model Reference Adaptive Control* (MRAC) in which

an observation error model is set up and used to compute the gains required in the fault estimation for actuator and sensor faults. The Wang *et al* (1997) approach has several weaknesses. The method requires *a priori knowledge* of the norms of the unknown inputs representing model uncertainties and/or the statistics of the process noise of the system, which are used to achieve stable fault estimation. Furthermore, the diagnostic strategy depends strongly on some *a priori* knowledge of spectral components of the unknown inputs in the frequency domain (Wang *et al*., 1997). It is unrealistic to need to depend on this information for real applications.

With this background in mind, the main contribution of this Chapter is to investigate the properties of an augmented state observer (ASO) approach for fault estimation in adaptive control for FTC, providing tolerance to actuator faults. The FTC controller is included within the structure of an augmented state system incorporating a full order state observer in which the actuator faults are estimated via additional state variables. The observer system for each case forms a part of the controller-compensator structure.

A useful topic outlined in Section 3.5 is the concept of the robustness of the ASO to modelling uncertainty. It is found that the adaptive mechanism compensates not only for the fault effect acting on the estimation error but also compensates for any unknown input signals. The consequence is that if the unknown input signals are decoupled from the ASO estimation error, the fault estimation will be improved but the control system is still affected by the uncertainty. It is demonstrated via the tutorial in Section 3.5 that a robust baseline controller is necessary for the FTC system to remain robust to uncertainty. It is also shown that by decoupling the uncertainty via the UIO approach, the fault estimates are very much improved but the sensitivity of the control loop to the modelling uncertainty still remains. Methods to achieve this robustness are not considered further for the ASO approach described in this Chapter.

It is important to note that the FTC schemes proposed in this Chapter are adaptive systems as the on-line fault estimates are updated continuously and the estimates are used to compensate the faults acting within the control channels. The compensation is achieved within the observer estimation error system with the consequence that the control signal has a time-varying component, the adaptive part of the control. This adaptive system cancels or reduces bounded uncertainty effects due to either faults or unknown input signals (or both together, for more discussion of this see Section 3.5) acting on the observer state estimation error. The use of on-line compensation means that the fault isolation task of FDI is not strictly required, although this function can be

useful. The possible value of including the full FDI function is discussed in the concluding statement of this Chapter. In this work the ideal residual generation problem of FDI, as described in Chapter 2, is replaced by *fault estimation*. In this Chapter the use of the residual generation process is obviated and attention is turned directly to the use of fault estimation embedded within the adaptive control scheme, to achieve good fault-tolerance.

There is no loss of generality in considering the process to be nonlinear. The procedures that are developed in this Chapter have the property of tolerance to faults. However, modelling uncertainties, for example as a consequence of applying the schemes to a nonlinear process will also be considered as "faults" in the adaptive process. Hence, both fault(s) and modelling uncertainties (unknown inputs) are estimated and compensated using an augmented state space structure with additional states corresponding to estimates of both faults and uncertainties. This property is discussed in Sections 3.4 and 3.5 using linear and nonlinear inverted pendulum example.

3.2 Augmented State Observer (ASO)

This approach is motivated by the work on estimation of unknown input directions for robust observer-based FDI by Chen and Patton (1999). In their work Chen and Patton used an augmented state observer to estimate the unknown input directions in a UIO observer description for robust unknown input de-coupling in FDI, based on both state observer and Kalman filter descriptions (Chen and Patton, 1996). The original idea was to estimate the unknown input direction parameters. Later Patton *et al* (2008a, 2009) extended this idea to the problem of fault(s) estimation to enhance the discrimination of some faults against other faults for the purpose of robust fault isolation applied to robust FDI of the Mars Express satellite system.

The work described below constitutes an original development of the use of an extended observer for unknown input estimation within the framework of an adaptive control scheme for fault compensation, the ASO. The approach has wide application to fault compensation, although this study focuses on the friction compensation control problem.

Hence, in this work the ASO forms an intrinsic part of an estimator-controller compensation mechanism which is quite different from the earlier studies based on Chen and Patton (1996, 1999). The details involved in the development of the ASO approach to actuator fault estimation are given prior to developing the mathematical description and stability of the complete ASO FTC compensator in Section 3.3.

The ideas of the ASO for fault estimation are now developed, based on the starting concept of actuator faults applied within a linear system.

Consider a state space representation of a linear system with actuator faults (Chen and Patton, 1999):

$$\begin{aligned} \dot{x}(t) &= Ax(t) + Bu(t) + F_a f_a(t) \\ y(t) &= Cx(t) \end{aligned} \qquad (3-1)$$

where: $x(t) \in \Re^n$ is the state vector, $y(t) \in \Re^p$ the output observation vector, $u(t) \in \Re^m$ the input control vector and F_a is the fault distribution matrix. (A, B) is a controllable pair with appropriate dimensions. Likewise (C, A) is an observable pair.

A full-order state observer for the system of Eq. (3 - 1) , driven by the outputs $y(t)$ can be designed with the following structure:

$$\begin{aligned} \dot{\hat{x}}(t) &= A\hat{x}(t) + BK_x\hat{x}(t) + L_x[y(t) - C\hat{x}(t)] \\ &= (A + BK_x)\hat{x}(t) + L_xC[x(t) - \hat{x}(t)] \end{aligned} \qquad (3-2)$$

where: $K_x \in R^{m \times n}$ is the feedback gain matrix obtained by a linear multivariable pole-placement state feedback design and $L_x \in R^{n \times p}$ are the observer gains to be designed [see ***Proposition 3.1*** and ***Theorem 3.1***].

Defining the state estimation error as $e_x(t) = x(t) - \hat{x}(t)$ so that:

$$\dot{e}_x(t) = (A - L_xC)e_x(t) + F_a f_a(t) \qquad (3-3)$$

This error state system is corrupted by the fault term $F_a f_a(t)$.

In this new contribution, the goal of a compensating observer-controller mechanism is to compensate for the term $F_a f_a(t)$. An ideal solution would be to combine the state feedback controller for the system of Eq. (3 - 1) with the state observer using a "actuator fault accommodating" controller of the form:

$$u(t) = \underbrace{K_x \hat{x}(t)}_{u_x} + \underbrace{K_a \hat{f}_a(t)}_{u_a} \qquad (3-4)$$

where $K_a \in R^{m \times m}$ is the actuator fault compensation gain to be designed.

The control signal $u(t)$ is sought to stabilise the fault-corrupted system Eq. (3 - 1) around the system equilibrium in the presence of unwanted actuator fault signals, where $u_x(t)$ is the control of the nominal system (fault-free case), and $u_a(t)$ is the compensating control to be added to compensate for the actuator fault $f_a(t)$ effect on the closed-loop system. The signals $\hat{x}(t)$ and $\hat{f}_a$ are state and actuator fault estimations, respectively.

3.3 ASO Strategy for Actuator Fault Estimation

The fault compensating observer-controller for the system of Eq. (3 - 1) can be achieved by replacing $u(t)$ in Eq. (3 - 1) with Eq. (3 - 4). Hence, the new state estimate feedback closed-loop system becomes:

$$\begin{aligned} \dot{x}(t) &= Ax(t) + B[K_x \hat{x}(t) + K_a \hat{f}(t)] + F_a f_a(t) \\ &= Ax(t) + B[u_x(t) + u_a(t)] + F_a f_a(t) \\ &= Ax(t) + Bu_x(t) + Bu_a(t) + F_a f_a(t) \end{aligned} \qquad (3-5)$$

In order to compensate the actuator fault in Eq. (3 - 1) , the control $u_a(t)$ must satisfy:

$$Bu_a(t) + F_a f_a(t) \approx 0 \qquad (3-6)$$

The solution of Eq. (3 - 6) can be obtained by:

$$u_a(t) \approx -\underbrace{B^+ F_a}_{K_a} \hat{f}_a(t) \qquad (3-7)$$

where B^+ is the *pseudo-inverse* of the matrix B. However, since $f_a(t)$ is an actuator fault, it is of interest here to let $F_a = B$ [i.e. $K_a = B^+ B$]. This assumption is retained throughout this Chapter.

It is hypothesized here that a suitable estimator $\hat{f}_a(t)$ for the actuator fault $f_a(t)$ can now be determined from the integral of the observer estimation error $e_x(t)$ as follows:

$$\dot{\hat{f}}_a(t) = L_a[y(t) - C\hat{x}(t)] \qquad (3-8)$$

where: $L_a \in R^{m\times p}$ are the observer gains to be designed [see ***Proposition 3.1*** and ***Theorem 3.1***].

The adaptive compensation control signal is calculated from Eq. (3 - 4) based on the estimates $\hat{x}$ and $\hat{f}_a$ and hence the solution must now be posed in terms of an *Augmented State Observer* (ASO) as follows:

Proposition 3.1

Following the new closed-loop system in Eq. (3 - 5) and the observer in Eq. (3 - 2), here the new error state $e_x(t) = x(t) - \hat{x}(t)$ in Eq. (3 - 3) can be written as:

$$\begin{aligned} \dot{x}(t) - \dot{\hat{x}}(t) &= A[x(t) - \hat{x}(t)] - L_x[y(t) - \hat{y}(t)] + BK_a\hat{f}_a(t) + F_a f_a(t) \\ \dot{e}_x(t) &= (A - L_xC)e_x(t) + BK_a\hat{f}_a(t) + F_a f_a(t) \end{aligned} \qquad (3-9)$$

In order to estimate the magnitude of the fault it is necessary to combine the two estimators of Eqs.(3 - 9) and (3 - 8) into one augmented system structure as follows:

$$\begin{bmatrix} \dot{e}_x(t) \\ \dot{\hat{f}}_a(t) \end{bmatrix} = \begin{bmatrix} A - L_xC & BK_a \\ L_aC & 0 \end{bmatrix}\begin{bmatrix} e_x(t) \\ \hat{f}_a(t) \end{bmatrix} + \begin{bmatrix} F_a \\ 0 \end{bmatrix} f_a(t) \qquad (3-10)$$

Eq. (3-10) can be re-arranged as:

$$\underbrace{\begin{bmatrix} \dot{e}_x(t) \\ \dot{\hat{f}}_a(t) \end{bmatrix}}_{\dot{\tilde{e}}(t)} = \left(\underbrace{\begin{bmatrix} A & BK_a \\ 0 & 0 \end{bmatrix}}_{A_0} - \underbrace{\begin{bmatrix} L_x \\ -L_a \end{bmatrix}}_{L_0}\underbrace{\begin{bmatrix} C & 0 \end{bmatrix}}_{C_0} \right)\underbrace{\begin{bmatrix} e_x(t) \\ \hat{f}_a(t) \end{bmatrix}}_{\tilde{e}(t)} + \underbrace{\begin{bmatrix} F_a \\ 0 \end{bmatrix}}_{F_0} f_a(t) \qquad (3-11)$$

Eq. (3-11) can be written in compact notation as:

$$\dot{\tilde{e}}(t) = (A_0 - L_0C_0)\tilde{e}(t) + F_0 f_a(t) \qquad (3-12)$$

Since the actuator faults $f_a(t)$ are bounded, one can always find a positive number β such that $\beta > \|f_a(t)\|$.

Let $\varepsilon \subset \Re^n$ be a bounded set, and then the following definition can be made.

Definition 3.1

The solution of $\tilde{e}(t)$ to the uncertainty system Eq. (3-12) is said to be ultimately bounded with respect to the set of ε if:

- On any finite interval the solution remains bounded, i.e. if $\|\tilde{e}(t_0)\| < \delta$ then $\|\tilde{e}(t)\| < d(\delta)$ for any $t \in [t_0, t_1]$
- In finite time the solution $\tilde{e}(t)$ enters the bounded set ε and remains there for all subsequent time.

The set ε is usually an acceptably small neighborhood of the origin and the concept is often termed *practical stability* (Edwards and Spurgeon, 1998).

Theorem 3.1

Consider the closed-loop system described by Eqs. (3-2) and (3-12) and assume that the pair (A, B) is controllable and the pair (C_0, A_0) is observable. If the observer gains L_0 in (3-12) are chosen such that there exists a S.P.D. matrix $P \in R^{(m+p)x(m+p)}$ satisfying:

$$P(A_0 - L_0C_0) + (A_0 - L_0C_0)^T P = -\alpha_{aso}\, \beta\, I \qquad (3\text{-}13)$$

where $\alpha_{aso} > 0$ and $\beta \geq \|f_a\|$ then $\tilde{e}(t)$ will be contained in a bounded region around the equilibrium independent of $e_x(0), \hat{x}(0)$ and $f_a(0)$. Furthermore, if the controller gains K_x are chosen such that the matrix $A + BK_x$ is *Hurwitz* then $\hat{x}(t)$ will also be contained in a bounded region around the equilibrium independent of $e_x(0), \hat{x}(0)$ and $f_a(0)$, meaning that the closed-loop system Eqs. (3-2) and (3-12) is *practically stable*.

Proof of Theorem 3.1

Consider a candidate Lyapunov function $V = \tilde{e}^T P \tilde{e}$ with its time derivative along trajectories of Eq. (3-12) as:

$$\begin{aligned} \dot{V} &= \tilde{e}^T P(A_0 - LC_0)\tilde{e} + \tilde{e}^T (A_0 - LC_0)^T P\, \tilde{e} + 2\tilde{e}^T P F_0\, f_a \\ &= \tilde{e}^T \underbrace{[P(A_0 - LC_0) + (A_0 - LC_0)^T P]}_{-\alpha_{aso}\, \beta\, I} \tilde{e} + 2\tilde{e}^T P F_0\, f_a \end{aligned} \qquad (3\text{-}14)$$

Substitution of Eq. (3-13) and $\beta \geq \| f_a \|$ into Eq. (3-14) results in:

$$\begin{aligned}\dot{V} &\le -\beta\alpha_{aso}\|\tilde{e}\|^2 + 2\beta\left\|\tilde{e}^T P F_0\right\| \\ &\le -\beta(\alpha_{aso}\|\tilde{e}\|^2 + 2\left\|\tilde{e}^T P F_0\right\|)\end{aligned} \tag{3-15}$$

Using the *Cauchy-Schwarz* inequality (Steele, 2004):

$$\left\|\tilde{e}^T P F_0\right\| = \sqrt{\tilde{e}^T P F_0 F_0^T P \tilde{e}} \le \sqrt{\lambda_{\max}(P F_0 F_0^T P)}\|\tilde{e}\| \tag{3-16}$$

where $\lambda_{\max}(\cdot)$ denotes the largest eigenvalue of the matrix defined in ( ).

Define:

$$\delta = \frac{2}{\alpha_{aso}}\sqrt{\lambda_{\max}(P F_0 F_0^T P)} \tag{3-17}$$

Then from Eqs (3-16) and (3-17) it follows that:

$$\begin{aligned}\dot{V} &\le -\beta\,\alpha_{aso}\|\tilde{e}\|^2 + 2\beta\sqrt{\lambda_{\max}(P F_0 F_0^T P)}\|\tilde{e}\| \\ &\le -\beta\,\alpha_{aso}\|\tilde{e}\|^2 + \alpha\,\beta\frac{2}{\alpha_{aso}}\sqrt{\lambda_{\max}(P F_0 F_0^T P)}\|\tilde{e}\| \\ &\le -\beta\,\alpha_{aso}\|\tilde{e}\|\left(\|\tilde{e}\| - \frac{2}{\alpha_{aso}}\sqrt{\lambda_{\max}(P F_0 F_0^T P)}\right) \\ &\le -\beta\,\alpha_{aso}\|\tilde{e}\|(\|\tilde{e}\| - \delta)\end{aligned} \tag{3-18}$$

Define a region $D_\delta = \{\tilde{e} : \|\tilde{e}\| < \delta\}$. Following Eq. (3-18) it can be concluded that $\dot{V} < 0 \;\; \forall \tilde{e} \notin D_\delta$. Therefore, there exists a time $t_0 > 0$ such that $\tilde{e}(t) \in D_\delta, \;\; \forall\, t > t_0$ independent of $e_x(0), \hat{x}(0)$ and $f_a(0)$, hence proving the first part of ***Theorem 3.1***. In other words, $\tilde{e}$ is ultimately bounded with respect to D_δ.

Since the matrix $A + BK_x$ is *Hurwitz*, the subsystem Eq. (3 - 2) is a stable linear system subject to inputs $e_x(t)$ that are bounded by D_δ around the origin. Therefore, $\hat{x}(t)$ will also be bounded around the origin and hence the last part of ***Theorem 3.1*** is proven. ■

Note that the controllability and observability conditions guarantee the existence of the controller gain K_x and observer gains L_0 satisfying the conditions in ***Theorem 3.1***. The magnitude of the steady state errors are defined by the region D_δ, which can be decreased by enlarging the design parameter α_{aso} as shown in Eq. (3-17).

Theorem 3.1 is also applicable for linear systems subject to unknown but bounded input disturbances/faults, i.e. it provides a bound for the input disturbances/faults.

3.4 Combine On-Line Fault Estimation and Compensation

Section 3.3 derives the condition for stability for the ASO used for actuator fault estimation in terms of a bound on the fault signal, in terms of the observer gain matrix L_0 of Eq. (3-12). This has been obtained from the use of ***Theorem 3.1*** and its proof. It is necessary now to consider the problem of joint fault and state estimation.

Consider again the Eqs (3 - 2) and (3 - 8) , these must be combined into one system as follows: [i.e on-line actuator fault estimation and compensation can be implemented as the closed-loop system depicted in Figure 3-1].

$$\begin{aligned}\begin{bmatrix}\dot{\hat{x}}(t)\\ \dot{\hat{f}}_a(t)\end{bmatrix} &= \begin{bmatrix}A+BK_x & 0\\ 0 & 0\end{bmatrix}\begin{bmatrix}\hat{x}(t)\\ \hat{f}_a(t)\end{bmatrix}+\begin{bmatrix}L_x\\ L_a\end{bmatrix}[y(t)-C\hat{x}(t)]\\ &= \begin{bmatrix}(A+BK_x-L_xC) & 0\\ -L_aC & 0\end{bmatrix}\begin{bmatrix}\hat{x}(t)\\ \hat{f}_a(t)\end{bmatrix}+\begin{bmatrix}L_x\\ L_a\end{bmatrix}y(t)\\ &= \left(\underbrace{\begin{bmatrix}A+BK_x & 0\\ 0 & 0\end{bmatrix}}_{A_x}-\underbrace{\begin{bmatrix}L_x\\ L_a\end{bmatrix}}_{L}\underbrace{[C\quad 0]}_{C_x}\right)\underbrace{\begin{bmatrix}\hat{x}(t)\\ \hat{f}_a(t)\end{bmatrix}}_{\tilde{\hat{x}}}+\underbrace{\begin{bmatrix}L_x\\ L_a\end{bmatrix}}_{L}y(t)\end{aligned} \qquad (3\text{-}19)$$

Eq. (3-19) can be re-written in simplified as:

$$\dot{\tilde{\hat{x}}} = (A_x - LC_x)\tilde{\hat{x}} + Ly \qquad (3\text{-}20)$$

The solution of Eq. (3-20) provides an estimate $\hat{f}_a(t)$ of the fault magnitude $f_a(t)$, which is the *last* component of the augmented state vector $\tilde{\hat{x}}(t)$, and a new control law as described in Eq. (3 - 4) is added to the nominal system in order to remove or reduce the actuator fault effects on the system [see Figure 3-1]

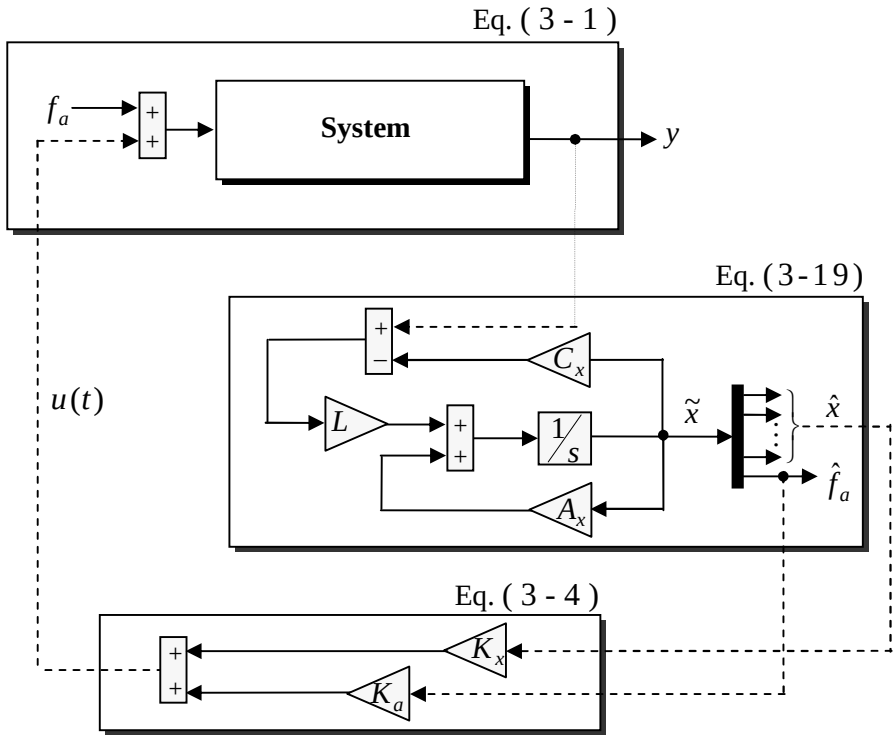

Figure 3-1: The ASO fault estimation and compensation scheme

Figure 3-1 shows the concept of the on-line observer-based adaptive controller strategy for on-line estimation and compensation in which the matrix parameters: A_x, C_x, K_x, K_a and L are determined and the stability of both the observer and control elements of this adaptive system as derived in Section 3.3.

3.4.1 Friction compensation case study

The control of systems that involve friction in the movement of mechanical components presents interesting challenges (Armstrong-Hélouvry *et al*., 1994; Olsson *et al*, 1998; Armstrong and Chen, 2008). The tendency in recent years has been to go down a road of more and more detailed modelling of the friction phenomena in order to evoke an on-line friction compensation procedure, thereby attempting to cancel out the effect of the friction in the feedback loop (Bona and Indri, 2005).

This is a natural development of the modelling requirements in robust and nonlinear control and estimation. Despite several important studies, the friction modelling problem remains a very difficult challenge, mainly because of the uncertain dynamic characteristics involved and that friction characteristics change over time due to, for example wear, temperature and humidity (Bona and Indri, 2005). From a control point of view, friction compensation strategies that require a detailed model of the friction

characteristics have limitations arising from non-smooth nonlinearity and the fact that friction modelling remains an imprecise subject, thereby resulting in a robustness problem. The new contributions are summarised as:

(1) The friction forces acting in a mechanical system can be viewed as "specific type of fault signals", facilitating the use of methods of fault estimation arising from FDI theory (Chen and Patton, 1999), thereby obviating completely the use of complex friction modelling.

(2) Estimates of friction forces can be used within an FTC structure to provide on-line friction compensation. The friction estimates provide important robustness indicators for the friction compensator design.

(3) FTC schemes for friction compensation can be developed which are adaptive in the sense of depending on bounded estimates of the friction forces.

These requirements are satisfied when the friction force itself is considered as *a specific type of fault*. The friction force may be tolerable in the feedback system, allowing acceptable performance. However, if the system performance is degraded to a significant extent, exhibiting limit cycle oscillation, action needs to be taken either to remove the "faulty" component (e.g. replace it or giving lubricated bearing) or to invoke an automatic fault-tolerant strategy in the control system. It is reasonable to consider the friction force as a fault as the friction in a mechanical system is an unwanted phenomenon in the majority of real systems (Patton *et al*., 2008b).

According to Eq. (3 - 1) when the system subject to friction forces acting in up to m of the input channels independently. For example, if this approach is extended to a multiple-joint actuated robot system, more than one friction signal would then be estimated and compensated so that for this general case:

$$\begin{aligned} \dot{x}(t) &= Ax(t) + B[u(t) - f_{fric}(t)] \\ y(t) &= Cx(t) \end{aligned} \qquad (3\text{-}21)$$

where: $f_{fric} = [f_{fric}^{1}, \ldots, f_{fric}^{m}]^{T}$ represents the friction forces acting on the system. Hence, the nonlinear friction force that reduces the effective force for a given control input can be represented as an actuator fault. The proposed friction compensation methods do not require a model of the nonlinear friction forces $f_{fric}(t)$. *The methods only require that the friction forces should be bounded, which is a valid assumption*

since the nonlinear friction force is bounded by its static friction level (Armstrong-Hélouvry *et al*., 1994; Olsson *et al*, 1998).

3.4.2 Inverted pendulum example

To illustrate the above discussion a tutorial example of the inverted pendulum with a cart is used here as friction compensation problem in the absence of friction model (see Figure 3-2). The cart is linked by a transmission belt which is used to drive the wheel via a DC motor to rotate the pendulum into vertical position in the vertical plane by force control $u(t)$ on the cart. The nonlinear equations of motion including friction on the cart are:

$$\begin{aligned}&(M+m)\ddot{x}_p + F_x\dot{x}_p + m(\ddot{\theta}_p\cos\theta_p - \dot{\theta}_p^2\sin\theta_p) = u(t) - f_{fric}(\dot{x}_p),\\ &J\ddot{\theta}_p + F_\theta\dot{\theta}_p - mlg\sin\theta_p + ml\ddot{x}_p\cos\theta_p = 0\end{aligned} \qquad (3\text{-}22)$$

where: x_p, θ_p are the cart position and the pendulum angle, respectively. The system parameters are given in Table 3-1.

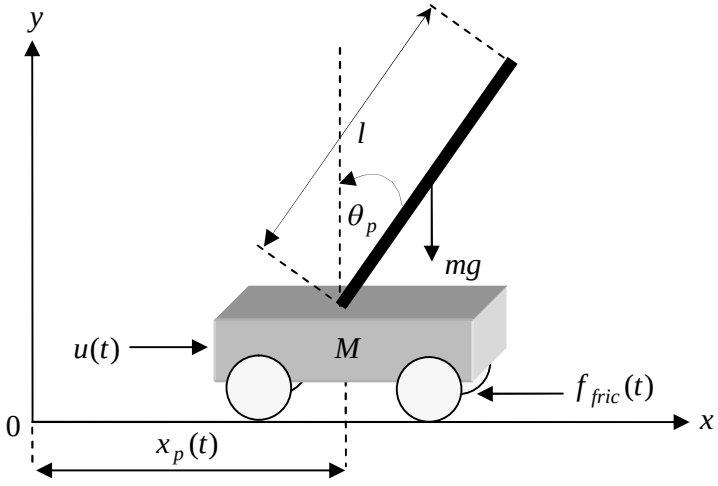

Figure 3-2: Inverted pendulum system

Constants	M	m	J	l	F_x	F_θ	g
Values	3.2	0.535	0.062	0.365	6.2	0.009	9.807
Units	Kg	Kg	Kg*m^2	m	Kg/s	Kg*m^2	m/s^2

Table 3-1: The inverted pendulum parameters

For simulation purposes the friction force acting on the cart is described by the discontinuous *Stribeck friction model* (Putra *et al*, 2004):

$$f_{fric} = g(\dot{x}_p)sign(\dot{x}_p), \quad \text{where } sign(x_p) \in \begin{cases} \{-1\} & \text{if} \quad \dot{x}_p < 0 \\ [-1,1] & \text{if} \quad \dot{x}_p = 0 \\ \{1\} & \text{if} \quad \dot{x}_p > 0 \end{cases} \qquad (3\text{-}23)$$

$g(\dot{x}_p) = F_c + (F_s - F_c)\exp(-\left|\dot{x}_p\right| / v_s)^{\delta_s}$ is the Stribeck friction function with F_c and F_s are the Coulomb and Static friction levels, respectively and $v_s, \delta_s > 0$ are the Stribeck velocity and shaping parameters, respectively. In the friction simulation, the following parameter values are used:

$$F_c = 5\ N,\ v_s\ = 0.15\ \text{ms}^{-1} \ \text{ and } \delta_s = 1.22$$

A linearization of the left hand side of Eq. (3-22) has been made around the equilibrium point: $\dot{x}_p = \dot{\theta}_p = \theta_p = 0$. These results in the system triple corresponding to single input $u(t)$ and measurements $y(t) \in \Re^3$. The three measurements (cart position, pendulum angular position and cart velocity) replicate the measurements of the laboratory system.

$$A = \begin{bmatrix} 0 & 0 & 1 & 0 \\ 0 & 0 & 0 & 1 \\ 0 & -1.9333 & -1.9872 & 0.0091 \\ 0 & 36.9771 & 6.2589 & -0.1738 \end{bmatrix}, B = \begin{bmatrix} 0 \\ 0 \\ 0.3205 \\ -1.0095 \end{bmatrix}, C = \begin{bmatrix} 1 & 0 & 0 & 0 \\ 0 & 1 & 0 & 0 \\ 0 & 0 & 1 & 0 \end{bmatrix},$$

It should be noted that in this study, it is assumed that only the position measurement of the cart (x_p) and the angle of the pendulum (θ_p) are available for the feedback loop, i.e. $C = \begin{bmatrix} 1\,0\,0\,0 \\ 0\,1\,0\,0 \end{bmatrix}$. The state feedback controller gain K_x is designed by placing the closed-loop pole at: -4.2,-4.4, -4.6 and -4.8, and given by:

$$K_x = [184.10\ \ 365.71\ 123.66\ \ 63.86]$$

The friction compensation gain is set to $K_a = 1$, which is appropriate for this example if $F_a\ =\ B$ and $(B^T B)^{-1} B^T F_a\ = 1$ [see Eq. (3 - 7)].

It can be verified that the pair (C_0, A_0) as in Eq. (3-12) is observable:

$$A_0 = \begin{bmatrix} 0.0000 & 0.0000 & 1.0000 & 0.0000 & 0.0000 \\ 0.0000 & 0.0000 & 0.0000 & 1.0000 & 0.0000 \\ 0.0000 & -1.9333 & -1.9872 & 0.0091 & -0.3205 \\ 0.0000 & 36.9771 & 6.2589 & -0.1738 & 1.0095 \\ 0.0000 & 0.0000 & 0.0000 & 0.0000 & 0.0000 \end{bmatrix}$$

$$C_0 = \begin{bmatrix} 1.0000 & 0.0000 & 0.0000 & 0.0000 & 0.0000 \\ 0.0000 & 1.0000 & 0.0000 & 0.0000 & 0.0000 \end{bmatrix}$$

The observer gains L_0 which correspond to eigenvalues of $(A_0 - L_0 C_0)$ placed at -12, -16, -13, -15 and -14 [satisfying condition Eq. (3-13)], are given by:

$$L_0 = \begin{bmatrix} 28.8285 & -3.5192 \\ -2.6301 & 39.0105 \\ 216.3432 & -92.7549 \\ -67.1367 & 513.3875 \\ -1705.2120 & 2119.5169 \end{bmatrix}$$

Simulation results for given initial values: $x(0) = col(1.1 \quad -1.1 \quad 0 \quad 0)$ are shown in Figure 3-3 and Figure 3-4.

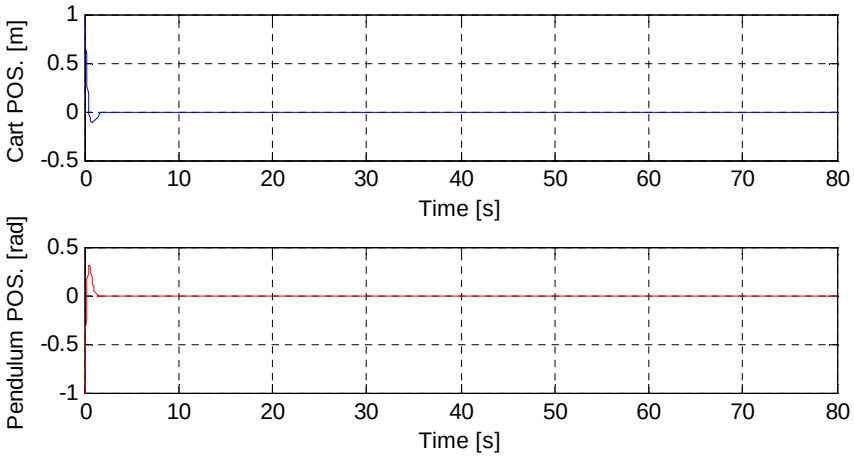

Figure 3-3: Nonlinear inverted pendulum system output responses (without friction force)

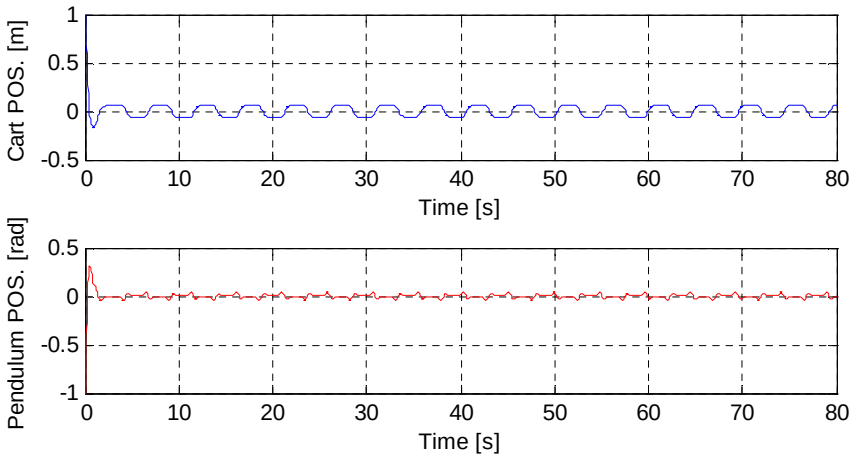

Figure 3-4: Nonlinear inverted pendulum system output responses (with friction force $F_s = 2.50\ N$)

Figure 3-5 shows the friction force and its estimate with the static friction level $F_s = 1.25\ N$ and with low estimation errors. Figure 3-6 demonstrates the on-line friction force estimation and compensation described in Section 3.4. It can be seen that before t = 40*s* (i.e the compensator is switched 'OFF') the inverted pendulum system exhibits limit cycle oscillation around the vertical equilibrium point (the origin). This is because the cart, which is affected by the friction, exhibits stick-slip (see ***Definition 3.1***) motion of dynamic friction. However, after t = 40*s*, the limit cycle oscillation is reduced to a very small neighbourhood around the equilibrium point as described in ***Theorem 3.1***. In this case the amplitude of the pendulum angle is less than 5*mrad* and the amplitude of the cart stick-slip motion is less than 2.5 *mm*. The limit cycle arises as a consequence of the friction phenomena and static and kinetic friction forces that tax or oppose the control force friction force, causing sudden change in position motion of the cart and pendulum. The control signal (force) on the cart increases to overcome the *stick-slip* and static friction force, causing a sudden jerk of the cart in one direction. As the cart moves beyond the reference position the feedback error changes sign causing the cart bearing to stick once again, the force from the control builds up causing a sudden jerk in the opposite direction. The process repeats giving a stable limit cycle oscillation.

***Definition 3.1*:** Stick-slip phenomenon

Patek, 2001 defined a stick-slip motion as '… *Stick-slip (or "slip-stick") refers to the phenomenon of a spontaneous jerking motion that can occur while two objects are sliding over each other. Stick-slip is caused by the surfaces alternating between sticking*

to each other and sliding over each other, with a corresponding change in the force of friction. Typically, the static friction coefficient between two surfaces is larger than the kinetic friction coefficient. If an applied force is large enough to overcome the static friction, then the reduction of the friction to the kinetic friction can cause a sudden jump in the velocity of the movement …'

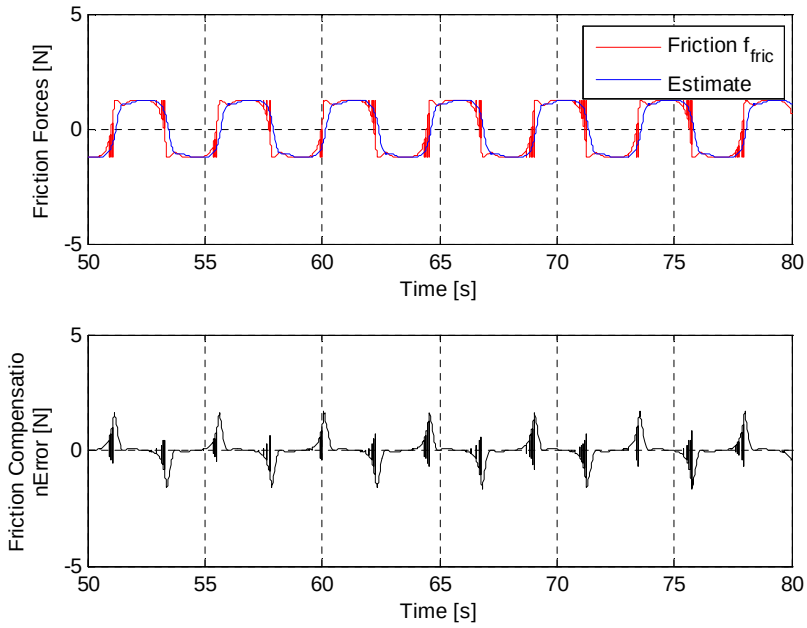

Figure 3-5: Comparison of the friction force (f_{fric}) and its estimate ($\hat{f}_{fric}$) (with F_s = 1.25 N)

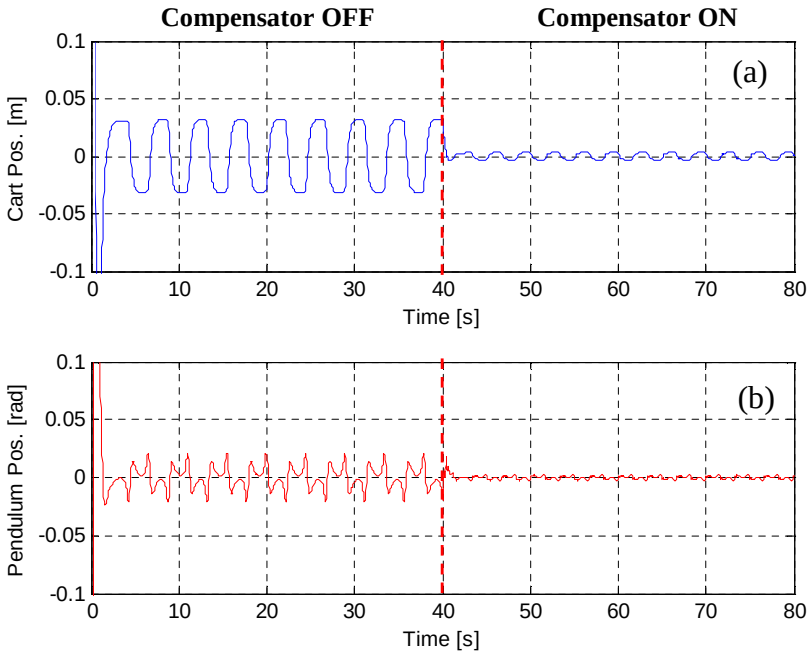

Figure 3-6: ASO simulation results (with F_s = 1.25 N) for friction compensation activated at time t = 40s.

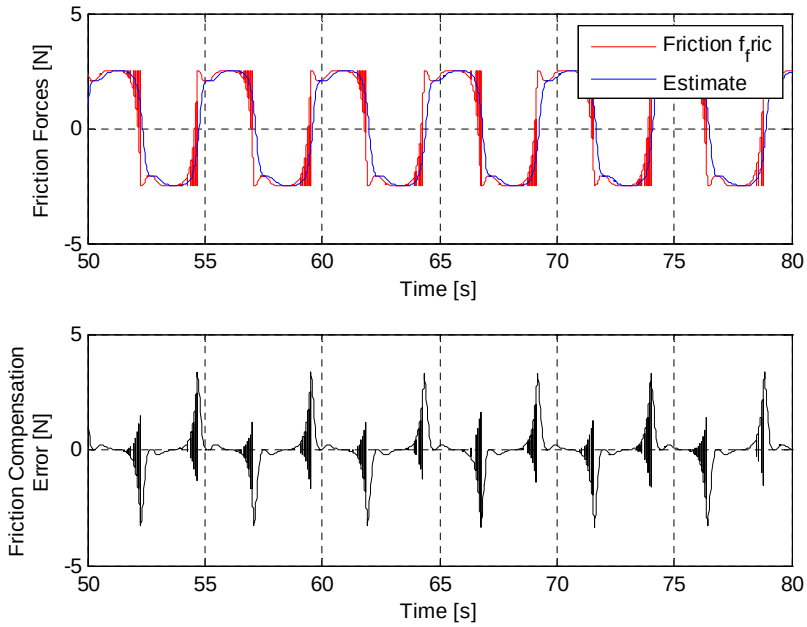

Figure 3-7: Comparison of the friction force (f_{fric}) and its estimate ($\hat{f}_{fric}$) (with F_s = 2.50 N)

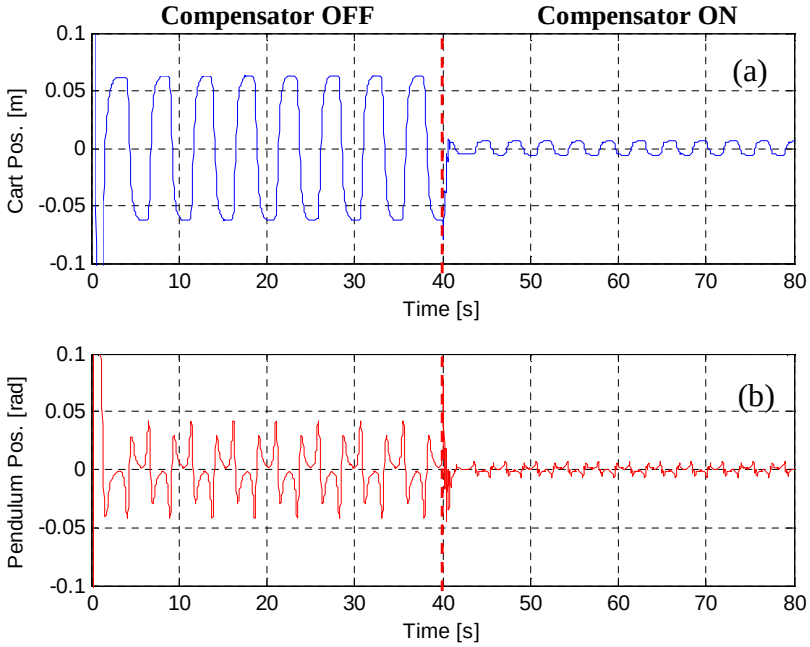

Figure 3-8: ASO simulation results (with F_s = 2.50 N) for friction compensation activated at time t = 40s.

Figure 3-7 and Figure 3-8 show the case when the static friction level is increased to $F_s = 2.50\ N$, the simulation results show that friction force estimation and compensation are still working very well with the increase of static friction magnitude. As discussed in Section 3.3 as long as the friction force is bounded the friction

estimation and compensation will work well. This leads to adaptive control in the sense of fault estimation and compensation in nonlinear system as an active FTC property.

Section 3.5 investigates the robustness of the ASO method based on the notion that modeling uncertainty and friction fault effects can compete in the compensation mechanism, since they may act at the same point in the system. The accuracy of the fault estimation can also be affected by the presence of modeling uncertainty or additional disturbance. The most obvious way to illustrate the robustness and FTC aspects of the ASO is to apply the ASO to a linear system with added nonlinear Stribeck friction. The separate and combined effects of the friction and modeling uncertainty are thus applied through the model example to illustrate the difference between the FTC action and the effect of modeling uncertainty and need for improved robustness of the controller.

3.5 Actuator Fault Estimation with Disturbance Decoupling

The aim here is to investigate the issue of designing fault estimation systems that are robust in the sense of decoupling the unknown input in the models. The main contribution is to incorporate the concept of *unknown input decoupling* described by Chen and Patton (1999) for diagnostic observers and outlined in Section 2.3.6, to achieve robustness in FDI. This is different from the work of Wang *et al* (1997), in which the norm of the unknown input vector is not *required* in the design of the proposed diagnostic algorithm. That is, the observation error, which is used to construct the diagnostic algorithm, does not depend on the effect of the unknown input.

Consider the system with actuator faults in Eq. (3 - 1) with the presence of an unknown input term $Ed(t)$:

$$\begin{aligned} \dot{x}(t) &= Ax(t) + Bu(t) + F_a f_a(t) + Ed(t) \\ y(t) &= Cx(t) \end{aligned} \qquad (3\text{-}24)$$

where: $E \in \Re^{nxq}$ is a full rank constant matrix, $d(t) \in \Re^q$ is the unknown input signal vector representing model uncertainties or/and input noise acting in the state space system. It is assumed that the pair (C, A) is observable and that the output vector $y(t) \in \Re^p$ is *output controllable* from the unknown input $Ed(t)$ [a control system is said to be (completely) output controllable if the output vector can be driven to the

origin in finite time and if the output is not everywhere zero-valued after application of the control input (MacFarlance and Karcanias, 1976; Katsuhiko O, 1997)]

A necessary condition for *decoupling* the unknown input $d(t)$ is that $rank(CE) = q, (q \le p)$, and it is assumed that $rank(CE) = rank(E)$ (Chen and Patton, 1999).

From Eqs (3-24), $\dot{y}(t)$ is obtained as:

$$\dot{y}(t) = CAx(t) + CBu(t) + CF_a f_a(t) + CEd(t) \tag{3-25}$$

And the *Moore-Penrose* generalised inverse matrix $(CE)^+$ can be obtained as (see discussion in Chen and Patton, 1999):

$$(CE)^+ = [(CE)^T (CE)]^{-1}(CE)^T, \in \Re^{pxq} \tag{3-26}$$

Thus, using Eq. (3-25) the unknown input signal $d(t)$ (assumed continuous) can be estimated by the following:

$$d(t) = (CE)^+[\dot{y}(t) - CAx(t) - CBu(t) - CF_a f_a(t)] \tag{3-27}$$

Substituting Eq. (3-27) into Eq. (3-24), the state equation which is independent of the unknown input term $Ed(t)$ is derived as:

$$\begin{aligned} \dot{x}(t) &= \underbrace{[I_n - E(CE)^+ C]A}_{\widetilde{A}} x(t) + \underbrace{[I_n - E(CE)^+ C]B}_{\widetilde{B}} u(t) \\ &\quad + \underbrace{[I_n - E(CE)^+ C]F_a}_{\widetilde{F}_a} f_a(t) + E(CE)^+ \dot{y}(t) \\ &= \widetilde{A}x(t) + \widetilde{B}u(t) + \widetilde{F}_a f_a + E(CE)^+ \dot{y}(t) \end{aligned} \tag{3-28}$$

The following derivation constitutes an original contribution in this research.

In a similar manner to Eqs (3-4)-(3-7), an observer-based adaptive controller is obtained by:

$$u(t) = \underbrace{\widetilde{K}_x \hat{x}(t)}_{u_x} + \underbrace{\widetilde{K}_a \hat{f}_a(t)}_{u_a} \tag{3-29}$$

where $\widetilde{K}_x \in R^{m \times n}$ and $\widetilde{K}_a \in R^{m \times m}$ are the feedback and actuator fault compensation gain obtained from the new system triple $(\widetilde{A}, \widetilde{B}, \widetilde{F}_a)$. Hence, Eq. (3-28) yields:

$$\dot{x}(t) = \widetilde{A}x(t) + \widetilde{B}\widetilde{K}_x \hat{x}(t) + \widetilde{B}\widetilde{K}_a \hat{f}_a(t) + \widetilde{F}_a f_a + E(CE)^+ \dot{y}(t) \tag{3-30}$$

Thus, the state estimate $\hat{x}$ is given by the solution to [see Eq. (3 - 2)]:

$$\begin{aligned}\dot{\hat{x}}(t) &= \tilde{A}\hat{x}(t) + \tilde{B}\tilde{K}_x\hat{x}(t) + L_x[y(t) - C\hat{x}(t)] + E(CE)^+\dot{y}(t) \\ &= (\tilde{A} + \tilde{B}\tilde{K}_x)\hat{x}(t) + L_x[y(t) - C\hat{x}(t)] + E(CE)^+\dot{y}(t)\end{aligned} \tag{3-31}$$

$$\hat{y}(t) = C\hat{x}(t) \tag{3-32}$$

Now, be defining a new state vector:

$$x_{new}(t) = \hat{x}(t) - E(CE)^+ y(t) \tag{3-33}$$

It can easily be seen that Eq. (3-33) removes the time derivative of the measurement output vector in Eq.(3-31) and leads to the following:

$$\begin{aligned}\dot{x}_{new}(t) &= \dot{\hat{x}}(t) - E(CE)^+\dot{y}(t) \\ &= \tilde{A}\hat{x}(t) + \tilde{B}\tilde{K}_x\hat{x}(t) + L_x[y(t) - C\hat{x}(t)]\end{aligned} \tag{3-34}$$

Re-forming Eq. (3-34) as:

$$\begin{aligned}\dot{x}_{new}(t) &= \tilde{A}\hat{x}(t) + \tilde{B}u_x(t) + L_x y(t) - L_x C\hat{x}(t) \\ &\quad + \tilde{A}[E(CE)^+]y(t) - \tilde{A}[E(CE)^+]y(t) \\ &\quad + L_x C[E(CE)^+]y(t) - L_x C[E(CE)^+]y(t) \\ &= \tilde{A}\left[\hat{x}(t) - E(CE)^+ y(t)\right] - L_x C\left[\hat{x}(t) - E(CE)^+ y(t)\right] \\ &\quad + \tilde{B}u_x(t) + L_x y(t) + \tilde{A}[E(CE)^+]y(t) \\ &\quad - L_x C[E(CE)^+]y(t) \\ &= \tilde{A}x_{new}(t) - L_x C x_{new}(t) + \tilde{B}u_x(t) + L_x y(t) + \tilde{A}[E(CE)^+]y(t) \\ &\quad - L_x C[E(CE)^+]y(t) \\ &= \tilde{A}x_{new}(t) - L_x C x_{new}(t) + \tilde{B}u_x(t) + \left[(\tilde{A} - LC)E(CE)^+ + L_x\right]y(t) \\ &= \underbrace{\left[\tilde{A} - L_x C\right]}_{\boldsymbol{A}_o} x_{new}(t) + \tilde{B}u_x(t) + \underbrace{\left[(\tilde{A} - L_x C)E(CE)^+ + L_x\right]}_{\boldsymbol{E}_o} y(t)\end{aligned} \tag{3-35}$$

Eq. (3-35) can now be rewritten as:

$$\dot{x}_{new}(t) = \boldsymbol{A}_o x_{new}(t) + \tilde{B}u_x(t) + \boldsymbol{E}_o y(t) \tag{3-36}$$

From this it follows that the state estimation without involving the time derivative of the measurement output $\dot{y}(t)$ is now given by:

$$\hat{x}(t) = x_{new}(t) + E(CE)^+ y(t) \tag{3-37}$$

and

$$\hat{f}_a(t) = L_a[y(t) - C\hat{x}(t)] \tag{3-38}$$

where $L_x \in R^{n\times p}$ and $L_a \in R^{m\times p}$ are the linear observer gains to be designed.

The system in Eq. (3-30) with the observer in Eq. (3-31), and the estimate $\hat{f}_a(t)$ in Eq. (3-38) can be arranged in the following closed-loop system:

$$\begin{aligned} \dot{x}(t) - \dot{\hat{x}}(t) &= \tilde{A}[x(t) - \hat{x}(t)] - L_x[y(t) - \hat{y}(t)] + \tilde{B}\tilde{K}_a \hat{f}_a(t) + \tilde{F}_a f_a(t) \\ \dot{e}_x(t) &= (\tilde{A} - L_x C)e_x(t) + \tilde{B}\tilde{K}_a \hat{f}_a(t) + \tilde{F}_a f_a(t) \end{aligned} \tag{3-39}$$

$$\begin{bmatrix} \dot{e}_x(t) \\ \dot{\hat{f}}_a(t) \end{bmatrix} = \begin{bmatrix} \tilde{A} - L_x C & \tilde{B}\tilde{K}_a \\ L_a C & 0 \end{bmatrix} \begin{bmatrix} e_x(t) \\ \hat{f}_a(t) \end{bmatrix} + \begin{bmatrix} \tilde{F}_a \\ 0 \end{bmatrix} f_a(t) \tag{3-40}$$

where $e_x(t) = x(t) - \hat{x}(t)$ is the state estimation error, and $e_y(t) = y(t) - \hat{y}(t)$ given by:

$$e_y(t) = Ce_x(t) \tag{3-41}$$

Eqs. (3-39) and (3-41) show that the unknown input disturbance term $Ed(t)$ does not affect the output error, i.e. the fault estimation given in Eq. (3-38) is robust against unknown disturbances.

Re-arranging Eq. (3-40) as:

$$\underbrace{\begin{bmatrix} \dot{e}_x(t) \\ \dot{\hat{f}}_a(t) \end{bmatrix}}_{\dot{\tilde{e}}} = \left(\underbrace{\begin{bmatrix} \tilde{A} & \tilde{B}\tilde{K}_a \\ 0 & 0 \end{bmatrix}}_{A_0} - \underbrace{\begin{bmatrix} L_x \\ -L_a \end{bmatrix}}_{L_0} \underbrace{\begin{bmatrix} C & 0 \end{bmatrix}}_{C_0} \right) \underbrace{\begin{bmatrix} e_x(t) \\ \hat{f}_a(t) \end{bmatrix}}_{\tilde{e}} + \underbrace{\begin{bmatrix} \tilde{F}_a \\ 0 \end{bmatrix}}_{F_0} f_a(t) \tag{3-42}$$

Eq. (3-42) can be re-written in the form:

$$\dot{\tilde{e}}(t) = (A_0 - L_0 C_0)\tilde{e}(t) + F_0 f_a(t) \tag{3-43}$$

This means that the compensation gain $\tilde{K}_a$ must design such that the pair $(A_0 - L_0 C_0)$ is observable. Again, since the actuator faults represented by the elements of (f_a) are bounded, one can always find a positive number β such that $\beta > \|f_a\|$ [see also ***Proposition 3.1*** and ***Theorem 3.1***].

3.5.1 Tutorial example of linear inverted pendulum system with friction

According to Eq. (3-24), when the system is subject to friction forces acting in up to m of the input channels independently together with the presence of an unknown input term $Ed(t)$ can be re-written as:

$$\begin{aligned} \dot{x}(t) &= Ax(t) + B[u(t) - f_{fric}(t)] + Ed(t) \\ y(t) &= Cx(t) \end{aligned} \qquad (3\text{-}44)$$

Consider as a simple tutorial example the linearised pendulum system with $E = col(0.5, 1, 1.5, 2)$ (chosen arbitrarily) and $d(t)$ is a zero-mean random noise signal with normal distribution and with variance 0.05. The parameters of the friction model used to generate $f_{fric}(t)$ and the matrices (A, B, C) of the linearised pendulum model (corresponding to the vertical equilibrium) are given in Section 3.4.1 .

For the purpose of this tutorial, in contrast to the nonlinear system simulation results as given in Section 3.4, here the ASO is applied to the linear system. Eq. (3-24) is used to investigate the trade-off and comparison of the fault compensation designs with and without robustness to uncertainty. The uncertainty here is defined to arise from the term $Ed(t)$ only and the friction signal $f_{fric}(t)$ is considered only as a fault signal.

The solution for the observer gain L_0 in Eq. (3-43) is used to investigate the combined effect of the friction $f_{fric}(t)$ and unknown input $Ed(t)$ signals, respectively. The simulation experiments are conducted as follows:

Simulation 1: As described in Section 3.3, consider the case that E is not taken into account for the design of on-line ASO fault estimation and compensation (i.e. robust estimation is not considered).

Figure 3-9 shows that before *t* = 40*s* without the augmented state $\hat{f}_{fric}$ to compensate the friction force, the inverted pendulum system exhibits limit cycle oscillation around the vertical equilibrium point (the origin). This is because the cart, which is affected by the friction, exhibits stick-slip motion.

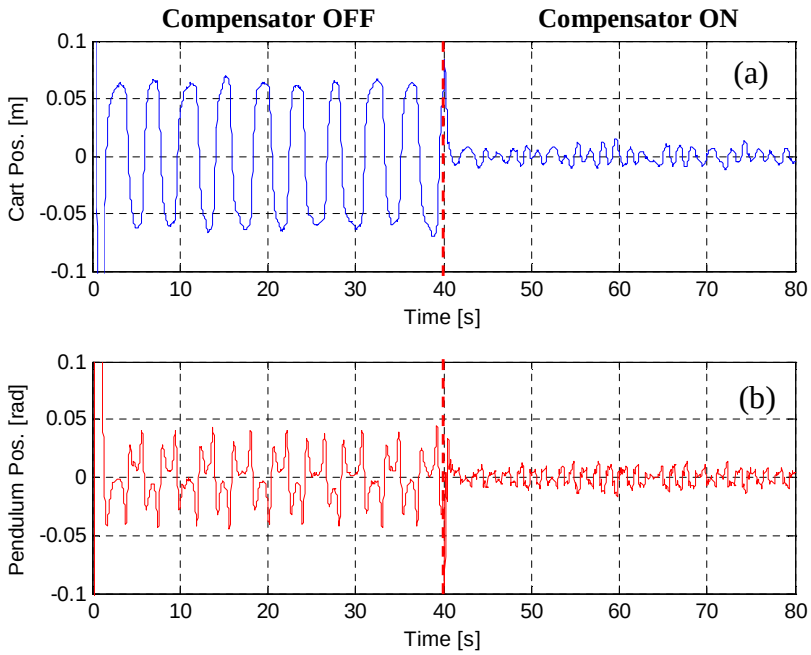

Figure 3-9: ASO simulation results (with $F_s = 2.50N$) for friction compensation activated at time t = 40s.

Figure 3-9 also shows that the activation of the friction compensation term after t = 40s. The limit cycle oscillation is significantly reduced. In this case the amplitude of the pendulum angle is less than 15$mrad$ and the amplitude of the cart stick-slip motion is less than 10mm.

These results can be achieved because the friction force is estimated by the ASO estimator [see Figure 3-10]. Once again as the on-line friction force estimate is updated continuously and used to compensate the friction force acting within the control channel using an observer-based adaptive controller in Eq. (3 - 4) .

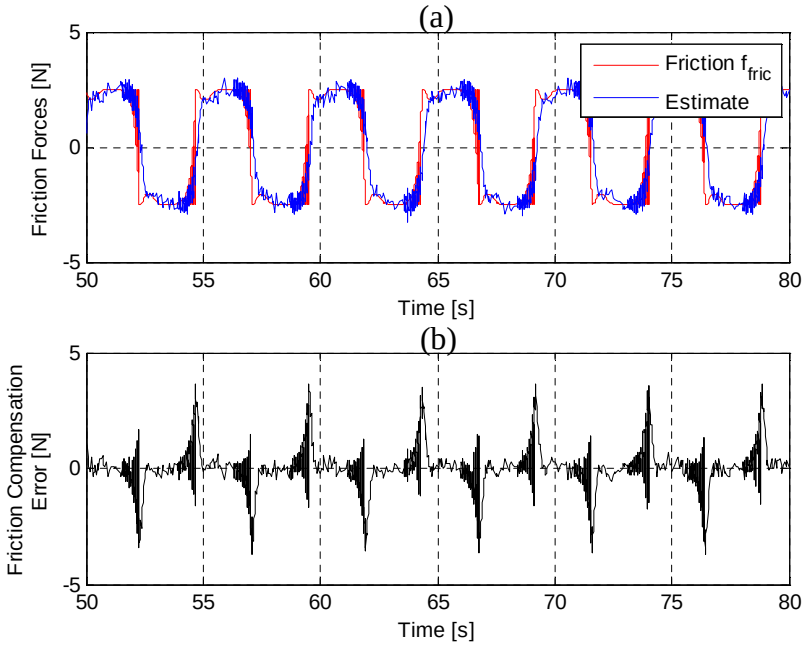

Figure 3-10: Comparison of the friction force (f_{fric}) and its estimate ($\hat{f}_{fric}$)

(with $F_s = 2.50N$)

Simulation 2: As described in Section 3.5, consider the case when the unknown input distribution E is taken into account for the design of on-line ASO fault estimation and compensation (i.e. robust estimation is considered).

Again, it can be verified that the pair (C_0, A_0) as in Eq. (3-43) is observable. The observer gains L_0 are designed such that the eigenvalues of $(A_0 - L_0 C_0)$ are placed at -4.5, -8.5, -5.5, -6.5 and -7.5 [satisfying condition Eq. (3-43)], is given by:

$$L_0 = \begin{bmatrix} 32.4478 & 22.7102 \\ -12.6867 & -4.3088 \\ 234.7925 & 264.4323 \\ -303.6056 & -299.7198 \\ -2403.7797 & -3142.3899 \end{bmatrix}$$

Similar to Figure 3-9, Figure 3-11 with same initial condition value, $x(0) = col(1.1 \quad -1.1 \quad 0 \quad 0)$ also shows that when friction compensation mechanism is turned 'ON' at time t = 40s, the limit cycle oscillation is reduced. In this case the amplitude of pendulum oscillation is less than 20*mrad* and the amplitude of the cart stick-slip motion is less than 18*mm*.

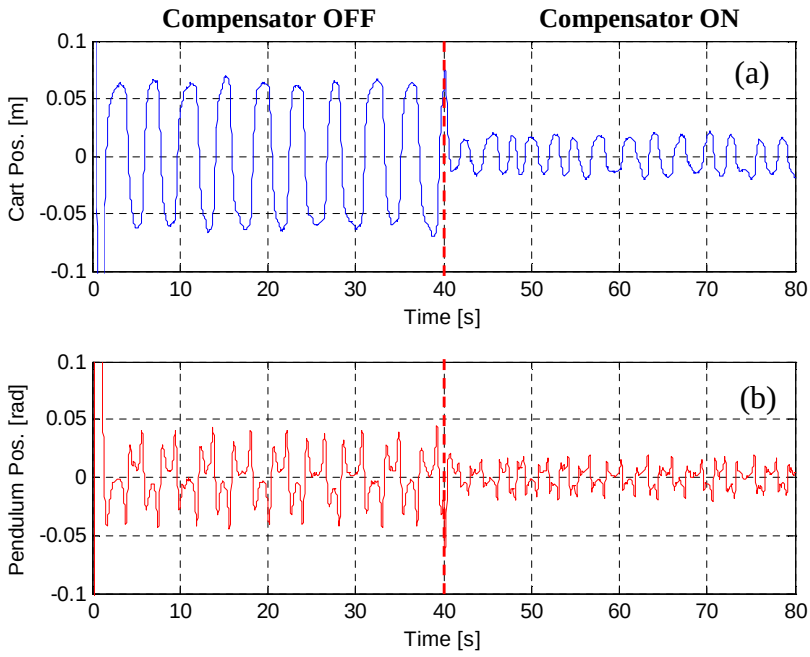

Figure 3-11: ASO simulation results ($F_s = 2.50N$) for friction compensation activated at time t = 40s.

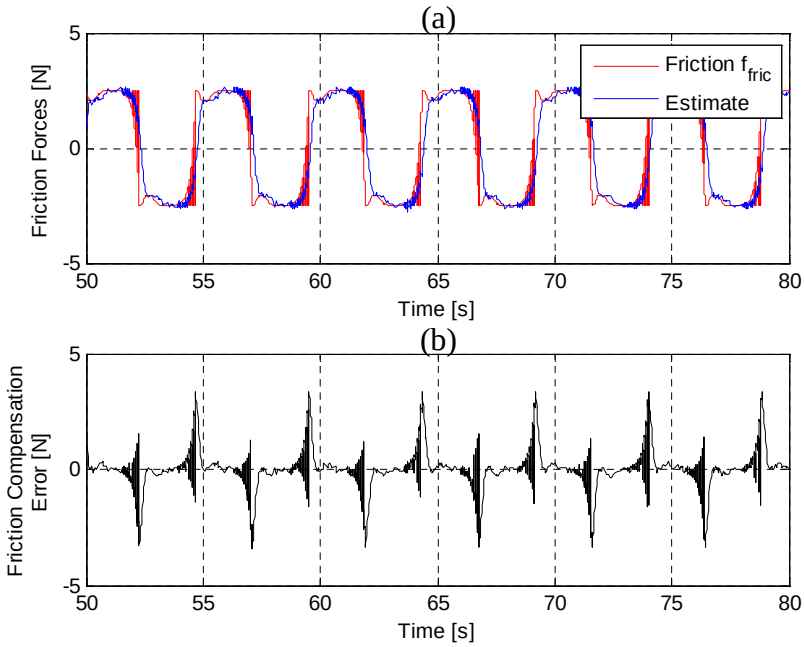

Figure 3-12: Comparison of the friction force (f_{fric}) and its estimate ($\hat{f}_{fric}$) with ($F_s = 2.50N$)

Figure 3-12 demonstrates clearly the robust property of the friction force estimation using the ASO estimator when the unknown input disturbance decoupling described in Section 3.5 is utilised. Whilst the friction estimation error is very small, the

compensation performance has been compromised by the inclusion of the unknown input de-coupling.

Hence, Figure 3-11 shows clearly that after the compensation mechanism is switched 'ON' the compensation result is not as good as that in Figure 3-9, even if the friction estimate in Figure 3-12 is very accurate with a small estimation error when compared with Figure 3-10.

It is very important to note here that for good FTC performance *robust compensation* is essential and *robust fault estimation* is not the main goal. On the other hand for robust control the effects of uncertainties must be compensated or minimised within the feedback control design. Small and bounded fault effects could be considered as uncertainty signals in this context but not through an FTC analysis (involving control adaption/fault compensation etc). This alternative robust control subject is essentially the *passive approach to FTC*.

When the joint estimation and compensation approach is used as illustrated in the above tutorial example the robustness problem is then not an issue as the compensation mechanism seeks to compensate for *both* bounded fault effects and uncertainties.
If one were to consider instead an FDI problem for detection and isolation of the friction fault using residual generation, the robustness of the residual with respect to the unknown input signal would have to be taken into account. This thesis does not pursue the FDI problem since the goal of the work of this Chapter is to develop adaptive strategies for fault compensation, based on fault estimation via a linear observer and adaptive control. This form of FTC employs adaptive control as the new control law given by Eq. (3 - 4) is a direct function of the bounded on-line fault estimate $\hat{f}_a(t)$. This is in keeping with the standard definition of adaptive control. For example, as given in the Wikipedia entry on Adaptive Control: '…*Adaptive control involves modifying the control law used by a controller to cope with the fact that the parameters of the system being controlled are slowly time-varying or uncertain. Adaptive control is different from robust control in the sense that it does not need a priori information about the bounds on these uncertain or time-varying parameters; robust control guarantees that if the changes are within given bounds the control law need not be changed, while adaptive control is precisely concerned with control law changes*...'.

See also the definition of adaptive control given by Aström and Wittenmark (1994): '…*An adaptive controller is a controller that can modify its behavior in response to changes in the dynamics of the processes and the character of the disturbances. In other*

words, an adaptive controller is a control with adjustable parameters and a mechanism for adjusting the parameters i.e. an adaptive control system can be thought of as having two loops. One loop is a nominal feedback control with the process and controller. The other loop is the parameter adjustment loop. The parameter adjustment loop is often slower than the nominal loop…'

3.6 Conclusion

This Chapter provides the strategy of fault estimation and compensation via the design of an augmented state approach, the augmented state observer, in which the new adaptive compensating control is designed based on the estimation error system. The idea of tutorial applications of uncertain systems is illustrated through the examples of friction compensation in an inverted pendulum (without any requirements of a friction force model). The simulation results show, based on a practical example, that the ASO has very good potential in fault estimation and compensation, with a simple design. From a practical standpoint, this method can be implemented well on real-time application systems, even when there are multiple faults.
Although this Chapter does not deal with systems with multiple faults, in Chapter 7 the ASO is further developed and applied to systems with multiple faults, focussed on a distributed system example.

The Chapter has discussed briefly the concepts of control robustness and robust estimation and robust fault compensation using a linear system example. An example of on-line friction estimation/compensation is provided, after defining the friction force acting in a mechatronic system as a fault to be compensated within the control loop. This is an important example as the work has shown clearly the potential of this approach to obviate the complexity problem that can arise when model-based friction compensation methods are used in which detailed models of friction phenomena are used. As friction phenomena are so difficult to model, these approaches may not yield better robustness and improved friction compensation, when compared with the ASO approach. It is clear, due to the adaptive nature of the ASO-based compensation FTC system that good robustness with respect to the friction model parameters is achieved. However, it is important to note that if the fault effect is small, the ASO fault compensator mechanism may not be necessary or may introduce an unwanted but small disturbance (residual error). For this case it would be of interest to use a robust FDI

scheme to detect the presence of a fault and isolate its location within a system, prior to switching on the estimation and compensation scheme.

This Chapter makes a strong case for the use of fault estimation in the problem of active FTC in which the faults acting on the system being controlled are estimated and compensated on-line, under well derived stability constraints on the feedback gains. For friction compensation this stability problem is very well posed since the dynamic friction forces are always bounded by their static levels and these are well know or can be well estimated for a give mechatronic system. The friction compensation problem is a nice example to illustrate the power and potential of this approach. However, it is now clear that the approach can be generalised to FTC problems in which the faults have different significance in terms of multi-faults and also in terms of actuator. Chapter 7 takes up some of these aspects as an extension to the work of this Chapter.

Chapter 4.
Fault Estimation and Compensation based on Sliding Mode Approach

4.1 Introduction

Variable structure control (VSC) was first developed in the USSR in the 50's as a control method applicable to uncertain dynamical systems (Zinober, 1990). Sliding mode control (SMC) is a special case of a VSC system and has received significant attention during the last two decades. Survey and tutorial papers, with numerous references, have been written on SMC by Utkin (1971, 1977, and 1978), Ryan and Corless (1984), Dorling and Zinober (1986), DeCarlo (1988) and books have been published by Zinober (1990), Utkin (1992) and Edwards and Spurgeon (1998).

The background material in this Chapter follows closely the presentation in (Edwards and Spurgeon1998) and Alwi (2008). In SMC, the controller performance depends on a sliding surface design. The state variables in state space are driven to the sliding surface and are forced to remain there by discontinuous (non-linear) feedback action. Once the state motion reaches the sliding surface (manifold) the motion remains within or near the manifold in what is effectively a reduced or system with strong insensitivity to parametric variations occurring in the space outside the sliding manifold. Hence, once the sliding surface or sliding manifold is reached, the system has a strong robustness

property to so-called “matched” disturbances. This robustness property of SMC is a strong motivation for the work described in this Chapter.

The main contribution of this Chapter is to combine, for on-line use in a practical system, the Sliding Mode Observer (SMO) for fault estimation with the SMC, to provide an effective and robust active FTC strategy (the detailed discussions describe in Section 4.4). The approach is illustrated using a nonlinear inverted pendulum with Stribeck friction (Putra *et al*., 2004). Necessary and sufficient conditions for estimation (as a matched uncertainty) are taken and modified from Edwards and Spurgeon (1998) and Alwi (2008).

As described in Chapter 3, the new ideas are two-fold (a) the concept of viewing friction as a fault-effect, and (b) the combined use of sliding mode fault estimation and control. This work develops and evaluates a powerful approach to on-line FTC for the friction compensation problem. The estimates of the friction force generated via the SMO theory of Edwards and Spurgeon are directly used in an adaptive SMC scheme. All the required mathematical conditions are given, including stability proofs underlying the SMC and SMO.

4.2 Sliding Mode Control

The objective of this Section is to summarise the SMC concept as described in (Dorling and Zinober, 1988; Zinober, 1990; Edwards and Spurgeon, 1998) including its basic properties as a mechanism for achieving good control performance via on-line fault estimation and compensation or FTC. An analysis and the tutorial example are based on a simple nonlinear inverted pendulum with cart system to illustrate the concept of SMC.

Generally, the design approaches for SMC controllers comprise *two* stages: (i) design the sliding surface, (ii) the switching control law can be designed so that sliding is attained and maintained on the surface. When perfect sliding occurs, there are two main advantages of SMC; there is a reduction in order, and the system has low sensitivity to some certain disturbances so-called *matched uncertainty* (Edwards and Spurgeon, 1998).

The SMC system can be viewed as partitioned into two subspaces, the so-called “range space” and the “null space” (the significance of these terms are explained in Section 4.2.1). The state motion corresponding to the range space dynamics is affected by

uncertainties and perturbations. On the other hand, once the state motion is driven into the sliding regime (or null space subsystem) the controlled system remains insensitive or with low sensitivity to the matched uncertainty and behaves as a "free" system in the ideal case, following an intersection of eigenvector directions into the equilibrium. State motion occurring precisely within the sliding manifold has zero sensitivity to the matched uncertainty, whereas motion close to the switching boundary of the sliding manifold takes on a finite but small sensitivity to uncertainty [Zinober, 1990].

Hence, the SMC have two feedback control components; (i) a linear component to stabilise the nominal linear system, and (ii) a nonlinear or discontinuous component. The linear control component brings about or ensures the reachability of the sliding regime of the system and the discontinuous controller component is used to cause the sliding motion (through switching action) and thereby cancel or reduce the effects of non-linearities and/or uncertainties in the system, as outlined above. Therefore the SMC is applicable for both non-linear and uncertain systems because of the use of the discontinuous component to induce sliding motion. These properties are discussed further in the Section 4.2.3.

4.2.1 Regular form for sliding hyperplane design

Consider the following linear time invariant (LTI) system:

$$\dot{x}(t) = Ax(t) + Bu(t) \qquad (4 - 1)$$

where $x \in \Re^n$ is the system state vector and $u \in \Re^m$ are the system inputs, and the system matrices are $A \in \Re^{nxn}, B \in \Re^{nxm}$. The matrix B is assumed to have full rank and the pair (A, B) is controllable.

Let $s : \Re^n \to \Re^m$ be a *switching function* represented as:

$$s(t) = Sx(t) \qquad (4 - 2)$$

where: $S \in \Re^{mxn}$ is full rank and so-called the *hyperplane*, and defined by:

$$S = \left\{ x \in \Re^n : \quad s(x) = 0 \right\} \qquad (4 - 3)$$

In the design procedure for SMC, it is well known that for the controllable system described in Eq. (4 - 1) [with $rank(B) = m$], there exists an invertible transformation, $T_r \in \Re^{nxn}$ defined as:

$$\begin{bmatrix} x_1(t) \\ x_2(t) \end{bmatrix} = T_r x(t) \qquad (4-4)$$

This transformation brings the system in Eq. (4 - 1) into the *regular form* as follows: (Edwards and Spurgeon, 1998).

$$\dot{x}_1(t) = A_{11}x_1(t) + A_{12}x_2(t) \qquad (4-5)$$

$$\dot{x}_2(t) = A_{21}x_1(t) + A_{22}x_2(t) + B_2u(t) \qquad (4-6)$$

where: $x_1(t) \in \Re^{n-m}$ and $x_2(t) \in \Re^m$. $B_2 \in \Re^{mxm}$ is non-singular and given by:

$$T_r B = \begin{bmatrix} 0 \\ B_2 \end{bmatrix} \qquad (4-7)$$

The purpose of the regular form above is to partition the transformed system into a suitable structure so that the null space [see Eq. (4 - 5)] and range space dynamics [see Eq. (4 - 6)] can be designed.

In the new coordinates the switching function in Eq.(4 - 2) becomes:

$$s(t) = S_1x_1(t) + S_2x_2(t) \qquad (4-8)$$

where: $S_1 \in \Re^{mx(n-m)}$ and $S_2 \in \Re^{mxm}$. The matrices S_1 and S_2 are the design parameters such that $\det(S_2) \neq 0$, and there exists a finite time t_s that satisfies:

$$s(t) = 0 \quad \text{for all } t \geq t_s \qquad (4-9)$$

Therefore, an ideal sliding motion takes place for all $t > t_s$, and during sliding, the motion is given by:

$$s(t) = S_1x_1(t) + S_2x_2(t) = S[x_1(t)\ x_2(t)] = 0 \qquad (4-10)$$

Re-arranging Eq.(4 - 1 0) yields:

$$x_2(t) = -S_2^{-1}S_1x_1(t) \qquad (4-11)$$

For simplicity, let $M = -S_2^{-1}S_1$. Substituting Eq. (4 - 1 1) into Eq. (4 - 5) gives:

$$\dot{x}_1(t) = (A_{11} - A_{12}M)x_1(t) \qquad (4-12)$$

In can be seen that Eq.(4 - 1 2) presents the dynamics of the closed-loop system in the sliding mode, which is equivalent to a classical state feedback problem i.e. the problem of finding a matrix M [$x_2(t) = -Mx_1(t)$] in Eq.(4 - 1 1) is equivalent to finding the gain matrix K in a state feedback problem [i.e. for $u(t) = -Kx(t)$] in Eq. (4 - 1) .

The stability of the closed-loop system in Eq. (4 - 1 2) depends on the $n-m$ reduced order pair (A_{11}, A_{12}) and the design matrix M which also based on pair (A_{11}, A_{12}) [e.g. the matrix $A_{11} - A_{12}M$ is *Hurwitz*]. It is straightforward to prove that the matrix pair (A_{11}, A_{12}) is controllable, if and only if the pair (A, B) is controllable (Edwards and Spurgeon, 1998; Alwi, 2008). Once the matrix M has been obtained, the sliding surface S can also be calculated as follows:

$$S = \begin{bmatrix} S_2 M & S_2 \end{bmatrix} \qquad (4\text{-}13)$$

where S_2 can be chosen arbitrarily as long as it is invertible, in this study, it is designed as $S_2 = I_m$.

Three main approaches have appeared in the literature for designing the state feedback matrix M .

(i). Robust pole-placement (Ryan and Corless, 1984)
(ii). Quadratic minimisation (Utkin and Young, 1978), and
(iii). Eigenstructure assignment (Zinober, 1990)

For this study approach (ii) has been used, and will be discussed in Section 4.2.5. Approach (iii) is an extension to (i) in which the multivariable design freedom in the design of M is used more fully to achieve an assignment of the eigenvectors of the reduced order null space dynamics as well as the assignment of the eigenvalues. The pole-placement problem is equivalent to only the eigenvalue part of the eigenstructure assignment problem (Zinober, 1990).

4.2.2 The reachability problem

Once the surface S is obtained, the next step of the procedure is the design of the control to ensure that the designed sliding mode is attained. Therefore, the problem of determining the control structure, which ensure that sliding surface is reached and motion on *S* is maintained, is called the '*reachability problem*'.

In other words, the reachability condition means that '… *the trajectory of the switching function* $s(t)$ *must be directed towards it…*' (Edwards and Spurgeon, 1998). Therefore need to design in order to satisfy the *reachability condition* (Utkin, 1977; Zinober, 1990). This can be expressed as: [see following Eqs (4-14) and (4-15)]

$$\lim_{s\to 0^+} \dot{s} < 0 \quad \text{and} \quad \lim_{s\to 0^-} \dot{s} > 0 \tag{4-14}$$

or equivalent to

$$s\dot{s} < 0 \tag{4-15}$$

Edwards and Spurgeon (1998), propose a strong condition to guarantee that the sliding surface is reached even in the presence of uncertainty and in *finite time*. This is given by:

$$s\dot{s} < -\eta_{reach}|s| \tag{4-16}$$

where: η_{reach} is a positive design scalar and so-called the η_{reach} *-reachability condition*'

4.2.3 Sliding properties under conditions of model uncertainty and disturbance

When the reachability condition Eq. (4-16) is satisfied the motion of the system moves to the sliding hyperplane subsystem. In general, the motion will remain within or close to the hyperplane switching boundary unless the system is disturbed. However, some disturbances and uncertainty will enable the motion to remain close to the sliding surface even in the presence of uncertainty. This invariance property of sliding mode control was first investigated by Draženović (1969) for the wider context of variable structure systems and holds for certain disturbance and parametric variations that lie within a bounded range and satisfy a given structural property defined in the state space.

This property is well known in the literature as the sliding motion matching condition and is referred as *matched uncertainty*. Utkin (1971) dealt with this problem for single input systems and Utkin (1977, 1978) deals with the multivariable control case. In fact, as the matching conditions (see below) are sometimes rather restrictive most of the work in the literature on this subject has been concerned with the problem of "mismatching", i.e. solutions for dealing with cases when the matching conditions do not hold.

To understand the matching conditions, consider the system in Eq.(4 - 1) with the presence of the uncertainty as follows:

$$\dot{x}(t) = Ax(t) + Bu(t) + D\xi(t,x) \qquad (4\text{-}17)$$

where: $\xi \in \Re_+ \; x \; \Re^n \rightarrow \Re^q$ is unknown function representing an uncertainty or exogenous disturbance acting on the system. $A \in \Re^{nxn}$, $B \in \Re^{nxm}$ and $D \in \Re^{nxq}$ are known matrices with appropriate dimensions.

At time t_s, if the system states lie on the sliding surface and remain there, that is:

$$s(t) = 0 \;\text{ and }\; \dot{s}(t) = 0 \qquad (4\text{-}18)$$

Eqs. (4 - 2) , (4-17), and (4-18) can be re-written in terms of the time derivative of $s(t)$ as:

$$\begin{aligned} \dot{s}(t) &= S\dot{x}(t) \\ &= S[Ax(t) + Bu(t) + D\xi(t,x)] \\ &= 0 \end{aligned} \qquad (4\text{-}19)$$

Thus, the control action for sliding motion can be obtained by:

$$u_{eq}(t) = -(SB)^{-1}[SAx(t) + SD\xi(t,x)] \quad \text{for all } t \geq t_s \qquad (4\text{-}20)$$

where: $u_{eq}(t)$ is the so–called *equivalent control*.

The equivalent control is basically the control that maintains the sliding motion without the high frequency (discontinuous component) (Utkin, 1977; El-Ghezawi, Zinober and Billings, 1983; Dorling and Zibober, 1986; Edwards and Spurgeon, 1998) and is clearly an idealised concept.

It can be seen that the equivalent control in Eq.(4-20) depends on the unknown uncertain signal $\xi(t,x)$. However, this uncertainty will still enable the sliding motion to remain close to the sliding surface [i.e. the sliding motion is insensitive to $\xi(t,x)$], if the following condition is satisfied (Edwards and Spurgeon, 1998).

Replacing the control input $u(t)$ in Eq. (4-17) with *equivalent control* action $u_{eq}(t)$ in Eq.(4-20) gives:

$$\begin{aligned} \dot{x}(t) &= Ax(t) - B(SB)^{-1}SAx(t) - B(SB)^{-1}SD\xi(t,x) + D\xi(t,x) \\ &= [I_n - B(SB)^{-1}S]Ax(t) + [I_n - B(SB)^{-1}S]D\xi(t,x) \end{aligned} \qquad (4\text{-}21)$$

Define:

$$P_s = I_n - B(SB)^{-1}S \tag{4-22}$$

where P_s is a projection operator, thus Eq. (2-19) can be rewritten as:

$$\dot{x}(t) = P_s Ax(t) + P_s D\xi(t,x) \tag{4-23}$$

There exists a matrix $R \in \Re^{mxq}$ such that $D = BR$, if $\mathbf{R}(D) \subset \mathbf{R}(B)$, and it follows that:

$$\begin{aligned} SP_s &= S[I_n - B(SB)^{-1}S] \\ &= S - \underbrace{(SB)(SB)^{-1}}_{I_m}S \\ &= 0 \end{aligned} \tag{4-24}$$

and

$$\begin{aligned} P_s B &= [I_n - B(SB)^{-1}S]B \\ &= B - B\underbrace{(SB)^{-1}(SB)}_{I_m} \\ &= 0 \end{aligned} \tag{4-25}$$

In the following the Eq. (4-25), thus Eq. (4-23) can be rewritten as:

$$\begin{aligned} \dot{x}(t) &= P_s Ax(t) + P_s D\xi(t,x) \\ &= P_s Ax(t) + \underbrace{P_s B}_{0}R\xi(t,x) \\ &= P_s Ax(t) \end{aligned} \tag{4-26}$$

It can be seen that during the sliding motion, Eq. (4-26) is not depend on the uncertain signal $\xi(t,x)$. This leads to the property that <u>the ideal sliding motion is totally insensitive to the uncertain function</u> in (4-17) if $\mathbf{R}(D) \subset \mathbf{R}(B)$ (Ryan and Corless, 1984; Dorling and Zinober, 1986; DeCarlo, 1988; Zinober, 1990; Edwards and Spurgeon, 1998).

Edwards and Spurgeon (1998) state that, '*…any uncertainty which can be expressed in the form of or as in Eq.* (4-17) *where* $\mathbf{R}(D) \subset \mathbf{R}(B)$ *is described as* <u>*matched uncertainty*</u>*. Any uncertainty which does not lie within the range space of the input distribution matrix is described as unmatched uncertainty . . .*'

If this matching condition is not satisfied the uncertainty does not lie within the range space of B, i.e. $\mathbf{R}(D) \not\subset \mathbf{R}(B)$ and several studies have proposed sliding control design methods that can preserve invariance for sliding under extended conditions (DeCarlo, 1988; Spurgeon, 1991; Spurgeon and Davies, 1993). The property which is probably

the most important for FTC in terms of handling actuator faults will be outlined in Section 4.4

4.2.4 Unit vector approach

The control structure for multivariable systems described in this Section is based on that of Ryan and Corless (1984), which is so-called the 'unit vector'. Consider a system which has only matched uncertainty (Edwards and Spurgeon, 1998):

$$\dot{x}(t) = Ax(t) + Bu(t) + f_m(t,x,u) \tag{4-27}$$

where $f_m(t,x,u) : \Re\ x\ \Re^n\ x\ \Re^m \rightarrow \mathbf{R}(B)$ is unknown but bounded and satisfies:

$$\left\| f_m(t,x,u) \right\| \leq k_m \left\| u(t) \right\| + \alpha(t,x) \tag{4-28}$$

where k_m is a known positive constant with $k_m < \sqrt{\lambda_{\min}(B^T B)}$ and $\alpha(\cdot)$ is a known function.

Without any loss of generality, the system in Eq. (4-27) can be transformed into regular form as follows [see Section 4.2.1]:

$$\dot{x}_1(t) = A_{11}x_1(t) + A_{12}x_2(t) \tag{4-29}$$

$$\dot{x}_2(t) = A_{21}x_1(t) + A_{22}x_2(t) + B_2u(t) + \bar{f}_m(t,x,u) \tag{4-30}$$

where: $\bar{f}_m$ represent a projection of f_m into the subspace $\mathbf{R}(B)$, then the following *Euclidean norm* is preserved and satisfied:

$$\left\| \bar{f}_m(t,x,u) \right\| \leq k_m \left\| u(t) \right\| + \alpha(t,x) \tag{4-31}$$

As described in Section 4.2.1, the switching function $s(t)$ can be presented as:

$$\begin{aligned} s(t) &= S_1x_1(t) + S_2x_2(t) \\ &= S_2M\,x_1(t) + S_2x_2(t) \end{aligned} \tag{4-32}$$

where: $M \in \Re^{mx(n-m)}$, and $S_2 \in \Re^{mxm}$ is designed matrix, a common choice here, is to let $S_2 = \Lambda B_2^{-1}$ for a non-singular diagonal design matrix $\Lambda \in \Re^{mxm}$, which implies that:

$$S_2B_2 = \Lambda \tag{4-33}$$

Define a second coordinate transformation by:

$$T_s = \begin{bmatrix} I & 0 \\ S_1 & S_2 \end{bmatrix} \tag{4-34}$$

Therefore, the system can be transformed into new partition as follows:

$$\begin{bmatrix} x_1(t) \\ s(t) \end{bmatrix} = T_s \begin{bmatrix} x_1(t) \\ x_2(t) \end{bmatrix} \tag{4-35}$$

In the following Eq.(4-35), the system in Eq. (4-29) can be re-arranged as:

$$\begin{bmatrix} \dot{x}_1(t) \\ \dot{s}(t) \end{bmatrix} = \begin{bmatrix} \overline{A}_{11} & A_{12} \\ \overline{A}_{21} & \overline{A}_{22} \end{bmatrix} \begin{bmatrix} x_1(t) \\ s(t) \end{bmatrix} + \begin{bmatrix} 0 \\ \Lambda \end{bmatrix} u(t) + \begin{bmatrix} 0 \\ S_2(t) \end{bmatrix} \bar{f}_m(t, x, u) \tag{4-36}$$

where: $\overline{A}_{11} = A_{11} - A_{12}M$, $\overline{A}_{21} = M\overline{A}_{11} + A_{21} - A_{22}M$ and $\overline{A}_{22} = MA_{12} + A_{22}$. The proposed control law consists of two components (Ryan and Coreless, 1984); a linear component and nonlinear or discontinuous component as follows:

$$u(t) = u_l(t) + u_n(t) \tag{4-37}$$

The linear control component is given by:

$$u_l(t) = -\Lambda^{-1}[S_2\overline{A}_{21}x(t) - (S_2\overline{A}_{22}S_2^{-1} - \Phi)s(t)] \tag{4-38}$$

where: $\Phi \in \Re^{mxm}$ is any stable design matrix.

The nonlinear component is given by:

$$u_n(t) = -\rho_c(t, x)\Lambda^{-1}\frac{P_2 s(t)}{\|P_2 s(t)\|} \qquad \text{for} \quad s(t) \neq 0 \tag{4-39}$$

where: $P_2 \in \Re^{mxm}$ is a S.P.D matrix satisfying the Lyapunov equation:

$$P_2\Phi + \Phi^T P_2 = -I_m \tag{4-40}$$

and $\rho_c(t, x)$ is any scalar function, which depends only on the magnitude of uncertainty, and satisfies:

$$\rho_c(t, x) \geq \frac{\|S_2\|(k_m\|u_l(t)\| + \alpha(t, x)) + \gamma_c}{(1 - k_m\|B_2^{-1}\|)} \tag{4-41}$$

In other words $\rho_c(t, x)$ must be greater than the magnitude of the uncertainty, and γ_c is a positive scalar design parameter.

Edwards and Spurgeon (1998), working in the original coordinates, show that Eq. (4-38) can be rewritten as:

$$u_l(t) = \underbrace{-\Lambda^{-1}(SA-\Phi S)}_{L_{sm}}x(t) \qquad (4\text{-}42)$$

It should be noted here that following the above analysis, the uncertainty is assumed to be matched. For the case when unmatched uncertainty terms can be included in the above analysis can be found in Edwards and Spurgeon (1998).

Sections 4.2.1 to 4.2.4 discuss the conditions required to achieve the design of the control law of Eq. (4-37). In Section 4.2.5, the design of the switching surface, namely the matrix S in the switching function of Eq. (4-2) is outlined.

4.2.5 Design of sliding surface using quadratic minimization

The section describes a design method for the switching hyperplane S. In this thesis, only the quadratic minimisation method is chosen (based on Section 4.2.2 in Edwards and Spurgeon, 1998). This method was proposed by Utkin and Young (1978) using a modified classical linear quadratic regulator (LQR) problem. In designing the sliding surface, the control inputs are not considered explicitly. This design problem involves the minimization of the quadratic cost:

$$J = \int_{t_s}^{\infty}(x^T Q x)dt \qquad (4\text{-}43)$$

Subject to Eq. (4-1) where Q is S.P.D and t_s indicates the start of sliding.

First, it is necessary to transform the system in Eq. (4-1) into regular form (see Section 4.2.1) using a coordinate transformation $z(t) = T_r x(t)$. Therefore, in regular form, the matrix Q in Eq. (4-43) can be partitioned as:

$$T_r Q T_r^T = \begin{bmatrix} Q_{11} & Q_{12} \\ Q_{21} & Q_{22} \end{bmatrix} \qquad (4\text{-}44)$$

where: $Q_{21} = Q_{12}^T$.

In the LQR problem, Eq. (4-43) can be represented in the $z(t)$ coordinate system as:

$$J = J = \frac{1}{2}\int_{t_s}^{\infty}\left(z_1^T(t)Q_{11}z_1(t) + 2z_1^T(t)Q_{12}z_2(t) + z_2^T(t)Q_{22}z_2(t)\right)dt \qquad (4\text{-}45)$$

It can be seen that Eq. (4-45) does not satisfy the standard form of the LQR problem. To overcome this problem, it is necessary to remove the cross term $2z_1^T(t)Q_{12}z_2(t)$ in Eq. (4-45). Utkin and Young (1978) proposed factorizing the last two terms of Eq. (4-45) yielding:

$$2z_1^T Q_{12}z_2 + z_2^T Q_{22}z_2 = (z_2 + Q_{22}^{-1}Q_{21}z_1)^T Q_{22}(z_2 + Q_{22}^{-1}Q_{21}z_1) - z_1^T Q_{22}^{-1}Q_{21}z_1 \qquad (4\text{-}46)$$

Using Eq. (4-46), hence Eq. (4-45) can be written as:

$$\begin{aligned} J &= \frac{1}{2}\int_{t_s}^{\infty}\left(z_1^T(t)Q_{11}z_1(t) + (z_2 + Q_{22}^{-1}Q_{21}z_1)^T Q_{22}(z_2 + Q_{22}^{-1}Q_{21}z_1) - z_1^T Q_{22}^{-1}Q_{21}z_1\right)dt \\ &= \frac{1}{2}\int_{t_s}^{\infty}\left(z_1^T \underbrace{(Q_{11} - Q_{12}Q_{22}^{-1}Q_{21})}_{\hat{Q}} z_1 + \underbrace{(z_2 + Q_{22}^{-1}Q_{21}z_1)^T}_{v_q} Q_{22} \underbrace{(z_2 + Q_{22}^{-1}Q_{21}z_1)}_{v_q} \right)dt \end{aligned} \qquad (4\text{-}47)$$

By defining:

$$\hat{Q} = Q_{11} - Q_{12}Q_{22}^{-1}Q_{21} \qquad (4\text{-}48)$$

and

$$v_q = z_2 + Q_{22}^{-1}Q_{21}z_1 \qquad (4\text{-}49)$$

Hence, Eq.(4-47) can be written as:

$$J = \frac{1}{2}\int_{t_s}^{\infty}\left(z_1^T\hat{Q}z_1 + v_q^T Q_{22}v_q\right)dt \qquad (4\text{-}50)$$

Recall that the transformed dynamical system in Eq. (4 - 5) is here given by:

$$\dot{z}_1(t) = A_{11}z_1(t) + A_{12}z_2(t) \qquad (4\text{-}51)$$

The $z_2(t)$ term in Eq. (4-51) can be eliminated by using Eq. (4-49), so that the modified constraint equation in Eq. (4-51) becomes:

$$\begin{aligned}\dot{z}_1(t) &= A_{11}z_1(t) + A_{12}[v_q - Q_{22}^{-1}Q_{21}z_1] \\ &= A_{11}z_1(t) + A_{12}v_q - A_{12}Q_{22}^{-1}Q_{21}z_1 \\ &= \underbrace{[A_{11} - A_{12}Q_{22}^{-1}Q_{21}]}_{\hat{A}}z_1 + A_{12}v_q \\ &= \hat{A}z_1(t) + A_{12}v_q(t)\end{aligned} \tag{4-52}$$

where $\hat{A} = A_{11} - A_{12}Q_{22}^{-1}Q_{21}$. The optimal $v_q(t)$ minimising Eq. (4-50) is given by:

$$v_q(t) = -Q_{22}^{-1}A_{12}^T P_1 z_1(t) \tag{4-53}$$

where P_1 satisfies:

$$P_1\hat{A} + \hat{A}^T P_1 - P_1 A_{12}Q_{22}^{-1}A_{12}^T P_1 + \hat{Q} = 0 \tag{4-54}$$

During sliding i.e. $s(t) = 0$ [see also Eq. (4-18)] and hence:

$$z_2(t) = -\underbrace{S_2^{-1}S_1}_{M}z_1(t) \tag{4-55}$$

The solution for v_q in Eqs. (4-49) and (4-53) leads to:

$$z_2 + Q_{22}^{-1}Q_{21}z_1 = -Q_{22}^{-1}A_{12}^T P_1 z_1(t) \tag{4-56}$$

or

$$z_2(t) = -Q_{22}^{-1}(A_{12}^T P_1 + Q_{21})z_1(t) \tag{4-57}$$

In the following Eq. (4-55), the matrix M can be represented by:

$$\begin{aligned}M &= S_2^{-1}S_1 \\ &= Q_{22}^{-1}(A_{12}^T P_1 + Q_{21})\end{aligned} \tag{4-58}$$

Therefore, when the matrix *M* is obtained, matrix S can also be determined (see Eq. (4-13)].

Whilst Section 4.2 outlines the main features and the potential of SMC, Section 4.3 describes the benefits of using the *Sliding Mode Observer* (SMO) for FDI, specifically for fault estimation.

4.3 Sliding Mode Observer for FDI and Fault Estimation

The SMO of Edwards and Spurgeon (1998) and Edwards *et al* (2000) has proved to be a powerful approach for nonlinear FDI methods. The idea of the SMO is to '*…design the observer gains such that the sliding surface is reached and maintained and so that the error between the plant and the observer states is equal to or converges to zero…*' (Alwi, 2008). Prior to the advent of the Edwards and Spurgeon SMO approach sliding mode observers have been used earlier for fault detection. For example, Sreedhar *et al* (1993) provide a sliding mode design procedure in which it is assumed that the states of the system are available (e.g. which is not practical in many real applications). Further approaches were developed by Yang *et al* (1995) and by Hermans and Zarrop (1996). The common idea was to ensure that the sliding motion is broken or destroyed when faults/failures occur and a residual is generated providing information about the fault.

The development of FDI in terms of the estimation/reconstruction of faults using SMO is provided by Edwards *et al*. (2000), with the concept of the '*equivalent output error injection signal*' to estimate/reconstruct faults. However, uncertainty was not considered in their early papers. This work was further developed by Tan and Edwards (2002) who considered the case of sensor faults. The work on robust estimation/reconstruction of sensor and actuator faults is developed further by Tan and Edwards (2003 and 2006). The advantage of these methods compared with some well known non-sliding observer based FDI approaches is that the sliding motion is not broken even in the event of faults/failures. This Section includes an introduction to a typical SMO and shows how the SMO can be used for fault estimation as suggested by Edwards and Spurgeon (1998).

4.3.1 A typical SMO

This Section introduces briefly one class of SMO which is used in Section 4.4 within an active FTC system. The SMO structure presented here evolved from the Walcott and Zak observer (1987 and 1988) and the Utkin observer (1992), and is well known as the Edwards and Spurgeon SMO (1998), described as follows:

Consider the nominal linear system with a class of uncertainty described by:

$$\dot{x}(t) = Ax(t) + Bu(t) + D\xi(t, x, u) \qquad (4\text{-}59)$$

$$y(t) = Cx(t) \qquad (4\text{-}60)$$

where: $A \in \Re^{nxn}, B \in \Re^{nxm}, C \in \Re^{pxn}, D \in \Re^{nxq}$ with $q \le p < n$, and the matrices B, C and D are of full rank, the function $\xi : \Re_+ \; x \; \Re^p \; p \to \Re_+$ is assumed to be unknown but bounded so that:

$$\left\| \xi(t, x, u) \right\| \;\; \le \;\; r_1 \left\| u(t) \right\| + \alpha(t, y) \qquad (4\text{-}61)$$

where: $\alpha(t, y) : \; \Re_+ \; x \; \Re^p \to \Re^q$ is a known function, and r_1 is a known scalar.

The general idea of the SMO design is to generate a state estimate $\hat{x}(t)$ such that the state error of the system $e_x^{sm}(t) = \hat{x}(t) - x(t)$ approaches zero asymptotically even the presence of the uncertainty.

The sliding surface is the *hyperplane* represented by:

$$S_o \; = \{ e_x^{sm} \in \Re^n \; : \; C e_x^{sm} = 0 \} \qquad (4\text{-}62)$$

The observer structure of the system in Eqs. (4-59) and (4-60) can be written in the form (Edwards and Spurgeon 1998):

$$\dot{\hat{x}}(t) \;\; = \;\; A\hat{x}(t) + Bu(t) - G_l e_y^{sm}(t) + G_n v_o(t) \qquad (4\text{-}63)$$

where: $G_l, G_n \in \Re^{nxp}$ are the design linear and nonlinear gain matrices, $e_y^{sm}(t) = \hat{y}(t) - y(t)$ is the output estimation error, and $v_o(t)$ is a discontinuous switched component to induce a sliding motion on sliding surface S_o.

Edwards and Spurgeon (1998) state '*…A sliding mode observer in Eq.* (4-61) *which rejects the uncertainty class in* Eq. (4-59) *exists if and only if the nominal linear system satisfies…*'

- $rank(CD) = q$
- *invariant zeros of* (A, D, C) *are stable.*

[Proof of the necessity is given in Proposition 6.2 in Edwards and Spurgeon (1998)]

Edwards and Spurgeon (1998) proposed the design of system which is transformed into observer *canonical form* via a transformation matrix T_o, so that $x \mapsto T_o x$, and the output distribution matrix becomes:

$$C T_o^{-1} = \begin{bmatrix} 0 & I_p \end{bmatrix} \qquad (4\text{-}64)$$

Therefore, the new coordinate system can be presented by:

$$\begin{aligned} \dot{x}_1(t) &= \mathcal{A}_{11}x_1(t) + \mathcal{A}_{12}y(t) + \mathcal{B}_1u(t) \\ \dot{y}(t) &= \mathcal{A}_{21}x_1(t) + \mathcal{A}_{22}y(t) + \mathcal{B}_2u(t) + \mathcal{D}_2\xi(t) \end{aligned} \tag{4-65}$$

where: $x_1(t) \in \Re^{(n-p)}$, $y(t) \in \Re^p$ and $\mathcal{A}_{11}$ has stable eigenvalues (Edward and Spurgeon, 1998).

Consider an observer of the form:

$$\begin{aligned} \dot{\hat{x}}_1(t) &= \mathcal{A}_{11}\hat{x}_1(t) + \mathcal{A}_{12}\hat{y}(t) + \mathcal{B}_1u(t) - \mathcal{A}_{12}e_y^{sm}(t) \\ \dot{\hat{y}}(t) &= \mathcal{A}_{21}\hat{x}_1(t) + \mathcal{A}_{22}\hat{y}(t) + \mathcal{B}_2u(t) - (\mathcal{A}_{22} - \mathcal{A}_{22}^s)e_y^{sm}(t) + v_o(t) \end{aligned} \tag{4-66}$$

where: $\mathcal{A}_{22}^s$ is stable design matrix, and v_o is defined as:

$$v_o(t) = \begin{cases} -\rho_o(t, y, u)\|\mathcal{D}_2\|\dfrac{P_2e_y^{sm}(t)}{\|P_2e_y^{sm}(t)\|} & \text{if } e_y^{sm}(t) \neq 0 \\ 0 & \text{otherwise} \end{cases} \tag{4-67}$$

where: P_2 is a S.P.D. matrix and satisfies Lyapunov equation as follows:

$$\mathcal{A}_{22}^{s\,T}P_2 + P_2\mathcal{A}_{22}^s = -I \tag{4-68}$$

and the scalar function $\rho_o(t, y)$ in Eq. (4-67) is chosen so that:

$$\rho_o(t, y) \geq r_1\|u(t)\| + \alpha(t, y) + \gamma_o \tag{4-69}$$

where: γ_o is a positive scalar.

The system state estimation error $e_{x_1}^{sm}(t) = \hat{x}_1(t) - x_1(t)$ and $e_y^{sm}(t)$ are associated as follows:

$$\dot{e}_{x_1}^{sm}(t) = \mathcal{A}_{11}e_{x_1}^{sm}(t) \tag{4-70}$$

$$\dot{e}_y^{sm}(t) = \mathcal{A}_{21}e_{x_1}^{sm}(t) + \mathcal{A}_{22}^s e_y^{sm}(t) + v_o(t) - \mathcal{D}_2\xi(t) \tag{4-71}$$

In the following Eqs.(4-66) to (4-71), the observer gains and the discontinuous vector $v_o(t)$ for the observer structure described in Eq. (4-63) are given by (Edwards and Spurgeon 1998):

The linear gain

$$G_l = T_o^{-1}\begin{bmatrix} \mathcal{A}_{12} \\ \mathcal{A}_{22} - \mathcal{A}_{22}^s \end{bmatrix} \tag{4-72}$$

and the non-linear gain

$$G_n = \| \mathcal{D}_2 \| T_o^{-1} \begin{bmatrix} 0 \\ I_p \end{bmatrix} \tag{4-73}$$

and

$$v_o(t) = \begin{cases} -\rho_o(t, y, u) \dfrac{P_2 C e_x^{sm}(t)}{\| P_2 C e_x^{sm}(t) \|} & \text{if } C e_x^{sm} \neq 0 \\ 0 & \text{otherwise} \end{cases} \tag{4-74}$$

4.3.2 The Edwards-Spurgeon observer for fault estimation

The SMO properties of interest that are important for fault reconstruction/estimation were based on the concept of the equivalent '*output error injection signals*' proposed in (Edwards and Spurgeon, 1998; Edwards *et al*, 2000). Their work forms the basis for the development of an active approach to FTC based on actuator faults, described in Section 4.4. Consider a nominal linear system with faults given by:

$$\dot{x}(t) = Ax(t) + Bu(t) + Df_a(t) \tag{4-75}$$

$$y(t) = Cx(t) + f_s(t) \tag{4-76}$$

where: $A \in \Re^{nxn}, B \in \Re^{nxm}, C \in \Re^{pxn}, D \in \Re^{nxq}$ satisfying $q \leq p < n$, and the matrices B, C and D are full rank. $f_a(t)$ and $f_s(t)$ are the functions that represent actuator and sensor faults, respectively. However, it is assumed that only $y(t)$ and $u(t)$ are measurable, whereas the states of the system are unknown.

Since an observer has been designed using Eq. (4-63), a sliding motion can be obtained, thus estimates of $f_a(t)$ and $f_s(t)$ can be determined from approximating the equivalent control (Edwards and Spurgeon, 1998; Edwards *et al*., 2000).

4.3.3 Actuator fault estimation

Following the work of Edwards and Spurgeon (1998), consider the case when $f_s(t) = 0$ but $f_a(t) \neq 0$. This implies that during the sliding motion, the output estimation error is equal to zero i.e. $e_y^{sm}(t) = 0$ and then $\dot{e}_y^{sm}(t) = 0$. Therefore, Eq. (4-71) becomes:

$$0 = \mathcal{A}_{21} e_{x_1}^{sm}(t) - \mathcal{D}_2 f_a(t) + v_{oeq}(t) \tag{4-77}$$

where v_{oeq} is the equivalent output error injection signal necessary to maintain sliding. From Eq. (4-70) it follows that: $e_{x_1}^{sm}(t) \to 0$ and hence that:

$$v_{oeq}(t) \to \mathcal{D}_2 f_a(t) \tag{4-78}$$

As $v_{oeq}(t)$ is a discontinuous signal, an appropriate approximation must be used in order to recover the equivalent output injection. The discontinuous component in Eq. (4-67) is now replaced by a continuous approximation:

$$v_{o\sigma}(t) = \rho_o \left\| \mathcal{D}_2 \right\| \frac{P_2 e_y^{sm}(t)}{\left\| P_2 e_y^{sm}(t) \right\| + \sigma_{sm}} \tag{4-79}$$

where σ_{sm} is a small positive scalar.

It is important to note that the equivalent feedback can be approximated, to any degree of accuracy, which depends on the choice of σ_{sm} (Edwards and Spurgeon 1998). Since $rank(\mathcal{D}_2) = q$ it follows from Eq. (4-78) that:

$$f_a(t) \approx -\rho_o \left\| \mathcal{D}_2 \right\| (\mathcal{D}_2^T \mathcal{D}_2)^{-1} \mathcal{D}_2^T \frac{P_2 e_y^{sm}(t)}{\left\| P_2 e_y^{sm}(t) \right\| + \sigma_{sm}} \tag{4-80}$$

From Eq. (4-80), it can be seen that the $f_a(t)$ term can be computed online, and depends only on the output estimation error $e_y^{sm}(t)$. '*…Therefore, $f_a(t)$ can be approximated to any degree of accuracy…*' (Edwards and Spurgeon, 1998).

4.3.4 Sensor fault estimation

Edwards and Spurgeon (1998) and Edwards *et al*, (2000) also consider the case when $f_a(t) = 0$ but $f_s(t) \neq 0$. Since the output of the system is represented by Eq. (4-76), it follows that:

$$e_y^{sm}(t) = Ce_x^{sm}(t) - f_s(t) \tag{4-81}$$

The state estimation error in the observer as described in Section 4.3.1, is now given by:

$$\dot{e}_{x_1}^{sm}(t) = \mathcal{A}_{11} e_{x_1}^{sm}(t) + \mathcal{A}_{12} f_s(t) \tag{4-82}$$

$$\dot{e}_y^{sm}(t) = \mathcal{A}_{21} e_{x_1}^{sm}(t) + \mathcal{A}_{22}^{s} e_y^{sm}(t) - \dot{f}_s(t) + \mathcal{A}_{22} f_s(t) + v_o(t) \tag{4-83}$$

It can be seen that the functions f_s and $\dot{f}_s$ appear as output disturbances, and thus the nonlinear gain $\rho_o(t, y, u)$ in Eq. (4-74) must be chosen sufficiently large in order to maintain the sliding and overcome the disturbance effect (Edwards and Spurgeon, 1998). As discussed in Section 4.3.3, during sliding $e_y^{sm}(t) = 0$ and then $\dot{e}_y^{sm}(t) = 0$, provided that a sliding motion in Eq. (4-83) can be obtained by:

$$0 = \mathcal{A}_{21} e_{x_1}^{sm}(t) - \dot{f}_s(t) + \mathcal{A}_{22} f_s(t) + v_{oeq}(t) \tag{4-84}$$

If it now be assumed that the sliding motion dynamics are fast $\dot{e}_{x_1}^{sm}(t) \approx 0$, then Eq. (4-82) can be rewritten as:

$$e_{x_1}^{sm}(t) \approx -\mathcal{A}_{11}^{-1} \mathcal{A}_{12} f_s(t) \tag{4-85}$$

For a slowly-varying fault i.e. $\dot{f}_s(t) \approx 0$, the dynamics of the sliding motion are sufficiently fast, so that by replacing $e_{x_1}^{sm}(t)$ in Eq. (4-84) with Eq. (4-85) gives:

$$\begin{aligned} v_{oeq}(t) &\approx \mathcal{A}_{21}[\mathcal{A}_{11}^{-1} \mathcal{A}_{12} f_s(t)] - \mathcal{A}_{22} f_s(t) \\ &\approx (\mathcal{A}_{21} \mathcal{A}_{11}^{-1} \mathcal{A}_{12} - \mathcal{A}_{22}) f_s(t) \\ &\approx -(\mathcal{A}_{22} - \mathcal{A}_{21} \mathcal{A}_{11}^{-1} \mathcal{A}_{12}) f_s(t) \end{aligned} \tag{4-86}$$

As described in Section 4.3.3, the equivalent control signal v_{oeq} can be calculated approximately from Eq. (4-79). If $(\mathcal{A}_{22} - \mathcal{A}_{21} \mathcal{A}_{11}^{-1} \mathcal{A}_{12})$ is non-singular, then the sensor fault signal can be obtained from:

$$f_s(t) \approx -(\mathcal{A}_{22} - \mathcal{A}_{21} \mathcal{A}_{11}^{-1} \mathcal{A}_{12})^{-1} v_{o\sigma}(t) \tag{4-87}$$

Edwards and Spurgeon (1998) and Edwards *et al* (2000) suggest that '*…even if* $(\mathcal{A}_{22} - \mathcal{A}_{21}\mathcal{A}_{11}^{-1}\mathcal{A}_{12})$ *singular, it may still be possible to estimate some of the sensor faults depending on the structure of the rank-deficiency...*'

However, this method was later improved for robust application in the presence of model uncertainty by Tan and Edwards (2003) using an LMI formulation. From Sections 4.2 and 4.3, it is clear that there are some inherent benefits of SMC and SMO for FTC. Section 4.4 highlights some of these advantages in terms of FTC via friction compensation example.

4.4 FTC Approach based on Sliding Mode

As discussed in the Section 4.2, once perfect sliding occurs, a reduced-order order motion is completely insensitive to matched and bounded uncertainty [i.e. any matched uncertainty does not have an effect on the sliding motion and the system performance]. This makes the SMC a powerful tool for controlling the system with the presence of uncertainty and has interesting potential for future research in the area (Edwards and Spurgeon, 1998; Alwi, 2008). The alternative idea used here is to consider actuator fault signals acting in the system as matched uncertainty terms and thereby use the well-known matching conditions summarised in Section 4.2.3.

Considering the dynamic system with actuator faults:

$$\begin{aligned} \dot{x}(t) &= Ax(t) + B(I - \eta^a)u(t) \\ &= Ax(t) + Bu(t) + \underbrace{(-B)}_{D}\underbrace{(\eta^a)u(t)}_{\xi(t,u,x)} \\ &= Ax(t) + Bu(t) + f_m(t,x,u) \end{aligned} \qquad (4\text{-}88)$$

This is equivalent to Eqs. (4-17) and (4-27).

where: η^a is the so called *fault-effect factor* of Chen *et al*, (1999) and Chen and Patton (2001), and $\eta^a = diag(\eta_1^a,\ldots,\eta_m^a)$, such that $0 \le \eta_i^a < 1$ represents a fault of the i^{th} actuator i.e. when $\eta_i^a = 0$ implies that the actuator operates normally. $\eta_i^a > 0$ means that some degree of fault effect occurs in the actuator. It can be seen that the system with the presence of an actuator fault in Eq. (4-88) fits very well to the definition for

matched uncertainty (Jones, 2005; Alwi, 2006, 2007, 2008). This is true as $D = B$ [i.e. $\mathbf{R}(D) \subset \mathbf{R}(B)$].

As described in Section 4.2.4, the effect of matched uncertainty (considered here as an actuator fault) can be removed or compensated depending only on the nonlinear gain $\rho_c(t, x)$. This means the system stability and sliding will always be guaranteed as long as the magnitude of $\rho_c(t, x)$ is chosen large enough to overcome the matched uncertainty or fault i.e. it must be greater than the magnitude of the actuator fault [see Section 4.4.1]. This adaptive property makes the SMC a powerful method for active FTC (Hess and Wells, 2003; Alwi, 2006, 2007, 2008). This is one motivation for work in this Chapter.

For the case when there are modelling uncertainties which are matched, the nonlinear gain must be large enough to encompass both the actuator fault effect factors and the uncertainty terms. This scenario is similar to the problem discussed in Section 3.5 for which the robustness of the fault estimator is not required for achieving fault compensation (within the context of the adaptive ASO scheme).

The equivalent problem in the sliding mode context is that the SMO does not take into account the model uncertainty but is assumed to be an estimator of the fault signal(s) which can be associated with the model uncertainty. Since the fault and uncertainty terms are assumed to be added, the fault estimation in the presence of modeling uncertainty will be compromised. The concept that is important is that the SMO estimation takes into account automatically the combination of both the actuator faults and matched uncertainty. In fact, the pure quality of the fault estimation is not the major issue, although the quality of the compensation of this signal is important. Hence, as stated in Section 3.5 there is a *trade-off* between estimation and compensation. Since the goal is to use the SMO and SMC schemes together to achieve good FTC performance good quality compensation will lead to good active FTC performance.

It is for this reason that the work of Tan and Edwards (2003) on robust estimation via SMO is not appropriate here. In fact it can be argued, in a similar manner to that shown (via an example) in Section 3.5, that the robust SMO estimator will not lead to good compensation performance when combined with an SMC in an adaptive FTC structure.

4.4.1 The stability of SMC with the presence of an actuator fault

The Section demonstrates that the two component controller of Eq. (4-37) will still induce sliding in the presence of actuator faults. As described in Eq. (4-88) the actuator faults acting in the system can be represented as uncertainty. Recall that the actuator faults [i.e. $B = D$] in Eq. (4-88) satisfy the matching condition. Hence, the problem of the stability of the closed–loop system under the effect of this actuator fault (i.e. matched uncertainty) becomes one of ensuring that sliding occurs, despite the presence of actuator faults. This is in fact a modification of the work described by Edwards and Spurgeon (1998) [Section 3.5 in Chapter 3] for the SMC stability condition in the matched uncertainty case [the unmatched case does not apply in this work as a consequence of the fault estimation bounds described in Eq. (4-88)].

Substituting the linear and nonlinear control components in Eq. (4-37) to (4-39) into Eq. (4-36) produces the following system:

$$\dot{x}_1(t) = \bar{A}_{11}x_1(t) + A_{12}S_2^{-1}s(t) \tag{4-89}$$

$$\dot{s}(t) = \Phi s(t) - \rho_c(t,x)\frac{P_2 s(t)}{\|P_2 s(t)\|} + S_2\bar{f}_m(t,x,u) \tag{4-90}$$

On applying the Lyapunov function $V(s) = s^T P_2 s$ and its time derivative $\dot{V}(s)$, it can be verified that:

$$\begin{aligned}
\dot{V}(s) &= \dot{s}^T P_2 s + s^T P_2 \dot{s} \\
&= (\Phi s - \rho_c(t,x)\frac{P_2 s}{\|P_2 s\|} + S_2\bar{f}_m)^T P_2 s \\
&\quad + s^T P_2(\Phi s - \rho_c(t,x)\frac{P_2 s(t)}{\|P_2 s(t)\|} + S_2\bar{f}_m) \\
&= s^T \underbrace{(\Phi^T P_2 + P_2\Phi)}_{-I_m} s - 2\rho_c(t,x)\frac{1}{\|P_2 s\|}(s^T P_2 P_2 s) + 2s^T P_2 S_2\bar{f}_m \\
&= -s^T s - 2\rho_c(t,x)\|P_2 s\| + 2s^T P_2 S_2\bar{f}_m
\end{aligned} \tag{4-91}$$

where $s^T P_2 P_2 s = \|P_2 s\|^2$ and $\|s^T P_2 S_2\bar{f}_m\| < \|P_2 s\|\|S_2\|\|\bar{f}_m\|$ from the *Cauchy–Schwarz* inequality:

$$\begin{aligned}
\dot{V} &\le -\|s\|^2 - 2\rho_c(t,x)\|P_2 s\| + 2\|P_2 s\|\|S_2\|\|\bar{f}_m\| \\
&\le -\|s\|^2 - 2\|P_2 s\|(\rho_c(t,x) - \|S_2\|\|\bar{f}_m\|)
\end{aligned} \tag{4-92}$$

By re-arranging $\rho_c(t,x)$ in (4-92) in terms of the uncertainty $\bar{f}_m$ using the definition of $\rho_c(t,x)$ given in Eq. (4-41). From Eqs (4-37) and (4-39) and using the triangle inequality property of norms:

$$\begin{aligned} \|u(t)\| &\leq \|u_l\| + \|u_n\| \\ &\leq \|u_l\| + \rho_c(t,x)\left\|\Lambda^{-1}\right\| \end{aligned} \tag{4-93}$$

where $S_2 B_2 = \Lambda$, then Eq. (4-41) can be written as:

$$\rho_c(t,x)(1 - k_m\left\|B_2^{-1}\right\|) \geq \|S_2\|(k_m\|u_l\| + \alpha(t,x)) + \gamma_c \tag{4-94}$$

Rearranging this inequality yields:

$$\begin{aligned} \rho_c(t,x) &\geq \|S_2\|(k_m\|u_l\| + \alpha(t,x)) + \gamma_c + \rho_c(t,x)k_m\left\|B_2^{-1}\right\| \\ &\geq \|S_2\|(k_m\|u_l\| + \alpha(t,x)) + \gamma_c + \rho_c(t,x)k_m\left\|S_2\Lambda^{-1}\right\| \\ &\geq \|S_2\|(k_m\|u_l\| + \rho_c(t,x)k_m\left\|\Lambda^{-1}\right\| + \alpha(t,x)) + \gamma_c \end{aligned} \tag{4-95}$$

Using Eqs (4-93) and (4-28), the Eq. (4-95) can be written as:

$$\begin{aligned} \rho_c(t,x) &\geq \|S_2\|\underbrace{(k_m\|u\| + \alpha(t,x))}_{\bar{f}_m} + \gamma_c \\ &\geq \|S_2\|\left\|\bar{f}_m\right\| + \gamma_c \end{aligned} \tag{4-96}$$

Substituting $\rho_c(t,x)$ in Eq. (4-96) into Eq. (4-92) yields:

$$\begin{aligned} \dot{V}(t) &\leq -\|s\|^2 - 2\|P_2 s\|(\|S_2\|\left\|\bar{f}_m\right\| + \gamma_c) + 2\|P_2 s\|\|S_2\|\,\bar{f}_m \\ &\leq -\|s\|^2 - 2\gamma_c\|P_2 s\| - 2\|P_2 s\|\|S_2\|\,\bar{f}_m + 2\|P_2 s\|\|S_2\|\,\bar{f}_m \\ &\leq -\|s\|^2 - 2\gamma_c\|P_2 s\| \end{aligned} \tag{4-97}$$

This inequality shows that the controller in the form Eq. (4-37) induces ideal sliding on S in finite time, despite the presence of the actuator fault(s) [the matched uncertainty in this context]. ■

4.5 Friction Compensation Case Study

To illustrate the above discussion a tutorial example of the nonlinear inverted pendulum simulation with a cart (as described in Section 3.4.2) is used here as a friction

compensation problem invoking the combined sliding estimator and VSC controller in on-line FTC system. In Sections 4.2 and 4.3, some ideas and benefits of using sliding mode schemes for FTC were discussed. In this Section the benefit of using SMC, especially when handling actuator faults is demonstrated using a realistic inverted pendulum model with the development of an online adaptive scheme for the nonlinear gain $\rho_c(t, x)$.

An on-line $\rho_c(.)$ gain is used in the nonlinear component of the control law of Eq. (4-39). The nonlinear adaptive gain reacts to the occurrence of the friction force (subject to the bounded magnitude of the online estimate of the friction force $\hat{f}_{fric}$) and attempts to maintain the sliding motion and nominal tracking performance (i.e. try to keep the switching function close to zero), however the linear control remains unchanged.

4.5.1 Friction estimation using SMO

This Section describes the properties of the SMO which can be used for friction estimation, based on the *equivalent output injection* concept (Edwards and Spurgeon, 1998). In Edwards *et al* (2000) the estimation problem (sensor and/or actuator faults) for the purpose of FDI is considered, whilst in this Chapter the actuator fault estimation problem is studied specifically as a basis for using the *FTC Approach to the Friction Compensation* (Patton *et al*., 2008b). Note that the isolation problem of FDI is not relevant as the type of fault and its action on the system is understood *a priori*.

Assume that an observer with the structure given in Eq. (4-63) has been designed and that a sliding motion has been established. Thus, the friction force ($\hat{f}_{fric}$) as presented in Eq. (3-21) can be computed via the so-called equivalent output injection (see Figure 4-1).

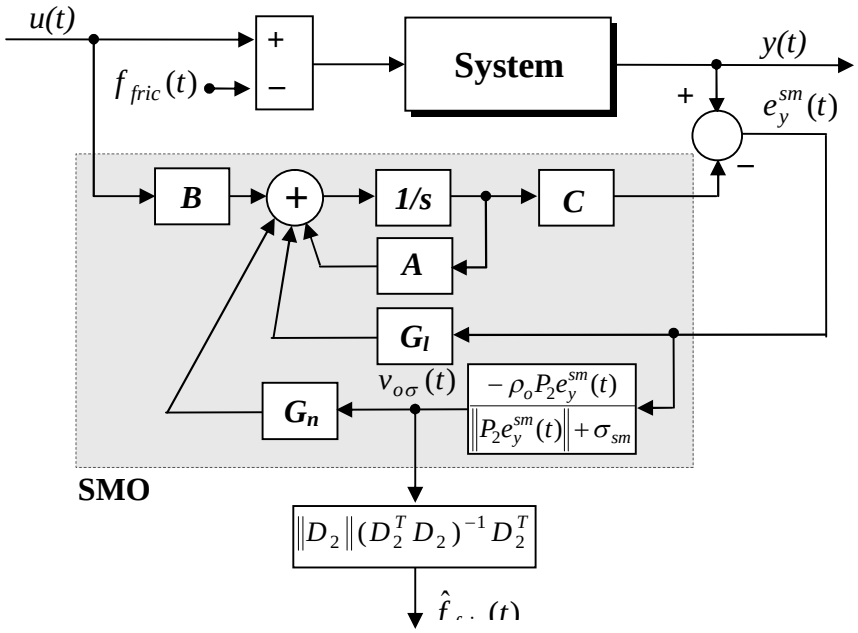

Figure 4-1: SMO and fault estimation
(adapted from Alwi, 2008)

The solution to Eq. (4-80) generates the estimates of the friction force, which are computed online so that an approximation for $\hat{f}_{fric}(t)$ can be obtained in real time (see Figure 4-1).

$$\hat{f}_{fric} \approx -\rho_o \|\mathcal{D}_2\|(\mathcal{D}_2^T\mathcal{D}_2)^{-1}\mathcal{D}_2^T \frac{P_2 e_y^{sm}(t)}{\|P_2 e_y^{sm}(t)\| + \sigma_{sm}} \qquad (4\text{-}98)$$

Using canonical from of Eq. (4-65) the system Eq. (3-21) becomes:

$$A = \left(\begin{array}{c|ccc} -10.0000 & 0.0000 & -67.6603 & 31.4960 \\ \hline 0.0000 & 0.0000 & 0.0000 & 1.0000 \\ 1.0000 & 0.0000 & 9.8548 & -3.1496 \\ 0.0091 & 0.0000 & -1.8437 & -2.0158 \end{array}\right),\ B = \begin{pmatrix} 0.0000 \\ 0.0000 \\ 0.0000 \\ 0.3205 \end{pmatrix} \text{ and}$$

$$C = \left(\begin{array}{c|ccc} 0.0000 & 1.0000 & 0.0000 & 0.0000 \\ 0.0000 & 0.0000 & 1.0000 & 0.0000 \\ 0.0000 & 0.0000 & 0.0000 & 1.0000 \end{array}\right)$$

The SMO design parameters are given as follows: the design of $A_{11} = -10$, and $A_{22}^s = diag[-11.5,-12.5,-13.5]$, with $\rho_o = 25.50$, $\sigma_{sm} = 0.045$, $D_2 = col[0,0,0.3205]$ and $P_2 = diag[0.0435, 0.0400, 0.0370]$ (see Section 4.3.3).

The associated gains from the observer representation in Eq. (4-63) are obtained by the modified scheme proposed in (Edwards *et al*, 2000) as:

$$G_l = \begin{pmatrix} 11.5000 & 0.0000 & 1.0000 \\ 0.0000 & 22.8548 & -3.1496 \\ 0.0000 & -1.8392 & 11.4842 \\ 0.0000 & 158.4500 & -35.7133 \end{pmatrix}$$

$$G_n = \begin{pmatrix} 0.3205 & 0.0000 & 0.0000 \\ 0.0000 & 0.3205 & 0.0000 \\ 0.0000 & 0.0000 & 0.3205 \\ 0.0000 & 3.3189 & -1.0095 \end{pmatrix}$$

The transformation matrix T_o is:

$$T_o = \begin{pmatrix} 0.0000 & -9.8548 & 3.1496 & 1.0000 \\ 1.0000 & 0.0000 & 0.0000 & 0.0000 \\ 0.0000 & 1.0000 & 0.0000 & 0.0000 \\ 0.0000 & 0.0000 & 1.0000 & 0.0000 \end{pmatrix}$$

The nonlinear inverted pendulum system is simulated in Matlab/Simulink and the Stribeck friction force f_{fric} is implemented as in (Putra *et al*, 2004).

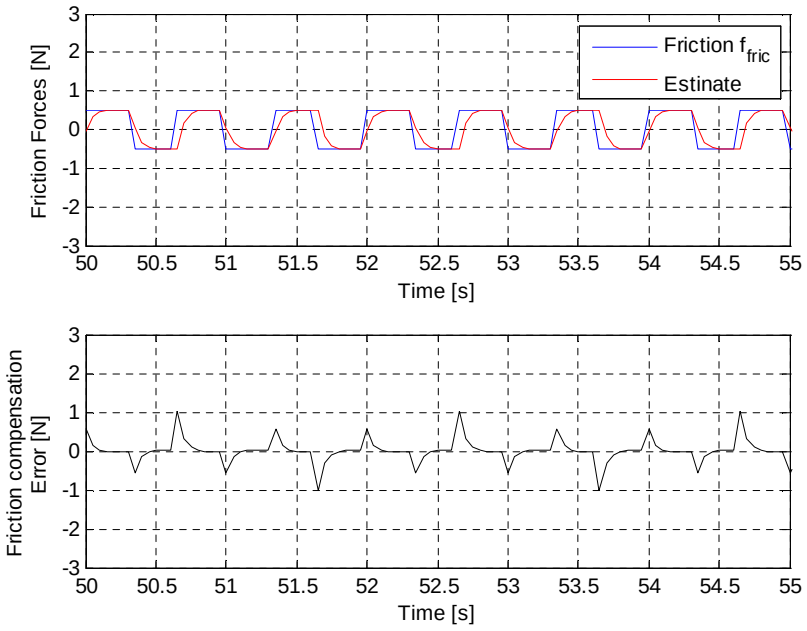

Figure 4-2: Simulation results of: (a) friction force, and its estimate, (b) friction force estimation error (with $F_s = 0.5N$)

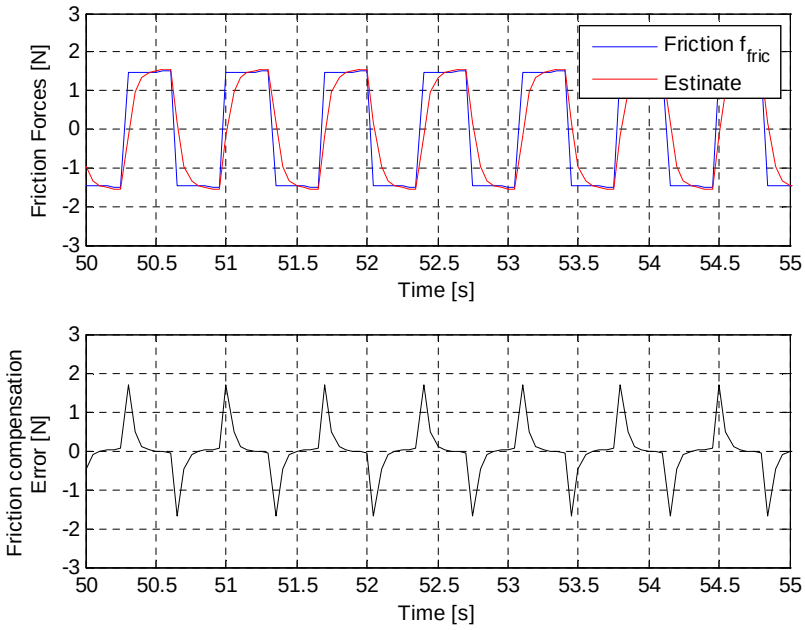

Figure 4-3: Simulation results of: (a) friction force, and its estimate, (b) friction force estimation error (with $F_s = 1.5N$)

Figure 4-2 and Figure 4-3 show a comparison of the simulated friction force f_{fric} with the simulated friction force estimate $\hat{f}_{fric}$ [see (a)]. Note that the estimates lag the simulated force due to the discontinuity of the friction force during reversed motion. The lower plot in (b) is the estimation error signal which reflects this discontinuous behaviour.

The following Section 4.5.2 , the friction force estimate $\hat{f}_{fric}(t)$ is used to achieve the FTC by compensating for the uncertain element of the control signal arising from the friction force.

4.5.2 Friction compensation sliding SMO/SMC system

The friction force estimate arises in the SMO analysis as an equivalent feedback signal as described in Section 4.5.1 and Figure 4-1 is used as the matched uncertainty in the SMC design for FTC. The approach describes the SMC as an adaptive control scheme designed to meet the FTC requirements, based on the friction force estimation. A bound derived from this estimation is used in the nonlinear component of the SMC.

Figure 4-4 illustrates the mechanism for combining the SMC and SMO/fault estimator structures together. The link is shown by the shaded box with continuous line edge,

giving the point at which the friction force estimate signal $\hat{f}_{fric}(t)$ enters the SMC structure from the SMO/estimator in term of $\hat{\eta}^{fric}(t)$ (so called *friction fault-effect factor*) (Chen *et al.*,1999).

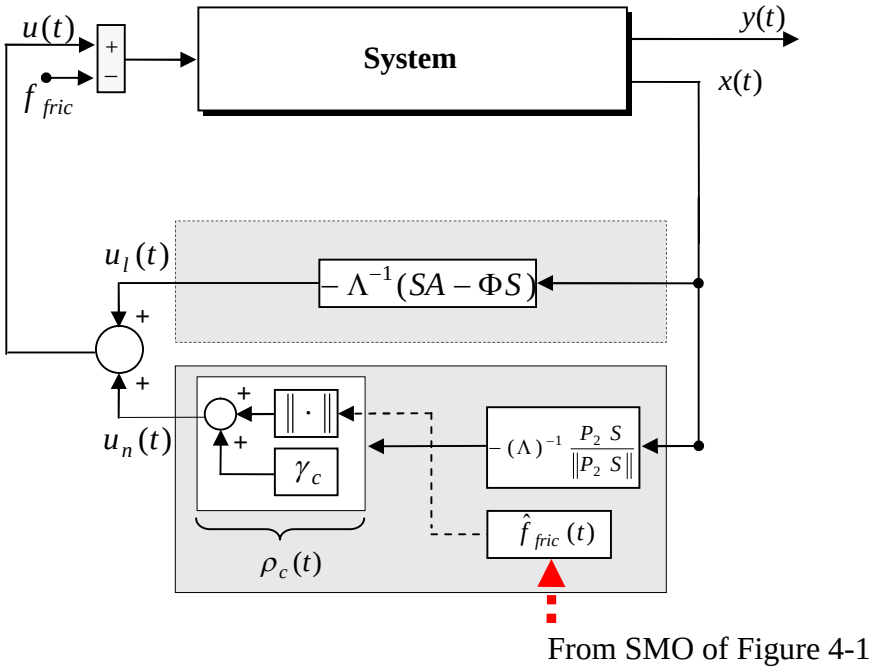

Figure 4-4: FTC strategy for friction compensation using SMC and SMO

Re-called Eq. (3-21) as follows:

$$\begin{aligned}\dot{x}(t) &= Ax + B[u(t) - f_{fric}(t)] \\ &= Ax + Bu(t) - Bf_{fric}(t)\end{aligned} \tag{4-99}$$

The online estimate of friction force $f_{fric}(t)$ in Eq. (4-99) is obtained from the SMO (as discussed in Section 4.4), and hence Eq. (4-99) can now be re-written into the term of $\hat{\eta}^{fric}(t)$ [i.e. since $\hat{f}_{fric}(t)$ is obtained] as follows:

$$\begin{aligned}\dot{x}(t) &= Ax(t) + Bu(t) + \underbrace{(-B)}_{D}\underbrace{(\hat{\eta}^{fric})u(t)}_{\xi(t,u,x)} \\ &= Ax(t) + Bu(t) + f_m(t,x,u)\end{aligned} \tag{4-100}$$

It can be seen that the friction force acting on the system [see the last term in the right-hand side of Eq. (4-100)] can be represented in the same way as the uncertainty acting on the system [similar to Eq. (4-88)] , i.e.

$$\xi(t,\, x,\, u) = (\hat{\eta}^{fric})u(t) \tag{4-101}$$

or

$$f_m(t,x,u) = D\xi(t,\,x,\,u) \\ = -B(\hat{\eta}^{\,fric})u(t) \tag{4-102}$$

It can be seen that the relationship between the Eq. (4-102) and Eq. (4-99) is equivalent to:

$$Bf_{fric}(t) = B(\hat{\eta}^{\,fric})u(t) \tag{4-103}$$

Thus, the matched uncertainty (considered here as a friction force) in Eq. (4-102) can be given by:

$$f_m(t,x,u) = -Bf_{fric}(t) \tag{4-104}$$

As discussed in Section 4.2.4 and Eqs. (4-28) and (4-41), for the matched *uncertainty condition*, and the scalar function $\rho_c(t,x)$ depends on the magnitude of the matched uncertainty. This can be any function satisfying:

Recall $\rho_c(t,x)$ from Eq. (4-96) as follows:

$$\rho_c(t,x) \;\geq\; \|S_2\|\|f_m(t,x,u)\| + \gamma_c \tag{4-105}$$

From Eqs. (4-105) and (4-106), it can be seen that $\rho_c(t,x)$ becomes a function of friction estimation $\hat{f}_{fric}(t)$ only as follows:

$$\rho_c(t) \;\geq\; \|S_2\|\left\| B\hat{f}_{fric}(t)\right\| + \gamma_c \tag{4-106}$$

This is shown in Figure 4-4, and for this design $\gamma_c = 0.065$, so that $\rho_c(t)$ must be greater than the magnitude of $\|S_2\|\left\| B\hat{f}_{fric}(t)\right\| + \gamma_c$, $\forall t$ (i.e. considered here as the matched uncertainty signal). In other words Eq. (4-106) forms an adaptive control mechanism in the SMC in term of $\rho_c(t)$ via the on-line generated friction estimates $\hat{f}_{fric}(t)$.

In the following Section 4.2, the parameters for the design of the SMC are given as follows:

$$S = [7.4040, 14.9867, 5.3020, 2.7326]$$

$$L_{sm} = [41.9427, 170.6191, 43.2255, 29.2265]$$

Giving a design matrices $P_2 = 0.0833$, Λ = -1.0592 and $Q = diag[10.00,1.00,1.00,0.10]$.

Simulation results for given initial values $x(0) = [1.1 \quad -1.1 \quad 0 \quad 0]^T$, and from Eqs (4-37) to (4-42), $u_l(t)$ and $u_n(t)$ can be obtained by:

$$u_l(t) = \underbrace{\begin{pmatrix} 41.9427 & 170.6191 & 43.2255 & 29.2265 \end{pmatrix}}_{L_{sm}} x(t) \tag{4-107}$$

$$u_n(t) = -\rho_c(t)\,\Lambda^{-1}\frac{P_2 s(t)}{\|P_2 s(t)\|} \tag{4-108}$$

where $\rho_c(t)$ is obtained from Eq. (4-106).

Simulation results will now be presented to illustrate the system operation with and without friction compensation.

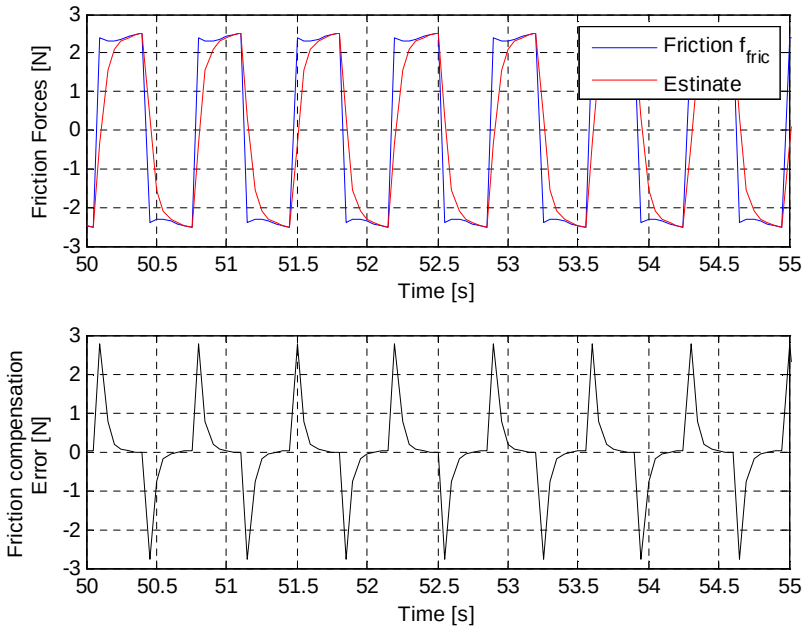

Figure 4-5: The simulation result of friction, its estimation ($\hat{f}_{fric}$), and estimation error (with $F_s = 2.5N$)

Figure 4-5 shows the Stribeck friction force (Putra *et al*, 2004), its estimate and estimation error implemented by the on-line SMO, as designed in Section 4.5.1.

Figure 4-6(a), Figure 4-7(a) and Figure 4-8(a) show that the dynamic sliding mode controller works well in the absence of friction force on the cart.

However, the controlled pendulum exhibits limit cycling in the presence of friction with $F_s = 2.5N$ as shown in the first *40s* of Figure 4-6(b), Figure 4-7(b) and Figure 4-8(b), respectively.

The Figure 4-6(c), Figure 4-7(c) and Figure 4-8(c) also shows that when the frictions force is compensated using $\hat{f}_{fric}(t)$ provided by the SMO in Eq. (4-98) and SMC mechanism in Eqs. (4-107) and (4-108), starting at *t=40s* the limit cycling is significantly suppressed.

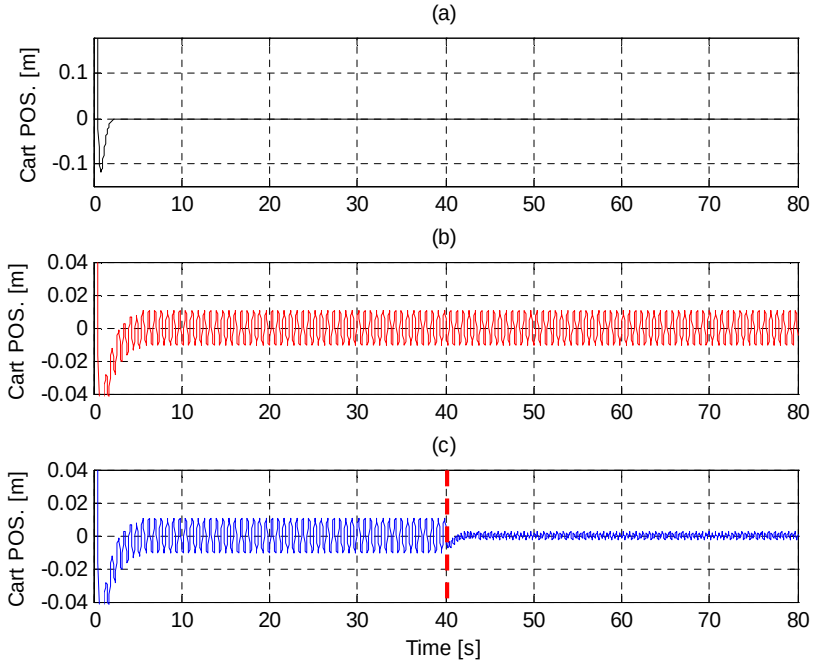

Figure 4-6: The output response of cart position: (a) without friction force, (b) with friction force and (c) with friction compensation mechanism activated at *t = 40s*

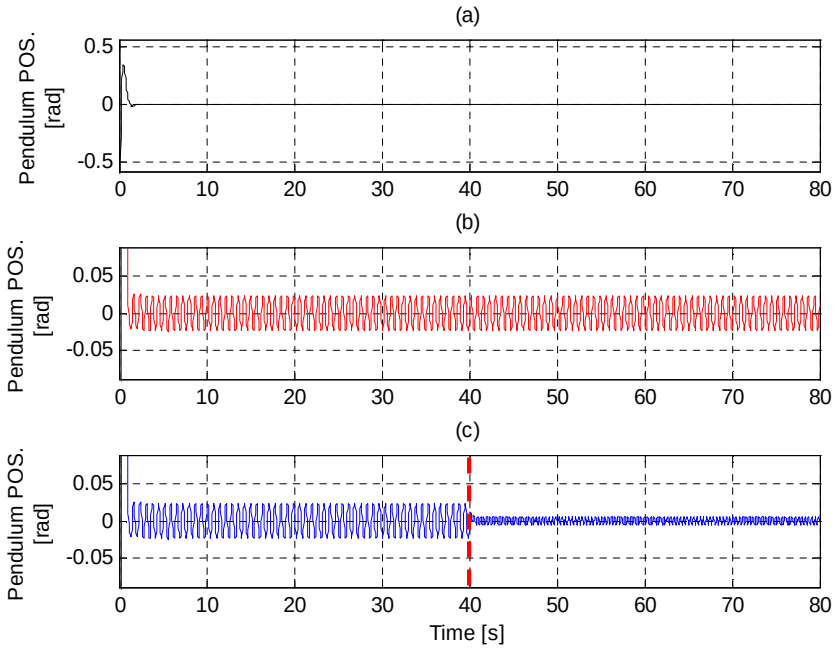

Figure 4-7: The output response of pendulum position: (a) without friction force, (b) with friction force and (c) with friction compensation mechanism activated at *t = 40s*

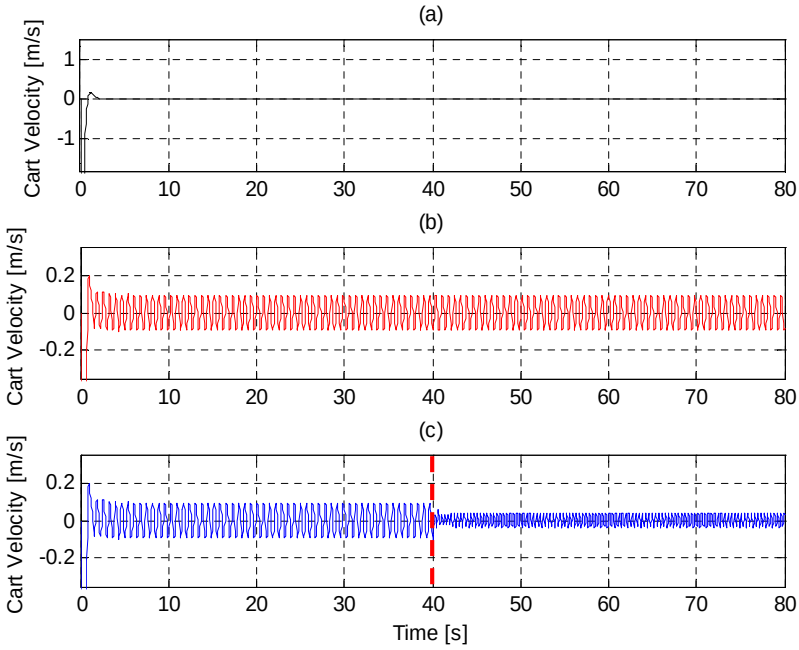

Figure 4-8: The output response of cart velocity: (a) without friction force, (b) with friction force and (c) with friction compensation mechanism activated at $t = 40s$

4.6 Conclusion

The purpose of this Chapter is to develop a framework for adaptive and active FTC, based on the sliding mode concept. The proposed FTC architecture uses a combination of SMO and SMC structures which jointly satisfy important stability bounds in terms of matched uncertainty via estimates of fault effect factors. To develop the required conditions for this new FTC architecture the Chapter examines carefully the design processes and concepts that accompany the individual SMO and SMC problems. Although much of the material is taken from well know research papers or books the description is important in order to develop the new FTC subject and outline some important new developments in this work.

The work proposed in this Chapter is an alternative approach to the scheme and architecture proposed in Chapter 3, with considerable new material presented in both cases. The main thrust of this Chapter is to replace the ASO/compensating adaptive controller scheme of Chapter 3 with the combination of the SMO and SMC. In this context this combination is a new contribution to the field of active and adaptive FTC. Whilst, the adaptive FTC approach described is applicable to a wide range of uncertain systems with faults, the example chosen formulates a new problem in its own right. This is the problem of considering the friction forces acting in mechatronic systems as

actuator-related faults which can be compensated with an adaptive control mechanism. In common with the material presented in Chapter 3, it is argued that this is a special case of an FTC problem with important potential application possibilities. The simulation results demonstrate the friction force compensation applied to a nonlinear inverted pendulum simulation including Stribeck friction. Another main advantage of the adaptive FTC approach to friction compensation is that it obviates the use of any form of mathematical model of the friction force phenomena. This is important since the friction phenomena are very difficult to model and it is difficult or almost impossible to develop control strategies based on inadequate friction modelling that have sufficient robustness to the friction modelling uncertainty

It is interesting to note that the sliding mode approach described in this Chapter offers some advantage over the equivalent FTC architecture described in Chapter 3. In this (sliding) approach the fault estimates are taken into account in the stability of the SMC, whilst in the ASO scheme of Chapter 3 the fault estimation is used within the control law and immediately affect the control performance.

Finally, all the ideas proposed in this Chapter can be immediately extended to cases of more general faults, for on-line FTC fault compensation and are not restricted to the friction case.

Chapter 5.
Fault Estimation and Compensation based on LPV Approach

5.1 Introduction

There has been significant interest in the control of time-varying systems over many years (Leith and Leithead, 2000; Balas, 2002). In recent years, Linear Parameter Varying (LPV) modelling methods have gained a great deal of interest, especially for applications related to vehicle, robust and aerospace control (Wu, 2001; Ganguli *et al*, 2002). The LPV approach is particularly appealing whenever nonlinear plants can be modelled as time-varying systems with on-line measurable state depending parameters.

Bokor and Balas (2004) introduced the concept of the use of fault detection filters for LPV systems and many other investigators have followed different aspects of this approach (Casavola *et al*, 2005a, 2005b, 2007, 2008; Henry *et al*, 2004; Marcos *et al*., 2005; Zolghadri *et al*, 2008; Weng *et al*, 2008; Henry, 2008).

For FTC, Chen *et al* (1999) tackled an FTC flight control design study using a *Linear Fractional Transformation* (LFT) approach via the LMI framework. Active FTC controllers are either based on on-line fault estimation (fault compensation) or FDI/FDD and control system reconfiguration. The fault estimate approaches require the generation of estimates of possible faults to allow the FTC controller to tolerate the

faults. Generally speaking the FDI problem is not relevant within this framework unless the more general problem of FDD is considered as this includes fault estimation. As discussed in Chapters 3 and 4, FTC via fault estimation is one powerful approach to on-line controller reconfiguration within the framework of adaptive control.

More recently, the idea of extending the control approach using LPV to encompass FTC schemes has been the subject of a number of studies (Shin and Belcastro, 2006; Rodrigues *et al*., 2005, 2007; Weng *et al*, 2007, 2008). Ganguli, Marcos and Balas (2002) use LPV ideas for the FTC problem based on actuator faults in aircraft. Their approach is immediately useful as a background to the work of this Chapter, although a different application subject is used.

This Chapter proposes a new design of an active FTC and polytopic LPV estimator for systems which can be characterized via a set of *Linear Matrix Inequalities* (LMIs) and can be obtained using efficient interior-point algorithms (Apkarian *et al*., 1995). In the work of this Chapter a polytopic LPV estimator is synthesized for providing actuator fault estimation which is used in an FTC scheme to schedule the state feedback gain. This gain is also calculated using LMIs in the fault-free case in order to maintain the system performance over a wide operating range within a proposed polytopic model. The resulting active FTC controller is a function of the fault effect factors as defined by Chen *et al* (1999) and Chen and Patton (2001) which can be derived on-line (in this case) from the residual vector of a polytopic LPV estimator mechanism.

Whilst the work uses well know results from Apkarian *et al* (1995) and several other investigators it has been motivated by:

(a) The research of Weng *et al* (2008) on fault estimation for rate bounded time-delay systems using LPV.

(b) The use of fault effect factors as described by Chen *et al* (1999) and Chen and Patton (2001)

The Weng *et al* (2008) work is limited only to fault estimation and does not include the full FTC problem, whilst the work of Chen *et al* (1999) and Chen and Patton (2001) pre-dates the development of the LPV approach to control and FTC in particular.

Hence, the novelty of this work lies in the combined use of fault estimation and fault compensation for FTC within an LPV framework. The effectiveness of the proposed method is demonstrated through a nonlinear two-link manipulator system with a fault in

the torque inputs at each manipulator joint. This is a nonlinear system that can be represented well by a polytopic model and this is also proposed in this Chapter.

5.2 General overview of the LPV approach

An LPV system is a mathematical realization/description of the linear parameter-varying nature of a system. LPV systems have state-space matrices that are fixed with some vector of varying parameters (Leith and Leithead, 2000; Wu 2001). From a practical point of view, the nonlinear systems can be reduced to an LPV representation by using the linearization along trajectories of the parameters. In other words, the idea in LPV is to obtain smooth semi–linear models that can vary or be scheduled using a parameter, for example an altitude and/or speed of an aircraft, so that the LPV model will mimic the actual nonlinear plant (Packard and Kantner, 1992; Shamma and Athans, 1992). Here, instead of choosing a combination of predefined linear models, the models change parametrically. The LPV model has the structure of a time-varying linear system with the parameter-dependent matrix quadruple $[A(\theta), B(\theta), C(\theta), D(\theta)]$.

where: $A(\theta) \in \Re^{nxn}$, $B(\theta) \in \Re^{nxm}$, $C(\theta) \in \Re^{pxn}$ and $D \in \Re^{pxm}$ as follows:

$$\begin{aligned} \dot{x}(t) &= A(\theta)x(t) + B(\theta)u(t) \\ y(t) &= C(\theta)x(t) + D(\theta)u(t) \end{aligned} \qquad (5 - 1)$$

where: θ is a vector of smoothly changing system parameters.

An LPV system can also reduced to a *Linear Time-Varying* (LTV) system with a given parameter trajectory and it can be reformed into a *Linear Time-Invariant* (LTI) system with a given a constant trajectory [i.e. θ is a constant]. From the control point of view, LPV control design is closely related to gain-scheduling (Apkarian *at el*., 1995; Leith and Leithead, 2000). It is motivated by the problem of obtaining and designing multiple models and controllers and the lack of performance and stability proofs for classical gain-scheduling (Balas, 2002; Ganguli *at el*., 2002). In comparison with the classical gain-scheduling methods where the gains arise from interpolations of predesigned controller gains, the LPV controllers are dependent on the parametric changes in the system.

The advantage of this LPV approach to nonlinear systems, compared with the multiple model switching and tuning (MMST) and interactive multiple model (IMM) methods is

that the LPV controllers do not need to be designed for all linearization points (Leith and Leithead, 2000; Wu, 2001).

5.3 Problem Statement

Consider the LPV system described by state-space equation as follows:

$$\begin{aligned} \dot{x}_p(t) &= A_p(\theta)x_p(t) + B_p(\theta)u(t) + E_p(\theta)d(t) + F_p(\theta)f(t) \\ y_p(t) &= C_p(\theta)x_p(t) + D_p(\theta)u(t) + G_p(\theta)d(t) + H_p(\theta)f(t) \end{aligned} \qquad (5-2)$$

where $x_p(t) \in \Re^n$, $u(t) \in \Re^p$, $y_p(t) \in \Re^m$, and $d(t) \in \Re^q$ are the states, control inputs, outputs, and disturbances. $f(t) \in \Re^g$ is the fault vector where each element $i = 1, 2, \ldots g$ corresponds to a specific fault, respectively. $\theta \in \Re^s$ is a time-varying parameter vector, and $A_p(\theta), B_p(\theta), C_p(\theta), D_p(\theta), E_p(\theta), F_p(\theta)$, $G_p(\theta)$ and $H_p(\theta)$ are the appropriate matrices with appropriate dimensions.

The assumptions that apply to system Eq. (5 - 2) are (Apkarian *et al*, 1995):

(A. 5-1) The system Eq. (5 - 2) is stable.

(A. 5-2) The vector $\theta(t)$ varies in a polytope Θ with vertices $\theta_1, \theta_2, \ldots, \theta_r$ ($r = 2^s$), i.e.:

$$\begin{aligned} \theta(t) \in \Theta &:= Co\{\theta_1, \theta_2, \cdots, \theta_r\} \\ &= \left\{ \sum_{i=1}^{r} \alpha_p^i \theta_i : \ \alpha_p^i \geq 0, \ \sum_{i=1}^{r} \alpha_o^i = 1 \right\} \end{aligned} \qquad (5-3)$$

(A. 5-3) The state-space matrices depend *affinely* on $\theta(t)$, the Eq. (5 - 2) is assumed to be polytopic, i.e.

$$\begin{pmatrix} A_p(\theta) & B_p(\theta) & E_p(\theta) & F_p(\theta) \\ C_p(\theta) & D_p(\theta) & G_p(\theta) & H_p(\theta) \end{pmatrix} \in Co\left\{ \begin{pmatrix} A_p(\theta_i) & B_p(\theta_i) & E_p(\theta_i) & F_p(\theta_i) \\ C_p(\theta_i) & D_p(\theta_i) & G_p(\theta_i) & H_p(\theta_i) \end{pmatrix}, \ i = 1, \cdots, r \right\} \qquad (5-4)$$

(A. 5-4) $C_p(\theta), D_p(\theta), G_p(\theta)$, and $H_p(\theta)$ are parameter independent, i.e.

$$C_p(\theta_i) = C_p, \quad D_p(\theta_i) = D_p, \quad G_p(\theta_i) = G_p, \quad H_p(\theta_i) = H_p, \quad i = 1, \ldots, r$$

The LPV systems encompass many relevant applications such as aircraft, missiles, multi-link robots, etc., particularly systems for which the time-varying state space parameters can be determined. The assumption **(A. 5-4)** can be removed by introducing some pre- and/or post-filtering and more details of this can be found in (Apkarian *at el*, 1995). This pre-and/or post-filtering is not necessary here the assumption **(A. 5-4)** is considered in its entirety.

5.4 The Polytopic LPV Estimator

Following from the motivation defined at the end of the Section 5.1, this Section proposes a structure [see Figure 5-1] which fits the objective of finding a estimator in order that the L_2-induced norm of the operator mapping $[u(t), d(t), f(t)]$ into the estimation error $e_f(t)$ is bounded by a scalar number γ, for all parameter trajectories (see the detailed discussion in ***Definition 5.1*** and Section 5.4.1).

Definition 5.1 (Garces *et al*., 2003)

The matrix $\boldsymbol{A}$ with n rows and m columns and real elements, $a_{ij} \in \Re$, $i = 1, \ldots, n$ and $j = 1, \ldots, m$, defines a linear mapping $x = \boldsymbol{A}z$ from $\Re^m$ to $\Re^n$ for the given vectors $x \in \Re^n$ and $z \in \Re^m$. The 'induced p-norm' of matrix $\boldsymbol{A}$ is defined as follows:

$$\|\boldsymbol{A}\|_p = \sup_{x \neq 0} \frac{\|\boldsymbol{A}z\|_p}{\|z\|_p} = \max_{\|z\|=1} \|\boldsymbol{A}z\|_p$$

where *sup* stands for supremum or least upper bound.

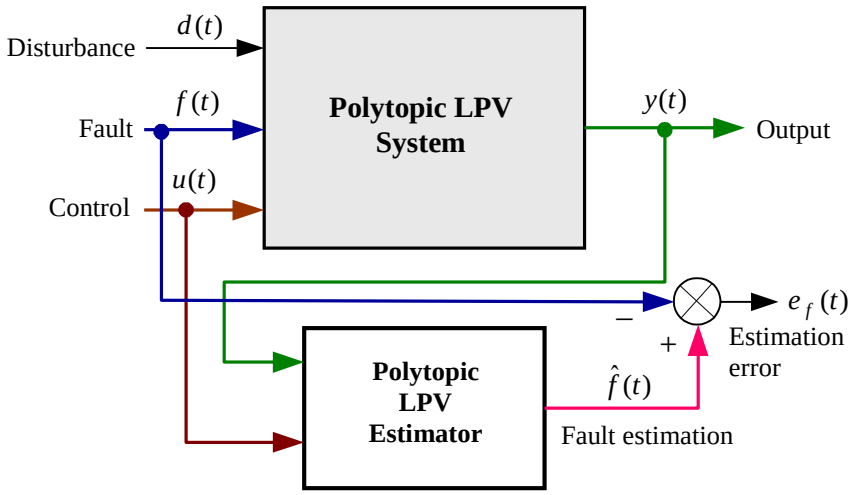

Figure 5-1: The polytopic LPV estimator structure

The design of a polytopic LPV estimator is given by:

$$\begin{aligned} \dot{x}_f(t) &= A_f(\theta)x_f(t) + B_f(\theta)\begin{pmatrix} u(t) \\ y_p(t) \end{pmatrix} \\ \hat{f}(t) &= C_f(\theta)x_f(t) + D_f(\theta)\begin{pmatrix} u(t) \\ y_p(t) \end{pmatrix} \end{aligned} \qquad (5-5)$$

such that the estimated error vector $e_f(t) = \hat{f}(t) - f(t) \in R^g$ is minimized.

Here $u(t)$ and $y_p(t)$ are defined by Eq.(5 - 1) , and $x_f(t) \in R^n$ is the state vector of the estimator, $\hat{f}(t)$ is the estimation of the fault $f(t)$. $A_f(\theta), B_f(\theta), C_f(\theta)$, and $D_f(\theta)$ are matrices with appropriate dimensions, to be designed. Therefore, the LPV estimator in Eq. (5 - 5) can be rewritten by:

$$\begin{aligned} \mathcal{F}(\theta) := & \begin{pmatrix} A_f(\theta) & B_f(\theta) \\ C_f(\theta) & D_f(\theta) \end{pmatrix} \in \\ & Co\left\{ \mathcal{F}_i = \begin{pmatrix} A_f(\theta_i) & B_f(\theta_i) \\ C_f(\theta_i) & D_f(\theta_i) \end{pmatrix}, \right. \\ & \left. i = 1, \cdots, r \right\} \end{aligned} \qquad (5-6)$$

The following system can be obtained from the combination of the LPV system of Eq. (5 - 2) with the fault estimator Eqs (5 - 5) and (5 - 6) :

$$
\begin{aligned}
\underbrace{\begin{bmatrix}\dot{x}_p(t)\\ \dot{x}_f(t)\end{bmatrix}}_{\dot{x}_{pf}(t)} &= \begin{bmatrix} A_p(\theta)x_p(t)+B_p(\theta)u(t)+E_p(\theta)d(t)+F_p(\theta)f(t) \\ A_f(\theta)x_f(t)+B_f(\theta)\begin{pmatrix} u(t) \\ C_p(\theta)x_p(t)+D_p(\theta)u(t)+G_p(\theta)d(t)+H_p(\theta)f(t)\end{pmatrix}\end{bmatrix} \\
&= \begin{bmatrix} A_p(\theta)x_p(t) \\ A_f(\theta)x_f(t)+B_f(\theta)\begin{pmatrix} 0 \\ C_p(\theta)x_p(t)\end{pmatrix}\end{bmatrix} \\
&\quad + \begin{bmatrix} B_p(\theta)u(t)+E_p(\theta)d(t)+F_p(\theta)f(t) \\ B_f(\theta)\begin{pmatrix} u(t) \\ D_p(\theta)u(t)+G_p(\theta)d(t)+H_p(\theta)f(t)\end{pmatrix}\end{bmatrix} \\
&= \underbrace{\begin{bmatrix} A_p(\theta) & 0 \\ B_f(\theta)\begin{pmatrix} 0 \\ C_p(\theta)\end{pmatrix} & A_f(\theta)\end{bmatrix}}_{\bar{A}(\theta)} \underbrace{\begin{bmatrix}x_p(t)\\ x_f(t)\end{bmatrix}}_{x_{pf}(t)} \\
&\quad + \underbrace{\begin{bmatrix} \begin{pmatrix}B_p(\theta) & E_p(\theta) & F_p(\theta)\end{pmatrix} \\ B_f(\theta)\begin{pmatrix} I & 0 & 0 \\ D_p(\theta) & G_p(\theta) & H_p(\theta)\end{pmatrix}\end{bmatrix}}_{\bar{B}(\theta)} \underbrace{\begin{bmatrix}u(t)\\ d(t)\\ f(t)\end{bmatrix}}_{w_{udf}(t)} \\
&= \bar{A}(\theta)x_{pf}(t)+\bar{B}(\theta)w_{udf}(t)
\end{aligned}
$$

(5 - 7)

$$
\begin{aligned}
e_f(t) &= \hat{f}(t)-f(t) \\
&= C_f(\theta)x_f(t)+D_f(\theta)\begin{bmatrix}u(t)\\ y_p(t)\end{bmatrix}-f(t) \\
&= C_f(\theta)x_f(t)+D_f(\theta)\begin{bmatrix}0\\ C_p(\theta)x_p(t)\end{bmatrix} \\
&\quad + \begin{bmatrix} D_f(\theta)u(t)-f(t) \\ D_f(\theta)D_p(\theta)u(t)+D_f(\theta)G_p(\theta)d(t)+D_f(\theta)H_p(\theta)f(t)-f(t)\end{bmatrix} \\
&= \underbrace{\begin{bmatrix} D_f(\theta)\begin{pmatrix} 0 \\ C_p(\theta)\end{pmatrix} & C_f(\theta)\end{bmatrix}}_{\bar{C}(\theta)} \underbrace{\begin{bmatrix}x_p(t)\\ x_f(t)\end{bmatrix}}_{x_{pf}(t)} \\
&\quad + \underbrace{\begin{bmatrix} D_f(\theta) & 0 & -I \\ D_f(\theta)D_p(\theta) & D_f(\theta)G_p(\theta) & D_f(\theta)H_p(\theta)-I\end{bmatrix}}_{\bar{D}(\theta)} \underbrace{\begin{bmatrix}u(t)\\ d(t)\\ f(t)\end{bmatrix}}_{w_{udf}(t)} \\
&= \bar{C}(\theta)x_{pf}(t)+\bar{D}(\theta)w_{udf}(t)
\end{aligned}
$$

(5 - 8)

Define:

$$\begin{aligned}\overline{A}(\theta) &= \begin{bmatrix} A_p(\theta) & 0 \\ B_f(\theta)\underbrace{\begin{pmatrix} 0 \\ C_p(\theta) \end{pmatrix}}_{C_2(\theta)} & A_f(\theta) \end{bmatrix} \\ &= \underbrace{\begin{bmatrix} A_p(\theta) & 0 \\ 0 & 0 \end{bmatrix}}_{A_0(\theta)} + \underbrace{\begin{bmatrix} 0 & 0 \\ I & 0 \end{bmatrix}}_{\mathcal{B}} \underbrace{\begin{bmatrix} A_f(\theta) & B_f(\theta) \\ C_f(\theta) & D_f(\theta) \end{bmatrix}}_{\mathcal{F}(\theta)} \underbrace{\begin{bmatrix} 0 & I \\ C_2(\theta) & 0 \end{bmatrix}}_{C} \\ &= A_0(\theta) + \mathcal{B}\mathcal{F}(\theta)C \end{aligned} \tag{5-9}$$

$$\begin{aligned}\overline{B}(\theta) &= \begin{bmatrix} \underbrace{\begin{pmatrix} B_p(\theta) & E_p(\theta) & F_p(\theta) \end{pmatrix}}_{B_1(\theta)} \\ B_f(\theta)\underbrace{\begin{pmatrix} I & 0 & 0 \\ D_p(\theta) & G_p(\theta) & H_p(\theta) \end{pmatrix}}_{D_{21}(\theta)} \end{bmatrix} \\ &= \underbrace{\begin{bmatrix} B_1(\theta) \\ 0 \end{bmatrix}}_{B_0(\theta)} + \underbrace{\begin{bmatrix} 0 & 0 \\ I & 0 \end{bmatrix}}_{\mathcal{B}} \underbrace{\begin{bmatrix} A_f(\theta) & B_f(\theta) \\ C_f(\theta) & D_f(\theta) \end{bmatrix}}_{\mathcal{F}(\theta)} \underbrace{\begin{bmatrix} 0 \\ D_{21}(\theta) \end{bmatrix}}_{\mathcal{D}_{21}} \\ &= B_0(\theta) + \mathcal{B}\mathcal{F}(\theta)\mathcal{D}_{21} \end{aligned} \tag{5-10}$$

$$\begin{aligned}\overline{C}(\theta) &= \begin{bmatrix} D_f(\theta)\underbrace{\begin{pmatrix} 0 \\ C_p(\theta) \end{pmatrix}}_{C_2(\theta)} & C_f(\theta) \end{bmatrix} \\ &= \underbrace{\begin{bmatrix} 0 & I \end{bmatrix}}_{\mathcal{D}_{12}} \underbrace{\begin{bmatrix} A_f(\theta) & B_f(\theta) \\ C_f(\theta) & D_f(\theta) \end{bmatrix}}_{\mathcal{F}(\theta)} \underbrace{\begin{bmatrix} 0 & I \\ C_2(\theta) & 0 \end{bmatrix}}_{C} \\ &= \mathcal{D}_{12}\mathcal{F}(\theta)C \end{aligned} \tag{5-11}$$

$$\begin{aligned}\overline{D}(\theta) &= \begin{bmatrix} D_f(\theta) & 0 & -I \\ D_f(\theta)D_p(\theta) & D_f(\theta)G_p(\theta) & D_f(\theta)H_p(\theta) - I \end{bmatrix} \\ &= \begin{bmatrix} 0 & 0 & -I \\ 0 & 0 & -I \end{bmatrix} + D_f(\theta)\underbrace{\begin{bmatrix} I & 0 & 0 \\ D_p(\theta) & G_p(\theta) & H_p(\theta) \end{bmatrix}}_{D_{21}} \\ &= \underbrace{\begin{bmatrix} 0 & 0 & -I \\ 0 & 0 & -I \end{bmatrix}}_{D_{11}} + \underbrace{\begin{bmatrix} 0 & I \end{bmatrix}}_{\mathcal{D}_{12}} \underbrace{\begin{bmatrix} A_f(\theta) & B_f(\theta) \\ C_f(\theta) & D_f(\theta) \end{bmatrix}}_{\mathcal{F}(\theta)} \underbrace{\begin{bmatrix} 0 \\ D_{21} \end{bmatrix}}_{\mathcal{D}_{21}} \\ &= D_{11}(\theta) + \mathcal{D}_{12}\mathcal{F}(\theta)\mathcal{D}_{21} \end{aligned} \tag{5-12}$$

Eqs (5 - 6) to (5-12) can be rewritten in the form:

$$\begin{aligned} \dot{x}_{pf}(t) &= \overline{A}(\theta)x_{pf}(t) + \overline{B}(\theta)w_{udf}(t) \\ e_f(t) &= \overline{C}(\theta)x_{pf}(t) + \overline{D}(\theta)w_{udf}(t) \end{aligned} \qquad (5\text{-}13)$$

where:

$$\begin{aligned} &x_{pf}(t) = \begin{bmatrix} x_p^T(t) & x_f^T(t) \end{bmatrix}^T, \qquad w_{udf}(t) = \begin{bmatrix} u^T(t) & d^T(t) & f^T(t) \end{bmatrix}^T \\ &\overline{A}(\theta) = A_0(\theta) + \mathcal{B}\mathcal{F}(\theta)C, \qquad \overline{B}(\theta) = B_0(\theta) + \mathcal{B}\mathcal{F}(\theta)\mathcal{D}_{21} \\ &\overline{C}(\theta) = \mathcal{D}_{12}\mathcal{F}(\theta)C, \qquad \overline{D}(\theta) = D_{11}(\theta) + \mathcal{D}_{12}\mathcal{F}(\theta)\mathcal{D}_{21} \end{aligned} \qquad (5\text{-}14)$$

and:

$$\begin{aligned} &A_0(\theta) = \begin{pmatrix} A_p(\theta) & 0 \\ 0 & 0 \end{pmatrix}, \qquad B_0(\theta) = \begin{pmatrix} B_1(\theta) \\ 0 \end{pmatrix}, \\ &\mathcal{B} = \begin{pmatrix} 0 & 0 \\ I & 0 \end{pmatrix}, \qquad C = \begin{pmatrix} 0 & I \\ C_2(\theta) & 0 \end{pmatrix}, \\ &\mathcal{D}_{21} = \begin{pmatrix} 0 \\ D_{21}(\theta) \end{pmatrix}, \qquad \mathcal{D}_{12} = \begin{pmatrix} 0 & I \end{pmatrix}, \\ &B_1(\theta) = \begin{pmatrix} B_p(\theta) & E_p(\theta) & F_p(\theta) \end{pmatrix}, \\ &D_{11}(\theta) = \begin{pmatrix} 0 & 0 & -I \end{pmatrix}, \\ &C_2(\theta) = \begin{pmatrix} 0 \\ C_p(\theta) \end{pmatrix}, \\ &D_{21}(\theta) = \begin{pmatrix} I & 0 & 0 \\ D_p(\theta) & G_p(\theta) & H_p(\theta) \end{pmatrix} \end{aligned} \qquad (5\text{-}15)$$

In order to solve the estimation problem of Eq. (5 - 5) the ***Problem 5.1*** must be defined:

Problem 5.1

For the LPV system Eq. (5 - 2) with assumptions **(A. 5-1)-(A. 5-4)**, design a polytopic LPV estimator Eq. (5 - 5), such that the L_2-induced norm of the operator mapping $w_{udf}(t)$ into $e_f(t)$ [see Eq. (5-13)] is bounded by a scalar number γ for all parameter trajectories $\theta(t)$ in the polytope Θ [see ***Lemma 5.1***].

5.4.1 LPV approach to robust fault estimation

Considering the structure of Eq. (5-13) and according to the assumptions **(A. 5-2)-(A. 5-4)**, it can be verified that the system Eq. (5-13) is a polytopic system, and the Lemma 5.1 can be used as an adaptation of the results from (Apkarian *at el*, 1995).

Lemma 5.1

For LPV system Eq. (5-13), the following statements are equivalent:

(1) L_2-induced norm of the operator mapping $w_{udf}(t)$ into $e_f(t)$ [see Eq. (5-13)] is bounded by a scalar number γ for all parameter trajectories $\theta(t)$ in the polytope Θ,

(2) There exists $X = X^T > 0$ satisfying the system of LMIs:

$$\begin{pmatrix} X\overline{A}(\theta_i) + \overline{A}^T(\theta_i)X & X\overline{B}(\theta_i) & \overline{C}^T(\theta_i) \\ \overline{B}^T(\theta_i)X & -\gamma I & \overline{D}^T(\theta_i) \\ \overline{C}(\theta_i) & \overline{D}(\theta_i) & -\gamma I \end{pmatrix} < 0 \qquad i = 1, \cdots, r \tag{5-16}$$

The main results of this Chapter can be stated through ***Theorem 5.1*** which provides the conditions leading to the solution of the ***Problem 5.1***.

Theorem 5.1 (Apkarian *at el*, 1995)

Consider the LPV system in Eq. (5-2) with assumptions **(A. 5-1)-(A. 5-4)**. There exists a polytopic LPV estimator in Eq. (5-5) that can determine the solution of ***Problem 5.1*** *if* there exist matrices $0 < R_o = R_o^T \in R^{n\times n}$, $0 < S_o = S_o^T \in R^{n\times n}$ such that:

$$\begin{pmatrix} \mathcal{N}_R & 0 \\ 0 & I \end{pmatrix}^T \begin{pmatrix} A_p(\theta_i)R_o + R_o A_p^T(\theta_i) & 0 & B_1(\theta_i) \\ 0 & -\gamma I & D_{11} \\ B_1^T(\theta_i) & D_{11}^T & -\gamma I \end{pmatrix} \begin{pmatrix} \mathcal{N}_R & 0 \\ 0 & I \end{pmatrix}^T < 0 \qquad i = 1, \cdots, r \tag{5-17}$$

$$\begin{pmatrix} \mathcal{N}_S & 0 \\ 0 & I \end{pmatrix}^T \begin{pmatrix} S_o A_p(\theta_i) + A_p^T(\theta_i)S_o & S_o B_1(\theta_i) & 0 \\ B_1^T(\theta_i)S_o & -\gamma I & D_{11}^T \\ 0 & D_{11} & -\gamma I \end{pmatrix} \begin{pmatrix} \mathcal{N}_S & 0 \\ 0 & I \end{pmatrix} < 0 \qquad i = 1, \cdots, r \tag{5-18}$$

$$\begin{pmatrix} R_o & I \\ I & S_o \end{pmatrix} \geq 0 \qquad (5\text{-}19)$$

Proof of Theorem 5.1

By ***Lemma 5.1*** [see Eq. (5 - 6)] and considering the notations in Eq. (5-14), there exists a polytopic LPV fault estimator Eq. (5 - 5) which solves the ***Problem 5.1*** if:

$$\Psi(\theta_i) + U_x^T \mathcal{F}(\theta_i) V + V^T \mathcal{F}^T(\theta_i) U_x < 0 \qquad i = 1, \cdots, r \qquad (5\text{-}20)$$

where:

$$\Psi(\theta_i) = \begin{pmatrix} XA_0(\theta_i) + A_0^T(\theta_i)X & XB_0(\theta_i) & 0 \\ B_0^T(\theta_i)X & -\gamma I & D_{11}^T \\ 0 & D_{11} & -\gamma I \end{pmatrix} \qquad (5\text{-}21)$$

$$U_x = \begin{pmatrix} \mathcal{B}^T X & 0 & \mathcal{D}_{12}^T \end{pmatrix} \qquad (5\text{-}22)$$

$$V = \begin{pmatrix} C & \mathcal{D}_{21} & 0 \end{pmatrix} \qquad (5\text{-}23)$$

Based on the *projection lemma* (Gahinet and Apkarian, 1994), the LMIs of Eq. (5-20) hold for some $\mathcal{F}(\theta_i)$ if and only if:

$$W_{U_x}^T \Psi(\theta_i) W_{U_x} < 0 \qquad (5\text{-}24)$$

$$W_V^T \Psi(\theta_i) W_V < 0 \qquad (5\text{-}25)$$

$$i = 1, \cdots, r$$

where W_{U_x} and W_V denote any bases of the null spaces of U_x and V, respectively.

Observing that:

$$U_X = \begin{pmatrix} \mathcal{B}^T & 0 & \mathcal{D}_{12}^T \end{pmatrix} \begin{pmatrix} X & 0 & 0 \\ 0 & I & 0 \\ 0 & 0 & I \end{pmatrix} \qquad (5\text{-}26)$$

$$U = \begin{pmatrix} \mathcal{B}^T & 0 & \mathcal{D}_{12}^T \end{pmatrix} \qquad (5\text{-}27)$$

A basis for the null space of U_x is given by:

$$W_{U_x} = \begin{pmatrix} X^{-1} & 0 & 0 \\ 0 & I & 0 \\ 0 & 0 & I \end{pmatrix} W_U \qquad (5\text{-}28)$$

where W_U denotes any basis of the null space of U. Hence, the inequality Eq. (5-24) can be rewritten as:

$$W_U^T \Omega(\theta_i) W_U < 0, \quad i = 1, \cdots, r \tag{5-29}$$

with:

$$\Omega(\theta_i) = \begin{pmatrix} A_0(\theta_i)X^{-1} + X^{-1}A_0^T(\theta_i) & B_0(\theta_i) & 0 \\ B_0^T(\theta_i) & -\gamma I & D_{11}^T \\ 0 & D_{11} & -\gamma I \end{pmatrix} \tag{5-30}$$

X and X^{-1} can be partitioned as:

$$X = \begin{pmatrix} S_o & N_o \\ N_o^T & * \end{pmatrix} \tag{5-31}$$

$$X^{-1} = \begin{pmatrix} R_o & M_o \\ M_o^T & * \end{pmatrix} \tag{5-32}$$

where $S_o, R_o, M_o, N_o \in R^{n \times n}$ and $S_o, R_o, M_o > 0$, and * stands for the matrix entries that we are not interested in.

These partitions of X and X^{-1} can now be substituted into Eq. (5-21) and Eq. (5-30), yielding $\Omega(\theta_i)$ and $\Psi(\theta_i)$ as:

$$\Omega(\theta_i) = \begin{pmatrix} A_p(\theta_i)R_o + R_o A_p^T(\theta_i) & A_p(\theta_i)M_o & B_1(\theta_i) & 0 \\ M_o^T A_p^T(\theta_i) & 0 & 0 & 0 \\ B_1^T(\theta_i) & 0 & -\gamma I & D_{11}^T \\ 0 & 0 & D_{11} & -\gamma I \end{pmatrix} \tag{5-33}$$

$$\Psi(\theta_i) = \begin{pmatrix} S_o A_p(\theta_i) + A_p^T(\theta_i)S_o & A_p^T(\theta_i)N_o & S_o B_1(\theta_i) & 0 \\ N_o^T A_p(\theta_i) & 0 & N_o^T B_1(\theta_i) & 0 \\ B_1^T(\theta_i)S_o & B_1^T(\theta_i)N_o & -\gamma I & D_{11}^T \\ 0 & 0 & D_{11} & -\gamma I \end{pmatrix} \tag{5-34}$$

Let $\mathcal{N}_R = \begin{pmatrix} U_1 \\ U_2 \end{pmatrix} = \begin{pmatrix} I \\ I \end{pmatrix}$ and $\mathcal{N}_S = \begin{pmatrix} V_1 \\ V_2 \end{pmatrix}$ be a basis of the null space of (C_2, D_{21}), then the bases for the null spaces of U and V are given by:

$$W_U = \begin{pmatrix} U_1 & 0 \\ 0 & 0 \\ 0 & I \\ U_2 & 0 \end{pmatrix}, W_V = \begin{pmatrix} V_1 & 0 \\ 0 & 0 \\ V_1 & 0 \\ 0 & I \end{pmatrix} \tag{5-35}$$

Observing that the *second row* is identically zero in the matrices of Eq. (5-35), thus the conditions Eqs. (5-29) and (5-25) can be reduced to the following LMIs:

$$\underbrace{\begin{pmatrix} U_1 & 0 \\ 0 & I \\ U_2 & 0 \end{pmatrix}^T}_{W_U^T} \underbrace{\begin{pmatrix} A_p(\theta_i)R_o + R_o A_p^T(\theta_i) & B_1(\theta_i) & 0 \\ B_1^T(\theta_i) & -\gamma I & D_{11}^T \\ 0 & D_{11} & -\gamma I \end{pmatrix}}_{\Omega(\theta_i)} \underbrace{\begin{pmatrix} U_1 & 0 \\ 0 & I \\ U_2 & 0 \end{pmatrix}}_{W_U} < 0 \tag{5-36}$$

$$i = 1, \cdots, r$$

$$\underbrace{\begin{pmatrix} V_1 & 0 \\ V_2 & 0 \\ 0 & I \end{pmatrix}^T}_{W_V^T} \underbrace{\begin{pmatrix} S_o A_p(\theta_i) + A_p^T(\theta_i) S_o & S_o B_1(\theta_i) & 0 \\ B_1^T(\theta_i) S_o & -\gamma I & D_{11}^T \\ 0 & D_{11} & -\gamma I \end{pmatrix}}_{\Psi(\theta_i)} \underbrace{\begin{pmatrix} V_1 & 0 \\ V_2 & 0 \\ 0 & I \end{pmatrix}}_{W_V} < 0 \tag{5-37}$$

$$i = 1, \cdots, r$$

Inequalities Eq. (5-36) and (5-37) resulting from the derivation of the bases of the null spaces of U and V have been modified in this thesis since the pair (B_2^T, D_{12}^T) does not appear in the derivation of Eq. (5 - 4) . The standard formulation by Apkarian *et al* (1995) can now be used based on the bases of W_U and W_V determined in inequalities Eq. (5-36) and (5-37) as follows:

$$\begin{pmatrix} \mathcal{N}_R & 0 \\ 0 & I \end{pmatrix}^T \begin{pmatrix} A_p(\theta_i)R_o + R_o A_p^T(\theta_i) & 0 & B_1(\theta_i) \\ 0 & -\gamma I & D_{11} \\ B_1^T(\theta_i) & D_{11}^T & -\gamma I \end{pmatrix} \begin{pmatrix} \mathcal{N}_R & 0 \\ 0 & I \end{pmatrix} < 0 \tag{5-38}$$

$$i = 1, \cdots, r$$

$$\begin{pmatrix} \mathcal{N}_S & 0 \\ 0 & I \end{pmatrix}^T \begin{pmatrix} S_o A_p(\theta_i) + A_p^T(\theta_i) S_o & S_o B_1(\theta_i) & 0 \\ B_1^T(\theta_i) S_o & -\gamma I & D_{11}^T \\ 0 & D_{11} & -\gamma I \end{pmatrix} \begin{pmatrix} \mathcal{N}_S & 0 \\ 0 & I \end{pmatrix} < 0 \tag{5-39}$$

$$i = 1, \cdots, r$$

Based on the matrix completion result (Zhou and Doyle, 1997), the condition $X > 0$ is equivalent to:

$$\begin{pmatrix} R_o & I \\ I & S_o \end{pmatrix} \geq 0 \qquad (5\text{-}40)$$

which completes the proof of ***Theorem 5.1*** ■

Once the matrices R_o and S_o are obtained, the LPV estimator described in Eq. (5 - 5) can be constructed as following algorithm:

Algorithm 5.1 (Apkarian, *et at*, 1995)

Step1. Computing the full rank matrices M_o, N_o using SVD such that:

$$M_o N_o^T = I - R_o S_o \qquad (5\text{-}41)$$

Step 2. Computing X as the unique solution of the linear matrix equation:

$$X\begin{pmatrix} I & R_o \\ 0 & M_o^T \end{pmatrix} = \begin{pmatrix} S_o & I \\ N_o^T & 0 \end{pmatrix} \qquad (5\text{-}42)$$

Step 3. Compute $\mathcal{F}(\theta_i)$ by solving the Eq. (5-20).

Step 4. Solve the polytopic LPV estimator:

$$\mathcal{F}(\theta) = \sum_{i=1}^{r} \alpha_p^i \mathcal{F}(\theta_i) \qquad (5\text{-}43)$$

where α_p^i is any solution of the convex decomposition problem:

$$\theta = \sum_{i=1}^{r} \alpha_p^i \theta_i \qquad (5\text{-}44)$$

5.5 Two-link Robot Case Study Example

To illustrate the mathematical discussion above, a tutorial example of the actuator fault compensation problem is considered using a nonlinear simulation of the two-link manipulator/robot. The field of robotics is concerned with the principle, design, manufacture, and application of robots, and is a broad application area involving many areas such as physics, mechanical design, motion analysis and planning, actuators and

drivers, control design, sensors, signal and image processing, computer algorithms, and study of behaviour of machines, animals, and even human beings (McKerrow, 1991; Slotine and Li, 1991; Hassen, *et al*., 2000).

The robot manipulators are familiar examples of position-controllable mechanical systems (Hassen, *et al*, 2000). However, their nonlinear dynamics present a challenging control problem, since traditional linear control approaches do not easily apply. The objective of this Section is to model the complete nonlinear dynamics of an example of a two-joint manipulator, so that the movement control, e.g. from one point to another in two-dimensional space, is facilitated.

5.5.1 Two-link manipulator dynamics

Basically, there are *three* types of dynamic torques that arise from the motion of the manipulator: *Inertial*, *Centripetal*, and *Coriolis* torques (McKerrow, 1991; Slotine and Li, 1991; Hassen, *et al*., 2000). Inertial torques are proportional to acceleration of each joint in accordance with Newton's second law. Centripetal torques arise from the centripetal forces which constrain a body to rotate about a point. They are directed towards the centre of the uniform circular motion, and are proportional to the square of the velocity. Coriolis torques result from vertical forces derived from the interaction of two rotating links and are proportional to the product of the joint velocities of those links.

For simplicity, the two-link robotic manipulator is considered to rotate in the vertical plane, and the equilibrium point is considered to be the upper vertical position, whose position can be described by a 2-vector $\varphi = (\varphi_1, \varphi_2)^T$ of joint angles, and whose actuator inputs consist of a 2-vector $u = (u_1, u_2)^T$ of torques applied at the manipulator joints as shown in Figure 5-2.

Using the vectors $\dot{\varphi}$ and $\ddot{\varphi}$ to denote the joint velocities and accelerations, respectively the dynamics of this simple manipulator can be written in the more general form (McKerrow, 1991; Slotine and Li, 1991; Hassen, *et al*, 2000) as:

$$\Xi(\varphi)\ddot{\varphi} + O(\varphi, \dot{\varphi})\dot{\varphi} + \mathcal{G}(\varphi) = u \qquad (5\text{-}45)$$

where: $\Xi(\varphi) \in \Re^{2x2}$ is the manipulator inertia tensor matrix (which is S.P.D.), $O(\varphi, \dot{\varphi})\dot{\varphi} \in \Re^2$ is the vector function containing the Centripetal and Coriolis torques, i.e. $O(\varphi, \dot{\varphi}) \in \Re^{2x2}$ and $g(\varphi) \in \Re^2$ are the gravitational torques.

Consider the following numerical example taken from (Kim 1997; Hassen, *et al*, 2000) and modified here as a demonstration for the proposed design strategy in Section 5.4. In this work a polytope representation of this model is given.

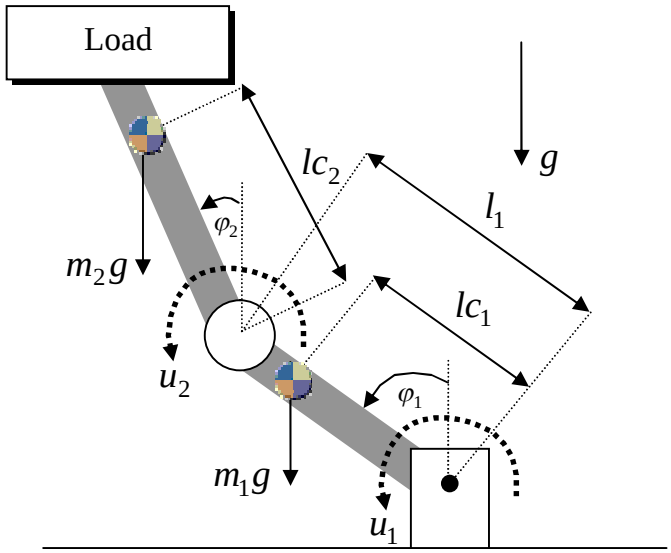

Figure 5-2: Two-link manipulator structure

The equations of motion are described by:

$$[m_1 lc_1^2 + m_2 l_1^2 + I_1]\ddot{\varphi}_1 + [m_2 l_1 lc_2 \cos(\varphi_1 - \varphi_2)\ddot{\varphi}_2 + m_2 l_1 lc_2 \sin(\varphi_1 - \varphi_2)\dot{\varphi}_2^2 - [m_1 lc_1 + m_2 l_1]g \sin(\varphi_1) = u_1 \quad (5\text{-}46)$$

$$[m_2 l_1 lc_2 \cos(\varphi_1 - \varphi_2)\ddot{\varphi}_1 + [m_2 lc_2^2 + I_2]\ddot{\varphi}_2 - [m_2 l_1 lc_2 \sin(\varphi_1 - \varphi_2)\dot{\varphi}_1^2 - m_2 g lc_2 \sin(\varphi_2) = u_2 \quad (5\text{-}47)$$

where:

I_1: Inertia of arm-1 and load

I_2: Inertia of arm-2

l_1 : Distance between joint-1 and joint-2

lc_1: Distance of joint-1 from centre of mass arm-1

lc_2: Distance of joint-2 from centre of mass arm-2

m_1: Mass of arm-1 and load

m_2: Mass of arm-2

Parameters	I_1	I_2	l_1	lc_1	lc_2	m_1	m_2	g
Values	0.833	0.417	1.0	0.5	0.5	10.0	5.0	9.80
Units	Kg*m^2	Kg*m^2	m	m	m	Kg	Kg	m/s^2

Table 5.1: Parameter values for the Two-link manipulator system

5.5.2 Polytopic model of two-link manipulator

Introduce intermediate variables to replace the constants as:

$$\begin{aligned} m_{11} &= m_1 lc_1^2 + m_2 lc_1^2 + I_1 \\ m_{12} &= m_2 l_1 lc_2 \\ m_{21} &= m_2 l_1 lc_2 \\ m_{22} &= m_2 lc_2^2 + I_2 \end{aligned} \qquad (5\text{-}48)$$

and

$$\begin{aligned} k_{11} &= -[m_1 lc_1 + m_2 l_1]g \\ k_{12} &= -m_2 g lc_2 \end{aligned} \qquad (5\text{-}49)$$

It is important to note that in this study the quadratic terms $O(\varphi, \dot{\varphi})$ are not considered because they are not bounded. This is different from the work by Adams *et al* (1996) as in their work, the $O(\varphi, \dot{\varphi})$ term is taken into account in the design of robust control approaches for a two-link flexible manipulator. However, it turns out that the two-link manipulator still works well (see the later results in Section 5.6.1), even if these bounds are not known *a priori*. Considering this limitation Eq. (5-45) becomes:

$$\Xi(\varphi)\ddot{\varphi} + g(\varphi) = u \qquad (5\text{-}50)$$

where:

$$\begin{aligned} \Xi(\varphi) &= \begin{bmatrix} m_{11} & m_{12}\cos(\varphi_1 - \varphi_2) \\ m_{21}\cos(\varphi_1 - \varphi_2) & m_{22} \end{bmatrix}, \\ g(\varphi) &= \begin{bmatrix} k_{11}\sin(\varphi_1) \\ k_{12}\sin(\varphi_2) \end{bmatrix} \end{aligned} \qquad (5\text{-}51)$$

The nonlinear term in $\Xi(\varphi)$ is clearly a bounded function:

$$\phi_1(\varphi) = \cos(\varphi_1 - \varphi_2) \qquad (5\text{-}52)$$

where: $-1 \le \phi_1 \le 1$, [see Figure 5-3 (a)]

Hence, $\Xi(\varphi)$ can be represented by a polytope whose vertices are defined by:

$$\Xi(\varphi) \in Co\{\Xi_1, \Xi_2\} \tag{5-53}$$

where:

$$\Xi_1 = \begin{pmatrix} m_{11} & m_{12} \\ m_{21} & m_{22} \end{pmatrix}, \qquad \Xi_2 = \begin{pmatrix} m_{11} & -m_{12} \\ -m_{21} & m_{22} \end{pmatrix} \tag{5-54}$$

To facilitate a state-space formulation, the vector field $g(\varphi)$ with $\varphi \in \Re^2$ can be arranged in the form of $G^g(\varphi)\varphi$ and function $\phi_2(\varphi)$ can now be defined which is bounded, as shown in Figure 5-3 (b).

$$\sin(\varphi_1) = \left(\frac{\sin(\varphi_1)}{\varphi_1}\right)\varphi_1 = \phi_2(\varphi)\varphi_1 \tag{5-55}$$

where $-0.2 \le \phi_2(\varphi) \le 1$ [see Figure 5-3 (b)]

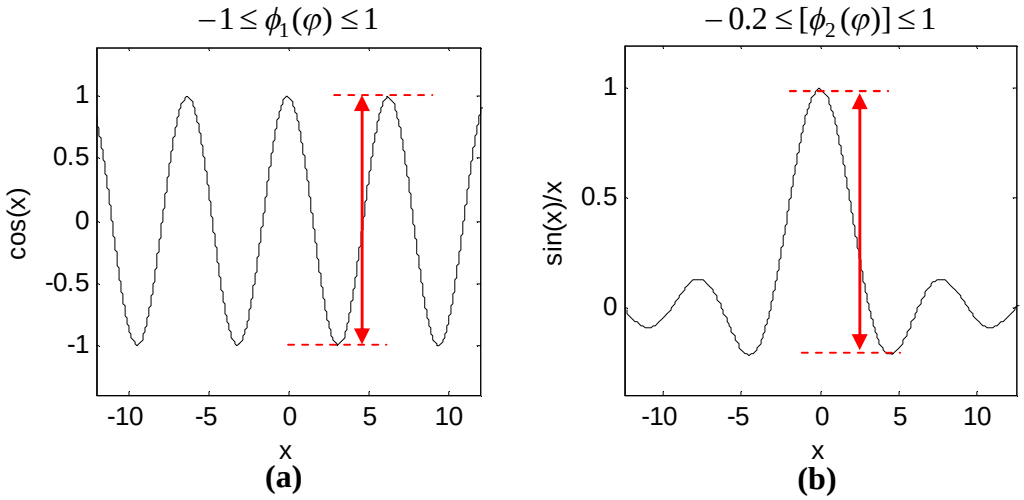

Figure 5-3: Variation of parameters used for the simulation

From the boundedness of functions $\phi_2(\varphi)$ in terms of the angle φ, $G^g(\varphi)$ is considered as a polytope as follows:

$$G^g(\varphi) \in Co\{G_1^g, G_2^g, G_3^g, G_4^g\} \tag{5-56}$$

where:

$$G_1^g = \begin{pmatrix} -0.2k_{11} & 0 \\ 0 & -0.2k_{12} \end{pmatrix}, \qquad G_2^g = \begin{pmatrix} k_{11} & 0 \\ 0 & -0.2k_{12} \end{pmatrix}$$

$$G_3^g = \begin{pmatrix} -0.2k_{11} & 0 \\ 0 & k_{12} \end{pmatrix}, \qquad G_4^g = \begin{pmatrix} k_{11} & 0 \\ 0 & k_{12} \end{pmatrix}$$

To define the state space representation of the two-link system, let:

$$x(t) = \begin{bmatrix} x_1(t) \\ x_2(t) \\ x_3(t) \\ x_4(t) \end{bmatrix} = \begin{bmatrix} \varphi_1(t) \\ \varphi_2(t) \\ \dot{\varphi}_1(t) \\ \dot{\varphi}_2(t) \end{bmatrix} \text{ and } W_b = \begin{bmatrix} 0 & 0 \\ 0 & 0 \\ 1 & 0 \\ 0 & 1 \end{bmatrix}$$

The LMI constraints with state feedback according to the nonlinear equations in Eqs (5-46) and (5-47) are then given by the following *descriptor system*:

$$\begin{pmatrix} I & 0 \\ 0 & \Xi(\varphi) \end{pmatrix} \begin{bmatrix} \dot{x}_1(t) \\ \dot{x}_2(t) \\ \dot{x}_3(t) \\ \dot{x}_4(t) \end{bmatrix} = \begin{pmatrix} 0 & I \\ -G^g(\varphi) & 0 \end{pmatrix} \begin{bmatrix} x_1(t) \\ x_2(t) \\ x_3(t) \\ x_4(t) \end{bmatrix} + W_b\, u(t) \qquad (5\text{-}57)$$

or the state space equation is presented as follows:

$$\dot{x}(t) = A(\varphi)x(t) + B(\varphi)u(t) \qquad (5\text{-}58)$$

Let the matrix Π be a non-singular matrix given by:

$$\Pi = \begin{pmatrix} I & 0 \\ 0 & \Xi(\varphi) \end{pmatrix} \qquad (5\text{-}59)$$

The proof that Π is non-singular follows form the $\Xi(\varphi)$ in the polytope of Eqs (5-53) and (5-54). As Π is block diagonal, its determinant is given by $\Xi(\varphi)$. It is thus only required to show that $m_{11}m_{22} \neq m_{12}\,m_{21}$. But $m_{12} = m_{21}$ (by symmetry) and $m_{11} > m_{22}$ since $I_1 > I_2$ and $m_1 > m_2$ and hence Π is non-singular. ■

It thus follows that:

$$A(\varphi) = \Pi^{-1} \begin{pmatrix} 0 & I \\ -G^g(\varphi) & 0 \end{pmatrix},$$
$$B(\varphi) = \Pi^{-1} W_b$$

5.5.3 Actuator fault estimation

Consider a nominal time-varying model [depending smoothly on the angle φ] of the nonlinear dynamical system of Eq. (5-58), subject to actuator faults $F_a f_a(t)$, as follows:

$$\begin{aligned}\dot{x}(t) &= A(\varphi)x(t) + B(\varphi)u(t) + F_a f_a(t) \\ &= A_{ij}x(t) + B_i u(t) + F_a f_a(t) \\ & i = 1, 2 \quad j = 1, 2, \ldots, 4\end{aligned} \tag{5-60}$$

where F_a fault distribution matrix and the vectored signal f_a represents actuator faults. These gives rise to a polytopic controller with *8*-vertex systems as follows:

Vertex system 1:

$$A_{11} = \begin{pmatrix} 0.0000 & 0.0000 & 0.0000 & 0.0000 \\ 0.0000 & 0.0000 & 0.0000 & 1.0000 \\ -19.5947 & -8.0159 & 0.0000 & 0.0000 \\ -29.3861 & 26.7184 & 0.0000 & 0.0000 \end{pmatrix}, B_1 = \begin{pmatrix} 0.0000 & 0.0000 \\ 0.0000 & 0.0000 \\ 0.2182 & -0.3272 \\ -0.3272 & 1.0905 \end{pmatrix}$$

Vertex system 2:

$$A_{12} = \begin{pmatrix} 0.0000 & 1.0000 & 0.0000 & 0.0000 \\ 0.0000 & 0.0000 & 0.0000 & 1.0000 \\ 19.5947 & 1.6032 & 0.0000 & 0.0000 \\ -29.3861 & -5.3437 & 0.0000 & 0.0000 \end{pmatrix}, B_1 = \begin{pmatrix} 0.0000 & 0.0000 \\ 0.0000 & 0.0000 \\ 0.2182 & -0.3272 \\ -0.3272 & 1.0905 \end{pmatrix}$$

Vertex system 3:

$$A_{13} = \begin{pmatrix} 0.0000 & 1.0000 & 0.0000 & 0.0000 \\ 0.0000 & 0.0000 & 0.0000 & 1.0000 \\ -3.9189 & -8.0159 & 0.0000 & 0.0000 \\ 5.8772 & 26.7184 & 0.0000 & 0.0000 \end{pmatrix}, B_1 = \begin{pmatrix} 0.0000 & 0.0000 \\ 0.0000 & 0.0000 \\ 0.2182 & -0.3272 \\ -0.3272 & 1.0905 \end{pmatrix}$$

Vertex system 4:

$$A_{14} = \begin{pmatrix} 0.0000 & 1.0000 & 0.0000 & 0.0000 \\ 0.0000 & 0.0000 & 0.0000 & 1.0000 \\ -3.9189 & 1.6032 & 0.0000 & 0.0000 \\ 5.8772 & -5.3437 & 0.0000 & 0.0000 \end{pmatrix}, B_1 = \begin{pmatrix} 0.0000 & 0.0000 \\ 0.0000 & 0.0000 \\ 0.2182 & -0.3272 \\ -0.3272 & 1.0905 \end{pmatrix}$$

Vertex system 5:

$$A_{21} = \begin{pmatrix} 0.0000 & 1.0000 & 0.0000 & 0.0000 \\ 0.0000 & 0.0000 & 0.0000 & 1.0000 \\ 19.5947 & 8.0159 & 0.0000 & 0.0000 \\ 29.3861 & 26.7184 & 0.0000 & 0.0000 \end{pmatrix}, B_2 = \begin{pmatrix} 0.0000 & 0.0000 \\ 0.0000 & 0.0000 \\ 0.2182 & 0.3272 \\ 0.3272 & 1.0905 \end{pmatrix}$$

Vertex system 6:

$$A_{22} = \begin{pmatrix} 0.0000 & 1.0000 & 0.0000 & 0.0000 \\ 0.0000 & 0.0000 & 0.0000 & 1.0000 \\ 19.5947 & -1.6032 & 0.0000 & 0.0000 \\ 29.3861 & -5.3437 & 0.0000 & 0.0000 \end{pmatrix}, B_2 = \begin{pmatrix} 0.0000 & 0.0000 \\ 0.0000 & 0.0000 \\ 0.2182 & 0.3272 \\ 0.3272 & 1.0905 \end{pmatrix}$$

Vertex system 7:

$$A_{23} = \begin{pmatrix} 0.0000 & 1.0000 & 0.0000 & 0.0000 \\ 0.0000 & 0.0000 & 0.0000 & 1.0000 \\ -3.9189 & 8.0159 & 0.0000 & 0.0000 \\ -5.8772 & 26.7184 & 0.0000 & 0.0000 \end{pmatrix}, B_2 = \begin{pmatrix} 0.0000 & 0.0000 \\ 0.0000 & 0.0000 \\ 0.2182 & 0.3272 \\ 0.3272 & 1.0905 \end{pmatrix}$$

Vertex system 8:

$$A_{24} = \begin{pmatrix} 0.0000 & 1.0000 & 0.0000 & 0.0000 \\ 0.0000 & 0.0000 & 0.0000 & 1.0000 \\ -3.9189 & -1.6032 & 0.0000 & 0.0000 \\ -5.8772 & -5.3437 & 0.0000 & 0.0000 \end{pmatrix}, B_2 = \begin{pmatrix} 0.0000 & 0.0000 \\ 0.0000 & 0.0000 \\ 0.2182 & 0.3272 \\ 0.3272 & 1.0905 \end{pmatrix}$$

Therefore, the actuator fault estimate $\hat{f}_a(t)$ in system Eq. (5-60) can be implemented by using ***Algorithm 5.1*** and solved using the MATLAB© LMI toolbox in Eqs (5-41)-(5-44). The solution for $\gamma = 2.7550$, after 39 iterations. The matrices R_o, S_o and M_o are given by:

$$R_o = \begin{pmatrix} 2.2245\text{E}+03 & -8.0233\text{E}+02 & -7.3705\text{E}+02 & -7.3705\text{E}+02 \\ -8.0233\text{E}+02 & 2.6290\text{E}+03 & -1.9536\text{E}+01 & -1.9536\text{E}+01 \\ -7.3705\text{E}+02 & -1.9536\text{E}+01 & 3.3488\text{E}+03 & 4.5642\text{E}+02 \\ -7.3705\text{E}+02 & -1.9536\text{E}+01 & 4.5642\text{E}+02 & 3.3488\text{E}+033 \end{pmatrix}$$

$$S_o = \begin{pmatrix} 2.9682\text{E}+03 & 3.1291\text{E}+01 & 1.9468\text{E}+01 & 1.9468\text{E}+01 \\ 3.1291\text{E}+01 & 2.9309\text{E}+03 & 7.5925\text{E}-01 & 7.5925\text{E}-01 \\ 1.9468\text{E}+01 & 7.5925\text{E}-01 & 2.8955\text{E}+03 & -4.1605\text{E}+01 \\ 1.9468\text{E}+01 & 7.5925\text{E}-01 & -4.1605\text{E}+01 & 2.8955\text{E}+03 \end{pmatrix}$$

$$M_o = \begin{pmatrix} 6.2022\text{E}+06 & -2.9214\text{E}+06 & 9.5678\text{E}-04 & 3.0969\text{E}+06 \\ -2.7157\text{E}+06 & 7.3022\text{E}+06 & -2.3657\text{E}-03 & 1.8940\text{E}+06 \\ -7.4692\text{E}+06 & -2.5404\text{E}+06 & -6.0069\text{E}+06 & 9.4147\text{E}+05 \\ -7.4692\text{E}+06 & -2.5404\text{E}+06 & 6.0069\text{E}+06 & 9.4147\text{E}+05 \end{pmatrix}$$

$$X = \begin{pmatrix} 2.968E+03 & 3.129E+01 & 1.947E+01 & 1.947E+01 \\ 3.129E+01 & 2.931E+03 & 7.593E-01 & 7.593E-01 \\ 1.947E+01 & 7.593E-01 & 2.895E+03 & -4.160E+01 \\ 1.947E+01 & 7.593E-01 & -4.160E+01 & 2.895E+03 \\ -4.983E-01 & 2.151E-01 & 5.939E-01 & 5.939E-01 \\ 3.369E-01 & -8.446E-01 & 2.943E-01 & 2.943E-01 \\ -1.126E-10 & 2.785E-10 & 7.071E-01 & -7.071E-01 \\ -7.989E-01 & -4.903E-01 & -2.464E-01 & -2.464E-01 \end{pmatrix}$$

$$\begin{pmatrix} -4.983E-01 & 3.369E-01 & -1.126E-10 & -7.989E-01 \\ 2.151E-01 & -8.446E-01 & 2.785E-10 & -4.903E-01 \\ 5.939E-01 & 2.943E-01 & 7.071E-01 & -2.464E-01 \\ 5.939E-01 & 2.943E-01 & -7.071E-01 & -2.464E-01 \\ 3.501E-04 & 1.969E-06 & 0.000E+00 & -2.988E-06 \\ 1.969E-06 & 3.435E-04 & -1.000E-15 & -5.660E-07 \\ 0.000E+00 & -1.000E-15 & 3.405E-04 & 0.000E+00 \\ -2.988E-06 & -5.660E-07 & 0.000E+00 & 3.350E-04 \end{pmatrix}$$

An estimator in Eq. (5 - 5) can be constructed by the ***Algorithm 5.1***. The polytopic LPV estimator in Eq. (5 - 43) are:

$$\mathcal{F}(\theta) = \left(\begin{array}{cccc} -4.347E+02 & -4.365E+02 & -3.126E+02 & -3.982E+02 \\ -2.174E+02 & -2.727E+02 & -4.662E+02 & -3.387E+02 \\ 8.814E+02 & 5.495E+02 & -1.420E+03 & -1.098E+02 \\ 1.479E+02 & 1.170E+01 & -6.757E+02 & -2.271E+02 \\ \hline -5.344E-02 & -4.086E-02 & 1.115E-01 & -1.721E-02 \end{array}\right.$$

$$\left.\begin{array}{cccc} 1.171E+06 & 1.359E+06 & -1.463E+06 & -1.667E+05 \\ 8.665E+05 & 1.018E+06 & -1.323E+06 & 6.172E+05 \\ -5.748E+05 & -5.788E+05 & -9.206E+05 & 4.979E+06 \\ 3.342E+05 & 4.078E+05 & -9.783E+05 & 1.827E+06 \\ \hline 7.742E+01 & 9.297E+01 & 1.193E+02 & -3.438E+02 \end{array}\right)$$

Figure 5-4 and Figure 5-5 show the result of the fault estimation, with a Gaussian random disturbance $d(t)$ of zero-mean and variance 0.015 and disturbance distribution matrix as follows:

$$E = \begin{pmatrix} 5.4832E-03 & 4.0004E-03 & 9.3071E-03 & 8.5417E-03 \\ 6.2289E-03 & 1.2001E-02 & 3.3493E-03 & 2.6570E-03 \\ 2.6745E-03 & 9.0829E-03 & 5.4991E-03 & 1.0490E-02 \\ 8.0437E-03 & 5.1494E-03 & 1.1667E-02 & 7.8598E-03 \end{pmatrix}$$

The polytopic system is simulated with scalar faults acting on the control input $u_1(t)$ [i.e. torque input at the manipulator joint-1], with: the parameter trajectories of $\phi_1(\varphi)$, and $\phi_2(\varphi)$ [as defined by Eqs. (5-52) and (5-55)], and the actuator fault signals [i.e. $f_a(t) = col[\, f_{a1}(t),\ f_{a2}(t)]$ as shown in Figure 5-4 and Figure 5-5 are:

$$f_a(t) = col[2.50e10^{-2}\sin(0.5t),\ 0.00] \quad \text{and} \quad f_a(t) = col[1.25e10^{-2}\sin(2t),\ 0.00],$$

Simulation results show that the designed polytopic LPV fault estimators provide very good estimation performance.

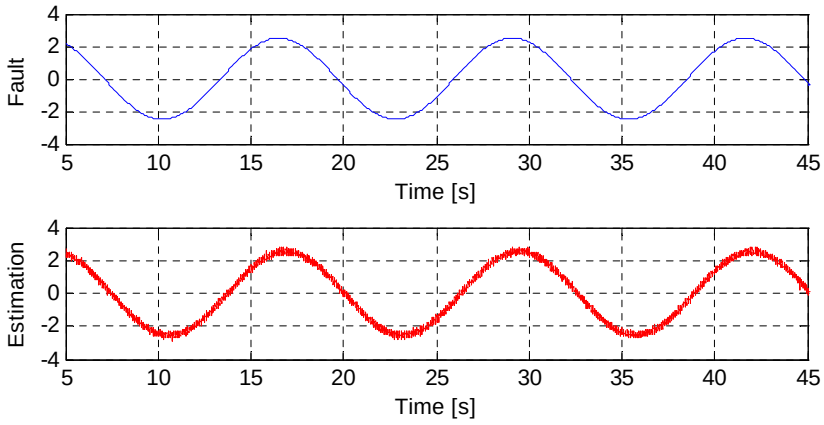

Figure 5-4: Fault estimation provided by the polytopic LPV estimator

$$[\, f_{a1}(t) = 2.50e10^{-2}\sin(0.5t)\,]$$

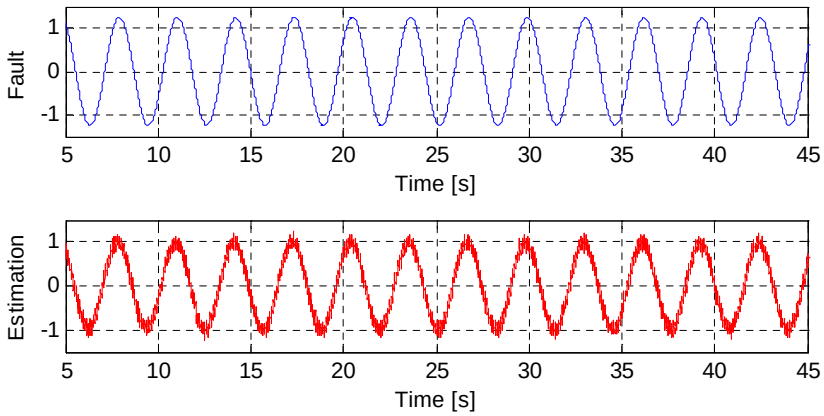

Figure 5-5: Fault estimation provided by the polytopic LPV estimator

$$[\, f_{a1}(t) = 1.25e10^{-2}\sin(2t)\,]$$

In this Section the design and performance of the fault estimator for the manipulator system have been given. After verifying the fault estimation performance the fault-free LPV controller design can now be described as a basis for the development of the active FTC system.

5.6 The Polytopic LPV Controller Design

In this Section, the case study robot manipulator as described in Section 5.5.2 is used to illustrate various control polytopic modelling issues and FTC design. The feedback control is developed for the nominal (fault-free) system of Eq. (5-50). The control objective is to compute the required actuator inputs to perform desired tasks (e.g. move the manipulated load to a desired position), given the measured system states, namely the vector φ of joint angles, and the vector $\dot{\varphi}$ of joint velocities.

5.6.1 Design of controller for nominal/fault-free case

Let a nominal state feedback control vector be $u_{nom}(t) = K_{lpv}x(t)$ [i.e. for the fault-free case], where $K_{lpv} \in \Re^{2x4}$ is controller gain matrix of the polytopic system to be designed. Before the nominal controller design can be completed it is first necessary to develop a stability condition that will be satisfied by all the LPV vertices.

The closed-loop nominal (fault-free) control system can be developed from the open-loop system of Eq. (5-58) as:

$$\begin{aligned} \dot{x}(t) &= [A(\varphi) + B(\varphi)K_{lpv}]x(t) \\ &= [A_{ij} + B_i K_{lpv}]x(t) \\ & \qquad i = 1, 2 \quad j = 1, 2, \ldots, 4 \end{aligned} \tag{5-61}$$

where;

$$\begin{aligned} A(\varphi) + B(\varphi)K_{lpv} &\in \{A_{11} + B_1K_{lpv}, \ldots, A_{14} + B_1K_{lpv}, A_{21} + B_2K_{lpv}, \ldots, A_{24} + B_2K_{lpv}\} \\ &\in \left\{\Pi^{-1}\begin{pmatrix} 0 & I \\ -G_1^g & 0 \end{pmatrix} + \Pi^{-1}WK_{lpv}, \ldots, \Pi^{-1}\begin{pmatrix} 0 & I \\ -G_4^g & 0 \end{pmatrix} + \Pi^{-1}WK_{lpv}\right\} \end{aligned}$$

and

$$\Pi \in Co\left\{\begin{pmatrix} I & 0 \\ 0 & \Xi_1 \end{pmatrix}, \begin{pmatrix} I & 0 \\ 0 & \Xi_2 \end{pmatrix}\right\}$$

The following quadratic stability conditions are now defined at each vertex for the S.P.D. Lyapunov matrix S_c:

$$(A_{ij} + B_i K_{lpv})S_c + S_c(A_{ij} + B_i K_{lpv})^T < 0 \tag{5-62}$$

or

$$\left(\Pi_i^{-1}\begin{pmatrix}0 & I\\ -G_j^g & 0\end{pmatrix}+\Pi_i^{-1}WK_{lpv}\right)S_c+S_c\left(\Pi_i^{-1}\begin{pmatrix}0 & I\\ -G_j^g & 0\end{pmatrix}+\Pi_i^{-1}WK_{lpv}\right)^T<0 \qquad (5\text{-}63)$$
$$i=1,2 \quad j=1,2,\ldots,4$$

Let $L_c = K_{lpv}S_c$, and then $K_{lpv} = L_c S_c^{-1}$ and the inequality is linear in the term of L_c and K_{lpv}:

$$A_{ij}S_c + B_i L_c + S_c A_{ij}^T + L_c^T B_i^T < 0 \qquad (5\text{-}64)$$
$$i=1,2 \quad j=1,2,\ldots 4$$

As discussed in Section 5.5.2, these LMIs lead to a polytopic controller with 8 vertex systems, with each system having *4* states, *2* inputs, and *2* outputs as follows:

$$\begin{aligned}
A_{11}S_c + B_1 L_c + S_c A_{11}^T + L_c^T B_1^T &< 0\\
A_{12}S_c + B_1 L_c + S_c A_{12}^T + L_c^T B_1^T &< 0\\
A_{13}S_c + B_1 L_c + S_c A_{13}^T + L_c^T B_1^T &< 0\\
A_{14}S_c + B_1 L_c + S_c A_{14}^T + L_c^T B_1^T &< 0\\
A_{21}S_c + B_2 L_c + S_c A_{21}^T + L_c^T B_2^T &< 0\\
A_{22}S_c + B_2 L_c + S_c A_{22}^T + L_c^T B_2^T &< 0\\
A_{23}S_c + B_2 L_c + S_c A_{23}^T + L_c^T B_2^T &< 0\\
A_{24}S_c + B_2 L_c + S_c A_{24}^T + L_c^T B_2^T &< 0\\
S_c = S_c^T &> I
\end{aligned} \qquad (5\text{-}65)$$

The following matrices S_c and L_c in inequalities of Eq. (5-65) are computed using the MATLAB©LMI toolbox after 24 iterations:

$$S_c = \begin{pmatrix} 0.0741 & 0.0000 & -0.2577 & 0.0000\\ 0.0000 & 0.7119 & 0.0000 & -2.2422\\ -0.2577 & 0.0000 & 1.2756 & -0.0000\\ 0.0000 & -2.2422 & -0.0000 & 8.7738 \end{pmatrix}$$

$$L_c = \begin{pmatrix} -7.2820 & 0.0000 & -23.9273 & -0.0000\\ -0.0000 & -8.3692 & 0.0000 & -40.7558 \end{pmatrix}$$

And the controller can be constructed as:

$$K_{lpv} = \begin{pmatrix} -550.0309 & 0.0000 & -129.8775 & 0.0000\\ 0.0000 & -135.2864 & 0.0000 & -39.2184 \end{pmatrix}$$

The simulation results in Figure 5-6 and Figure 5-7 with polytopic LPV controller design as described in Section 5.6.1 show that the two-link manipulator remains stable

although the quadratic terms, $O(\varphi, \dot{\varphi})$ are neglected in the design of the polytopic model [see Eq. (5-50) in Section 5.5.2].

Figure 5-6 shows that the two-link robot arm is commanded to move from the initial condition with joint angles (0, 0) to the joint angles (10, 20). Figure 5-7 demonstrates the movement of the two-link manipulator from the larger initial condition (20, 40) back to (0, 0).

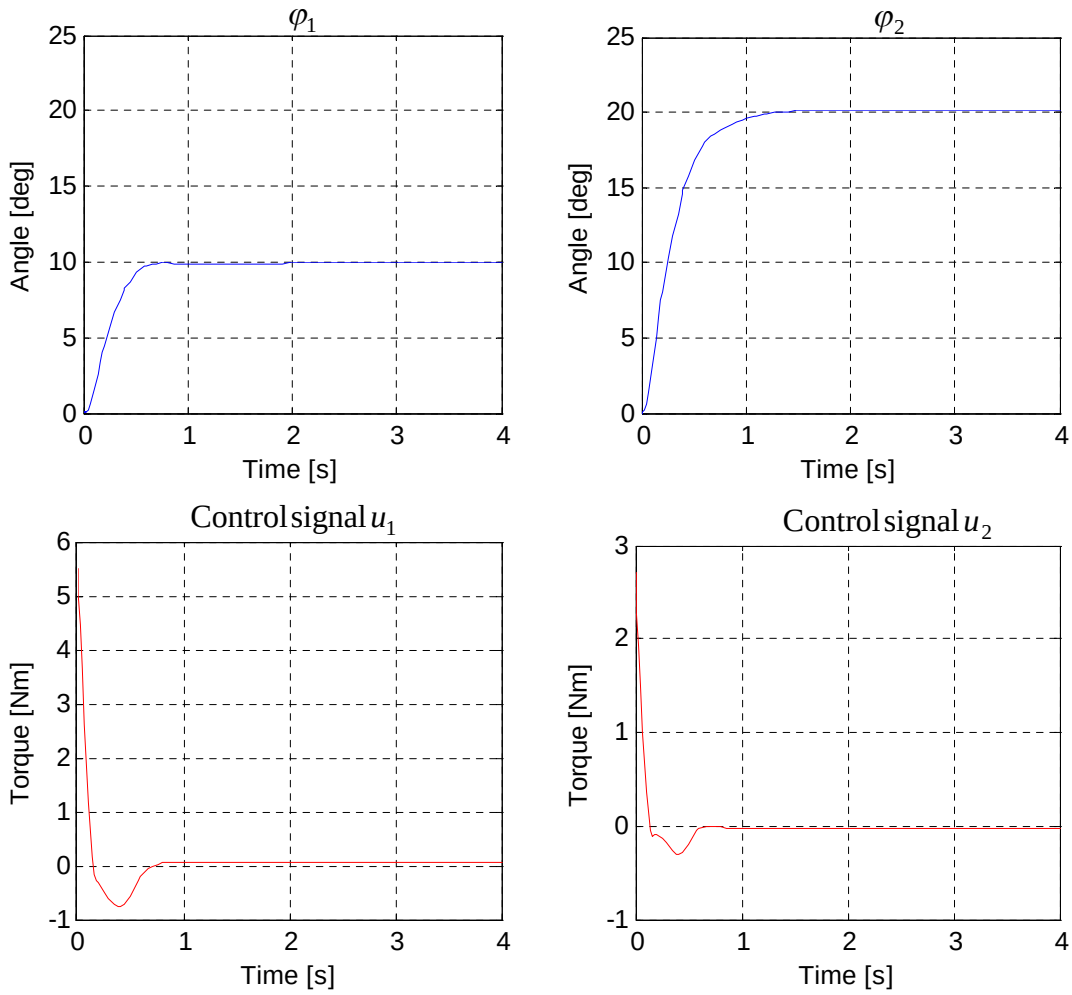

Figure 5-6: The control/output responses of the nonlinear system moving from (0, 0) to (10, 20)

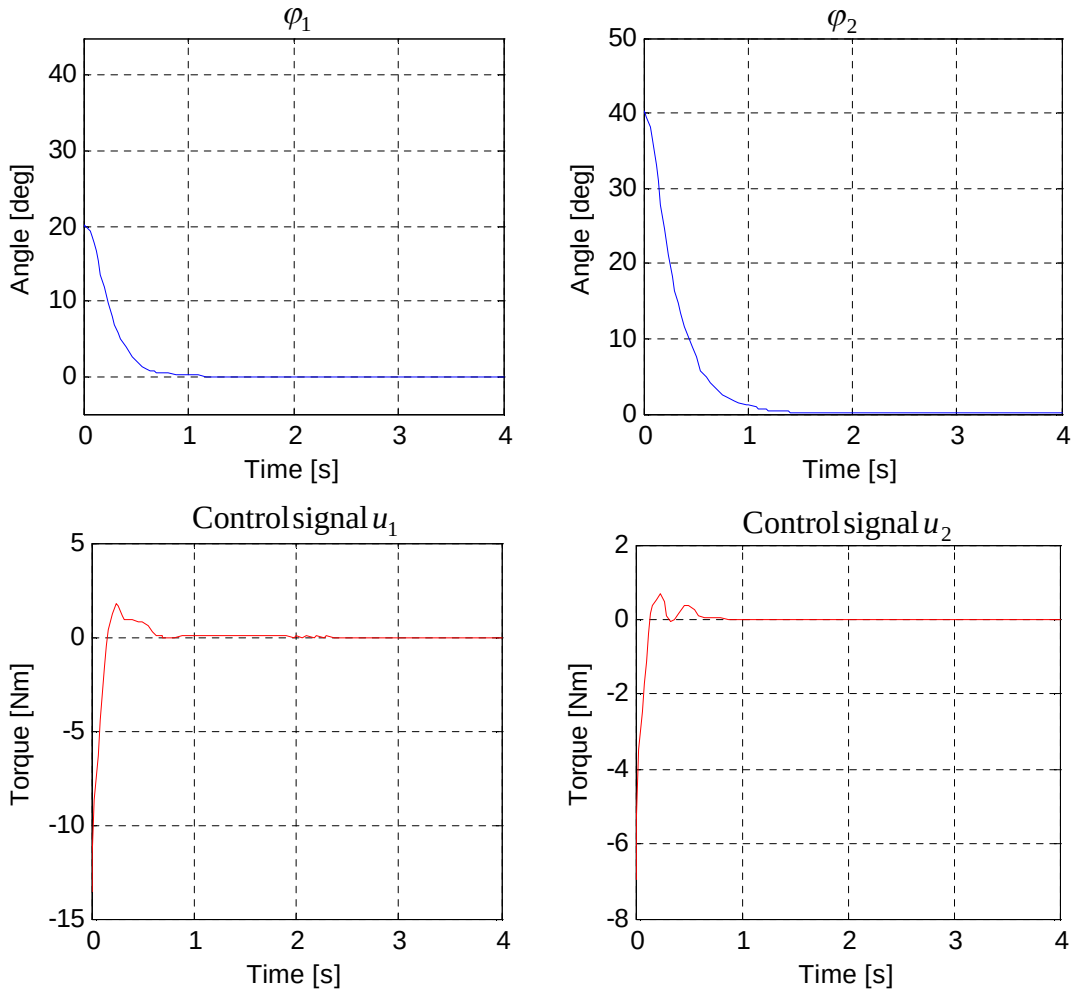

Figure 5-7: The control/output responses of the nonlinear system moving from (20, 40) to (0, 0)

5.6.2 Design of controller for active FTC

As described in Section 5.5.3, the dynamic system of in Eq. (5-60) includes an additive description of the actuator faults. However, the faults can have a multiplicative effect in the system representation. A multiplicative actuator fault representation can be defined as:

$$\dot{x}(t) = A_{ij}x(t) + B_i[I_m - \eta^a(t)]u(t) \qquad i = 1, 2 \quad j = 1, 2, \ldots 4 \tag{5-66}$$

where η^a is the so-called *fault-effect factor*, and $\eta^a = diag[\eta_1^a, \eta_2^a, \ldots, \eta_m^a]$, and $0 \le \eta_i^a < 1$ represents a fault in the i^{th} actuator and $\eta_i^a = 0$ means that i^{th} actuator operates normally (fault-free), whist $\eta_i^a > 0$ means that some degree of fault effect

occurs in the actuator. The state space equations in (5-60) and (5-66) is equivalent to:

$$F_a f_a(t) = -B\eta^a(t)u(t) \tag{5-67}$$

where the distribution matrix F_a is equal to the matrix B in an actuator fault case. The estimation of *fault-effect factor* $\hat{\eta}^a(t)$ is determined from the fault estimation $\hat{f}_a(t)$ provided by the fault estimator as described in Section 5.4.

The adaptive (time-varying) active FTC scheme can be developed by considering the system with the actuator fault vector $f_a(t)$ described in Eq. (5-66) in terms of $\hat{\eta}^a(t)$ and based on the nominal controller synthesized in Section 5.6.1. This is achieved under the assumption that the fault occurrence and fault effect factors η^a are known, i.e. they are provided by the polytopic LPV estimator described Section 5.4.

Theorem 5.2

From a design consideration consider the system in Eq. (5-66) with $i = 1, 2, \ldots, m$ actuator faults ($\eta^a \neq 0$) acting independently within each of the m vertex control systems with identical gain matrix K_{lpv} The new control action (assuming non-zero fault effects) is given as:

$$\begin{aligned} u_{FTC}(t) &= \underbrace{[I - \hat{\eta}^a(t)]^+ K_{lpv}}_{K_{FTC}} x(t) \\ &= K_{FTC}(\hat{\eta}^a) x(t) \end{aligned} \tag{5-68}$$

where $(I - \hat{\eta}^a)^+$ is the *Pseudo-Inverse* of $(I - \hat{\eta}^a)$ [see Figure 5-8], and $K_{FTC}(\hat{\eta}^a)$ is the adaptive controller gain for the FTC mechanism, depending on the on-line estimation $\hat{\eta}^a$.

Figure 5-8 shows a design structure of the active FTC system, where $P(\theta)$ is the polytopic LPV closed-loop system with exogenous disturbances and actuator faults as defined in Eq. (5-2). $K_{FTC}(\hat{\eta}^a)$ is the on-line adaptive controller gain matrix for the active FTC system as in Eq. (5-68), and the $\hat{\eta}^a$ is an estimate of η^a, which can be estimated on-line using a suitable polytopic LPV estimator as in Eq. (5-5).

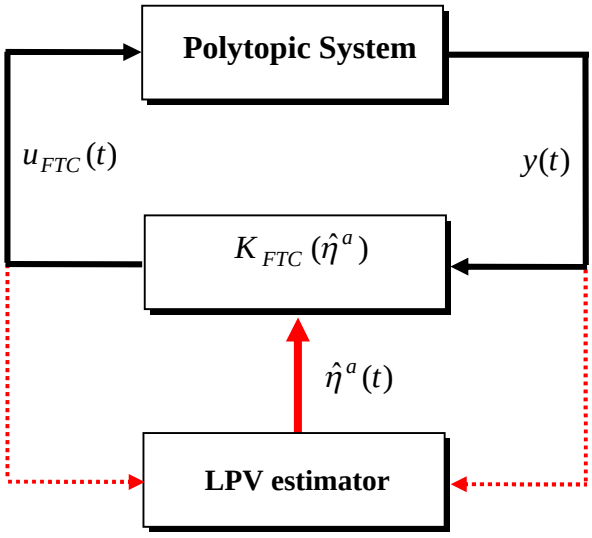

Figure 5-8: Active fault-tolerant control scheme

Proof of Theorem 5.2

Consider Eq. (5-66) When an actuator fault occurs in a given vertex system, the controller of the complete polytope system is given by:

$$\dot{x}(t) = Ax(t) + B[I - \eta^a(t)]u(t) \tag{5-69}$$

The new closed-loop LPV system is determined by substituting the new control law from Eq. (5-68) into the fault-corrupted system of Eq. (5-69), yielding:

$$\begin{aligned}
\dot{x}(t) &= Ax(t) + B[I - \eta^a(t)]u_{FTC} \\
&= Ax(t) + B[I - \eta^a(t)]K_{FTC}(\hat{\eta}^a)x(t) \\
&= Ax(t) + B\underbrace{[(I - \eta^a(t)][(I - \hat{\eta}^a(t)]^+}_{\approx I_m}K_{lpv}x(t) \\
&= Ax(t) + BK_{lpv}x(t) \\
&= Ax(t) + Bu_{nom}(t)
\end{aligned} \tag{5-70}$$

It can be seen that the term $(I - \eta^a)$ acting on the system of Eq. (5-66) can be removed by replacing u with u_{FTC} in Eq. (5-68), which completes the proof. ■

Figure 5-9 shows the system simulation, with a fault acting on the torque input at the manipulator joint [i.e. control input (u_1) is interrupted by $f_{a1}(t)$ in fault vector $f_a(t) = col[\, f_{a1}(t),\ f_{a2}(t)]]$ with $f_a(t) = col[1.25e10^{-2}\sin(t), 0.00]$ at $t = 1s$. It can be seen that the control and output performances are very poor and an oscillation is clearly visible as the robot aim moves from joint angle coordinates (5, 10) to

coordinates (0, 0). The closed-loop LPV system becomes unstable when the magnitude of the actuator fault increases to $f_{a1}(t) = 5.50e10^{-2}\sin(t)$ at $t = 10s$ [see Figure 5-10].

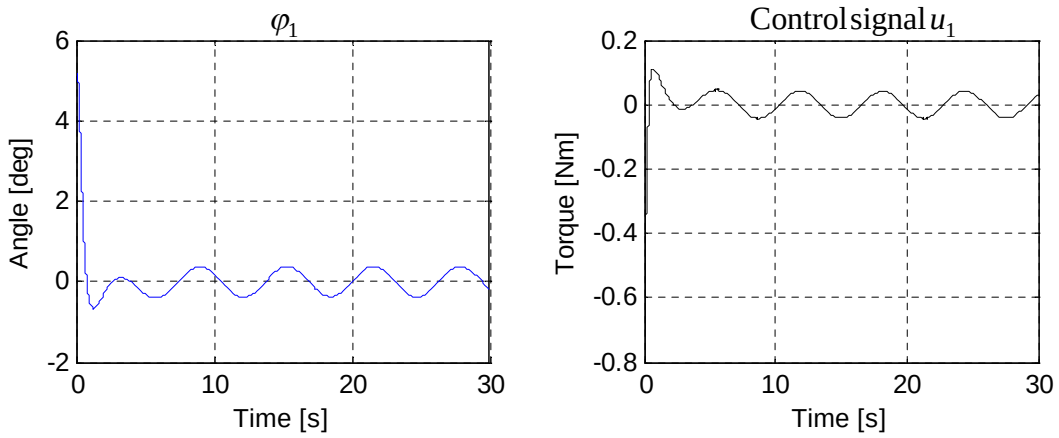

Figure 5-9: The control/output responses of the system without FTC, when the actuator fault [$f_{a1} = 1.25e10^{-2}\sin(t)$] occurred at $t = 1s$

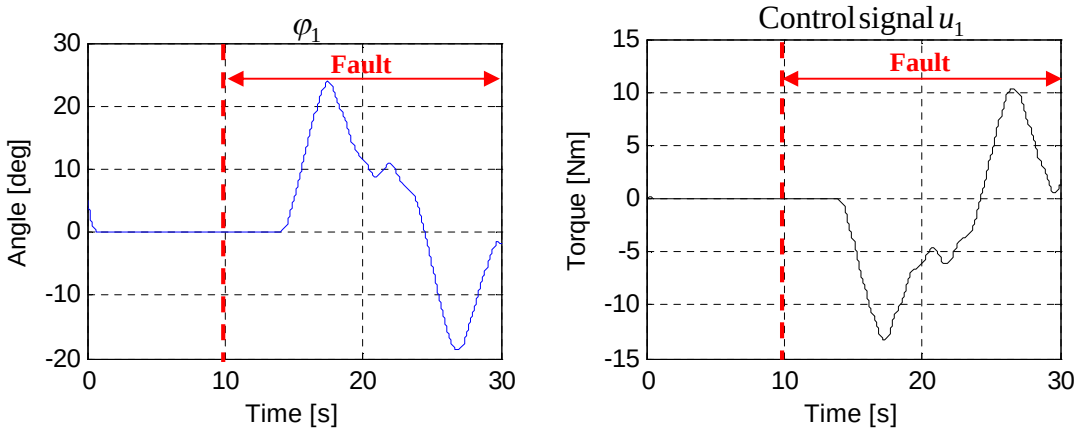

Figure 5-10: Control/output responses of the unstable system without FTC, when the actuator fault [$f_{a1} = 5.50e10^{-2}\sin(t)$] occurred at $t = 10s$

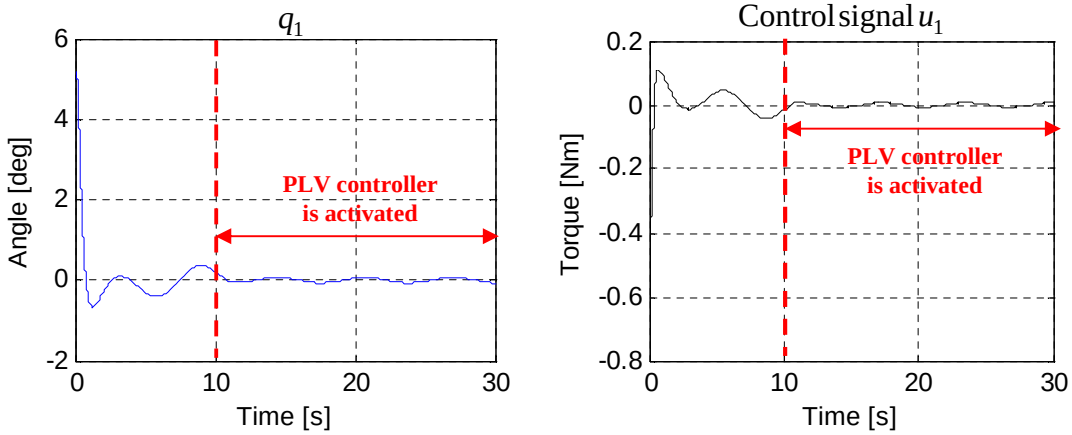

Figure 5-11: The control/output responses of the system with FTC activated at $t = 10s$, when the actuator fault [$f_{a1} = 1.25e10^{-2}\sin(t)$] occurred at $t = 1s$

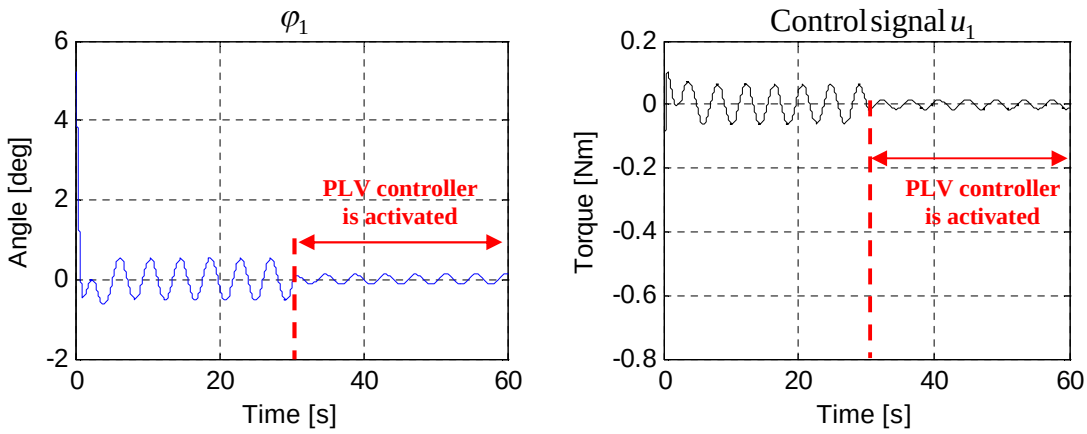

Figure 5-12: The control/output responses of the system with FTC activated at $t = 30s$, when the actuator fault [$f_{a1} = 2.50e10^{-2}\sin(1.5t)$] occurred at $t = 1s$

Figure 5-11 shows that if the polytopic LPV controller is employed under the assumption that the $\hat{\eta}^a(t)$ can be estimated perfectly by the polytopic LPV estimator in Eq. (5 - 5), then the actuator fault can be compensated using new LPV control law in Eq. (5-68). It can be seen that the control and output performances soon return to their nominal/reference values with a very small amount of oscillation.

Figure 5-12 shows that even if the actuator fault increases to $f_{a1} = 2.50e10^{-2}\sin(1.5t)$ [twice the previous magnitude], the system is still stable and provides a very good control performance after the polytopic LPV controller mechanism is activated at $t > 30s$. This demonstrates very well the fault-tolerance of the LPV active FTC system. However, when the actuator fault magnitude increases to $f_{a1} = 5.50e10^{-2}\sin(t)$, the system becomes unstable and the FTC performance is very poor.

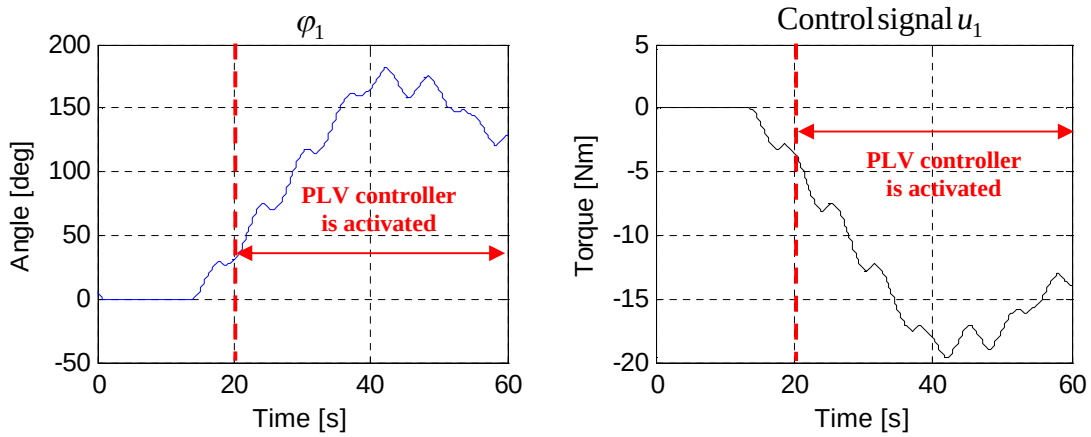

Figure 5-13: The control/output responses of the system with FTC activated at $t = 20s$, when the actuator fault [$f_{a1} = 5.50e10^{-2}\sin(t)$] occurred at $t = 10s$

5.7 Conclusion

This Chapter proposes a new strategy of an active FTC and polytopic LPV estimator for systems which can be implemented via a set of LMIs using efficient interior-point algorithms (Apkarian *et al*., 1995).

In the work of this Chapter an on-line polytopic LPV estimator is synthesized for providing the estimate of actuator fault which is used in an active FTC strategy to schedule predefined state feedback gains. These gains are also calculated using LMIs for nominal and faulty cases in order to maintain the system performances over a wide operating range within a proposed polytopic model. This can be implemented easily via the MATLAB©LMI toolbox.

The active FTC controller is a function of the *fault effect factors* as defined by Chen *et al* (1999) and Chen and Patton (2001) which can be derived on-line (in this case) from the residual vector of a polytopic LPV estimator mechanism. The proposed active FTC scheme is investigated using the two-link manipulator with an actuator fault acting on the torque input of the first manipulator joint.

Simulation results show that the design of polytopic LPV estimator can follow the fault rapidly and effectively with robustness to disturbance signal. This gives the system continue operating safely via on-line active FTC controller mechanism.

Chapter 6.
Fault-tolerance in Distributed Control Systems

6.1 Introduction

The concept of control of distributed systems is becoming an important subject in control systems, bringing with it challenges to the control of inter-connected and complex processes. It turns out that the requirements for control of an inter-connected system are quite different from the classical view of control. Classical control is built around the idea of point-to-point control, whereas the distributed control problem necessarily has a many-to-many connection structure with some closeness to the concept of "control of a network" (Patton *et al*, 2006). The distributed network system has special requirements focused on the importance of re-configurability and the need for control of an uncertain inter-connected system, leading to powerful robustness in control. The uncertainly arises from the inter-connected dynamic system structure and can also be a consequence of complexity from uncertain dynamic behaviour. The uncertain behaviour can also arise as the inter-connected dynamical subsystems must have some degree of automatic reconfiguration, i.e. avoiding such behaviour and providing reliable FTC is a currently a subject of research interest (Brennan *et al*., 2002; Maturana *et al*., 2003).

This Chapter proposes modifications to the architecture and framework for FTC for distributed control systems proposed by Patton *et al* (2007). The Patton *et al* (2007) work does not describe or consider methods for FDI as it is assumed in that work that the global control action provides a degree of fault compensation (fault accommodating control) for certain bounded faults. The new work considers the dynamic behaviour of the overall inter-connected system and includes fault-tolerance using the integration of FDI and control functions at the local as well as reconfiguration task at global levels (Patton *et al*, 2007; Kambhampati *et al*., 2007; Klinkhieo *et al*, 2008).

6.2 Challenges of FTC in Distributed Systems

In a classical point-to-point architecture, control loops are considered one at a time with the system components and inter-connections (sensors and physical networked links) being permanently linked/wired (Patton *et al*, 2006). The control of complex and uncertain systems such as the distributed/inter-connected network cannot simply involve the analysis of one or more control loops as the complexity is dependent upon dynamic (i.e. changing) interactions between system (perhaps embedded) components. The presence of uncertain components (e.g. affected by disturbances or faults) means that the control of the inter-connected system requires an architecture that can provide fault-tolerant properties. In other words it must able to reconfigure autonomously subject to faults (or due to other anomalies defined as faults), and self-repair or accommodate to anomalies e.g. uncertain behaviour and faults, as stated in (Patton *et al*, 2007) "*It becomes clear that point-to-point control architectures do not easily support system reconfiguration, subsequent to fault events*".

However, an FTC system is essentially a connection of embedded systems with the complexity arising from a number of factors:

- The number of components in the overall system,
- Interactions between the various components that could result in *a priori* un-modelled behaviour,
- Faults which cannot be taken into account *a priori*, and
- Effect of propagation of faults from one sub-system to another.

Classical FDI procedures for single-point control structures e.g. use either signal-based or model-based approaches. Both approaches use the concept of local modelling and are only applicable to the single-point control structure system (Patton *et al*., 2007). In the

quantitative model-based approach the local models are explicit, whilst in the signal-based (or data-driven) approaches implicit models are used. It becomes clear that distributed/inter-connected systems need a different form of modelling philosophy as the classical methods of FDI are no longer applicable (Patton *et al*., 2007).

From the above discussion, the complexity/uncertainty in the control of distributed system implies that '…*we must move away from the use of point-to-point classical control strategies as they do not offer an efficient way of achieving reliable FTC*…' (Patton *et al*, 2007). Therefore, the analytical tools and design methods for handling with such complexities/uncertainties of the distributed and inter-connected systems are mainly required. For example, the reconfiguration and accommodation require mechanisms for monitoring, detecting unusual system changes or faults in order to achieve fault tolerance.

In a classical sense the FDI is based on redundant analytical relationships between the various inputs and outputs of the process using local system modelling (as described in Chapter 2). When many such local components are inter-connected together the challenges of FDI and even control become much greater as the system is difficult to model using classical modelling concepts. Currently, FTC studies only include the effects of faults at either component or local controller levels. One can see very clearly that '…*the autonomous FTC system has a distributed nature involving fault diagnosis and control at various local to global levels of system embedding.*…' (Patton *et al*, 2007).

The key challenge at a global level of a distributed or inter-connected system is to make sure that the system functions safely, and reliably. This requires that the system has a strong and reliable capability to detect and accommodate faults via a reconfiguration of the design system architecture. The simplified structure of a distributed system can be represented as different inter-connected levels with: (i) a coordinating level, (ii) local levels, and (iii) subsystem (or component) level (Patton *et al*., 2006). Thus the framework required would involve the following:

1. Architectures for the design of systems with learning, fault tolerance and self-repairing features.
2. Computational strategies for modelling complex systems
3. New control strategies for complex embedded systems
4. Optimal decision-support systems for enhanced autonomy and fault-tolerance

Each subsystem is capable of control, identifying and locating faults and/or changes in system behaviour and inter-communication with other subsystems in the overall system, ensuring the maintenance of the required local and global objectives. Re-configurability is dependent on the connectivity (and hence redundancy) in the multi-subsystem structure.

It is clear that a deep interaction must take place between these levels, and the information and decisions taken one effect the system as a whole. This leads to the proposed concept of the Autonomous Coordination and Supervision Scheme (ACSS) whose goal is to take into account the uncertainty in the system (e.g. state of the system, faults and the effect of the environment) using a on-line adaptive learning strategy (Patton *et al*., 2007; Kambhampati *et al*., 2007; Klinkhieo *et al*, 2008).

6.3 Integrated FTC and FDI in Distributed Control

Generally, in a distributed or even de-centralise FTC structure each subsystem would have both a FDI and a control function tasks. The tasks use localised knowledge, supplemented by information received from other tasks, for decision-making (see Figure 6-1).

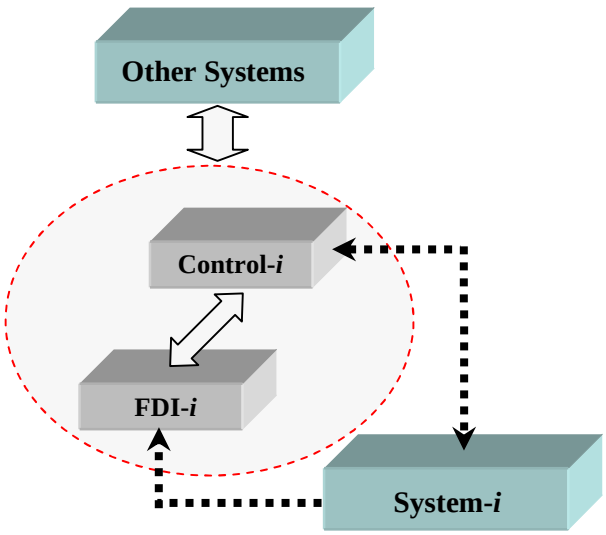

Figure 6-1 : The structure of the control and FDI tasks in distributed system

The drawback of this structure is that all the tasks need to be communicated with each other. *In other words every task has information regarding all other tasks whether it is required or not*. The problem is involved with "bottle-necks" in the communication network which could induce additional uncertainty in terms of un-modelled time-delays,

etc. (Patton *et al*., 2006). This adds a further complexity to the robustness requirements of distributed control over the network. Furthermore, the various tasks cause multiple-time scales, having an additional level where a coordinator task must coordinate the all activities of the overall tasks.

The two main features of the control strategy of distributed system are re-configurability and *plug and play*. The latter refers to the property that the system might have to add or remove subsystems or other elements of the system. A desirable plug and play feature will mean that the overall system performance can be taken into account in a flexible way when such system elements are added/removed. This implies that sub-systems could be plugged and un-plugged from the distributed system whilst at the same time maintaining the performance. This imposes a constraint on the ability to both analyze and design suitable architectures. This is reflected by an *additively separable* performance criterion property defined as follows:

An additively separable performance criterion is one in which the overall performance of combined systems (subsystems) is combined additively so that if any one subsystem is excluded from the system the performance of the remaining subsystems are obtained collectively by simply removing the local performance criterion of the removed subsystem.

Tutorial Example of additively separable concept:

Consider a system consisting of two sub-systems and the index of performance is given by: $J = \int [x_1 x_2 + x_1^2 + x_2^2 + u_1^2 + u_2^2]dt$. This is *not* separable into two separate indices representing each of the two sub-systems.

On the other hand $J = \int [x_1 + x_2 + x_1^2 + x_2^2 + u_1^2 + u_2^2]dt$ is separable, in that $J_1 = \int [x_1 + x_1^2 + u_1^2]dt$ and similarly $J_2 = \int [x_2 + x_2^2 + u_2^2]dt$. ■

The examples show the performance indices corresponding to the two subsystems are independent of each other. It can be seen that when there are cross-products within one performance index these are only associated with the given index and are not reflected in the global performance of the system. For the above examples the global performance is given as: $J = J_1 + J_2$.

6.3.1 Development of a two-level architecture

Figure 6-2 shows the architecture for implementing a task-based solution to the problem of FTC in distributed systems. This demonstrates the coordination of *N* inter-connected systems, each having local FDI and control tasks. The diagram has been adapted from Patton *et al* (2007) by incorporating an important link between the local FDI and Reconfiguration Tasks.

The ACSS use the indicators of faults (e.g. residual signals), set-point changes, disturbances, and unusual plant operation to monitor the performance of each subsystem and compare their performances against global requirements used to co-ordinate the overall inter-connected system performance, stability and fault-tolerance (Patton *et al*., 2007; Kambhampati *et al*., 2007).

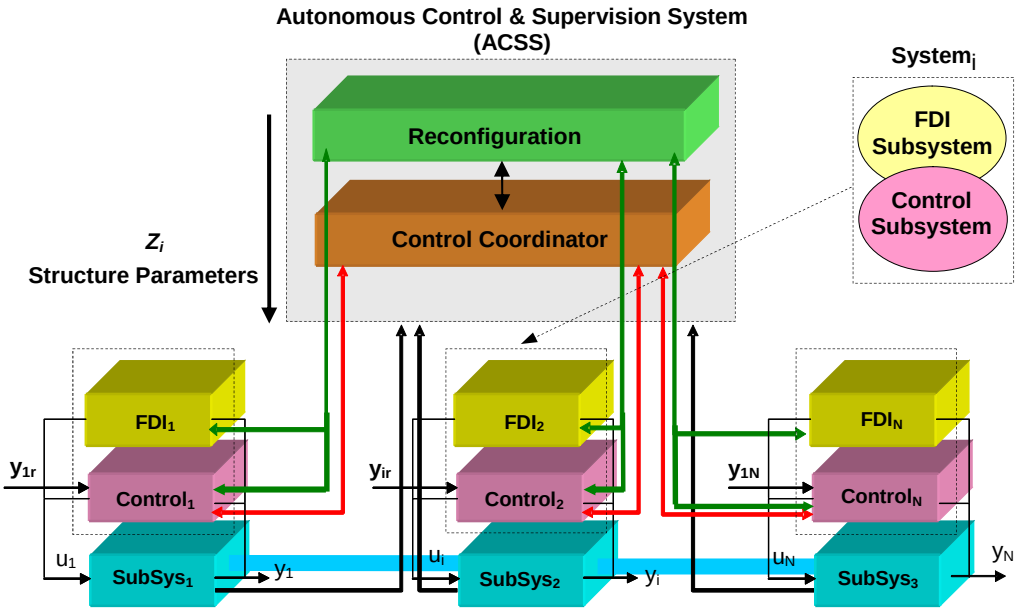

Figure 6-2: Autonomous Coordination & Supervision Scheme (ACSS) [adapted from Patton *et al*, 2007]

The ACSS architecture must satisfy the requirements as follows:

(i) A dynamic representation of the system for detecting and diagnosing faults,

(ii) A predictive approach for the design of FTC (Bemporad *et al*., 1997; Camacho and Bordons, 2004; Casavola *et al*., 2005a; Casavola *et al*., 2005b), and

(iii) Re-configurability enabling criteria

There are *four* types of tasks within the ACSS architecture (Figure 6-2). These are shown in Figure 6-3:

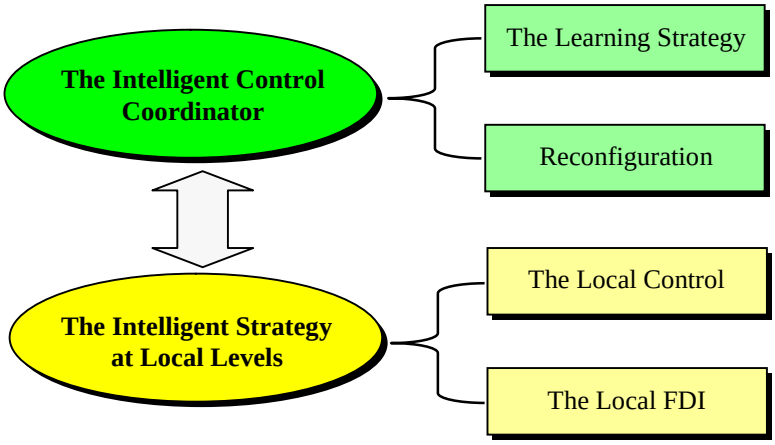

Figure 6-3: The four tasks of two-level ACSS architecture

6.4 FDI and Control Intelligence at Local Levels

6.4.1 Formulation of the inter-connected system structure

The system structure at a local level can be represented by the following:

$$\begin{aligned} \dot{x}_i(t) &= F_i(x_i, z_i, u_i) \\ &= f_i(x_i, u_i) + h_i(z_i) \\ y_i(t) &= \pi_i(x_i) \end{aligned} \qquad (6-1)$$

where: $(x_i, z_i, u_i) \to F_i(x_i, z_i, u_i) : \Re^{n_i} \times \Re^{l_i} \times \Re^{m_i} \to \Re^{n_i}$, $x_i(t)$, $z_i(t)$ and $u_i(t)$ are the states, interconnections and the control signals of the i^{th} subsystem, for $i = 1, 2, \ldots N$, respectively. Furthermore, $(x_i, u_i) \to f_i(x_i, u_i) : \Re^{n_i} \times \Re^{m_i} \to \Re^{n_i}$ is a local model of the i^{th} subsystem, and $(z_i) \to h_i(z_i) : \Re^{l_i} \to \Re^{l_i}$ is the inter-connection mappings affecting the local system (Patton *et al*, 2007; Kambhampati *et al*., 2007).

The inter-connection states are given by:

$$z_i(t) = \sum_{\substack{j=1 \\ i \neq j}}^{N} H_{ij} x_j(t) \qquad (6-2)$$

where: the H_{ij} are inter-connection matrices of appropriate dimensions as shown in Figure 6-4.

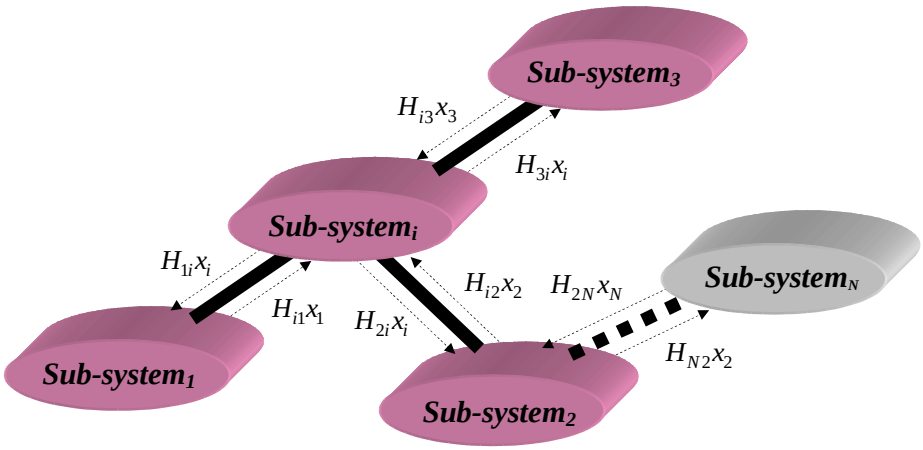

Figure 6-4: A set of interconnected nonlinear systems

On combining Eqs (6 - 1) and (6 - 2), the overall inter-connected system is given by:

$$\begin{aligned} \dot{x}(t) &= \tilde{f}(x,u) \\ y(t) &= \tilde{\pi}(x) \end{aligned} \qquad (6-3)$$

where $(x,u) \to \tilde{f}(x,u) : \Re^n \times \Re^m \to \Re^n$ satisfies $\tilde{f}(0,0) = 0$

As discussed in Section 6.2, in this inter-connected system un-modelled or unpredicted system behaviour is something which the system should be capable of dealing with. However, in a complex inter-connected system (e.g. arising from a nonlinear dynamical structure), all possible behaviours cannot be modelled as the effects of interconnections are not fully known or modelled. This is the case as the individual subsystems are considered as isolated systems with time-varying inter-connections between them. The isolated system is a special case of the subsystem defined in Eq. (6 - 3) in which the interconnection terms are assumed absent or ignored, according to the following general definition:

Definition 6.1: The following system (Kambhampati *et al*., 2007):

$$\begin{aligned} \dot{x}_i(t) &= f_i(x_i,u_i) \\ &= f_i(x_i,t) + g_i(x_i)u_i^{local} \end{aligned} \qquad (6-4)$$

is called an *isolated system* of Eq.(6-1), and $(x_i,u_i) \to f_i(x_i,u_i) : \Re^{n_i} \times \Re^{m_i} \to \Re^{n_i}$

Section 6.4.2 discusses in some detail the strategy used for the identification of all the individual (isolated) subsystems using a recurrent neural network (RNN) approach. The

work is a development of the work of Delgado *et al* (1996) and Garces *et al* (2003) which was based only on the identification of a single system.

6.4.2 RNN for subsystem identification

The identification of the individual local level subsystems (isolated systems) of the inter-connected and distributed system defined above can be solved using a neural network approach if the neural network is capable of representing/identifying a dynamical system. It is well known that a *Recurrent Neural Network* (RNN) can model a dynamical system as a consequence of its recurrent (recursive) structure (Nelles, 2001). Alternatively, other soft-computing paradigms (e.g. genetic algorithms) can be used. Here, an RNN procedure is used as an extension of the work of Delgado *et al* (1996) and Garces *et al* (2003). The strategy is one of identifying a RNN for the local systems, and then using the resulting "isolated systems" in the FDI and local control strategies. The advantages of using this RNN identification procedure are that:

(a) precise knowledge of the plant is not required
(b) the neural network will pick up the relevant structural information regarding the plant dynamics, e.g. the structure of the *weight matrices*, and the relative plant dynamic order.

The artificial NN consists of several interconnections of simple nonlinear systems or so-called neurons (Delgado *et al*., 1995). A dynamic RNN is a network of dynamic neurons with forward and backward connections i.e. the introduction of feedback into feedforward NN architecture provides a state space dynamic model.

Therefore, a dynamic RNN is a collection of dynamic neurons partially interconnected to a function of their own output which is represented by a differential equation (Garces *et al*., 2003). This dynamic structure is illustrated in Figure 6-5.

Consider the generalised nonlinear inter-connected system of Eq. (6 - 3) , the network can be described by a state space neural system of the form (Garces *et al*., 2003; Kambhampati *et al*., 2007):

$$\begin{aligned} \dot{x} &= -\tau x + w\sigma(x) + \Gamma u \\ y &= Cx \end{aligned} \qquad (6-5)$$

where $x \in \Re^n$, $u \in \Re^m$, $\tau = diag[\tau_1, \tau_2, ..., \tau_n]$, $w \in \Re^{nxn}$, $\Gamma \in \Re^{nxm}$, $C = I_{mxn}$, and with the smooth and differentiable nonlinear functions; $\sigma(x) = [\sigma(x_1), \ldots, \sigma(x_n)]^T$, respectively (See also the proof in Delgado *et al*., 1995).

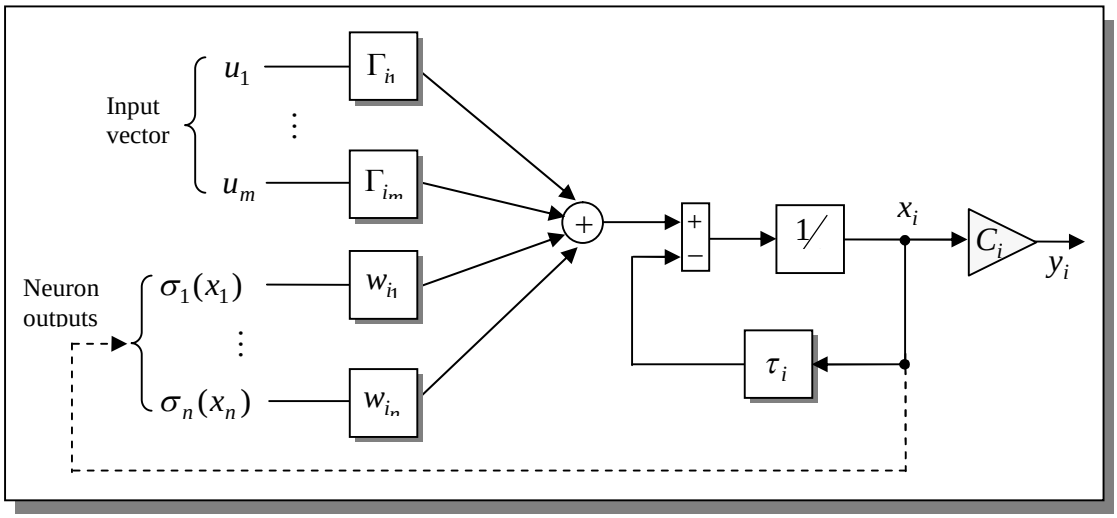

Figure 6-5: The dynamic structure of RNN (from Garces *et al*., 2003)

The identification scheme assumes that the plant is "black box" and the only available information is input $u(t)$-output $y(t)$ data (see Figure 6-6).

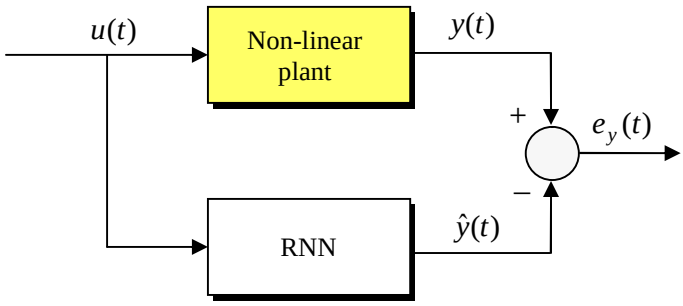

Figure 6-6: The system identification using RNN

Figure 6-6 shows the nonlinear plant and the dynamic RNN during the identification process, where $e_y(t) = y(t) - \hat{y}(t)$ is the output estimation error. The training is carried out repetitively over the fixed time interval $[0, t_f]$ to minimize the Mean-Squared-Error (MSE) performance index:

$$J = \left[\frac{1}{t_f} \int_o^{t_f} e_y^2(t)\, dt \right]^{1/2} = \left[\frac{1}{t_f} \int_o^{t_f} [y(t) - \hat{y}(t)]^2\, dt \right]^{1/2} \qquad (6\text{-}6)$$

As an extension of the work of Delgado *et al* (1996) and Garces *et al* (2003) and in order to model the i^{th} subsystem which is inter-connected within the overall system described by Eq. (6 - 3) , the dynamic RNN structure of Eq. (6 - 5) must be modified as:

$$\dot{x}_i = -\tau_i x_i + w_i \sigma(x_i) + \Gamma_i u_i + \tilde{w}_i \sigma(z_i) \qquad (6\text{-}7)$$

where $x_i \in \Re^{n_i}$, $u_i \in \Re^{m_i}$, $\tau_i = diag[\tau_1^i, \tau_2^i, ..., \tau_{n_i}^i]$, $w_i \in \Re^{n_i x n_i}$, $\Gamma_i \in \Re^{n_i x m_i}$, $C_i = I_{m_i x n_i}$. The smooth nonlinear functions are given by $\sigma(x_i) = [\sigma(x_1), \ldots, \sigma(x_{n_i})]^T$ and $\sigma(z_i) = [\sigma(z_1), \ldots, \sigma(z_{n_i})]^T$, respectively, where the $\tilde{w}_i \sigma(z_i)$ represent the interconnections between the subsystems.

If the functions $\sigma(z_i)$ from $\tilde{w}_i \sigma(z_i)$ can be considered approximately linear (subject to some assumed equilibrium condition, e.g. resulting from control action), then Eq. (6 - 7) becomes (Kambhampati *et al*., 2007):

$$\dot{x}_i = -\tau_i x_i + w_i \sigma(x_i) + \Gamma_i u_i + \sum_{\substack{j=1 \\ i \neq j}}^{N} H_{ij} x_j \qquad (6\text{-}8)$$

It is important to note that the structural properties of the RNN of Figure 6-5 are dependent on the identified plant. The overall identified system matrices τ , w and Γ in Eq. (6 - 5) are obtained using the Neural Network MATLAB© toolbox, together with the modified procedure of Garces *et al* (2003). For this interconnected/distributed system this is based on the concept of linearization for each subsystem [τ_i , w_i and Γ_i].

The identified interconnected system has the structure of Eqs (6 - 9) -(6 - 1 1) in terms of the subsystem states x_i :

$$\dot{x}_i = \underbrace{(-\tau_i + w_i)}_{A_i} x_i + \underbrace{\Gamma_i}_{B_i} u_i + \boldsymbol{H}_i \bar{\chi}_i \qquad (6\text{-}9)$$

The terms $\boldsymbol{H}_i \bar{\chi}_i$ for $i = 1, 2, \ldots N$, represent the identified interconnection signals between the subsystems, where $\boldsymbol{H}_i = (H_{i1}, \ldots, H_{(i)(i-1)}, H_{(i)(i+1)}, \ldots H_{iN})$ and

$\bar{x}_i = col(x_1, \ldots, x_{i-1}, x_{i+1}, \ldots x_N)$. The block-partitioned matrices $A_i = (-\tau_i + w_i)$, $B_i = \Gamma_i$ and $\boldsymbol{H}_i$ are also determined through the partition of the overall inter-connected system ($A_{overall}$, $B_{overall}$) as follows:

$$A_{overall} = \begin{bmatrix} -\tau_1 + w_{11} & w_{12} & \cdots & w_{1N} \\ w_{21} & -\tau_2 + w_{22} & \cdots & w_{2N} \\ \vdots & \vdots & \ddots & \vdots \\ w_{N1} & w_{N2} & \cdots & -\tau_N + w_{NN} \end{bmatrix} \qquad (6\text{-}10)$$

$$B_{overall} = \begin{bmatrix} \Gamma_1 & * & \cdots & * \\ * & \Gamma_2 & \cdots & * \\ \vdots & \vdots & \ddots & \vdots \\ * & * & \cdots & \Gamma_N \end{bmatrix} \qquad (6\text{-}11)$$

where:

$$\begin{aligned} A_1 &= (-\tau_1 + w_{11}) & B_1 &= \Gamma_1 \\ A_2 &= (-\tau_2 + w_{22}) & B_2 &= \Gamma_2 \\ \vdots &= \vdots \quad , & \vdots &= \vdots \quad , \\ A_N &= (-\tau_N + w_{NN}) & B_N &= \Gamma_N \end{aligned}$$

$[*]$ represents matrices that are indefinite (do not need to be known),

$$\begin{aligned} \boldsymbol{H}_1 &= [w_{12}, w_{13,} \ldots, w_{1N}] \\ &= [H_{12}, H_{13,} \ldots, H_{1N}], \\ \boldsymbol{H}_2 &= [w_{21}, w_{23,} \ldots, w_{2N}] \\ &= [H_{21}, H_{23,} \ldots, H_{2N}], \\ &\vdots \\ \boldsymbol{H}_N &= [w_{N1}, w_{N2,} \ldots, w_{N,N-1}] \\ &= [H_{N1}, H_{N2,} \ldots, H_{NN-1}] \end{aligned}$$

The identified system structure given by Eqs (6 - 9) -(6 - 1 1) is applied within a strategy for detecting and isolating faults in each of the *N* local subsystems. It will be shown in Section 6.4.5 that the identified system structure can also be used for the development and design of the local control functions in the distributed system. However, for the local control of each subsystem the term $\boldsymbol{H}_i \bar{x}_i$ is considered as a disturbance term. This concept is described in Section 6.4.4. Section 6.4.3 now deals with definition and design problem for the local FDI task.

6.4.3 The local FDI problem

Section 6.3 states that a suitable FDI method must have a very specific role to play in enabling fault-tolerance in the distributed control system (see Figure 6-2). The FDI algorithms must distinguish between local and neighboring subsystem faults, inform the control supervisor that (a) a fault has occurred, (b) where it has occurred and (c) information about possible either the overall control requirements or re-configuration of the system. In the other situation when a subsystem is added or removed from the inter-connected systems the FDI structure should recognise this situation and inform the control coordinator which should then restructure its coordination efforts.

At a local level, the FDI task needs the presence of an estimator and the corresponding residual generator as described in Chapter 2. The residuals represent the differences between the observed behaviour and some nominal behaviour of the system (Chen and Patton, 1999; Kambhampati *et al*., 2007; Klinkhieo *et al*., 2008). These can be obtained by extending the system description given by Eq. (6 - 1) to take into account the faults represented by the fault vector f_i corresponding to the i^{th} subsystem.

$$\text{Model of subsystem } i: \quad \begin{cases} \dot{x}_i &= F_i(x_i, u_i) \\ &= f_i(x_i, u_i) + F_i^a f_i \\ y_i &= \pi_i(x_i) + F_i^s f_i \end{cases} \qquad (6\text{-}12)$$

where f_i is the local fault vector, F_i^a and F_i^s are the local fault distribution matrix for the local states and local measurements with appropriate dimensions, respectively. For this at a local level, based on the residuals generated by the observers, the various fault conditions can be identified. Thus the FDI observer and residual generator have the following form:

$$\text{FDI observer and residual generator}: \begin{cases} \dot{e}_i(t) &= \alpha_i(e_i, u_i, y_i, t) \\ r_i(t) &= \chi_i(e_i, u_i, y_i, t) \end{cases} \qquad (6\text{-}13)$$

where: $e_i(t)$ is a generalised error system, leading to a corresponding form for the residuals $r_i(t)$. The residuals thus generated should satisfy the following conditions:

$$\| r_i(t) \| \begin{cases} \approx 0 & \text{when} \quad f_i(t) = 0 \\ >> 0 & \text{when} \quad f_i(t) \neq 0 \end{cases} \qquad (6\text{-}14)$$

It should be noted that the estimator can have many forms (Chen and Patton, 1999; Kambhampati *et al*., 2007; Klinkhieo *et al*., 2008). A "fault" refers to any unwanted internal or external changes from the nominal (expected) system behaviour which could be a result of parametric and structural deviations and also unpredicted behaviour.

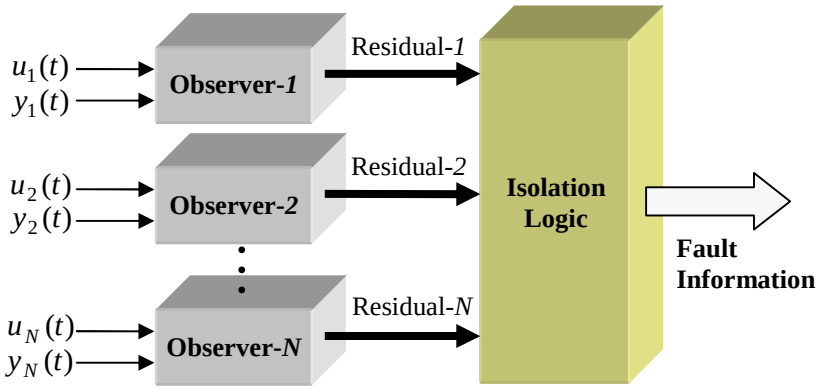

Figure 6-7: FDI structure without considering the network

It can be seen from Eqs. (6-13) and (6-14) that the FDI scheme has a highly local function [see Figure 6-7]. Indeed, it would indicate that a local fault has occurred as a result of getting faulty interconnection (z_i) which may cause FDI function giving a wrong fault indication. To take into account the interconnection faults, Eq. (6-12) should be extended as follows [see Figure 6-8]:

$$\text{Model of subsystem } i: \begin{cases} \dot{x}_i &= F_i(x_i, z_i, u_i) \\ &= f_i(x_i, u_i) + h_i(z_i) + F_i^a f_i \\ y_i &= \pi_i(x_i) + F_i^s f_i \end{cases} \qquad (6\text{-}15)$$

The added feature with the structure given by Eq. (6-15) is that in a *plug-and-play* situation if a subsystem is added or removed, all that is required is for the coordinator to be given the relevant information for augmenting the relevant terms, $h_i(z_i)$. These involve the effect of the new subsystem on the overall interconnection system. Once such structural information is available (via system identification), a *structural analysis*

here can be performed in order to assess the *Detectability* and *Isolability* of the faults in the plant (Chen and Patton, 1999; Boumama *et al*, 2006; Klinkhieo and Patton, 2008).

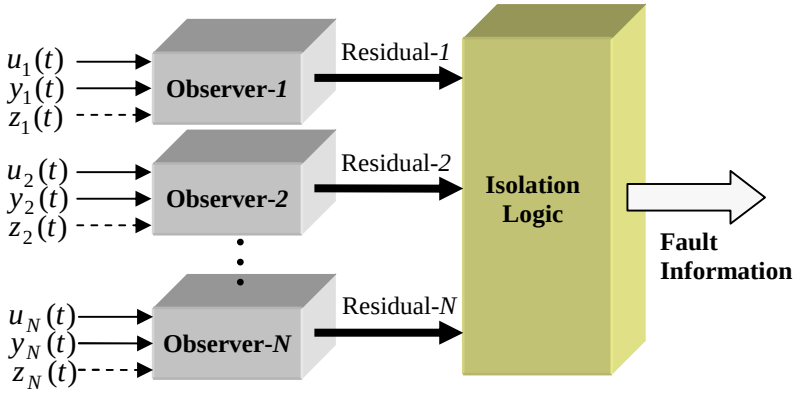

Figure 6-8: FDI with interconnections for local FDI

The linearised form of Eq. (6-15) is given as follows (see Section 6.4.2):

$$\left.\begin{aligned} \dot{x}_i &= (-\tau_i + w_i)x_i + \Gamma_i u_i + H_i \bar{x}_i + F_i^a f_i \\ y_i &= C_i x_i + F_i^s f_i \end{aligned}\right\} \qquad (6\text{-}16)$$

Thus, the local FDI based residual generator has the simple form:

$$\left.\begin{aligned} \dot{\hat{x}}_i &= (-\tau_i + w_i)\hat{x}_i + \Gamma_i u + L_i(y_i - C_i\hat{x}_i) \\ r_i &= y_i - C_i\hat{x}_i \end{aligned}\right\} \qquad (6\text{-}17)$$

where the L_i are the observer gains designed via the UIO approach (see description of this approach in Chapter 2). The simulation results of these robust local FDI approaches will be discussed and demonstrated in Chapter 7.

An alternative approach to this is to use overlapping decomposition techniques to design overlapping observers for FDI along the lines of (Singh *et al*., 1983; Ferrari *et al*., 2007). However, this approach has not been considered in this work.

6.4.4 The local control problem

Background and Motivation

In this thesis the task of the control at a local level is defined using a *receding horizon control* (RHC) problem formulation, based on the work of Keerthi and Gilbert (1988) and Mayne and Michalska (1990). In some limited sense the RHC problem is equivalent to the *model based predictive control* (MBPC) strategies which are popular

in the “process control” domain (Camacho and Bordons, 2004). However, the MBPC approach is usually based on input-output system information to optimize a control objective function, whereas the RHC formulation is based entirely in the state-space and applies to nonlinear system problems with no loss of generality (due to the local optimization within the time horizon). At first it would appear that the RHC formulation is therefore more general and is particularly suited to nonlinear system applications. From the literature it is clear that RHC and MBPC have initially developed along different lines of investigation.

The Mayne and Michalska (1990) results are limited to single level control, whereas Singh and Titli focus on multi-level control with a special emphasis on the applicability of the two-level special case. Focusing further on distributed and interconnected systems, Patton *et al* (2007) combine the work of Singh and Titli (1978) with that of Mayne and Michalska (1990) through the use of two-level RHC. The RHC formulation follows very naturally from the Singh and Titli results as it provides a powerful way of realising the two-level control goals in terms of a subsystem regulator control problem, based on constrained *Linear Quadratic Regulator* (LQR) Control.

Although Goodwin and Quevedo (2004) also discuss the potential of RHC for distributed and networked systems they focus only on single-level nonlinear interconnected systems. It turns out that the two-level approach is a very important development for FTC for distributed systems. This is an important emphasis in this thesis and the main ideas will be discussed more in this Section. It appears that the solutions for dealing with single level distributed control problems are complex and difficult to solve, simply as the high level control function is missing. The higher level in the two-level formulation provides some necessary information concerning the subsystem interconnection states and this is very important in the design of local FTC.

Hence, the minimization of interconnection states is a key to achieving good FTC action, when the interconnection states are bounded. This concept increases in importance as the number of subsystems becomes large. Although Singh and Titli reported their work in terms of large-scale systems, the issue of whether or not the system is large-scale or not is irrelevant since a distributed system with a significantly large number of interconnected subsystems becomes a large-scale system.

The main difference between the approaches of Singh and Titli (1978) and Keerthi and Gilbert (1988) is that the earlier work considers the Lagrange multipliers in terms of cooperation effort between the subsystems, i.e. to develop a good balance between the

subsystems under global control. In Keerthi and Gilbert (1988) and Mayne and Michalska (1990) the Lagrange multipliers are considered in terms of the co-states in a classical LQR optimization problem applied to a smooth nonlinear system.

In combining the work of Singh and Titli (1978) and Mayne and Michalska (1990), Patton *et al* (2007) show that this is a convenient formulation for distributed control problems as it facilitates the development of a control strategy for nonlinear and time-varying systems in which the effects of subsystem interconnections on the performance of the system can be evaluated in a transparent way. The Patton *et al* (2007) work on two-level control uses as a basis the optimality analysis arising from the concept of the isolated system in RHC of nonlinear systems, given by Mayne and Michalska (1990). This leads to powerful FTC properties for the control of uncertain interconnected and distributed systems.

Singh and Titli (1978) work proposes the use of the Interaction-Prediction Principle via a gradient optimization approach to the coordination function (higher level in two-level control). In contrast to this Patton *et al* (2007) include in their work the use of a learning coordinator based on interaction-prediction together with a new development in the use of RHC as a constrained regulator problem. This form of two-level control has been adopted further in this research.

The appropriate intersection of these studies provides a powerful framework for FTC in distributed and networked control systems in which robust FDI of the local subsystems can be added to further enhance the value of the two-level control approach. This thesis goes beyond the work of Patton *et al* (2007) by taking into account the effects of larger faults arising from the subsystems in addition to the time-varying subsystem interactions (which affect the robustness of the local FDI problem).

The development of RHC for the distributed control problem

In RHC, the current control at time t and state $x(t)$ are obtained by determining the predicted on-line (open-loop) optimal control $\hat{u}$ for the *horizon interval* $[t, t+T]$ and by setting the current control equal to $\hat{u}(t)$ (i.e. at time *t*) (Mayne and Michalska, 1990). A feedback control law is then obtained by repeatedly determining this optimal control law [since $\hat{u}(t)$ clearly depends on the current state $x(t)$]. The optimal control problem is usually posed as an on-line minimization of a quadratic function over the horizon $[t, t+T]$, subject to the terminal constraint $x(t+T) = 0$.

When RHC is applied to a nonlinear or time-varying distributed system with inter-connected local subsystems, the goal of the control is to minimise some local performance index subject to nonlinear interconnection constraints between the subsystems. This problem is now analysed in order to determine:

(1) the set of properties which would ensure (a) a solution to the problem, and (b) the stability of the solution provided by the control strategy, and

(2) a numerically efficient strategy which is globally suboptimal but locally optimal.

(2) above is important when dealing with either a distributed system or with a *plug and play* system (see discussion in Section 6.3), for which it is more efficient to determine locally optimal control laws together with bounds placed on the control inputs to account for the effects of subsystem interactions.

The local (single) level control problem

The distributed system can be stated as follows Mayne and Michalska, 1990): for a given Lagrangian multiplier $\lambda \in \Re^n$, determine a feedback control u^λ which minimizes $V(x,t;u) + \lambda^T x^\lambda(t+T;x,t)$ where $x^\lambda(t+T;x,t)$ is the solution of Eq. (6-3). Although λ is the classical Lagrangian multiplier, it is considered here as the *coordinating effort* (Singh and Titli, 1978) between the various subsystems, where $V(x,t;u)$ is the following receding horizon cost:

$$V(x,t;u) = \frac{1}{2}\int_{t}^{t+T}(x^T Q x + u^T R u)dt \qquad (6\text{-}18)$$

where the overall distributed system state and control performance weighting matrices Q and R, respectively are block-diagonal partitioned according to $Q = diag[Q_i], R = diag[R_i]$. The matrices $Q_i \in \Re^{n_i x n_i}$ are positive semi-definite and the matrices $R_i \in \Re^{m_i x m_i}$ are positive definite.

Since the performance index Eq. (6-18) is *additively separable* (see Section 6.3 for definition), Eq. (6-18) can be transformed into:

$$V(x,t;u) = \sum_{i=1}^{N}\left(\frac{1}{2}\int_{0}^{t_f}(x_i^T Q_i x_i + u_i^T R_i u_i)dt\right) = \sum_{i=1}^{N} V_i(x_i,t;u_i) \qquad (6\text{-}19)$$

where t_f is the time-horizon.

The development of the two-level control strategy

The control problem for the distributed system can now be solved by decomposing the problem into smaller sub-problems, one for each subsystem (Mesarovic *et al*, 1970; Singh and Titli, 1978). The decomposition is achieved by minimizing the following Lagrangian for the distributed system:

$$L(x,u,\lambda,p,z) = \sum_{i=1}^{N}\left(\int_{0}^{t_f}\frac{1}{2}(x_i^T Q_i x_i + \frac{1}{2}u_i^T R_i u_i + \lambda_i^T\left[z_i - \sum_{\substack{j=1\\ i\neq j}}^{N} H_{ij}x_j\right] + p_i^T\left[F_i(x_i,z_i,u_i)\right])\right)dt \qquad (6\text{-}20)$$

where $\lambda_i(t)$ is coordination variables [e.g. interactions taking place between the i^{th} subsystem and the other i-1 subsystems] and $p_i \in \Re^{n_i}$ are the classical co-states of the local system.

It can be seen that the Eq.(6-20) is also additively separable for any given z_i and λ_i. To satisfy the necessary conditions for global optimality within a two-level computational structure, Eq. (6-20) can be re-written the Lagrangian L as:

$$L = \sum_{i=1}^{N} L_i = \sum_{i=1}^{N}\left(\int_{0}^{t_f}\frac{1}{2}(x_i^T Q_i x_i + \frac{1}{2}u_i^T R_i u_i + \lambda_i^T z_i - \sum_{\substack{j=1\\ i\neq j}}^{N}\lambda_j^T H_{ji}x_i + p_i^T\left[F_i(x_i,z_i,u_i)\right])\right)dt \qquad (6\text{-}21)$$

The additively separable property of Eq. (6-21) facilitates the design of a two-level structure for the control of the distributed and interconnected system, as shown in Figure 6-2. The i^{th} local control problem is given by:

$$P(x_{i_0},t) = \begin{cases}\min\limits_{x_i,z_i,u_i} & V_i(x_i,u_i)\\ \text{subject to} & \dot{x}_i = F_i(x_i,z_i,u_i);\ x_i(t_0) = x_{i0}\end{cases} \qquad (6\text{-}22)$$

From Eq. (6-22) the i^{th} control function depends on both the local subsystem states $x_i \in \Re^{n_i}$ and the subsystem interconnection states $z_i \in \Re^{l_i}$. It thus becomes clear that the subsystem control has *two* components, namely (a) a control component based on local information and (b) a component based on the interactions, as discussed by Patton *et al* (2007). Thus:

$$u_i = u_i^{local} + u_i^{int.} \tag{6-23}$$

where u_i^{local} is the control for the i^{th} subsystem in isolation, and $u_i^{int.}$ is the compensating control for the interactions.

Ideally, each local controller requires on-line updated values of z_i and λ_i. There is clearly a computational requirement for iteratively improving the z_i and λ_i such that *N* local optimal can be achieved. In fact some coordination rules are required which can be derived from a consideration of the optimality conditions for solving Eq. (6-22). The development of the ACSS coordination rules are given in Section 6.5.

As given in the ***Definition 6.1*** (see Section 6.4.1) the optimal control law for each isolated subsystem with states $x_i \in \Re^{n_i}$ defined in terms of a single control component $u_i = u_i^{local}$ [compare with Eq. (6-23)] which is the solution to the problem defined by:

$$\begin{cases} \min\limits_{x_i, u_i} & V_i(x_i, u_i) \\ \text{subject to} & \dot{x}_i = f_i(x_i, u_i);\ x_i(t_0) = x_{i0} \end{cases} \tag{6-24}$$

This Section discuses the RHC law for an *isolated system*, as a precursor to defining the global control strategy, i.e. by considering just one subsystem and ignoring all the interconnections. The term *isolated system* is defined in ***Definition 6.1***. The solution to the problem of RHC has been investigated by a number of authors (Keerthi and Gilbert, 1988; Mayne and Michalska, 1990; Kambhampati *et al*, 2000) and a moving horizon approach to *networked control system* (NCS) design by (Goodwin and Quevedo, 2004). It is important to note here that whilst the NCS problem is certainly a form of distributed system, Goodwin and Quevedo, (2004) do not consider the two-level strategy for distributed control which is important in the work of this thesis.

Therefore, the following assumptions on the interconnections are required to establish the required pareto-optimal strategy required to balance the performance indices of the overall system.

Assumption 6.1:

It is assumed that the interconnection function $h_i(z_i)$ is smooth and that there exists a *Lipschitz Constant* $\kappa_i > 0$ such that $\|h_i(z_i)\| \leq \kappa_i \|x\|; x \in \tilde{\Omega}$, where x is the global state.

The ***Assumption 6.1*** is the result of the continuity of the interconnection mappings, and can be satisfied with relative ease by all inter-connection systems.

The determination of the required local distributed control is thus a three-stage process:

Stage 1: Determine the control for each isolated system (u_i^{local}),

Stage 2: Determine the interconnection-control $(u_i^{int.})$ and

Stage 3: Combine Stages 1 and 2 to give the i^{th} local control $u_i = u_i^{local} + u_i^{int.}$.

It should be recalled that the role of the ACSS coordinator is to update the interconnection states z_i (as an estimate) to balance the distributed system in terms of control performance. The update of the z_i {and hence the $h_i(z_i)$} is bounded as long as the iterative learning function of the coordinator is convergent.

6.4.5 Distributed system of *N* interconnected linear systems

Consider once again the lower level control problem, as discussed in Section 6.4.2 we now consider the case in which all the subsystems are linear. For this problem the results of Mayne and Michalska (1990) can still be applied as a trivial case of their work.

From Eq. (6-21) the Hamiltonian for the i^{th} linear isolated subsystem problem can be re-written as (Kambhampati *et al*., 2007):

$$H_i^{am} = \frac{1}{2} x_i^T Q_i x_i + \frac{1}{2} u_i^T R_i u_i + \lambda_i^T z_i - \sum_{\substack{j=1 \\ i \neq j}}^{N} \lambda_j^T H_{ji} x_i) + p_i^T \left[F_i(x_i, z_i, u_i) \right] \qquad (6\text{-}25)$$

For optimality let $\frac{\partial}{\partial x_i} H_i^{am} = 0$ Eq. (6-25) then leads to the following:

$$\dot{p}_i = -Q_i x_i - \tilde{A}_i p_i + \sum_{\substack{j=1 \\ i \neq j}}^{N} [\lambda_j^T H_{ji}]^T \qquad (6\text{-}26)$$

where $\tilde{A}_i = \frac{\partial}{\partial x_i} F_i(x_i, z_i, u_i)$ together with a linear system of state equations:

$$\dot{x}_i = F_i(x_i, z_i, u_i) \qquad (6\text{-}27)$$

Where the $\frac{\partial}{\partial x_i}$ denotes partial differentiation with respect to the x_i and the initial conditions $p_i(t_f) = 0$, $x_i(t_0) = x_{i0}$

Consider the linear system representation of Eq. (6-27):

$$\dot{x}_i = A_i x_i + B_i u_i + E_i z_i \qquad (6\text{-}28)$$

where A_i, B_i, E_i are known matrices with appropriate dimensions, then Eq. (6-26) are reduced to the following:

$$\dot{p}_i = -Q_i x_i - A_i^T p_i + \sum_{\substack{j=1 \\ i \neq j}}^{N} [\lambda_j^T H_{ji}]^T \qquad (6\text{-}29)$$

The well known LQR control input to the i^{th} system is given by:

$$u_i = -R_i^{-1} B_i^T p_i \qquad (6\text{-}30)$$

Now consider:

$$p_i = S_i x_i + \aleph_i \qquad (6\text{-}31)$$

where S_i and $\aleph_i$ are the solutions to the *Riccati Equations* Eqs. (6-37) together with the *Interaction Compensation* equations of Eq. (6-38) (Singh and Titli, 1978):

Then it follows that:

$$\dot{p}_i = S_i \dot{x}_i + \dot{S}_i x_i + \dot{\aleph}_i \qquad (6\text{-}32)$$

Substituting Eq. (6-30) into Eq. (6-28) gives

$$\dot{x}_i = A_i x_i - B_i R_i^{-1} B_i^T S_i x_i - B_i R_i^{-1} B_i^T \aleph_i + E_i z_i \qquad (6\text{-}33)$$

Since Eq. (6-32) is equivalent to Eq. (6-29), thus this giving:

$$S_i \dot{x}_i + \dot{S}_i x_i + \dot{\aleph} = -Q_i x_i - A_i^T p_i + \sum_{\substack{j=1 \\ i \neq j}}^{N} [\lambda_j^T H_{ji}]^T \qquad (6\text{-}34)$$

Substituting Eqs (6-31) and (6-33) into Eq. (6-34), then Eq. (6-34) can be rewritten as follows:

$$\dot{S}_i x_i + S_i A_i x_{ii} - S_i B_i R_i^{-1} B_i^T S_i x_i - S_i B_i R_i^{-1} B_i^T \aleph_i + S_i E_i z_i + \dot{\aleph}_i + Q_i x_i + A_i^T S_i x + A_i^T \aleph_i - \sum_{\substack{j=1 \\ i \neq j}}^{N} \left[\lambda_j^T H_{ji}\right]^T = 0 \qquad (6\text{-}35)$$

or

$$[\dot{S}_i + S_i A_i + A_i^T S_i - S_i B_i R_i^{-1} B_i^T S_i + Q_i] x_i + \left[\dot{\aleph}_i + A_i^T \aleph_i - S_i B_i R_i^{-1} B_i^T \aleph_i + S_i E_i z_i - \sum_{\substack{j=1 \\ i \neq j}}^{N} \left[\lambda_j^T H_{ji}\right]^T \right] = 0 \qquad (6\text{-}36)$$

Since Eq. (6-36) is valid for arbitrary x_i, it follows that:

$$\dot{S}_i + S_i A_i + A_i^T S_i - S_i B_i R_i^{-1} B_i^T S_i + Q_i = 0; \quad S_i(t_f) = 0 \qquad (6\text{-}37)$$

$$\dot{\aleph}_i = \left[S_i B_i R_i^{-1} B_i^T - A_i^T\right] \aleph_i - S_i E_i z_i + \sum_{\substack{j=1 \\ i \neq j}}^{N} \left[\lambda_j^T H_{ji}\right]^T; \quad \aleph_i(t_f) = 0 \qquad (6\text{-}38)$$

$$u_i = \underbrace{-R_i^{-1} B_i^T S_i}_{u_i^{local}} x_i - \underbrace{R_i^{-1} B_i^T \aleph_i}_{u_i^{int.}} \qquad (6\text{-}39)$$

It can be seen that the *Riccati Equation* Eq. (6-37) is independent from the states of the subsystems. Conversely, Eq. (6-38) depends on all the states of the interconnected system [i.e. z_i depend on vector of the neighbouring states $(x_1, \ldots x_{i-1}, x_{i+1}, \ldots, x_N)$]. It should also be noted that Eq. (6-39) has the same structure as Eq. (6-23), where $u_i^{local} = -R_i^{-1} B_i^T S_i x_i$ and $u_i^{int.} = -R_i^{-1} B_i^T \aleph_i$.

6.5 The Intelligent Control Coordinator

This Section focuses on the development of the system global controller, its structure and optimisation under the action of the ACSS. The global controller is developed as an intelligent learning from the knowledge base of the ACSS. Methods developed in the field of learning control systems are used together with on-line constrained

optimisation strategies [see Eq.(6-20)] together with the two-level strategy of Singh and Titli (1978).

The coordination problem is appropriate if the system is considered to be either distributed or decentralised. In a *centralised structure* the subsystems are all being controlled by one controller, whereas in a *distributed or decentralised structure*, the local systems require information regarding the behaviour of the other systems.

As discussed in Eq.(6-20) is additively separable, this implies that for any given z_i and λ_i, the optimality with respect to the other variables can be obtained by N independent minimisations. This leaves the problem of improving the accuracy z_i and λ_i such that the global optimum for the ensemble of subsystems is achievable. Considering the Lagrangian L given by Eq. (6-20), necessary conditions are:

$$\frac{\partial L}{\partial z_i} = 0 \quad \rightarrow \quad \lambda_i = -\frac{\partial}{\partial z_i} F_i(x_i, z_i, u_i) p_i \qquad (6\text{-}40)$$

$$= -F_i^z(x_i, z_i, u_i) p_i$$

$$\frac{\partial L}{\partial \lambda_i} = 0 \quad \rightarrow \quad z_i = \sum_{\substack{j=1 \\ i \neq j}}^{N} H_{ij} x_j \qquad (6\text{-}41)$$

Re-arranging Eqs (6-40) and (6-41), leads to:

$$\begin{bmatrix} \lambda_i(t) \\ z_i(t) \end{bmatrix}^{t+\Delta t} = \begin{bmatrix} -F_i^z(x_i, z_i, u_i) p_i \\ \sum_{\substack{j=1 \\ i \neq j}}^{N} H_{ij} x_j \end{bmatrix}^{t} \qquad (6\text{-}42)$$

for a given p_i and x_i, i.e. the p_i and x_i which are obtained from the independent minimization in Eq. (6-20) are used in Eqs (6-40) and (6-41) to get the values of λ_i and z_i (i.e. from the iteration t to $t + \Delta t$) [Kambhampati *et al*., 2007].

It can be seen that if Eq. (6-42) consists of i distinct components corresponding to the i subsystems, this would require that all the subsystems be provided information regarding all other subsystems, whether that subsystem is physically interacting with it or not. An architecture that allows sharing of information between subsystems only adds to the complexity of the overall system and limits the fault-tolerance capabilities of the FTC scheme. This of course would also have an important consequence of the applicability of FTC for a Networked Control System (NCS), based on the "Control of the Network" problem.

On the other hand, by solving this problem at a higher level, as in the ACSS (see Figure 6-2), a more efficient information structure is achieved in that all the interaction information is sent to one point for evaluation and distribution. Furthermore, the proposed architecture shown in Figure 6-2 not only enables the coordination of the performance but also allows for reconfiguration and fault accommodation without a rapid increase in information traffic.

Note that this is in total contrast the normally accepted scenario in which a "consensus" rule applies. The traditional networked control problem based on consensus may not be so clever or efficient in terms of reliable FTC. The approach in Eq. (6-42) employed here is the interaction prediction principle (IPP) approach of (Takahara, 1965; Sadati and Moment, 2005). The IPP approach facilitates the interpretation of faults of a certain magnitude as wrong interaction predictions or prediction error, and thus enables the coordinator to accommodate these faults and ensures a smooth fault-tolerant operation of the system (e.g. learning method).

The solution to the problem given by Eq. (6-42) has two components, (i) a coordination variable which encapsulates the effort required for coordinating the various subsystems and (ii) predictions of the interactions. This is in line with the concept of coordination and reconfiguration, in that the coordinator ensures proper system functioning/performance even in situations which are unforeseen, modelling uncertainty or faults.

6.5.1 The learning strategy

The neural network employed to solve the global problem is a multilayered feed forward network (see Figure 6-9) which is architecturally similar to a radial basis function network [e.g. function approximation, time series prediction, and control]. Here the activation functions associated with the nodes can have any of the standard forms, including the various radial basis functions (see ***Definitions 6.2*** and ***6.3***)

.

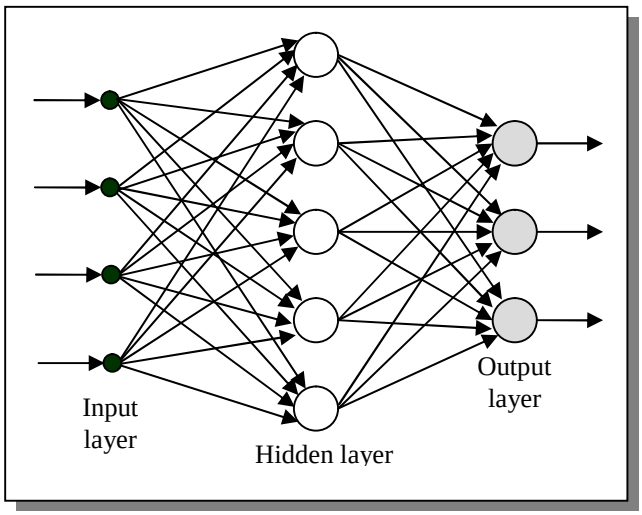

Figure 6-9: Fully Connected Feed Forward NN (taken from Haykin, 1994)

Definition 6.2

A radial basis function network: an artificial network the uses '*radial basis functions*' as activation functions. It is a linear combination of radial basis functions. They are used in function approximation, time series prediction, and control (Buhmann, 2003).

Definition 6.3

Radial Basis Functions: is a real-valued function whose value depend only on the distance from the original, so that $\tilde{\phi}(x) = \tilde{\phi}(\|x\|)$; or alternatively on the distance from some other point c, called a centre, so that $\tilde{\phi}(x, c) = \tilde{\phi}(\|x\| - c)$, Any function that satisfies the property $\tilde{\phi}(x) = \tilde{\phi}(\|x\|)$ is a radial function (Haykin, 1994; Buhmann, 2003)

It should be noted that the connections between the input-layer and the hidden layer are unity-weighted. The learning algorithm provides the weights between the hidden layer and the outputs (see Figure 6-9). For the problem defined at the coordination level Eq. (6-42) the inputs of the neural network are $[x_1(t), x_2(t), \ldots, x_N(t)]$ and $[\lambda_1(t), \lambda_2(t), \ldots \lambda_p(t)]$. The outputs of the system will be $[\lambda_1(t+\Delta t), \lambda_2(t+\Delta t), \ldots \lambda_p(t+\Delta t)]$ and $[z_1(t+\Delta t), z_2(t+\Delta t), \ldots z_p(t+\Delta t)]$, which are the inputs of the systems at the local level. The coordination level neural network should find the output values according to its inputs and sends them to the local levels and adjust the weights of the neural network.

6.5.2 The Hebbian learning method

The approach used for learning is a *reinforcement strategy* and has the following form (Haykin, 1994):

1. Start with a reasonable network configuration: assign the weights and the threshold level of each neuron.
2. Forward computation: Calculate the output of the neural network by proceeding forward through the network. The *linear combiner output* or net internal activity level $v_j^o(t)$ for neuron j is:

$$v_j^o(t) = \sum_{i=0}^{g} w_{ji}(t)\mathcal{X}_i(t) \qquad (6\text{-}43)$$

where $\mathcal{X}_1, \mathcal{X}_2, \ldots \mathcal{X}_g$ is the input signals and w_{ji} is the *synaptic weight* of neuron. The output signal $y_j(t)$ of neuron j is:

$$y_j(t) = \tilde{\varphi}(v_j^o) \qquad (6\text{-}44)$$

where $\tilde{\varphi}(\cdot)$ is the activation function (see Figure 6-10).

3. Update the synaptic weights of the neural network according to the learning algorithm selected.
4. If a stopping criteria reached then stop, otherwise go to step 2.

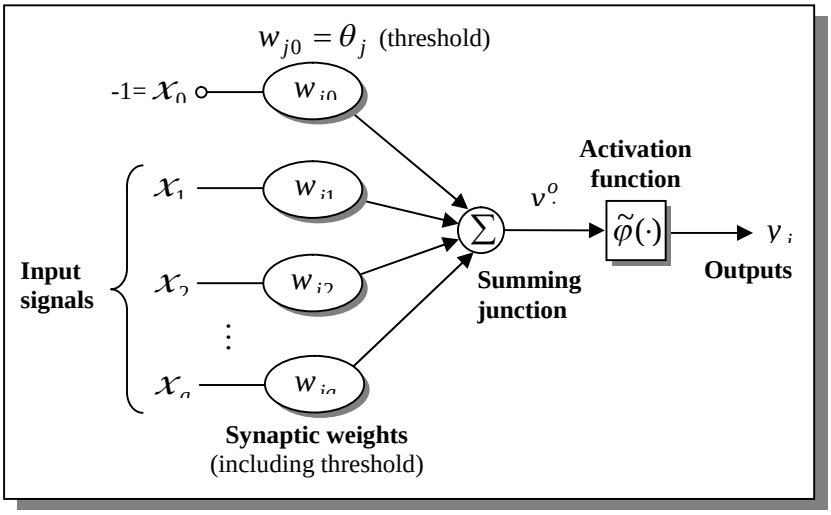

Figure 6-10: The nonlinear model of a neuron (Haykin, 1994)

In Step 3, adjusting the weights of the neural network may be done by using two different ways which are: (i) *Hebbian learning method* and (ii) *Error Backward propagation method*.

(i) The first way for the learning process or updating the synaptic weights is Hebbian learning as a totally unsupervised learning method. The next values for the weights in Hebbian learning are obtained by the information of the input and output values of the related neuron or alternatively activation degree of the two neurons at the each end of the synaptic weight. The weight between two neurons will increase if the two neurons activate simultaneously. Mathematically $\Delta w_{ji}(t)$ is calculated by the following equation (see Chapter 9 in Haykin, 1994)

$$\begin{aligned}\Delta w_{ji}(t) &= \eta\left(y_j(t)x_i(t) - y_j(t)\sum_{k=0}^{j-1} w_{ji}(t)y_k(t)\right) \\ &= \eta\, y_j(t)\left(x_i(t) - \sum_{k=0}^{j-1} w_{ji}(t)y_k(t)\right)\end{aligned} \qquad (6\text{-}45)$$

where: x_i is the i^{th} input and $y_j(t)$ is the output of the j^{th} neuron.

(ii) An alternative to this is to employ pseudo-supervised learning, where the supervisor assumes that the previous values are the correct values, and provides new outputs to ensure that the differences are minimised. Error back propagation needs desired values at the output level of the system to find the error output level (see Chapter 6 in Haykin, 1994). For the coordination problem given by Eq. (6-42) the desired values for $z_{d1}, z_{d2}, \ldots, z_{dp}$ can be calculated by the following:

$$z_{di} = \sum_{j=1}^{N} H_{ij}\, x_j(t - \Delta t) \qquad (6\text{-}46)$$

and the error can be obtained by the following:

$$e_{z_i} = z_{di} - z_i(t) \qquad (6\text{-}47)$$

The errors related with $\lambda_1, \lambda_2, \ldots, \lambda_p$ are obtained by using the previous values of $\lambda_i, i = 1, \ldots, p$ as given below:

$$e_{\lambda_i} = \lambda_i(t - \Delta t) - \lambda_i(t) \qquad (6\text{-}48)$$

Using the Eqs (6-47) and (6-48) and errors are calculated and the update of the weights is as follows:

$$\Delta w_{ji}(t) = \eta \delta_j y_i(t) \qquad (6\text{-}49)$$

where w_{ji} is the weight between neuron i and j, η are a constant that determines the rate of learning; $y_i(t)$ is the output of the neuron i and $\delta_j(t)$ is the local gradient of neuron at time *t*, defined by:

$$\delta_j(t) = e_j(t)\tilde{\varphi}'(v_j^o(t)) \qquad (6\text{-}50)$$

The local gradient points to required change in synaptic weight. According to Eq. (6-50), the local gradient for output neural *j* is equal to the product of the corresponding error signal $e_j(t)$ and derivative $\tilde{\varphi}'(v_j^o(t))$ of the associated actuation function.

Therefore, in Step 3, updating the synaptic weights of the neural network can be obtained by substituting either Eq. (6-45) or (6-49) into the following Eq. (6-51) [i.e. depend on the learning methods chosen] into following equation:

$$w_{ji}(t + \Delta t) = w_{ji}(t) + \Delta w_{ji}(t) \qquad (6\text{-}51)$$

Remark: Both of these formulations provide the required coordination. However, a reinforcement strategy is recommended in that the error back-propagation strategy employs a '*pseudo-teacher*', and as a result is a lot slower when compared to the Hebbian learning.

6.5.3 Reconfiguration

The re-configurability implies that when a fault has occurred and the system is diagnosable, a new set of performance constraints are identifiable which ensures the system performance does not deteriorate.

Within the context of a control of distributed or interconnected systems, the reconfiguration task has to perform a number of tasks, these can be summarised as: (a) re-distribution of performance requirements, and (b) ensuring that the faulty subsystems

which are beyond repair cannot cause a total failure of the overall system. Thus the reconfiguration task has two-levels of operation:

(1) Decide whether reconfiguration is required [Compare the symptoms for decision-making], e.g. reconfiguration task (see Figure 6-2) gets residual information from the local FDI and makes a decision as to whether reconfiguration is required or not, based on the residuals.

(2) A mechanism which reconfigures the performance criteria and sets new constraints.

Here the decision for reconfiguration would *be based on the nature and size of the fault. If the fault is small and bounded, reconfiguration is not required*. The reason for this is that the control coordinator will compensate for this, as it would assume that an error has occurred in the prediction of the interactions. Typically, the output sensor FDI problem is relatively simpler when compared to that of actuator FDI. Indeed in the distributed systems, the output sensor fault becomes an actuator fault because of the connectivity between the subsystems. This research only deals with the actuator fault case.

6.6 A simple Tutorial Example

Consider a simple system consisting of two interconnected subsystems as described in Figure 6-11. Typically these could be two simple chemical processes inter-connected and represented by an RNN.

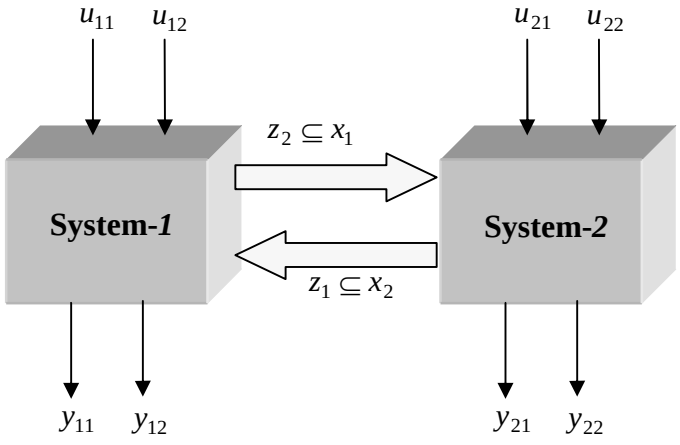

Figure 6-11: A simple situation of two subsystems

The independent dynamics of each of the *nonlinear* systems can be given by the following set of normalised linear subsystem dynamic equations:

Nonlinear system-1

$$\begin{aligned} \dot{x}_1(t) &= -\tau_1 x_1(t) + w_1\sigma(x_1) + \Gamma_1 u_1(t) + \boldsymbol{H}_1\bar{x}_1(t) \\ y_1(t) &= x_1(t) \end{aligned} \qquad (6\text{-}52)$$

Nonlinear system-2

$$\begin{aligned} \dot{x}_2(t) &= -\tau_2 x_2(t) + w_2\sigma(x_2) + \Gamma_2 u_2(t) + \boldsymbol{H}_2\bar{x}_2(t) \\ y_2(t) &= x_2(t) \end{aligned} \qquad (6\text{-}53)$$

where x_i are the normalised local states, u_i the local control and the block $\boldsymbol{H}_i$ represents the possible interconnections and consists of the effect of all H_{ij}, and $\sigma(x_i)$ can be any smooth *nonlinearity*. However, for the purpose of this example $\sigma(x_i) = \dfrac{1}{1+e^{-x_i}}$ (which can represent chemical kinetics) for $i = 1, 2$. Without any loss of generality consider a situation in which two subsystems each having 2-inputs, 2-output and 5-states as follows:

$x_1 = [x_{11} \;\; x_{12} \;\; x_{13} \;\; x_{14} \;\; x_{15}]^T$, $x_2 = [x_{21} \;\; x_{22} \;\; x_{23} \;\; x_{24} \;\; x_{25}]^T$,

$\bar{x}_1 = x_2, \quad \bar{x}_2 = x_1$

$\boldsymbol{H}_1 = H_{12}, \quad \boldsymbol{H}_2 = H_{21}$

$\tau_1 = diag([-0.5, -0.1, -0.02, -0.1, -0.1])$,

$\tau_2 = diag([-0.2, -0.1, -0.02, -0.1, -0.1])$,

$\Gamma_1 = [1 \;\; 1 \;\; 0 \;\; 0]^T$, $\Gamma_2 = [0 \;\; 0 \;\; 1 \;\; 1]^T$

The two $5x5$ matrices w_1 and w_2 are given by:

$$w_1 = \begin{bmatrix} -0.2000 & 0.0100 & 0 & 0.0300 & 0 \\ 0 & -0.2000 & 0 & 0.025 & 0.0015 \\ 0.0010 & 0.0030 & -0.2000 & 0.0010 & 0 \\ 0.0050 & 0.0210 & 0.0010 & -0.5000 & 0.0016 \\ 0.0010 & 0.0110 & 0 & 0 & -0.2000 \end{bmatrix}$$

$$w_2 = \begin{bmatrix} -0.1000 & 0 & 0.0160 & 0.0160 & 0 \\ 0 & -0.2000 & 0 & 0.0110 & 0 \\ 0.0076 & 0 & -0.5000 & 0 & 0.0010 \\ 0 & 0.0450 & 0.0010 & -0.3000 & 0 \\ 0.0067 & 0 & 0.0023 & 0 & -0.2000 \end{bmatrix}$$

The two systems exhibit the following two properties: (i) $f_i(0,0) = 0, \quad i = 1, 2$ and (ii) are asymptotically stable and the eigenvalues of the linearised systems around the origin $(0,0)$ (the only equilibrium point) of system-*1* and system-*2* are given as: {-0.7015, -0.6003, -0.2200, -0.2948, -0.3034}, {-0.5206, -0.4047, -0.3005, -0.2990, -0.2953}, respectively.

6.6.1 Two isolated subsystems

The behaviour of each system in *isolation* can be seen from Figure 6-12.

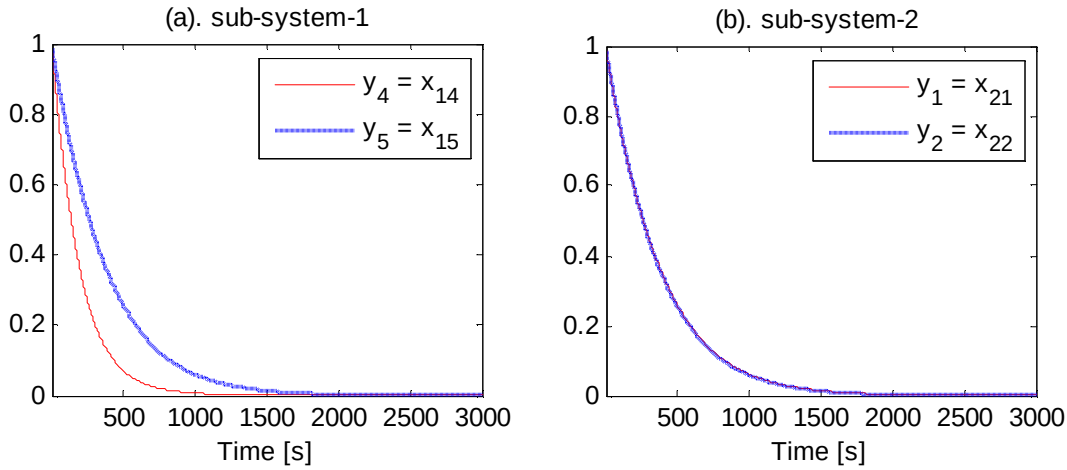

Figure 6-12: Both systems exhibit stable behaviour

6.6.2 Two interconnected subsystems

With an appropriate choice of interconnections the system exhibits stable behaviour (see Figure 6-13 (a). However, an inappropriate choice yields an unstable system [see Figure 6-13 (b)]. Indeed, this is a typical situation when dealing with distributed systems where a major constraint could be the available interconnections. It is important to keep in mind that the resulting system could be unstable.

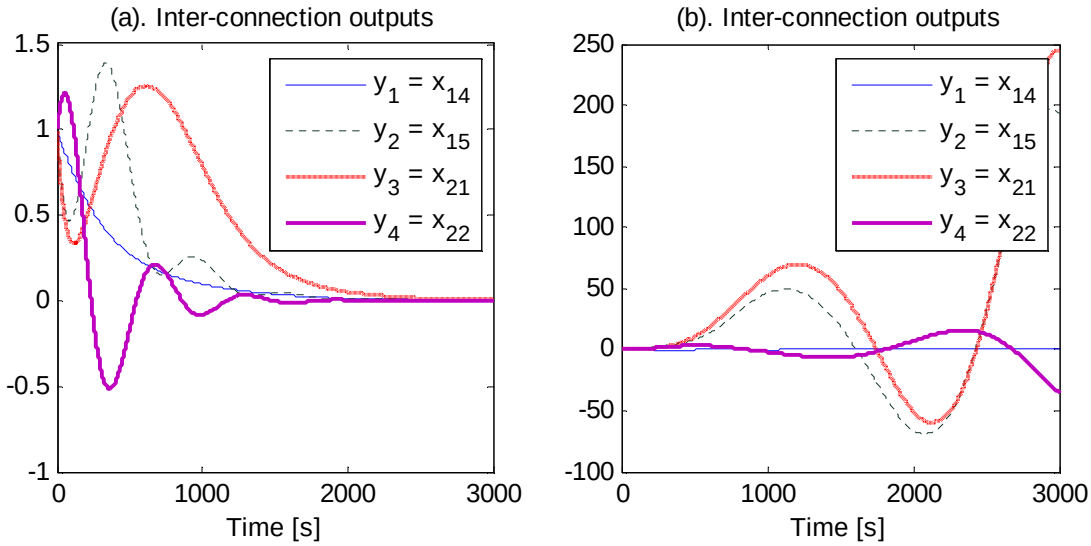

Figure 6-13: The output responses of the inter-connected systems:
(a) An appropriate design of interconnection yields stable behaviour, and
(b) An inappropriate design of interconnection yields an unstable system

In the following sections will illustrate the development of the proposed controller, and learning approach architecture for coordinating the activities and autonomous fault tolerant control.

6.6.3 The two subsystem control strategy

As discussed in Section 6.4, a set of appropriate performance indicators are selected.

$$J_i = \int_0^t (x_i^T Q_i x_i + u_i^T R_i u_i) dt \qquad (6\text{-}54)$$

The global index is the sum of the two indices for the individual subsystems: $J = J_1 + J_2$. As a first stage for the illustration of the requirement of a coordinating architecture considers the case where the two systems are not connected but are individually controlled. The results are given in the Figure 6-14. If the two systems are now interconnected [see Figure 6-15], it can be seen that the global performance of the system is not as desired, in that the tracking of the set-points is poor. This illustrates the need to take into account the interactions taking place between the two subsystems.

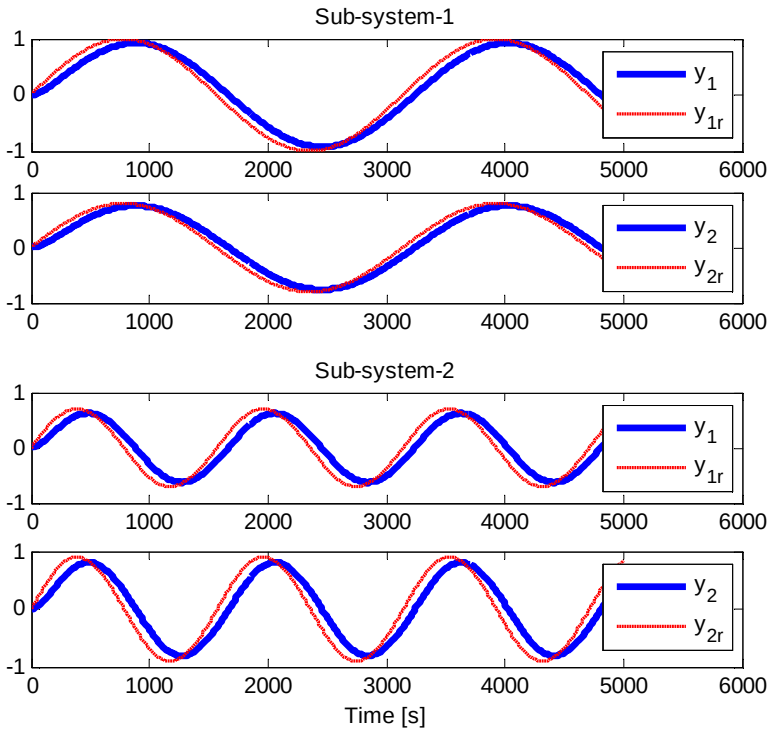

Figure 6-14: The output response of the systems not connected, individually controlled

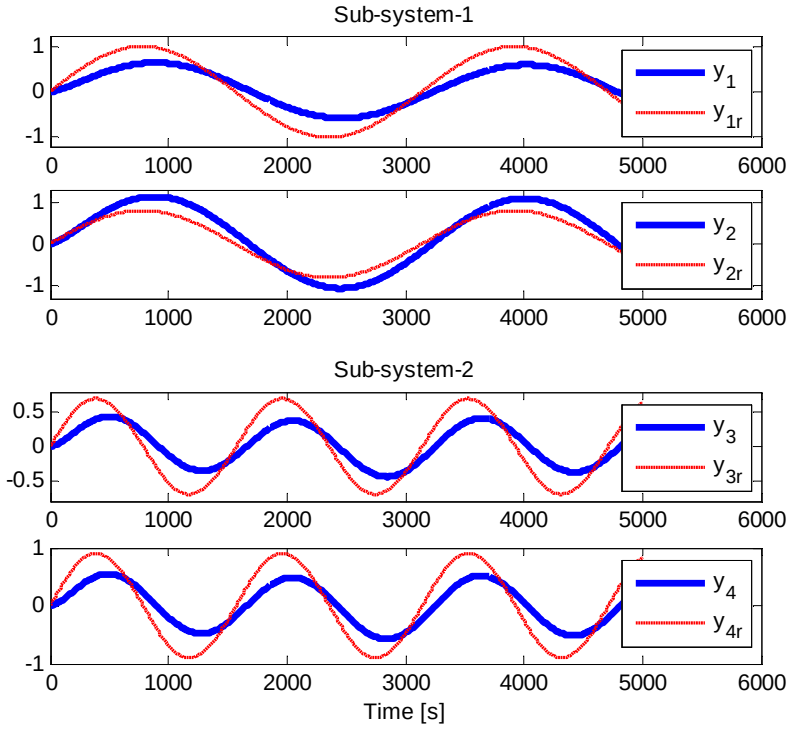

Figure 6-15: The output response of the systems interconnected

When the two controllers are being designed individually the interconnections, $h_i(z_i)$ are ignored. However, these come into play when the two sub-systems are inter-connected and in this initial design the controller is unable to compensate for the effect

of the interconnections $h_i(z_i)$. These interconnections are taken as exogenous disturbances. The reason for this is that the effect of interconnections is being recycled and being magnified by the interconnection of the two sub-systems. The only way to avoid this is to take account of the interconnections $h_i(z_i)$ as described in Section 6.4.

6.6.4 The Control Strategy using the learning approach

The simulation results without using a NN learning approach in the global level are given in Sections 6.6.3. In this Section the same example is performed by the integration of the global level control using NN learning approach.

The system is simulated initially without any faults and from Figure 6-16 it can be seen that the outputs track the reference signal. The initial oscillations in the outputs are due to the co-ordinator learning the co-ordination task for the two subsystems.

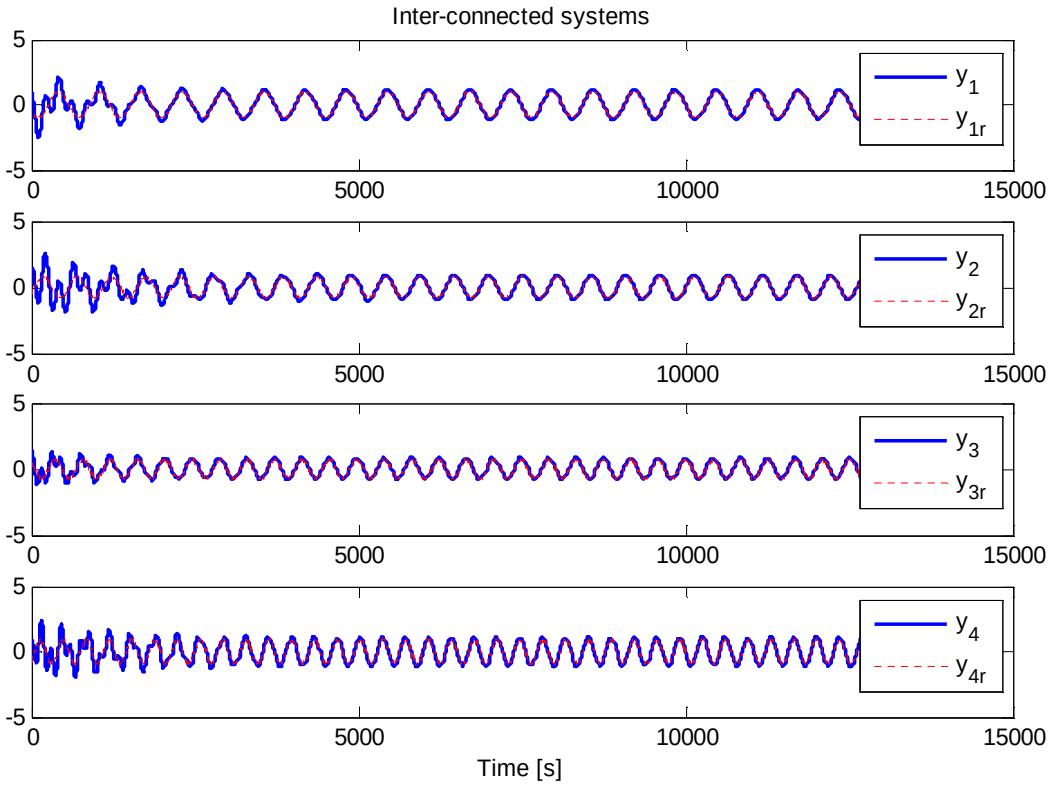

Figure 6-16: Input and output of the system without fault

It can be seen in Figure 6-17 that the cost function is also minimised. It can also be noted that the initial oscillations of the cost function corresponds to the coordinator learning phase.

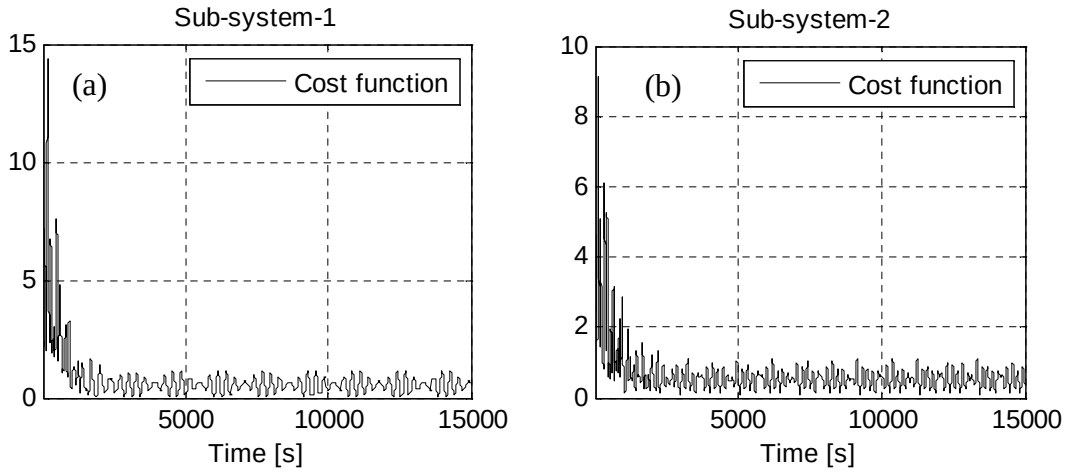

Figure 6-17: The cost functions of the local systems 1 and 2 without faults

The following simulation results were carried out with bias faults 10% and 50% on the 1st control channel. The results of these simulations are shown in Figure 6-18 (a), Figure 6-18 (b).

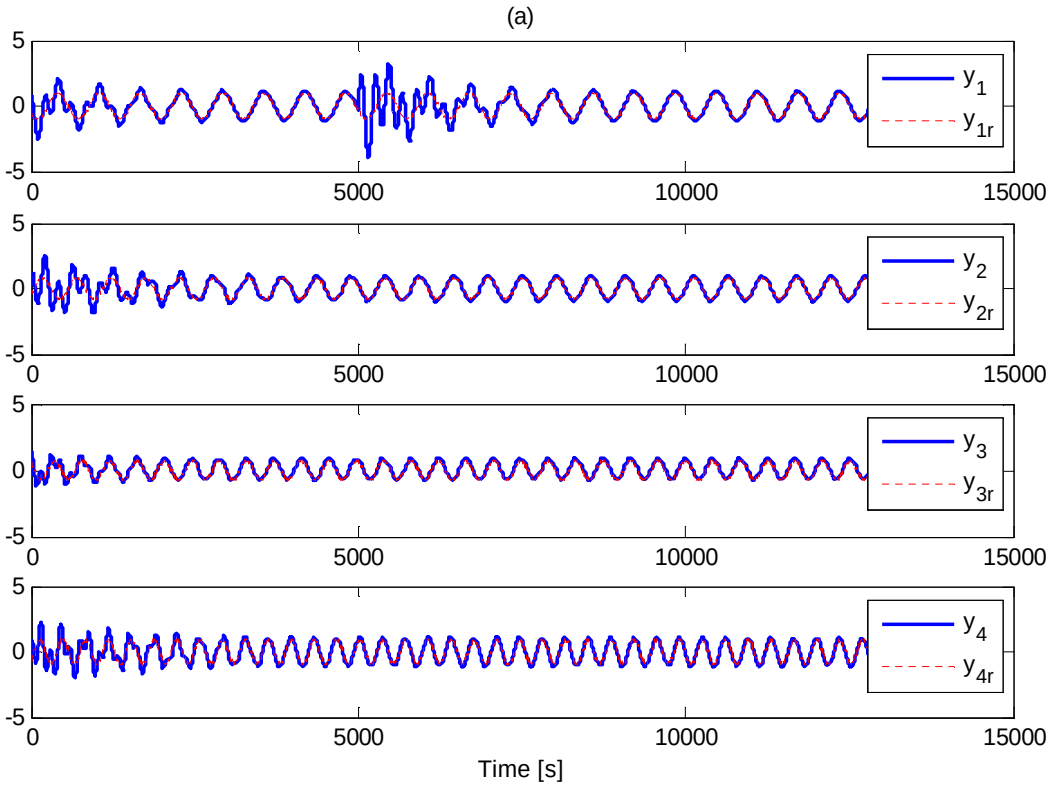

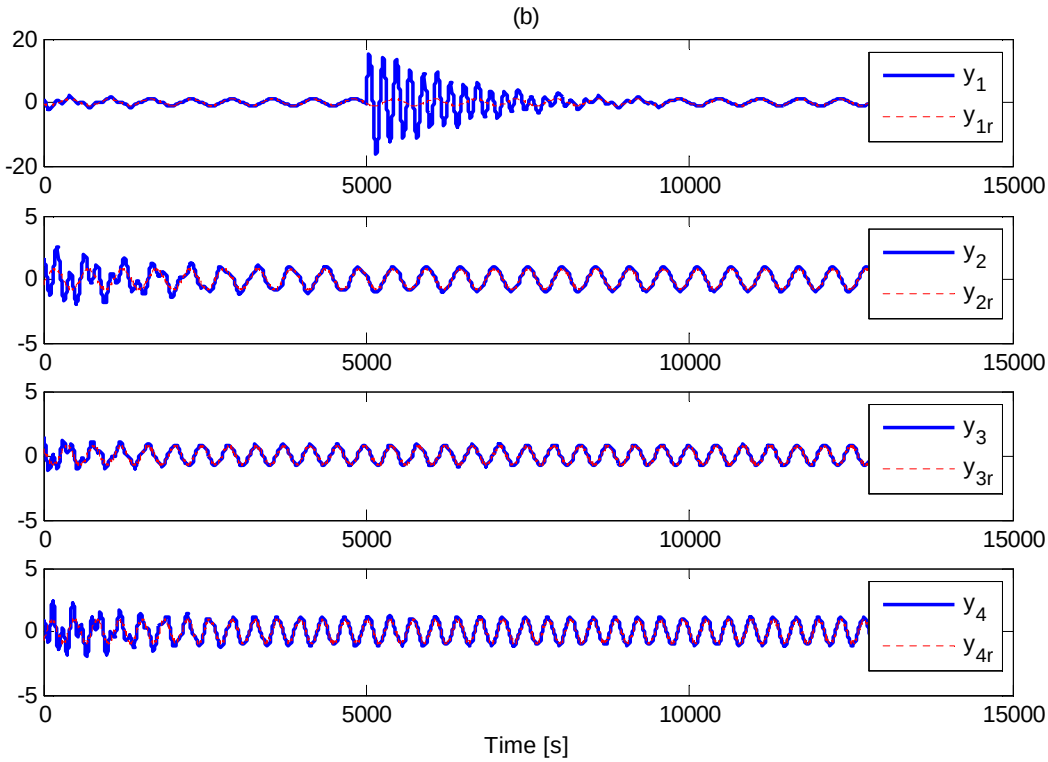

Figure 6-18: Input/Output of the system with a bias fault at the 1st control channels: (a) 10% and (b) 50%

In each case it can be seen that the outputs are tracked as before. However, when the faults are introduced, the system oscillates and then settles. As the magnitude of fault is increased, these oscillations increase in magnitude as well.

Figure 6-18 illustrates that when the faults have occurred; the control coordinator receives information about the state of the two subsystems and compares these with its predictions (as a prediction error) of the same states when the errors occur. The co-ordinator then determines a new set of predictions to minimise this error and maintains the stability on each of the two subsystems even when faults are present.

6.7 Conclusion

This Chapter describes and develops fault-tolerant architectures with a view to demonstrating that the classical concepts of FTC, namely of *active* and *passive* FTC can be related to equivalent (although more complex) concepts in distributed systems. The comparison can be made according to whether or not the structure requires Reconfiguration and/or FDI via fault estimation concept. The study confirms that the

de-centralized approach to FTC in distributed systems suffers from a difficult challenge as to how to compensate for fault effects occurring throughout the overall system.

On the other hand, the distributed hierarchical architecture that is described illustrates the notion that, under a scheme of Control Co-ordination, the equivalent to the classical active FTC is achievable. This architecture can be implemented using a Global Coordination Task, making use of the *Principle of Interaction Predictions*. Methods proposed in the field of learning control systems are used together with on-line constrained optimisation strategies. The solutions are achieved using two tasks of neural network: (i) at a local level, RNN is used for subsystem identification and FDI structure, and (ii) at the higher (global) level, a feed-forward network is used along with Hebbian learning to learn the coordinating function.

Once the system structure is set up in terms of global and local units, the performance measures are "additively separable", a concept coming form large-scale systems theory (Singh and Titli, 1978). This additive separable ensures suitable flexibility for control reconfiguration.

It has been shown that for small faults the autonomous FTC system compensates for faults through an adaptive mechanism as the classical active (or adaptive) FTC. For larger faults, fault estimation is required, to facilitate the Reconfiguration Task of this distributed hierarchical structure.

This Chapter forms the basis for work to be continued in Chapter 7.

Chapter 7.
Three Tank System Application Study

7.1 Introduction

To illustrate the discussion in previous Chapter a tutorial example of a 3-tank inter-connected system is used here as a benchmark problem of fault estimation for FTC in distributed system. The model represents a real 3-tank system (Figure 7-1) from the Research Centre for Automatic Control in CRAN-UHP, Nancy, France (http://www.strep-necst.org/). The concepts presented in Chapter 6 will be later tested on this benchmark system. In fact the basic concepts of the distributed control design for this example have been applied on the real three tank system at Nancy via the collaboration with Dr Cahit Perkgoz at Hull University and this has been reported in internal report [Reference: Integration of NeCST Concepts in OPC].

7.2 Three-Tank Benchmark Simulation

In this Chapter, the simulation of an inter-connected 3-tank level and temperature control system is described within the Simulink/Matlab© environment (Sauter *et al*., 2005).

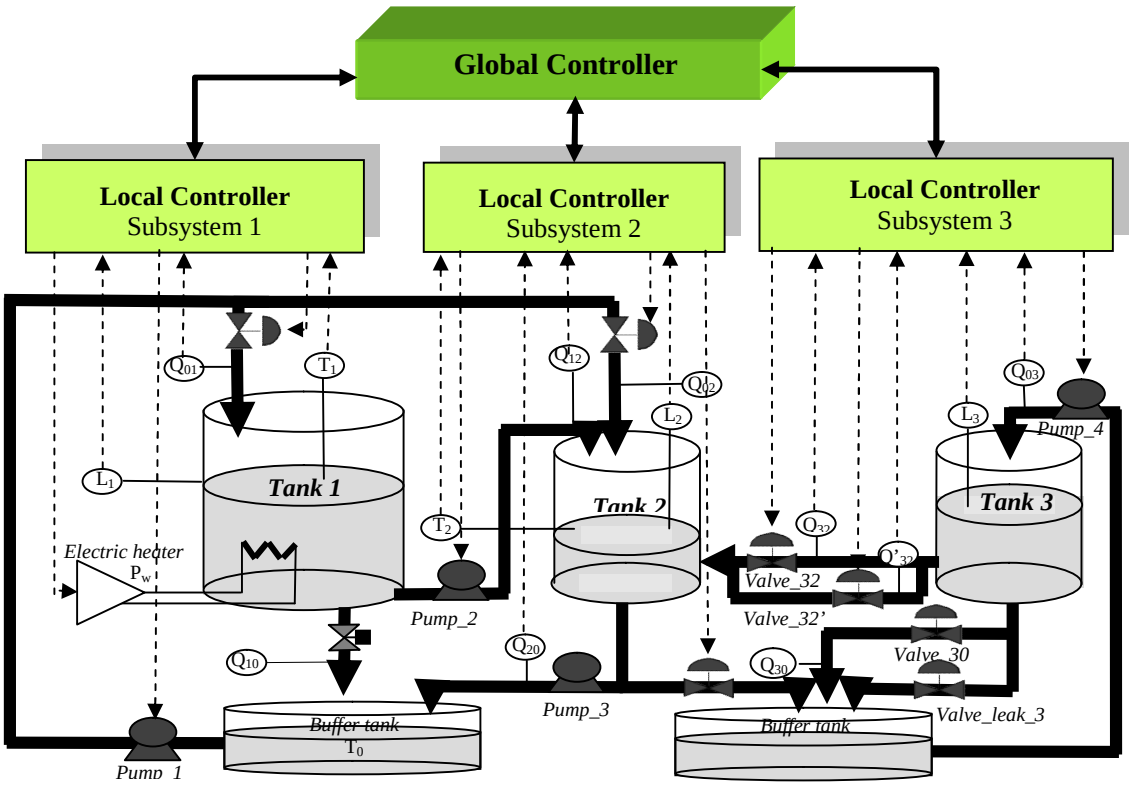

Figure 7-1: The schematic diagram of the Three-Tank Benchmark System (NeCST FP6 STREP project)

It can be seen that Figure 7-1 shows: [see the abbreviations in table 7.1]

Subsystem-1 has 3 inputs (Q_{01}, P_w and Q_{12}) and 3 states [$x_1 = col(L_1, T_1, V_{12})$] with the following dynamics:

$$\begin{aligned} S_1 \dot{L}_1 &= Q_{01} - Q_{12} - Q_{10} \\ S_1 L_1 \dot{T}_1 &= Q_{01}(T_0 - T_1) + \frac{P_w}{\rho c} \\ \dot{V}_{12} &= Q_{12} \end{aligned} \qquad (7\text{-}1)$$

Subsystem-2 has 2 inputs (Q_{02} and Q_{20}) and 3 states [$x_2 = col(L_2, T_2, V_{20})$] with the following dynamics:

$$\begin{aligned} S_2 \dot{L}_2 &= Q_{12} + Q_{02} - Q_{20} + (Q_{32} + Q'_{32}) - Q_{leak\,2} \\ S_2 L_2 \dot{T}_2 &= Q_{12}(T_1 - T_2) + Q_{02}(T_0 - T_2) + (Q_{32} + Q'_{32})(T_0 - T_2) \\ \dot{V}_{20} &= Q_{20} \end{aligned} \qquad (7\text{-}2)$$

Subsystem-3 has 2 inputs (Q_{03} and Q_{32}) and 2 states [$x_3 = col(L_3, V_{32})$] with following dynamics:

$$
\begin{aligned}
S_3 \dot{L}_3 &= Q_{03} - (Q_{32} + Q'_{32}) - Q_{30} - Q_{leak3} \\
\dot{V}_{32} &= Q_{32}
\end{aligned}
\qquad (7 - 3)
$$

where S_i, L_i, T_i, V_{ij}, Q_{ij}, Q_{leak_i} $i = 0, 1, 2, 3$ are the cross-sectional areas of each tank, the level of liquid in Tank-*i*, the temperature of liquid at the centre of the Tank-*i*, the volume of liquid passing from Tank-*i* to Tank-*j*, the liquid flow rates between Tank-*i* to tank-*j*, and the leak from tank-*i*, respectively. *ij =0* means the buffer tank. P_w is the power input. ρ and C are the density and the specific heat capacity of the liquid inside the tank. The abbreviations used in Eqs. (7 - 1) – (7 - 3) are given are given:

Variable	Definition	Unit
S_i	Cross-sectional area of i^{th} tank.	M^2
L_i	Level of liquid in i^{th} tank.	M
T_i	Temperature of liquid in i^{th} tank. (0 means the buffer tank)	^oC
Q_{ij}	Flow-rate from i^{th} tank to j^{th} tank.	M^3/sec
V_{ij}	Amount of liquid passing from i^{th} tank to j^{th} tank.	m^3
P_w	Power input	kW
ρ	Density of the liquid	kg/ m^3
c	Specific heat capacity of the liquid	$J/kg\text{-}K$
Q_{leaki}	Flow-rate of the leakage from i^{th} tank.	M^3/sec

Table 7.1: The tree tank system abbreviations

It should be noted that the flow-rates on the system are controlled by either pumps or valves. The system working as follows:

- Pump_1 is kept constant at 0.75 m^3/sec.
- Tank-1 is fed by *Valve01* (Q_{01}).
- Tank-2 is fed by *Valve02* (Q_{02}) and *Pump_2* (Q_{12}).
- Tank-3 is fed by *Pump_3* (Q_{03}).

The liquid inside the Tank-1 is heated by an electrical heater. The Tank-2 is taking preheated liquid from the Tank-1 (Q_{12}) and mixes it with a solution coming from the Tank-3 (*Q32*). *Valve32', Valve_leak_1, Valve_leak_2, and Valve_leak_3* are totally closed ($Q'_{32} = Q_{10} = Q_{leak2} = Q_{leak3} = 0$) and *Valve30* is totally opened during the simulation.

The performance objectives for the system are as follows:

- Maintain the levels of each tank, L_1 at 0.75 m, L_2 at 0.3 m, and L_3 at 0.5 m.

- Maintain the temperature of 1^{st} and 2^{nd} tank, T_1 at 30°C and T_2 at 28°C.

An alternative to using this first principles model would be to use a data-driven approach for example, recurrent neural networks (Garces *et al.*, 2003) in which the states of the individual subsystems would be defined as follows:

(1) Subsystem-1 has 3 inputs (Q_{01}, P_w and Q_{12}) and 3 states $[L_1, T_1, V_{12}]$,

(2) Subsystem-2 has 2 inputs (Q_{02} and Q_{20}) and 3 states $[L_2, T_2, V_{20}]$, and

(3) Subsystem-3 has 2 inputs (Q_{03} and Q_{32}) and 2 states $[L_3, V_{32}]$

The models based on recurrent networks were trained using data collected from the simulations over a period of 9,000s. These data were based on the open-loop system, i.e. without application of feedback control. The RNN in Eq. (6 - 5) is trained with overall states $n = 8$ and $\sigma(x) = \tanh(x)$ to identify the nonlinear Three Tank system in Eqs. (7 - 1) -(7 - 3). The initial condition for the neuron states are: [-0.7773, -0.6199, -0.5342, 0.0748, -0.7261, -0.4979, -0.0186, -0.4959] and the training inputs are given as follows:

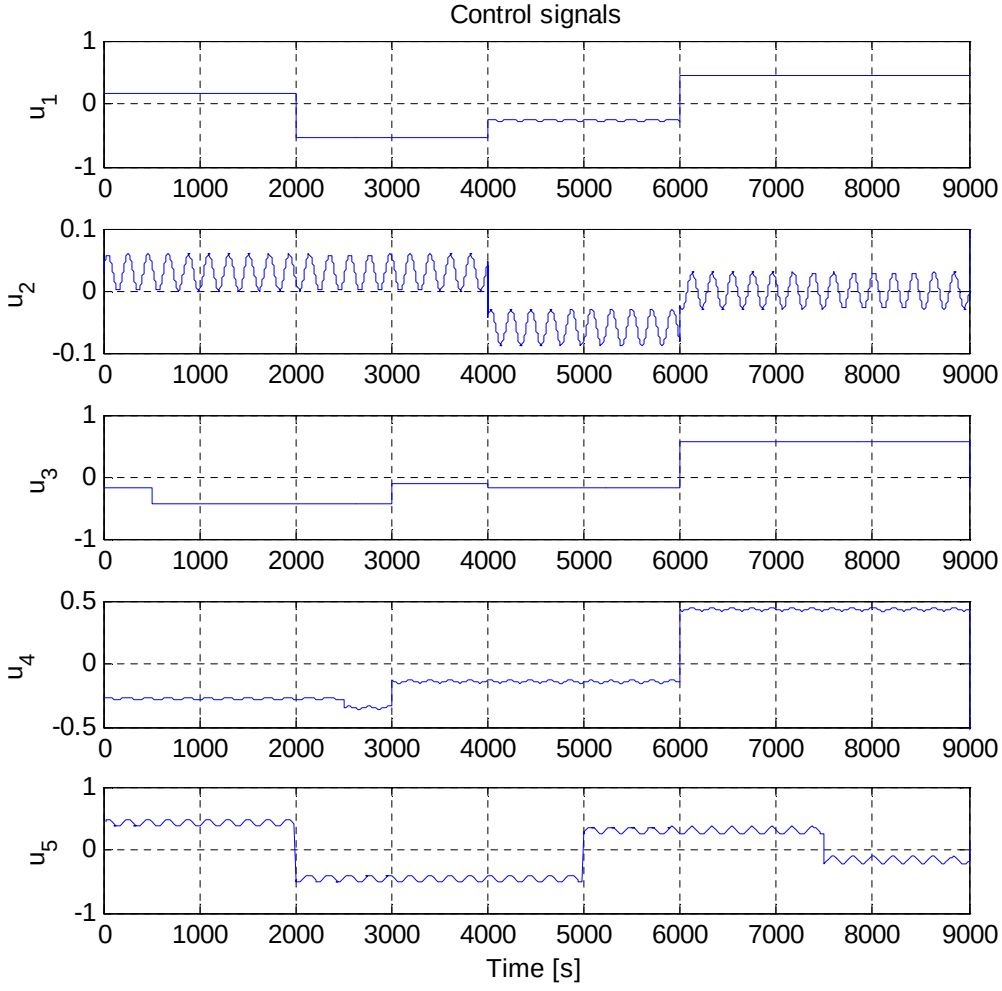

Figure 7-2: The control inputs for RNN training

All the trained RNNs were able to model the data well to the desired accuracy, and some of the results are shown in Figure 7-3.

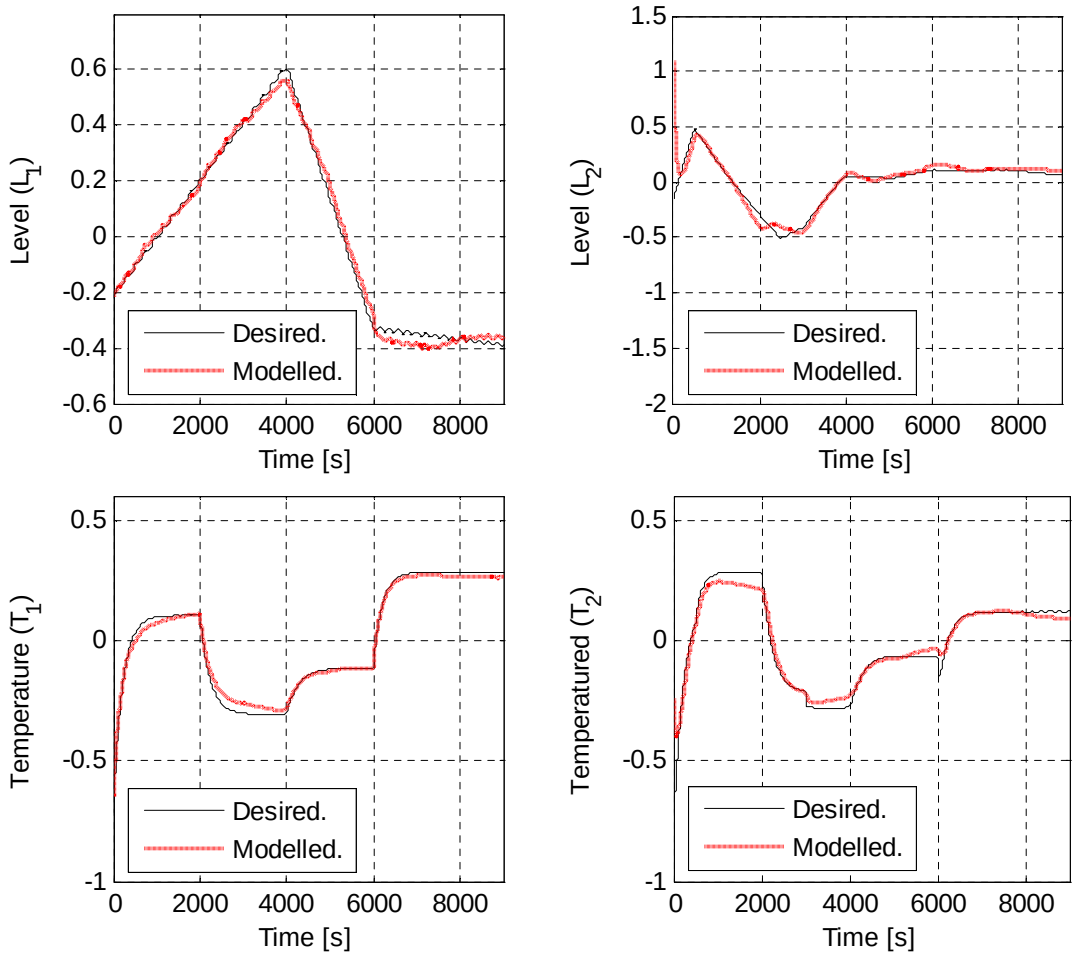

Figure 7-3: The system modelling based on RNN

Following the discussion of RNN for system identification presented in Section 6.4.2, and the solutions of Eqs. (6 - 8) to (6 - 1 1) obtained the linear systems of the Tank-1, 2 and 3 as given below:

$$A_{overall} =$$

$$\left(\begin{array}{ccc|ccc|cc}
-0.0581 & -0.0347 & 0.0298 & -0.0309 & -0.0074 & 0.0205 & 0.0192 & 0.0493 \\
-0.0244 & -0.3504 & 0.0561 & 0.0115 & 0.0446 & 0.0446 & 0.0446 & 0.0439 \\
0.0153 & 0.0163 & -0.0900 & -0.0559 & 0.0143 & 0.0244 & -0.0005 & 0.0557 \\
\hline
-0.0550 & 0.0323 & -0.0354 & -0.1098 & 0.0154 & -0.0467 & 0.0348 & -0.0338 \\
0.0230 & 0.0310 & 0.0357 & 0.0348 & -0.1517 & -0.0467 & 0.0500 & 0.0061 \\
-0.0061 & 0.0411 & 0.0440 & -0.0215 & -0.0149 & -0.1337 & -0.0004 & -0.0047 \\
\hline
0.0244 & 0.0308 & 0.0073 & 0.0258 & 0.0105 & -0.0049 & -0.0915 & -0.0022 \\
0.0444 & -0.0018 & 0.0721 & -0.0070 & 0.0167 & 0.0918 & 0.0244 & -0.2232
\end{array}\right) \quad (7-4)$$

$$\Gamma_{overall} = \left(\begin{array}{ccc|cc|cc} 0.0000 & 0.0511 & -0.0158 & * & * & * & * \\ 0.1329 & -0.0143 & 0.0000 & * & * & * & * \\ 0.0000 & 0.0000 & 0.0657 & * & * & * & * \\ \hline * & * & * & 0.0551 & -0.0301 & * & * \\ * & * & * & -0.1051 & 0.0052 & * & * \\ * & * & * & 0.0053 & 0.0111 & * & * \\ \hline * & * & * & * & * & 0.0441 & -0.0273 \\ * & * & * & * & * & 0.0000 & 0.0218 \end{array}\right) \quad (7-5)$$

Then:

Tank-1

$$A_1 = \begin{pmatrix} -0.0581 & -0.0347 & 0.0298 \\ -0.0244 & -0.3504 & 0.0561 \\ 0.0153 & 0.0163 & -0.0900 \end{pmatrix}, \; B_1 = \begin{pmatrix} 0.0000 & 0.0511 & -0.0158 \\ 0.1329 & -0.0143 & 0.0000 \\ 0.0000 & 0.0000 & 0.0657 \end{pmatrix} \text{ and}$$

$$\boldsymbol{H}_1 = \left(H_{12} \,\vdots\, H_{13}\right) = \left(\begin{array}{ccc|cc} -0.0309 & -0.0074 & 0.0205 & 0.0192 & 0.0493 \\ 0.0115 & 0.0446 & 0.0446 & 0.0446 & 0.0439 \\ -0.0559 & 0.0143 & 0.0244 & -0.0005 & 0.0557 \end{array}\right)$$

Tank-2

$$A_2 = \begin{pmatrix} -0.1098 & 0.0154 & -0.0467 \\ 0.0348 & -0.1517 & -0.0467 \\ -0.0215 & -0.0149 & -0.1337 \end{pmatrix}, \; B_2 = \begin{pmatrix} 0.0551 & -0.0301 \\ -0.1051 & 0.0052 \\ 0.0053 & 0.0111 \end{pmatrix}, \text{ and}$$

$$\boldsymbol{H}_2 = \left(H_{21} \,\vdots\, H_{23}\right) = \left(\begin{array}{ccc|cc} -0.0550 & 0.0323 & -0.0354 & 0.0348 & -0.0338 \\ 0.0230 & 0.0310 & 0.0357 & 0.0500 & 0.0061 \\ -0.0061 & 0.0411 & 0.0440 & -0.0004 & -0.0047 \end{array}\right)$$

Tank-3

$$A_3 = \begin{pmatrix} -0.0915 & -0.0022 \\ 0.0244 & -0.2232 \end{pmatrix}, \; B_3 = \begin{pmatrix} 0.0441 & -0.0273 \\ 0.0000 & 0.0218 \end{pmatrix}, \text{ and}$$

$$\boldsymbol{H}_3 = \left(H_{31} \,\vdots\, H_{32}\right) = \left(\begin{array}{ccc|ccc} 0.0244 & 0.0308 & 0.0073 & 0.0258 & 0.0105 & -0.0049 \\ 0.0444 & -0.0018 & 0.0721 & -0.0070 & 0.0167 & 0.0918 \end{array}\right)$$

The system is simulated initially without any faults via the two-level control strategy purposed in Chapter 6, and from Figure 7-4 it can be seen that the outputs follow the reference signal. The desired values (references) for each control objective are shown in the red dashed lines.

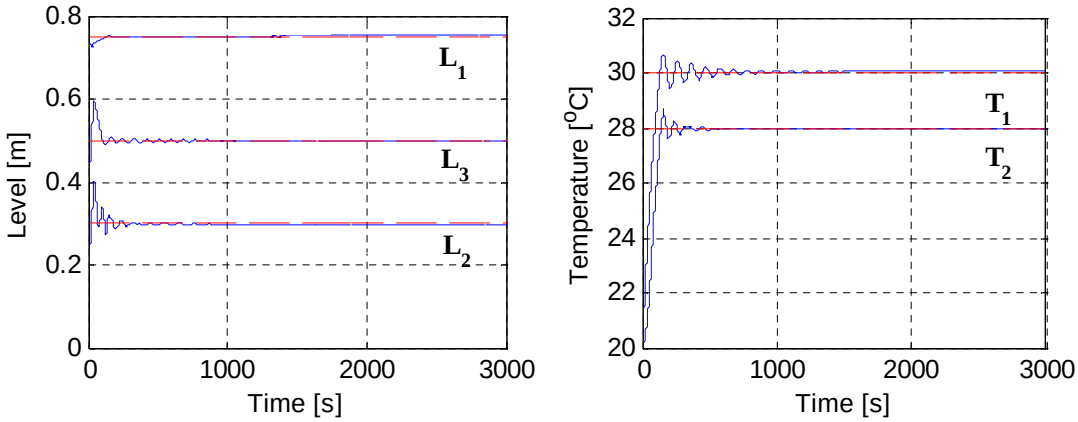

Figure 7-4: Fault-free System Outputs

It can be seen in Figure 7-5 that the cost function is also minimized.

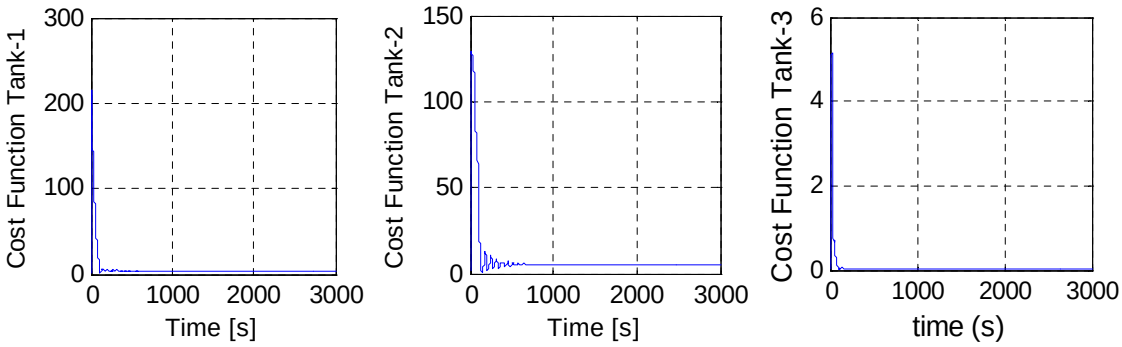

Figure 7-5: Cost Function of the Tank-1, 2 and 3 without fault

The next sets of simulation results were carried out with bias faults (20%, 40%, and 60%) of the electrical heater operating points after t = 1500 seconds. The results of these simulations are shown in Figure 7-6 to Figure 7-8, respectively.

Essentially, when the fault has occurred, the co-ordinator gets information about the state of the three subsystems and when it compares these with its predictions of the same states an error occurs. This results in the co-ordinator determining a new set of predictions to minimise this error. In each case it can be seen that the outputs are tracked as shown in Figure 7-6 and Figure 7-7.

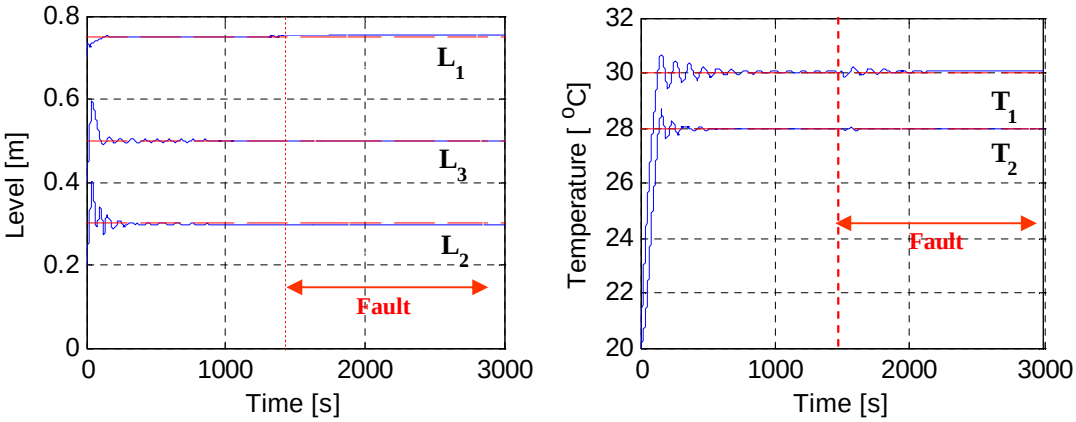

Figure 7-6: Outputs of the System with a Bias Fault (20% of heater operating point)

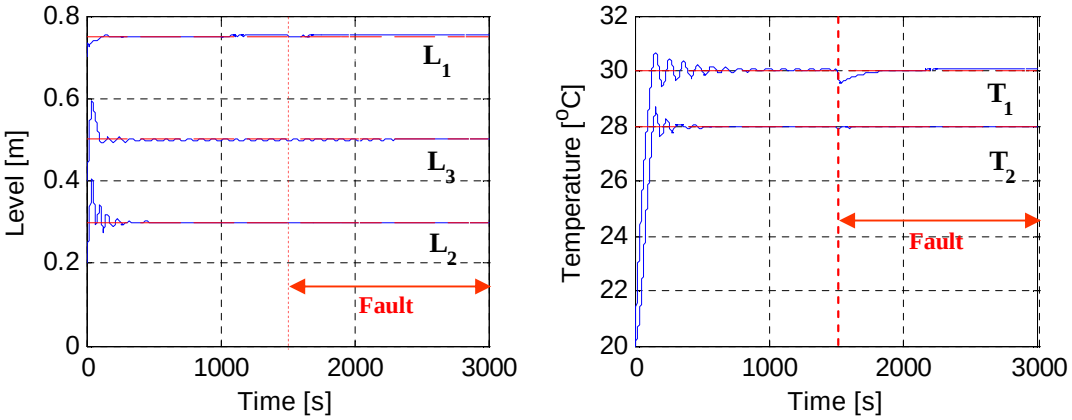

Figure 7-7: Outputs of the System with Bias Fault (40% of heater operating point)

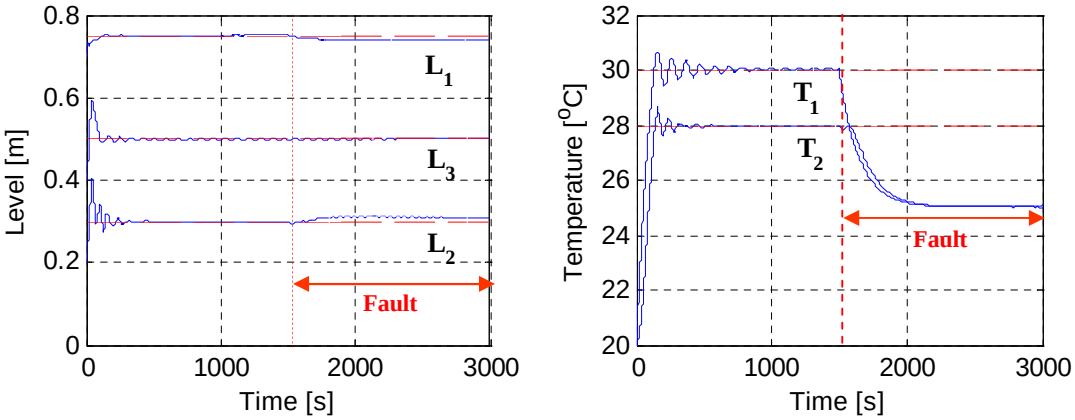

Figure 7-8: Outputs of the System with Bias Fault (60% of heater operating point)

As the magnitude of the fault is increased the system can handle tracking up to a certain level (Figure 7-7), after that the system becomes uncontrollable and the system cost function requires reconfiguration. This can be seen in Figure 7-8 in which the cost function reaches a new (higher) level. This is the cost that has to be paid for reconfiguration as a result of the fault.

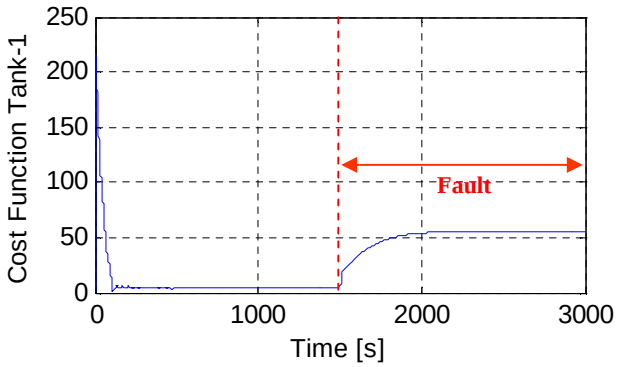

Figure 7-9: Cost Function of the Subsystem 1 with 60% bias on heater operating point

However, this particular feature of tolerance to faults is limited to certain magnitudes of faults. Beyond this magnitude, it is suggested that alternative strategies based on active reconfiguration would have to be considered. Establishing this bound for the fault magnitude is a design feature which could be similar to the use of a threshold employed in model-based FDI methods (see Section 7.3). For achieving robust local FDI, the unknown input observers (UIOs) as described in Chapter 2 is chosen here for the design approach of robust de-coupling FDI in distributed systems.

7.3 Robust De-coupling FDI via UIO Approach

This Section focuses on the development of a suitable FDI strategy for application to a system of inter-connected and distributed subsystems, as a basis for achieving fault-tolerance in two-level distributed control systems. The idea is to use robust FDI methods to facilitate the discrimination between faults acting within one subsystem and faults acting in others, so that a powerful form of robust FTC can be implemented, through an autonomous coordinator. The problem of unknown input de-coupling; subject to autonomous coordination is an interesting challenge in which the interactions between the subsystems (including modeling uncertainty, interconnection disturbance) are considered as *unknown inputs*.

The essential concept is that robust FDI can be achieved within a given subsystem, without requiring a consensus of FDI information across the ensemble of subsystems. A set of residual generators based on the UIO concept provide robust FDI within a given subsystem. As illustrated in Section 2.3.6, Figure 2-11 consists of a group of decoupling UIOs for generating a number of residuals for fault detection isolation. Each

observer in the group is designed to be sensitive to a subset of faults (that have to be detected and isolated).

Considering the system identification in Eqs (7 - 4) and (7 - 5) , the robust FDI for each subsystem can be obtained by Eq. (2 - 2 1) :

Tank-1

$$\begin{aligned}\dot{x}_1(t) &= A_1 x_1(t) + B_1 u_1(t) + z_1(t) \\ &= A_1 x_1(t) + B_1 u_1(t) + \underbrace{\begin{bmatrix} H_{12} & H_{13} \end{bmatrix}}_{E_1} \underbrace{\begin{bmatrix} x_2(t) & x_3(t) \end{bmatrix}^T}_{d_1(t)}\end{aligned} \qquad (7-6)$$

Tank-2

$$\begin{aligned}\dot{x}_2(t) &= A_2 x_2(t) + B_2 u_2(t) + z_2(t) \\ &= A_2 x_2(t) + B_2 u_2(t) + \underbrace{\begin{bmatrix} H_{21} & H_{23} \end{bmatrix}}_{E_2} \underbrace{\begin{bmatrix} x_1(t) & x_3(t) \end{bmatrix}^T}_{d_2(t)}\end{aligned} \qquad (7-7)$$

Tank-3

$$\begin{aligned}\dot{x}_3(t) &= A_3 x_3(t) + B_3 u_3(t) + z_3(t) \\ &= A_3 x_3(t) + B_3 u_3(t) + \underbrace{\begin{bmatrix} H_{31} & H_{32} \end{bmatrix}}_{E_3} \underbrace{\begin{bmatrix} x_1(t) & x_2(t) \end{bmatrix}^T}_{d_3(t)}\end{aligned} \qquad (7-8)$$

where $d_i(t) \in \Re^{q_i}$ is the unknown input or interconnection disturbance, $E_i \in \Re^{n_i x q_i}$ is disturbance distribution direction for $i = 1, 2, 3$. The disturbance estimated this way is also expected to take into account the un-modelled dynamics and interconnection disturbance. Decoupling this direction from the residuals will also make the FDI design robust against unknown inputs. An evaluation of these residuals is carried out in the *Fault Isolation Logic* (see Figure 2-11) unit in order to determine the location of the fault.

The next simulation result illustrates the ability of the i^{th} local FDI tasks to detect faults and also to be able to identify the subsystem where the fault is located. It is stated that when a fault occurs the FDI structure should detect that a fault occurred and where the fault occurred (Klinkhieo and Patton, 2008).

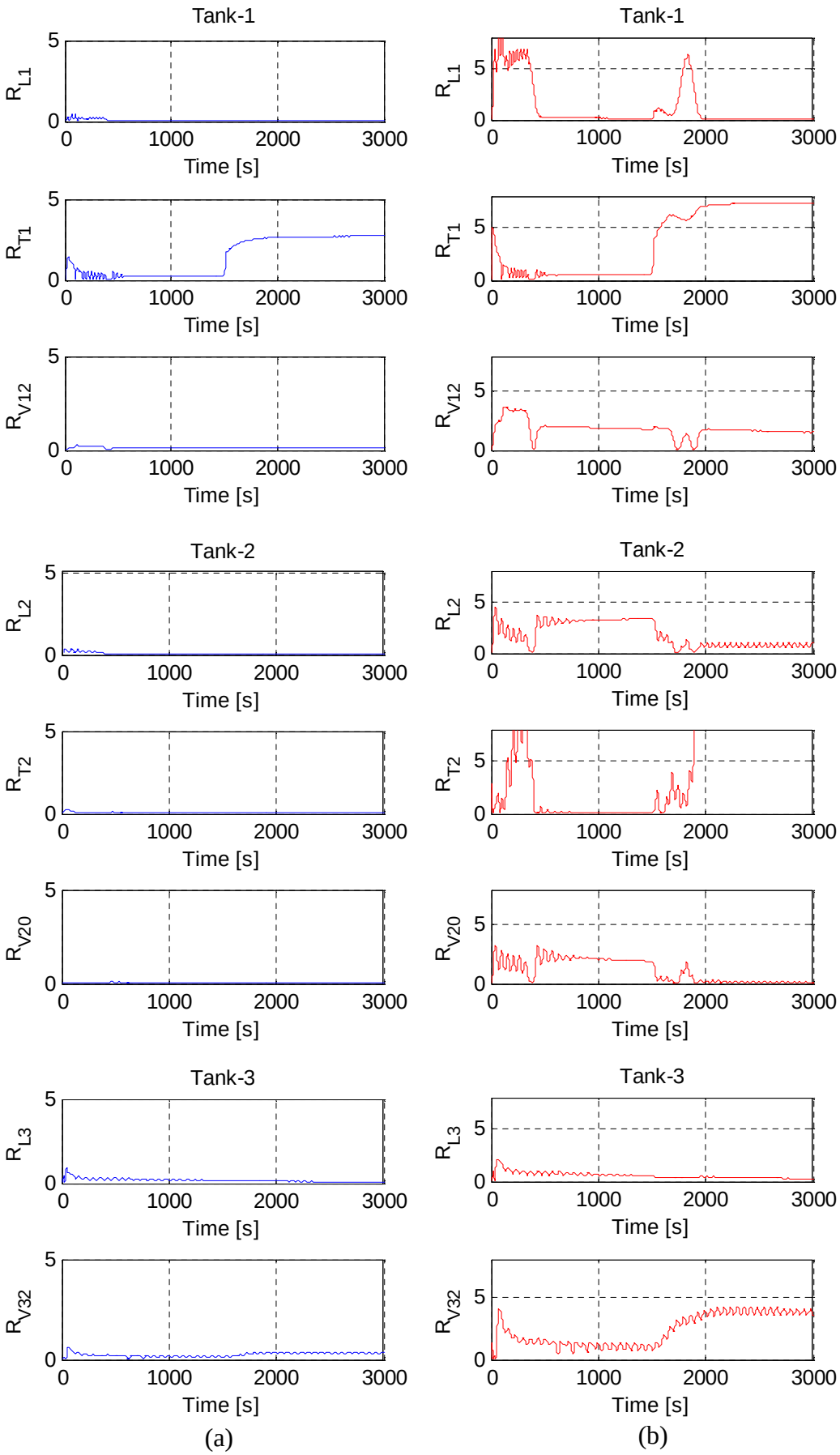

Figure 7-10: Residuals for Tank-1, 2 and 3 with 60% bias on heater operating point (a) with decoupling, (b) without decoupling

Figure 7-10 shows the robustness of residuals to interconnection faults, based on the levels $L_1, L_2, \& L_3$ and Temperatures $T_1 \& T_2$ and inter-tank flows $V_{12}, V_{20}, \& V_{32}$. The fault condition is as for the faulty subsystem is the same as the last case where a 60% bias error on the electrical heater has occurred describing in Figure 7-8.

Figure 7-10 (a) correspond to the case when the 3-UIOs with the disturbance distribution matrix $E_i \neq 0^{n_i x q_i}$ are implemented [see Section 2.3.6], demonstrating clearly that the T_1 residual can be used to isolate the heater fault (i.e. the FDI task can detect the fault and its location in the system)

For Figure 7-10 (b), the 3-UIOs with the disturbance distribution matrix $E_i = 0^{n_i x q_i}$ used for each subsystem [see Section 2.3.6], showing clearly the inability to isolate the heater fault via the T_1 measurement in Tank-1.

As it is discussed extensively above the local control together with the control coordinator can tolerate the faults up to a particular limit (or bound) (see Figure 7-7). Within this limit the control coordinator assumes an error in the interaction prediction and compensate for this error.

However, when a fault exceeds this bound (see Figure 7-8), the FTC methodologies cannot tolerate the faults anymore and the system should be reconfigured. The reconfiguration task acquires residual information from the local FDI tasks and makes a decision as whether or not the reconfiguration is required, based on the comparisons of residual signals and threshold (e.g. adaptive or fixed threshold) (see Figure 7-11).

This gives the reconfiguration task has two levels of operation; (i) a decision task, which decides on whether reconfiguration of performance objectives is needed and (ii) a task which reconfigures the performance criteria and sets new constraints.

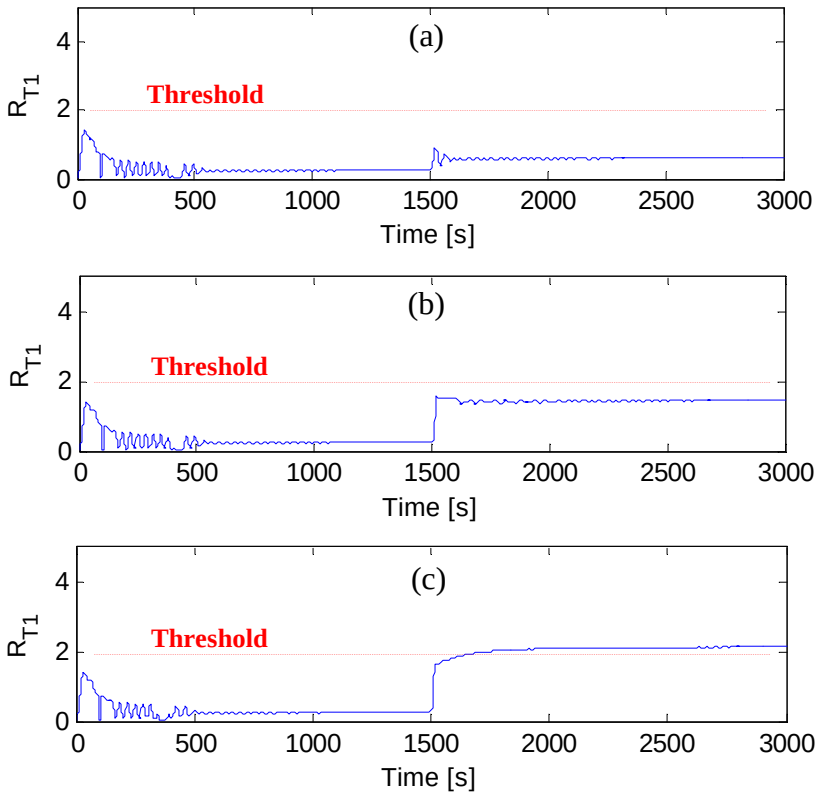

Figure 7-11: The reconfiguration based on the threshold level with a bias fault (20%, 40% and 60% of heater operating point, respectively)

Figure 7-11 (c) shows that the reconfiguration task can be declared once the i^{th} residual signal exceeds some predetermined threshold.

For the Three-tank application problem, the reconfiguration in task (ii) is accomplished by the (hardware) redundant actuators included in the system. There is one heater (*Heater_R*), one pump (*Pump_3_R*) and one valve (*Valve_03_R*) as redundant elements. See Figure 7-12.

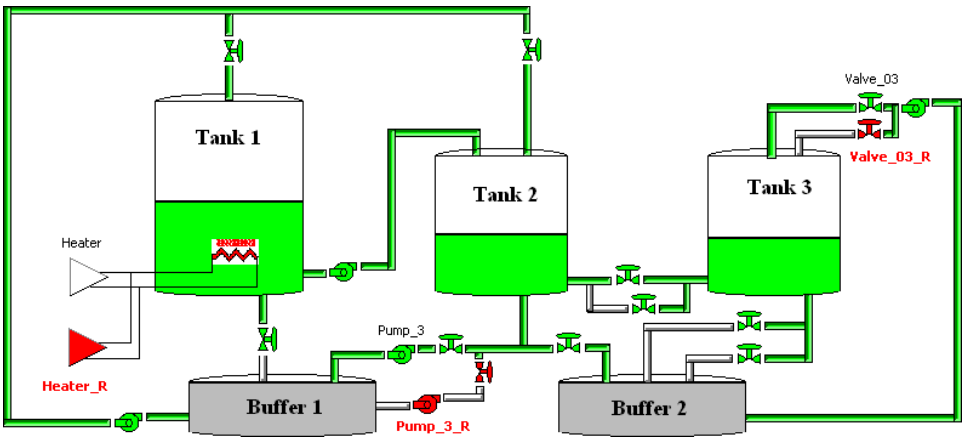

Figure 7-12: Three-Tank system with Redundant Elements

In order to illustrate the reconfiguration the experiments have been carried out. As described above there are three hardware redundancies in the system: *Heater_R*, *Pump-3_R* and *Valve-03_R*. Thus when severe faults occur on the *Heater*, *Pump-3* or *Valve-03* the FTC strategies cannot compensate the faults and the hardware redundant elements of the system become necessary.

When the fault magnitudes are too large the control scheme cannot compensate for the faults (see Figure 7-8). It can then be seen that the temperature (T_1) in Tank-1 moves away from its set-point value, the residual signal reaches the chosen threshold level [see Figure 7-11 (c)], therefore the Reconfiguration Task will disconnects the *Heater* and activates the redundant *Heater_R*.

Figure 7-13 shows that after the reconfiguration T_1 soon settles back to its normal value under coordinated closed-loop control.

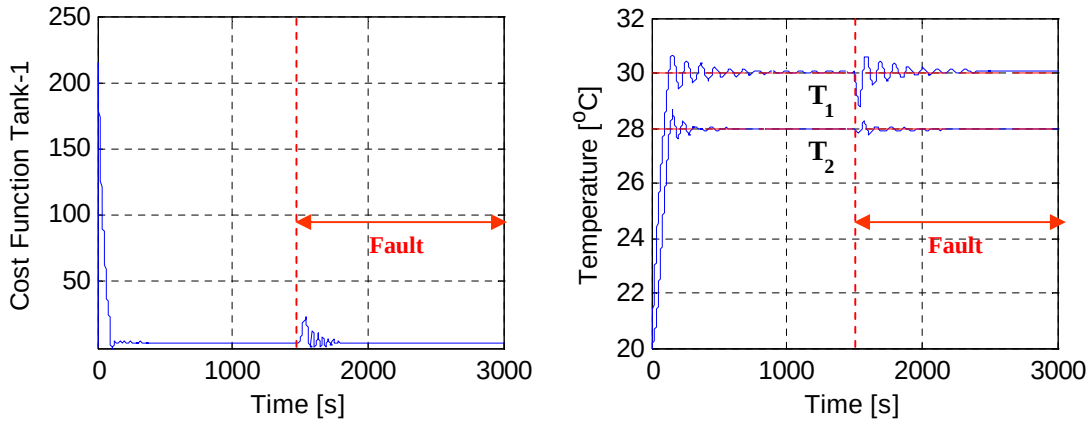

Figure 7-13: Three-Tank-System with reconfiguration using redundant elements

However, in some cases the redundant elements are not available, perhaps for space limitations, or (for military aircraft: weight and even increased operating costs, etc). Section 7.4 provides the alternative ways for achieving FTC via adaptive control in which the reconfiguration (i.e. hardware redundancies) is not required.

7.4 The ASO Approach to FTC of Distributed Systems

As mentioned in Chapters 6, the complexity of the distributed system is quite different from the classical view of control, with special requirements focused on the importance of re-configurability and the need for control of a complex inter-connected system

(Patton *et al*., 2007). In this Section, the ASO (see Chapter 3) is employed to dealing with these problems.

7.4.1 The ASO approach for the single-level control strategy

As described in Chapter 6, distributed and interconnected systems are difficult to stabilise with single controllers due to computational complexity caused by large dimensions and effects of interconnections (Singh and Titli, 1978; Patton *et al*., 2007). Therefore, for designing a distributed control system, it is necessary to divide the entire system into several interconnected subsystems, and utilise a single (local) de-centralised controller to stabilise each subsystem.

For the problem in which the control is only single level, the coordinator is not used and the problem becomes a special case of the one developed in Chapter 6. Hence, an alternative and appropriate method of estimation and compensation for the subsystem interaction states is attractive, since this role is no longer provided by the coordinator.

In this Section, the nonlinear Three-Tank interconnected system of Section 7.2 is reconsidered without the use of the learning coordinator and ACSS. The parameters of this system are given in Eqs. (7 - 4) and (7 - 5). Here, the ASO method (Patton, Klinkhieo and Putra, 2008) described in Chapter 3 is used to handle the problem of interconnection disturbances in the local subsystem, using the assumption that the system is in a fault-free state. In Section 7.4.2 the system is considered with faults acting and the full system with both faults and estimation and compensation of state interactions is demonstrated.

Consider as a special case of Section 6.4.5 an interconnected system composed of N subsystem as follows:

$$\begin{aligned} \dot{x}_i(t) &= A_i x_i(t) + B_i u_i(t) + z_i(t) \\ y_i(t) &= C_i x_i(t) \\ & \qquad i = 1, 2, \ldots, N \end{aligned} \qquad (7\text{-}9)$$

where $z_i \in \Re^{n_i}$ is the state/interconnection term of the i^{th} subsystem. The isolated control strategy for interconnection, estimation and compensation is illustrated in Figure 7-14.

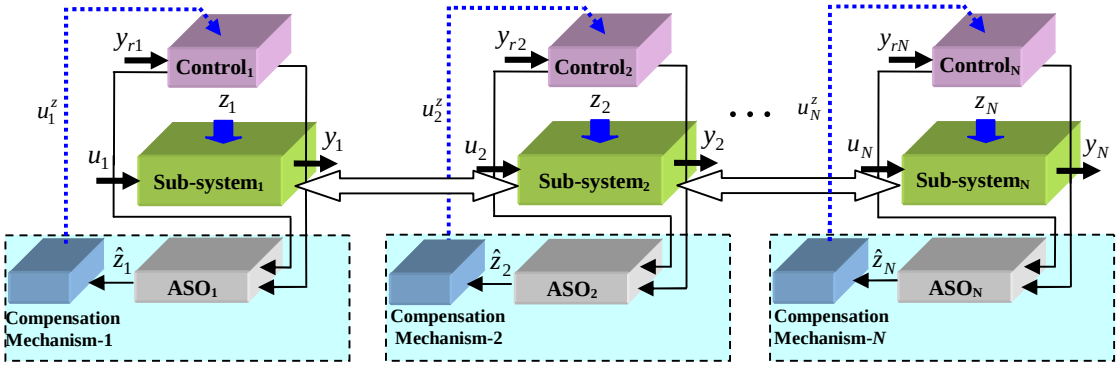

Figure 7-14: The ASO approach for interconnected disturbance compensation

Figure 7-14 shows that the interconnection terms (z_i) acting on each subsystem are estimated via i^{th} subsystem local ASO units. The information about the magnitude of estimated signals ($\hat{z}_i$) are sent to the *compensation mechanism* section where the interconnected compensating control (u_i^z) is computed.

In a similar manner to the actuator fault estimation case described in Section 3.2, here the new compensating control is added into the nominal control signal to compensate or reduce the interconnection effects. This estimation-controller structure is given by:

$$u_i = \underbrace{K_i^x \hat{x}_i}_{u_i^x} + \underbrace{K_i^z \hat{z}_i}_{u_i^z} \qquad i = 1, 2, \ldots, N \tag{7-10}$$

where u_i^x is the control of nominal system for the fault-free case, u_i^z is the compensating control to be added to compensate for the interconnection (z_i) acting upon the i^{th} system, and the signals $\hat{x}$ and $\hat{z}_i$ are state and actuator fault estimations, respectively. $K_i^x \in R^{m_i \times n_i}$ is the feedback gain matrix obtained by linear pole-placement state feedback design. $K_i^z \in R^{m_i \times l_i}$ is the actuator fault compensation gain to be designed [see the details described in Section 3.2].

The interconnection compensation can be achieved by replacing u_i in Eq. (7-9) with the new u_i in Eq. (7-10), yielding the local closed-loop system given by:

$$\begin{aligned} \dot{x}_i &= A_i x_i + B_i K_i^x x_i + B_i K_i^z \hat{z}_i + z_i \\ &= (A_i + B_i K_i^x) x_i + B_i K_i^z \hat{z}_i + z_i \end{aligned} \tag{7-11}$$

where i^{th} subsystem estimated state is given by:

$$\begin{aligned}\dot{\hat{x}}_i &= A_i\hat{x}_i + B_iK_i^x\hat{x}_i + L_i^x(y_i - \hat{y}_i) \\ &= (A_i + B_iK_i^x)\hat{x}_i + L_i^xC_i(x_i - \hat{x}_i)\end{aligned} \qquad (7\text{-}12)$$

and the i^{th} subsystem interconnection state estimation is given by:

$$\dot{\hat{z}}_i = L_i^z(y_i - C_i\hat{x}_i) \qquad (7\text{-}13)$$

Following Eqs (3 - 2) and (3 - 8) , here Eqs (7-12) and (7-13) giving:

$$\underbrace{\begin{bmatrix}\dot{\hat{x}}_i \\ \dot{\hat{z}}_i\end{bmatrix}}_{\dot{\tilde{x}}_i} = \left(\underbrace{\begin{bmatrix}A_i + B_iK_i^x & 0 \\ 0 & 0\end{bmatrix}}_{A_i^x} - \underbrace{\begin{bmatrix}L_i^x \\ L_i^z\end{bmatrix}}_{L_i}\underbrace{\begin{bmatrix}C_i & 0\end{bmatrix}}_{C_i^x}\right)\underbrace{\begin{bmatrix}\hat{x}_i \\ z_i\end{bmatrix}}_{\tilde{x}_i} + \underbrace{\begin{bmatrix}L_i^x \\ L_i^z\end{bmatrix}}_{L_i}C_ix_i \qquad (7\text{-}14)$$

and

$$\dot{\tilde{x}}_i = (A_i^x - L_iC_i^x)\tilde{x}_i + L_iC_i^x \qquad (7\text{-}15)$$

where $L_i^x \in R^{n_i \times p_i}$ and $L_i^z \in R^{n_i \times p_i}$ are the observer gains to be designed. Hence, solving the Eq. (7-15) gives an estimation of the magnitudes z_i, which is the *last component* of the augmented state vector $\tilde{x}_i$.

Thus, the interconnected system in Eq. (7-9) with the observer Eq. (7-12) can be arranged in the following closed-loop system:

$$\begin{bmatrix}\dot{e}_i^x \\ \dot{\hat{z}}_i\end{bmatrix} = \begin{bmatrix}A_i - L_i^xC & B_iK_i^z \\ L_i^xC & 0\end{bmatrix}\begin{bmatrix}e_i^x \\ \hat{z}_i\end{bmatrix} + \begin{bmatrix}I_{n_i} \\ 0\end{bmatrix}z_i \qquad (7\text{-}16)$$

where $e_i^x = x_i - \hat{x}_i$ is the state estimation error. Re-arranging Eq. (7-16) as:

$$\underbrace{\begin{bmatrix}\dot{e}_i^x \\ \dot{\hat{z}}_i\end{bmatrix}}_{\dot{\tilde{e}}_i} = \left(\underbrace{\begin{bmatrix}A_i & B_iK_i^z \\ 0 & 0\end{bmatrix}}_{A_i^0} - \underbrace{\begin{bmatrix}L_i^x \\ -L_i^z\end{bmatrix}}_{L_i^0}\underbrace{\begin{bmatrix}C & 0\end{bmatrix}}_{C_i^0}\right)\underbrace{\begin{bmatrix}e_i^x \\ \hat{z}_i\end{bmatrix}}_{\tilde{e}_i} + \underbrace{\begin{bmatrix}I_{n_i} \\ 0\end{bmatrix}}_{I_{n_i}^0}z_i \qquad (7\text{-}17)$$

$$\dot{\tilde{e}}_i = (A_i^0 - L_i^0C_i^0)\tilde{e}_i + I_{n_i}^0z_i \qquad (7\text{-}18)$$

Section 3.2 provides the stability proof for the ASO control compensating problem. Furthermore, as the interconnected terms (z_i) are bounded, it follows from ***Proposition 3.1*** and ***Theorem 3.1***, that the gains L_1^o, L_2^o and L_3^o for the i^{th} subsystem, where $i = 1, 2, 3$ can result in a stable implementation of this system. To guarantee stability of

each ASO subsystem it is necessary to ensure that the eigenvalues of the estimation error system Eq. (7-18) are assigned with negative real values. A suitably chosen eigenvalue placement will also ensure good tracking/estimation of the interaction states, as required for rapid compensation.

For this example, the matrix subsystem pairs (A_1^0, C_1^0), (A_2^0, C_2^0) and (A_3^0, C_3^0) are observable, and the observer gains L_i^o are designed such that the eigenvalues of $(A_i^o - L_i^o C_i^o)$ are placed as follows:

Tank-1

$$A_1^o = \begin{bmatrix} -0.0581 & -0.0347 & 0.0298 & 1.0000 & 0.0000 & 0.0000 \\ -0.0244 & -0.3504 & 0.0561 & 0.0000 & 1.0000 & 0.0000 \\ 0.0153 & 0.0163 & -0.0900 & 0.0000 & 0.0000 & 1.0000 \\ 0.0000 & 0.0000 & 0.0000 & 0.0000 & 0.0000 & 0.0000 \\ 0.0000 & 0.0000 & 0.0000 & 0.0000 & 0.0000 & 0.0000 \\ 0.0000 & 0.0000 & 0.0000 & 0.0000 & 0.0000 & 0.0000 \end{bmatrix}$$

$$C_1^o = \begin{bmatrix} 0.5000 & 0.0000 & 0.0000 & 0.0000 & 0.0000 & 0.0000 \\ 0.0000 & 1.0000 & 0.0000 & 0.0000 & 0.0000 & 0.0000 \\ 0.0000 & 0.0000 & 1.0000 & 0.0000 & 0.0000 & 0.0000 \end{bmatrix}$$

$$L_1^o = \begin{bmatrix} 84.8837 & -0.0347 & 0.0298 \\ -0.0488 & 24.9911 & -1.2046 \\ 0.0307 & -1.2456 & 29.5685 \\ 900.0000 & 0.0000 & 0.0000 \\ 0.0000 & 154.6957 & -17.3332 \\ 0.0000 & -17.3526 & 214.0543 \end{bmatrix}$$

The eigenvalues of $(A_1^o - L_1^o C_1^o)$ are: -22.50, -20.00, -10.00, -12.50, -15.00, -17.50

Tank-2

$$A_2^o = \begin{bmatrix} -0.1098 & 0.0154 & -0.0467 & 1.0625 & -0.0156 & -0.3750 \\ 0.0348 & -0.1517 & -0.0051 & -1.0000 & 0.6250 & 1.5000 \\ -0.0215 & -0.0149 & -0.1337 & 0.0625 & 0.0625 & 1.1250 \\ 0.0000 & 0.0000 & 0.0000 & 0.0000 & 0.0000 & 0.0000 \\ 0.0000 & 0.0000 & 0.0000 & 0.0000 & 0.0000 & 0.0000 \\ 0.0000 & 0.0000 & 0.0000 & 0.0000 & 0.0000 & 0.0000 \end{bmatrix}$$

$$C_2^o = \begin{bmatrix} 1.0000 & 0.0000 & 0.0000 & 0.0000 & 0.0000 & 0.0000 \\ 0.0000 & 1.0000 & 0.0000 & 0.0000 & 0.0000 & 0.0000 \\ 0.0000 & 0.0000 & 0.8000 & 0.0000 & 0.0000 & 0.0000 \end{bmatrix}$$

$$L_2^o = \begin{bmatrix} 3.7856 & -0.0867 & 0.5606 \\ -0.1020 & 3.2351 & -0.0662 \\ 0.5099 & -0.0630 & 4.6122 \\ 32.6822 & -2.0716 & 22.0641 \\ 37.5854 & 43.3485 & -53.8429 \\ 4.7067 & -2.8627 & 36.7357 \end{bmatrix}$$

The eigenvalues of $(A_2^o - L_2^o C_2^o)$ are: -27.50, -10.00, -12.50, -15.00, -22.50, -20.00

Tank-3

$$A_3^o = \begin{bmatrix} -0.0915 & -0.0022 & 1.0000 & 0.0000 \\ 0.0244 & -0.2232 & 0.0000 & 1.0000 \\ 0.0000 & 0.0000 & 0.0000 & 0.0000 \\ 0.0000 & 0.0000 & 0.0000 & 0.0000 \\ 0.0000 & 0.0000 & 0.0000 & 0.0000 \end{bmatrix}$$

$$C_3^o = \begin{bmatrix} 0.3000 & 0.0000 & 0.0000 & 0.0000 \\ 0.0000 & 0.1000 & 0.0000 & 0.0000 \end{bmatrix}$$

$$L_3^o = \begin{bmatrix} 133.0282 & -0.0216 \\ 0.0814 & 222.7683 \\ 1250.0000 & 0.0000 \\ 0.0000 & 1250.000 \end{bmatrix}$$

The eigenvalues of $(A_3^o - L_3^o C_3^o)$ are: -25.00, -15.00, -12.50, -10.00

Figure 7-15 shows the *three* components of the interconnected state vector for Tank-2, given by: $z_2 = col(z_{2_1}, z_{2_2}, z_{2_3})$.

Figure 7-16 shows the level output (L_2) in Tank-2 with (a) the output response including the (uncompensated) interconnection effect (z_2) i.e. without the ASO compensation mechanism. It can be seen that the L_2 output does not follow its reference/set-point well and there is a considerable off-set value (d_{offset}). Case (b) demonstrates the excellent performance of the controlled output (L_2) as a consequence of the interconnection compensation mechanism employing the three ASO. Clearly, in case (b), the off-set (d_{offset}) is reduced practically to zero by adding the new interconnected compensating control described in Eq. (7-10).

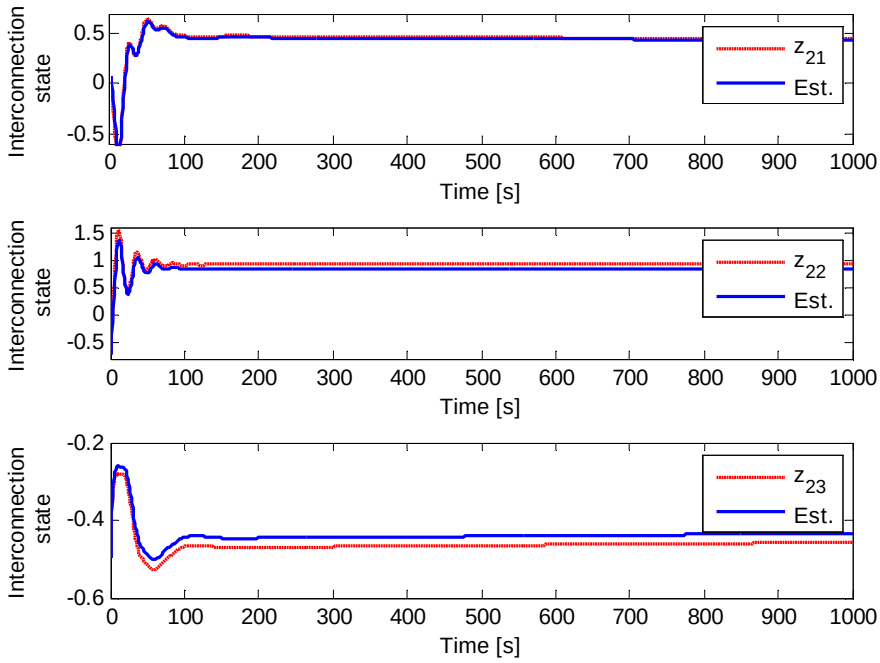

Figure 7-15: The interconnected signal (z_2) and its estimate ($\hat{z}_2$) using ASO

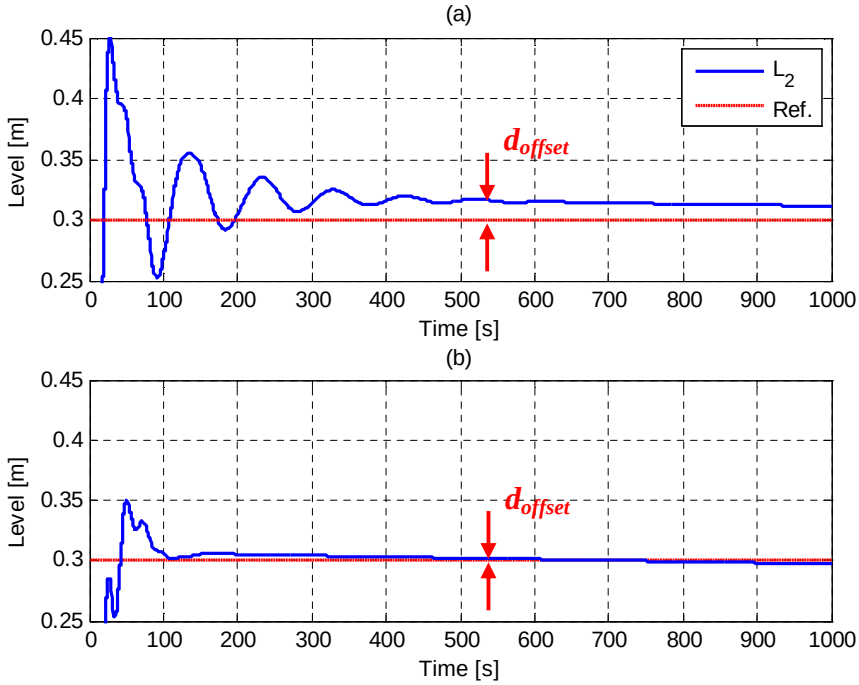

Figure 7-16: The level output (L_2) with and without interconnection compensation

7.4.2 The Combination of two-level control and ASO approach

The coordination principles for the optimization problem of distributed systems are introduced in Chapter 6 through the application of the Principle of Interaction-Prediction. This uses as a basis the idea that the distributed system can be decomposed into smaller subsystems, and that there is an ability to be able to predict and coordinate

possible interactions between these subsystems. By using this Principle the autonomous system coordinator is able to use current state information together with interaction state information to balance the system. The coordinator optimizes and balances the global system performance and this gives rise to an excellent opportunity to achieve good FTC action (Singh and Titli, 1978; Patton *et al*., 2007; Kambhampati *et al*., 2007).

This Section provides a novel strategy for extending the concept of the two-level control architecture. This comprises a local level fault compensating control mechanism the additive fault compensating control using ASO (see description in Section 3.2), with the coordinated two-level control (ACSS) scheme as illustrated in Figure 7-17 . In the manner described in Chapter 6, this two-level control approach is used to deal with the problem of interconnection disturbances, whereas the ASO compensates for any bounded local faults.

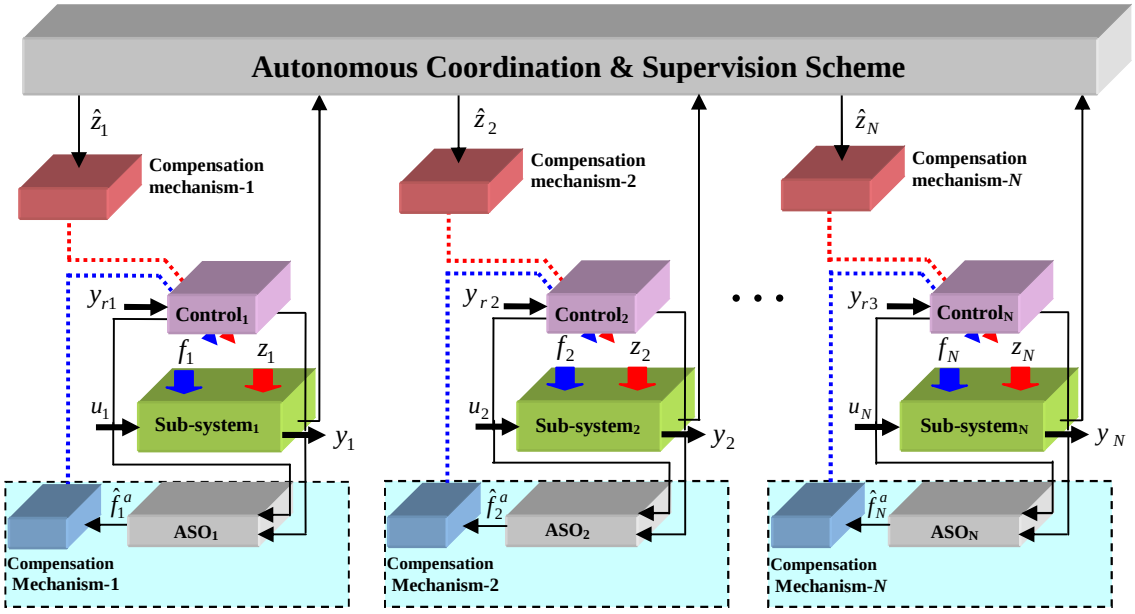

Figure 7-17: The interconnection and local fault compensation scheme

In contrast to the architecture shown in Figure 7-17, it is now possible to deal with the simultaneous estimation and compensation of both subsystem interaction states and local faults. The linearised representation for each subsystem within this structure is given, in the presence of simultaneous actuator fault and interconnection disturbances by:

$$\begin{aligned} \dot{x}_i(t) &= A_i x_i(t) + B_i u_i(t) + F_i^a f_i^a(t) + z_i(t) \\ y_i(t) &= C_i x_i(t) \end{aligned} \qquad (7\text{-}19)$$

where f_i^a is the actuator fault effect on the i^{th} subsystem. For the actuator fault case the matrix F_i^a is identical to B_i. Once again the z_i represent the interconnection states. subsystems acting on i^{th} subsystem.

By following the ASO approach presented in Section 3.2 and similar to the interconnection estimation case described in Section 7.4.1, here again the new compensating control is added into the nominal control signal to compensate or reduce the actuator fault effects. This estimation-controller structure is given by:

$$u_i = \underbrace{K_i^x \hat{x}_i}_{u_i^x} + \underbrace{K_i^a \hat{f}_i^a}_{u_i^a} \qquad i = 1, 2, \ldots, N \tag{7-20}$$

where u_i^x is the control of nominal system for the fault-free case, and u_i^a is the compensating control to be added to compensate for the actuator fault ($\hat{f}_i^a$) acting upon the i^{th} system. The signals $\hat{x}$ and $\hat{f}_a$ are state and actuator fault estimations, respectively. $K_i^x \in R^{m_i \times n_i}$ is the feedback gain matrix obtained by a linear multivariable state feedback design $K_i^a \in R^{m_i \times m_i}$ is the actuator fault compensation gain to be designed (see Section 3.2).

The actuator fault compensation

The actuator fault compensation can be achieved by replacing u_i in Eq.(7-19) as an isolated system [i.e. by not considering $z_i(t)$ here, as this term can be compensated later by using the two level control approach] and obtaining a new local control signal u_i in Eq. (7-20), yields the local closed-loop system given by:

$$\begin{aligned} \dot{x}_i &= A_i x_i + B_i K_i^x x_i + B_i K_i^a f_i^a + F_i^a f_i^a \\ &= (A_i + B_i K_i^x) x_i + B_i K_i^a f_i^a + F_i^a f_i^a \end{aligned} \tag{7-21}$$

where i^{th} subsystem estimated state is given by:

$$\begin{aligned} \dot{\hat{x}}_i &= A_i \hat{x}_i + B_i K_i^x \hat{x}_i + L_i^x (y_i - \hat{y}_i) \\ &= (A_i + B_i K_i^x) \hat{x}_i + L_i^x C_i (x_i - \hat{x}_i) \end{aligned} \tag{7-22}$$

and the i^{th} actuator fault estimation is given by:

$$\dot{\hat{f}}_i^a = L_i^a (y_i - C_i \hat{x}_i) \tag{7-23}$$

Following Eqs (3 - 2) and (3 - 8) , here Eqs (7-22) and (7-23) giving:

$$\underbrace{\begin{bmatrix}\dot{\hat{x}}_i\\ \dot{\hat{f}}_i^{\,a}\end{bmatrix}}_{\dot{\tilde{x}}_i} = \left(\underbrace{\begin{bmatrix}A_i + B_i K_i^x & 0\\ 0 & 0\end{bmatrix}}_{A_i^x} - \underbrace{\begin{bmatrix}L_i^x\\ L_i^a\end{bmatrix}}_{L_i}\underbrace{\begin{bmatrix}C_i & 0\end{bmatrix}}_{C_i^x}\right)\underbrace{\begin{bmatrix}\hat{x}_i\\ \hat{f}_i^{\,a}\end{bmatrix}}_{\tilde{x}_i} + \underbrace{\begin{bmatrix}L_i^x\\ L_i^a\end{bmatrix}}_{L_i} C_i x_i \qquad (7\text{-}24)$$

and

$$\dot{\tilde{x}}_i = (A_i^x - L_i C_i^x)\tilde{x}_i + L_i C_i^x \qquad (7\text{-}25)$$

where $L_i^x \in R^{n_i \times p_i}$ and $L_i^z \in R^{m_i \times p_i}$ are the observer gains to be designed. Hence, solving the Eq. (7-25) gives an estimation of the actuator faults $f_i^{\,a}$, which is the *last component* of the augmented state vector $\tilde{x}_i$.

Thus, the isolated system in Eq. (7-19) and the observer Eq. (7-22) can be arranged in the following closed-loop system:

$$\begin{bmatrix}\dot{\hat{e}}_i^x\\ \dot{\hat{f}}_i^{\,a}\end{bmatrix} = \begin{bmatrix}A_i - L_i^x C & B_i K_i^a\\ L_i^x C & 0\end{bmatrix}\begin{bmatrix}\hat{e}_i^x\\ \hat{f}_i^{\,a}\end{bmatrix} + \begin{bmatrix}F_i^a\\ 0\end{bmatrix} f_i^{\,a} \qquad (7\text{-}26)$$

where $e_i^x = x_i - \hat{x}_i$ is the state estimation error. Re-arranging Eq. (7-26) as:

$$\underbrace{\begin{bmatrix}\dot{e}_i^x\\ \dot{\hat{f}}_i^{\,a}\end{bmatrix}}_{\dot{\tilde{e}}_i} = \left(\underbrace{\begin{bmatrix}A_i & B_i K_i^a\\ 0 & 0\end{bmatrix}}_{A_i^0} - \underbrace{\begin{bmatrix}L_i^x\\ -L_i^z\end{bmatrix}}_{L_i^0}\underbrace{\begin{bmatrix}C & 0\end{bmatrix}}_{C_i^0}\right)\underbrace{\begin{bmatrix}e_i^x\\ \hat{f}_i^{\,a}\end{bmatrix}}_{\tilde{e}_i} + \underbrace{\begin{bmatrix}F_i^a\\ 0\end{bmatrix}}_{F_i^0} f_i^{\,a} \qquad (7\text{-}27)$$

$$\dot{\tilde{e}}_i = (A_i^0 - L_i^0 C_i^0)\tilde{e}_i + F_i^0 f_i^{\,a} \qquad (7\text{-}28)$$

Section 3.2 provides the stability proof for the ASO control compensating problem. Furthermore, since the actuator fault terms ($\hat{f}_i^{\,a}$) are bounded, it follows from ***Proposition 3.1*** and ***Theorem 3.1***

<u>The interconnection compensation</u>

Now following the two-level control approach described in the Eqs (6-23) and (6-39), together with Eq. (7-20) defined with respect to the interconnected states [i.e. using linear quadratic optimization for obtaining the feedback gain matrix], the compensating control can be re-written as:

$$
\begin{aligned}
u_i^x &= \underbrace{R_i^{-1}(B_i)^T S_i \hat{x}_i}_{u_i^{local}} + \underbrace{R_i^{-1}(B_i)^T \aleph_i}_{u_i^{int.}} \\
&= u_i^{local} + u_i^{int.}
\end{aligned}
\qquad (7\text{-}29)
$$

where S_i and $\aleph_i$ are the solutions of the appropriate modified *Riccati Equations* (see Section 6.4.5) and the *Interaction Compensation Equations* respectively,. The first two terms (u_i^{local}) correspond to the control for the i^{th} isolated subsystem following Eq. (6-23), whilst the last term ($u_i^{int.}$) is the compensating control for the interactions.

By following Eqs (7-20) and (7-29), at this point, it can be seen that the new control law now has <u>*three*</u> components, namely (i) a control component based on local information, (ii) a component based on the interactions, and (iii) a component based on the local fault [see Figure 7-17]. Therefore, the total control for i^{th} subsystem is given by:

$$
\begin{aligned}
u_i &= u_i^x + u_i^a \\
&= u_i^{local} + u_i^{int.} + u_i^a
\end{aligned}
\qquad (7\text{-}30)
$$

where u_i^{local} is the compensator for the i^{th} subsystem in isolation, $u_i^{int.}$ is the compensating control for the interaction disturbances, and u_i^a is the compensating control to be added to compensate for the actuator fault (f_i^a) effect on the i^{th} subsystem.

To demonstrate the above discussion, the nonlinear distributed three-tank system is used as a simultaneous interconnection (z_i) and fault (f_i^a) compensation problem. The important task here is to design the new control law in order to reduce or compensate <u>*both*</u> interconnection and fault effecting on i^{th} subsystem simultaneously, and then the local FTC task can be achieved.

For this example, the matrix subsystem pairs (A_1^0, C_1^0), (A_2^0, C_2^0) and (A_3^0, C_3^0) are observable, and the observer gains L_i^o are designed such that the eigenvalues of $(A_i^o - L_i^o C_i^o)$ are placed as follows:

Tank-1

$$A_1^o = \begin{bmatrix} -0.0581 & -0.0347 & 0.0298 & 0.0000 & 0.0511 & -0.0158 \\ -0.0244 & -0.3504 & 0.0561 & 0.1329 & -0.0143 & 0.0000 \\ 0.0153 & 0.0163 & -0.0900 & 0.0000 & 0.0000 & 0.0657 \\ 0.0000 & 0.0000 & 0.0000 & 0.0000 & 0.0000 & 0.0000 \\ 0.0000 & 0.0000 & 0.0000 & 0.0000 & 0.0000 & 0.0000 \\ 0.0000 & 0.0000 & 0.0000 & 0.0000 & 0.0000 & 0.0000 \end{bmatrix}$$

$$C_1^o = \begin{bmatrix} 0.5000 & 0.0000 & 0.0000 & 0.0000 & 0.0000 & 0.0000 \\ 0.0000 & 1.0000 & 0.0000 & 0.0000 & 0.0000 & 0.0000 \\ 0.0000 & 0.0000 & 1.0000 & 0.0000 & 0.0000 & 0.0000 \end{bmatrix}$$

$$L_1^o = \begin{bmatrix} 32.2462 & 0.2404 & 1.6325 \\ 1.0046 & 14.7727 & -0.5545 \\ 4.0169 & -0.3654 & 17.3557 \\ 327.2741 & 419.2859 & 31.6413 \\ 2538.4626 & 18.6535 & 621.3612 \\ 541.9950 & -42.3754 & 1114.0933 \end{bmatrix}$$

The eigenvalues of $(A_1^o - L_1^o C_1^o)$ are: -11.25, -5.00, -10.00, -6.25, -7.50 and -8.75

Tank-2

$$A_2^o = \begin{bmatrix} -0.1098 & 0.0154 & -0.0467 & 0.8619 & -0.0892 \\ 0.0348 & -0.1517 & -0.0051 & -0.0892 & 0.9423 \\ -0.0215 & -0.0149 & -0.1337 & -0.3332 & -0.2153 \\ 0.0000 & 0.0000 & 0.0000 & 0.0000 & 0.0000 \\ 0.0000 & 0.0000 & 0.0000 & 0.0000 & 0.0000 \end{bmatrix}$$

$$C_2^o = \begin{bmatrix} 1.0000 & 0.0000 & 0.0000 & 0.0000 \\ 0.0000 & 1.0000 & 0.0000 & 0.0000 \\ 0.0000 & 0.0000 & 0.8000 & 0.0000 \end{bmatrix}$$

$$L_2^o = \begin{bmatrix} 33.2218 & 0.6153 & -0.9703 \\ -1.1655 & 37.8389 & -8.3162 \\ -4.6280 & -5.1310 & 27.8675 \\ 299.7352 & 45.2720 & -67.8204 \\ -0.0836 & 374.4786 & 173.2831 \end{bmatrix}$$

The eigenvalues of $(A_2^o - L_2^o C_2^o)$ are: -13.75, -23.75, -21.25, -18.75 and -16.25

Tank-3

$$A_3^o = \begin{bmatrix} -0.0915 & -0.0022 & 0.0441 & -0.0273 \\ 0.0244 & -0.2232 & 0.0000 & 0.0218 \\ 0.0000 & 0.0000 & 0.0000 & 0.0000 \\ 0.0000 & 0.0000 & 0.0000 & 0.0000 \end{bmatrix}$$

$$C_3^o = \begin{bmatrix} 0.3000 & 0.0000 & 0.0000 & 0.0000 \\ 0.0000 & 0.1000 & 0.0000 & 0.0000 \end{bmatrix}$$

$$L_3^o = \begin{bmatrix} -2.7004 & 55.3001 \\ 380.6707 & 1915.0792 \\ -349.1169 & 3711.0336 \end{bmatrix}$$

The eigenvalues of $(A_3^o - L_3^o C_3^o)$ are: -4.00, -2.00, -2.50 and -3.00

Figure 7-18 shows; (a) the fault signal acting on (2^{nd} actuator) in Tank-1 with $f_{1_1}^a = 0$, $f_{1_2}^a = 0.25\sin(0.30t)$ and $f_{1_3}^a = 0$, respectively, where actuator fault vector of Tank-1 is given by: $f_1^a = col[\, f_{1_1}^a, f_{1_2}^a, f_{1_3}^a\,]$ [see Eq. (7-19)], (b) the estimation of the fault magnitude, and (c) the estimation error, respectively. It can be seen that the fault estimator as presented in Eq. (7-24), provides excellent estimation of $\hat{f}_i^a$, with very small estimation error.

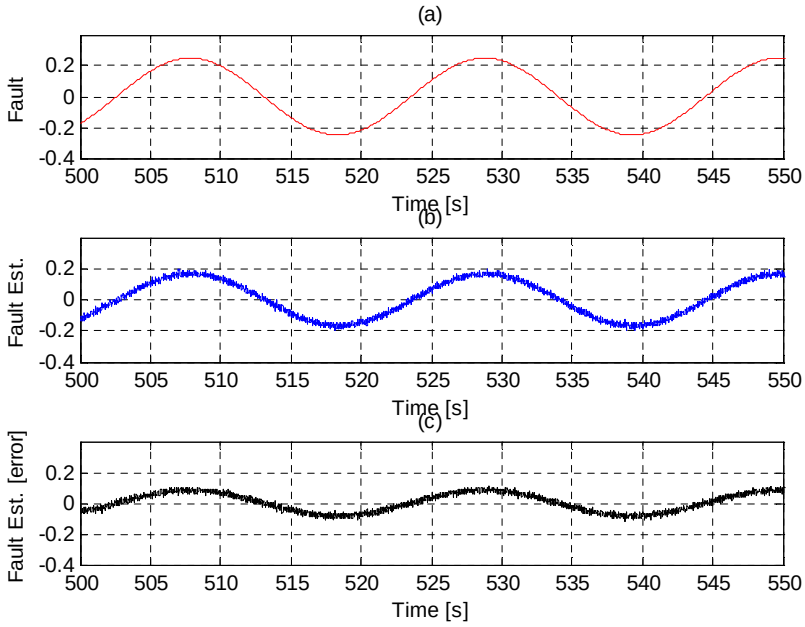

Figure 7-18: The fault signal, fault estimation and estimation error acting on 2^{nd} actuator in Tank-1

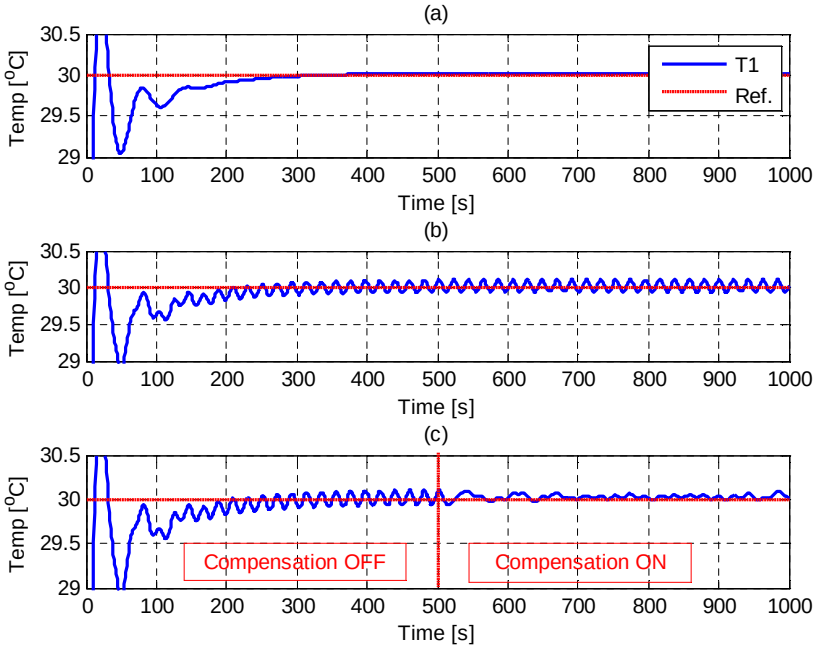

Figure 7-19: The interconnection and fault compensation on Tank-1 where the compensation mechanism is activated at time t = 500s.

Figure 7-19 shows the output response of the temperature (T_1) in Tank-1; (a) in the present of fault free case, (b) with fault acting on (2^{nd} actuator) [i.e. $f_1^a = col(0.00,\ 0.25\sin(0.30t),\ 0.00)$], and (c) with the compensating control mechanism, activated at $t = 500s$. Figure 7-19 (c) shows that after compensating control mechanism "ON", T_1 soon settles back to its normal value due to the interconnection and fault effects are compensated/reduced under coordinated closed-loop control.

The next simulation considers the case when the fault is present on (the 1^{st} actuator) in Tank-1, where fault ($f_{2_1}^a$) is a *pulse signal* with Magnitude: 0.25, period: 10secs and with Pulse Width: 50% of period [MATLAB; Pulse Generator], $f_{1_2}^a = 0$ and $f_{1_3}^a = 0$, respectively.

Figure 7-20 also demonstrates the very good estimation using ASO method following: (a) the fault signal ($f_{1_1}^a$) acting on the 1^{st} actuator in Tank-1, (b) the fault estimation ($\hat{f}_{1_1}^a$), and (c) the estimation error, respectively.

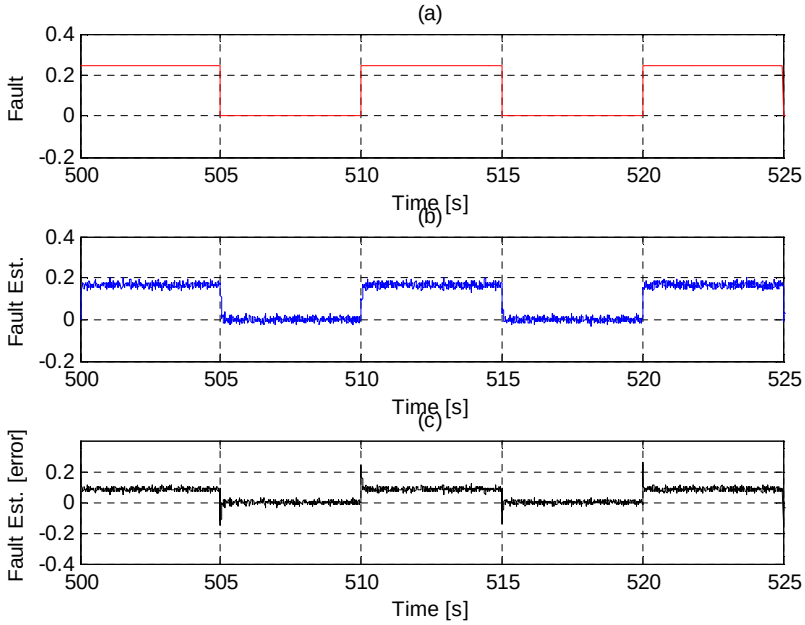

Figure 7-20: The fault signal, fault estimation and estimation error acting on 1^{st} actuator in Tank-1

Figure 7-21 presents the simulation result of: (a) the tank level output response (L_1) for fault free case, (b) the tank level (L_1) when fault is presented on the 1^{st} actuator in Tank-1, and (c) the tank level (L_1) settles back to its normal value after the compensation mechanism "ON" at $t = 500$s.

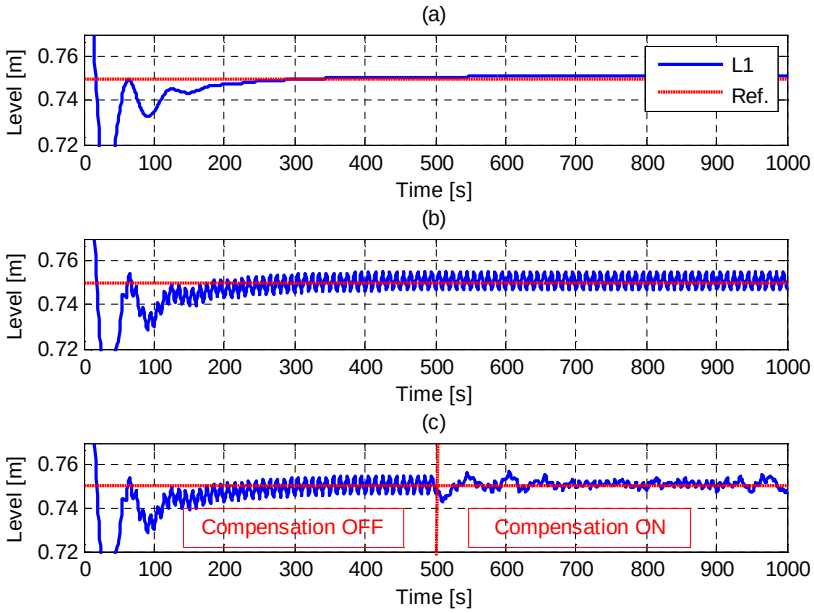

Figure 7-21: The interconnection and fault compensation on Tank-1; the compensation mechanism is activated at time t = 500s.

7.5 Conclusion

This Chapter show the proposed strategies described Chapter 3 and 6 to the interconnection or/and fault estimation and compensation via the design of two-level control and ASO method, the new compensating control design is computed using the estimate interconnection disturbance or/and fault. The tutorial application of the complex systems is illustrated through the examples of the interconnection disturbance together with fault acting on the nonlinear Three-Tank interconnected systems. A new approach to FTC of distributed/interconnected systems is proposed based on ASO and tow-level control strategies.

The ASO is employed to deal with the local fault estimation and compensation whereas the two-level control approach is used to handle the interconnection effecting on each subsystem, simultaneously. This combination gives a powerful way for the on-line fault estimation and compensation as an active FTC in the distributed systems. As discussed in Chapter 3, if the fault effect is small the fault compensator mechanisms described above may not be necessary or may introduce and unwanted but small disturbance (residual error). For this case it would be of interest to use a robust FDI scheme to detect the presence of a fault and isolate its location within a subsystem, prior to switching on the estimation and compensation scheme.

Chapter 8.
Conclusions

8.1. Conclusions and Summary

This thesis focuses on the well known topics of FD and FTC as well as a new concept in the augmented state observer (ASO), the use of joint sliding mode estimation and, linear parameter-varying (LPV) systems and some extensions of the work of Patton *et al* (2007) based on Autonomous Coordination and Supervision Scheme (ACSS). The ACSS is used in the problem of on-line fault estimation and compensation/accommodation, within the framework of active FTC applied to an uncertain and distributed system. The work presented has made some contribution within each of the topics outlined above. A review of the literature shows that the joint problem of fault estimation and fault compensation is actively studied as a topic in FTC and the recent research has formed a good basis for the work of this thesis. The faults are considered as significant uncertainties affecting the system control variables and their estimates are used in an adaptive control compensation mechanism [i.e. the faults can be considered as uncertainties affecting the control system].

The thesis deals with the active approach to FTC, based on on-line estimation and control adaption and not the use of control system reconfiguration. This problem to be addressed is outlined in Chapter 1 where the definitions and significance of faults, failures and the different types of faults have been presented briefly, along with the

industry drivers and practical requirements. Chapters 1 and 2 provide an introduction and overview of the traditional/modern model-based FD approaches and control reconfiguration approaches to FTC. The issues of increasing demand of reliable and safe control systems, FD and the need for FTC solutions as well as predictive maintenance, are discussed. The unknown input observer (UIO) approach to robust residual design for FDI is described in Chapter 2 as this is used in Chapter 7.

In Chapter 3, the new ASO scheme for FTC fault compensation is described. The concept of estimation of fault magnitudes is set up using an augmented state space structure with the fault variables comprising the additional states. The faults are estimated and compensated via an adaptive scheme in which one control signal component is a function of the estimated fault(s). The Chapter provides a thorough derivation of the stability conditions that apply to the ASO system, given that the fault(s) is/are bounded. From a practical point of view this new ASO method can be implemented well on real-time application systems using a simple design procedure.

A tutorial application study of adaptive estimation and compensation in an uncertain system uses the concept of friction force compensation in an inverted pendulum, as an FTC problem. It is shown that the friction compensation for a mechanical system can indeed be viewed as an FTC problem which does not require a model of the friction forces. The proposed approach is illustrated using a non-linear inverted pendulum with Stribeck friction, which avoids the use of any form of mathematical model of the friction force. Although, most studies consider the friction force to have an uncertain effect on the system, it is more constructive in the work of Chapter 3 and later in Chapter 4 to view the friction force as a specific fault. The proposed theory and approach has wide application to more complex problems in which actuator, sensor as well as multiplicative faults and unknown input signals can all be compensated together using the system description and proposed stability conditions.

Chapter 3 has also demonstrated, through a linear tutorial example with both unknown input disturbance and faults. It is shown that the effects of faults and unknown input uncertainties compete in the estimation/compensation mechanism. A discussion of this problem as a robustness issue is given using the example. The work described in Chapter 3 forms a basis for the material presented in Chapters 4 and 5, where the robustness issue is discussed further. It is expected that this work will stimulate further research into this method, its robustness and comparison with other approaches.

The sliding mode approach is investigated in Chapter 4 in which the main motivation is to replace the ASO/compensating adaptive controller scheme of Chapter 3 with the combination of the SMO of Edwards and Sprurgeon (1998) and SMC which is also considered to be a new contribution to the field of active and adaptive FTC. The contribution of this Chapter involves the adaptive term for the nonlinear unit vector gain which compensates for the fault effects. Once again, the friction compensation problem is used as an FTC example. The estimates of the friction force (via friction–effect factor) generated via the SMO theory are used directly in an adaptive SMC scheme. The results demonstrate the power of this on-line FTC approach, via the friction compensation example. It is important to note that the approaches used in Chapters 3 and 4 can be generalised to FTC problems in which the faults have different significance in terms of multi-faults and also in terms of actuator. Chapter 7 takes up some of these aspects as an extension to the work of this ASO approach via the study of distributed FTC problem.

Chapter 5 proposes a new alternative design of an active FTC for nonlinear systems that are difficult to linearise, e.g. robotic systems. The design of a polytopic state-space model is made using LPV theory and the polytope models are characterized via sets of LMIs. It is recognized that, in practice, the nonlinear systems can be reduced to LPV representations via the linearization along trajectories of the parameters. In other words, the idea in LPV is to obtain smooth semi–linear models that can vary or be scheduled using a parameter. A polytopic LPV estimator is synthesized for providing fault estimate which can be used in an FTC strategy to schedule some predefined state feedback gains (i.e. in a similar manner to the fault estimation and compensation concept described in Chapter 3 and 4). In the fault-free case, the controller gains are calculated using LMIs, whilst the resulting active FTC controller is a function of the fault effect factor estimate which can be implemented on-line from the polytopic LPV estimator mechanism. The new contribution in this work is the ccombined use of fault estimation and fault compensation for FTC using an LPV framework. The effectiveness of the proposed method is demonstrated through a nonlinear two-link robotic manipulator system with a fault in the torque inputs at each manipulator joint.

The common problem considered in Chapters 3, 4 and 5 is the design strategy for an active FTC for uncertain systems. In each of these Chapters the ideas and concepts have been illustrated using appropriate tutorial examples.

Chapter 6 focuses on a different application domain, namely that of the development of FTC schemes for distributed and inter-connected system. The work uses a global control strategy which uses constrained receding-horizon optimal control, under the coordination of the ACSS using the *two-level* control concept. The global controller is designed as an intelligent learning coordination from the knowledge base of the ACSS. The methods proposed in the field of learning control systems are used together with on-line constrained optimisation strategies. The system structure is set up in terms of global and local levels, the performance measures are additively separable, a concept coming from large-scale systems theory of Singh and Titli (1978). The *additively separable* property ensures suitable flexibility for control reconfiguration. It has been shown that for small faults the autonomous FTC system compensates for faults through an adaptive FTC mechanism. For larger faults in this distributed hierarchical structure, fault estimation is required to facilitate the reconfiguration task (i.e. either the use of hardware or analytical redundancy).

The strategies described in Chapters 3 and 6 are demonstrated in Chapter 7 on the two-level distributed system. The separate and combined designs of two-level control and ASO approaches are described, dealing with the larger faults via new reconfigurable control. The Patton *et al* (2007) work does not describe or consider methods for FDD as it is assumed in their work that the global control action provides a degree of fault compensation (fault accommodating control) for certain bounded faults. Hence, the new contributions in Chapter 7 focus on the dynamic behaviour of the overall inter-connected systems. Fault-tolerance is included using the integration of FDD and control algorithms at the local (subsystems) levels as well as the reconfiguration task at the global level.

The compensating control is computed using on-line estimation of the interconnection disturbance and local fault. The tutorial application is illustrated through the example of a non-linear Three-Tank interconnected system with the presence of the interconnection disturbances together with actuator faults. An active FTC scheme for distributed/interconnected systems is achieved based on the design of: (i) ASO approach, to handle local fault estimation and compensation, and (ii) whereas the two-level control approach is used to deal with interconnection disturbance affecting on each subsystem. This combination gives a powerful way for the on-line interconnection disturbance/fault estimation and compensation as an active FTC in the distributed systems.

References

Adams R J, Apkarian P, and Chretien J P (1996), Robust control approaches for a two-link flexible manipulator, *3rd International Conference on Dynamics and Control of Structures in Space*, pp. 101–116, Cranfield, U.K.

Ahmed-Zaid F, Ioannou P, Gousman K and Rooney R (1991), Accommodation of failure in the F-16 aircraft using adaptive control. *IEEE Control Systems Magazine*, vol. 11, no.1, pp. 73–78.

Alwi H (2008), *Fault Tolerant Sliding Mode Control Schemes with Aerospace Applications*, PhD thesis, The University of Leicester.

Alwi H and Edwards C (2005), Fault tolerant control of a civil aircraft using a sliding mode based scheme, *44th IEEE Conference on Decision and Control*, December 12-15, 2005, Seville, Spain.

Alwi H and Edwards C (2006), Fault tolerant control of a large civil aircraft using a sliding mode based scheme, *Proceedings of the IFAC Symposium SAFEPROCESS '06*, August 29th -September 1st , Beijing.

Alwi H and Edwards C (2007), Application of fault tolerant control using sliding modes with on-line control allocation on a large civil aircraft, *16th IEEE Conference on Control Applications*.

Alwi H and Edwards C (2009), A Fault Tolerant Sliding Mode Control Allocation Benchmark Evaluation, *7th IFAC Symposium on Fault Detection, Supervision and Safety of Technical Processes*, 30th June-3rd July, Barcelona, Spain.

Apkarian P, Gahinet P and Becker G (1995), Self-scheduled H_∞ control of linear parameter-varying systems: a design example. *Automatica*, vol. 31, pp. 1251-1261.

Armstrong B S R and Chen Q (2008), The Z-properties chart, *IEEE Control Systems Magazine*, vol. 28, no. 5, pp. 79-90.

Armstrong-Hélouvry B, Dupont P and Canudas de Wit C (1994), A survey of models, analysis tools, and compensation methods for the control of machines with friction, *Automatica*, vol. 30, no. 7, pp. 1083–1138.

Åström K J, Albertos P, Blanke M, Isidori A, Schaufelberger W and Sanz R (editors) (2001), *Control of Complex Systems*, Springer-Verlag, ISBN-13: 9781852333249

Åström K J and Wittenmark B (editors), (2 ed), (1994), *Adaptive Control*, Prentice Hall, ISBN 0201558661.

Balas G J (2002), Linear, parameter–varying control and its application to a turbo-fan engine. *International Journal of Robust and Nonlinear Control*, no.12, pp. 763–796.

Basseville M (1988), Detecting changes in signal and systems-a survey, *Automatica*, vol. 24, no. 3, pp. 309-326.

Beard R V, (1971), *Failure accommodation in linear system through self reorganization*, Ph.D. thesis, Department of Aeronautics and Astronautic, MIT, Cambridge, USA

Belcastro C M (2001), Application of fault detection, identification, and accommodation methods for improved aircraft safety, *American Control Conference*, pp. 2623–2624, June 25th -27th , Arlington, VA.

Bemporad A, Casavola A and Mosca E (1997), Nonlinear control of constrained linear systems via predictive reference management, *IEEE Trans. Auomatic Control*, vol. 42, no. 3, pp. 340-349.

Blanke M, Frei C, Kraus F, Patton R J and Staroswiecki M (2000), What is fault-tolerant control?, *4th IFAC symposium on fault detection, supervision and safety for technical process*, pp. 40–51.

Blanke M, Izadi-Zamanabadi R, Bogh R, and Lunau Z P (1997), Fault tolerant control systems-A holistic view, *Control Engineering Practice*, vol. 5, no. 5, pp. 693–702.

Blanke M, Kinnaert M, Lunze J and Staroswiecki M (editors) (2003), *Diagnosis and Fault-Tolerant Control*, Springer-Verlag. ISBN: 3540010564.

Blanke M, Kinnaert M, Lunze J and Staroswiecki M (editors) (2006), *Diagnosis and Fault-Tolerant Control*, (2nd ed.), Springer.

Blanke M, Staroswiecki M and Wu N E (2001), Concepts and methods in fault-tolerant control, *American control conference*, pp. 2606–2620.

Bodson B, Groszkiewicz M J (1997), Multivariable adaptive algorithms for reconfigurable flight control, *IEEE Transactions on Control Systems Technology*, vol. 5, no. 2, pp. 217–229.

Bogh S A, Zamanabadi I and Blanke M (1995), On board supervisor for the ϕrsted satellite attitude control system. *Artificial Intelligence and Knowledge Based System for Space*, 5th workshop, pp. 137-152, Noordwijk.

Bokor J and Balas G (2004), Detection filter design for LPV systems – a geometric

approach, *Automatica*, vol. 40, pp. 511-518.

Bokor J, Szabó, Z and Stikkel G (2002), Failure detection for quasi LPV systems, *Proc. of the American Control Conf.*, pp. 4421–4426

Bona B and Indri M (2005), Friction Compensation in Robotics: an Overview, *Proc. the joint 44th IEEE Conference on Decision and Control and the European Control Conference 2005*, pp. 4360-4367, 12-15 December , Seville, Spain.

Boskovic J D and Mehra R K (2000), Intelligent adaptive control of a tailless advanced fighter aircraft under wing damage, *Journal of Guidance, Control, and Dynamics*, vol. 23, no. 5, pp.876–884.

Boskovic J D, Bergstrom S E and Mehra R K (2005), Robust integrated flight control design under failures, damage, and state-dependent disturbances, *Journal of Guidance, Control, and Dynamics*, vol. 28, no.5, pp. 902–917.

Boskovic J D, Prasanth R and Mehra R K (2007), Retrofit fault-tolerant flight control design under control effectors damage, *Journal of Guidance, Control, and Dynamics*, vol. 30, no. 3, pp. 703–712.

Boskovic, J D and Mehra R K (2002), Multiple-model adaptive flight control scheme for accommodation of actuator failures, *Journal of Guidance, Control, and Dynamics*, vol. 25, no. 4, pp. 712–724.

Brennan R, Fletcher M. and Norrie D (2002), An Agent-Based Approach to Reconfiguration of Real-Time Distributed Control Systems, *IEEE Trans. on Robotics & Automation*, vol. 18, no. 4, pp. 444-451.

Buhmann M D (2003), *Radial Basis Functions: Theory and Implementations*, Cambridge University, ISBN 0-521-63338-9.

Buncefield Major Incident Investigation Board (2006), Initial Report to the Health and Safety Commission and Environment Agency of the investigation into the explosions and fires at the Buncefield storage and transfer depot, Hemel Hempstead, on 11 December 2005. Available: http://www.buncefieldinvestigation.gov.uk/reports/initialreport.pdf.

Burcham F W, Burken J, Maine T A and Bull J (1997), Emergency flight control using only engine thrust and lateral center-of-gravity offset: A first look, *Technical Memorandum NASA/TM-4789*, NASA.

Burcham F W, Fullertron C G and Maine T A (2004), Manual manipulation of engine throttles for emergency flight control, *Technical Report NASA/TM-2004-212045*, NASA.

Burcham F W, Maine T A, Burken J and Bull J (1998), Using engine thrust for emergency flight control: MD–11 and B–747 results. *Technical Memorandum NASA/TM–1998– 206552*, NASA.

Burcham F W, Maine T A, Kaneshinge J, and Bull J (1999), Simulator evaluation of simplified propulsion only emergency flight control system on transport aircraft, *Technical Report NASA/TM-1999-206578*, NASA.

Caccavale F and Villani L (2003), *Fault Diagnosis and Fault Tolerance for Mechatronic Systems: Recent Advances*, Springer.

Calado J M F, Korbicz J, Patan K, Patton R J and Costa J M G (2001), Soft Computing Approaches to Fault Diagnosis for Dynamic Systems, Invited Special Issue Paper, *European Journal of Control*, vol. 7, no. 2-3, pp. 248-286.

Camacho E F and Bordons C, *Model Predictive Control* (2nd Ed) (2004), Springer-Verlag.

Caraces F, Becerra V M, Kambhampati C and Warwick K (editors) (2003), *Strategy for feedback linearisation: A dynamic Neural Network Approach*, Springer-Verlage, London, ISDN 1852335017.

Casavola A, Famularo D and Franz`e G (2005a), Norm-bounded Robust MPC strategies for constrained control of nonlinear systems, *IEE Proceedings Control Theory Appl.*, vol. 152, no. 3, pp. 266-272.

Casavola A, Famularo D, Franz`e G and Sorbara M (2005b), Supervision of networked dynamical systems subject to coordination constraints, *Proceedings of the NeCST 1st Workshop on Networked Control Systems*, Corsica.

Casavola A, Famularo D, Franze G and Patton R J (2008), A Fault Detection Filter Design Method for a class of Linear Time-Varying Systems, *16th Mediterranean Conference on Control and Automation*, 25-27 June, Corsica.

Casavola A, Famularo D, Franze G and Sorbara M (2007), A fault detection filter design method for linear parameter-varying systems, *Proc. J. IMechE Part I*, pp. 865-874.

Chandler P (1984), Self-repairing flight control system reliability & maintainability program executive overview, *Proc. Nat. Aero. & Electr. Conf.*, Dayton, pp. 586-590.

Chen J and Patton R J (1996), Optimal filtering and robust fault-diagnosis of stochastic systems with unknown disturbances, *IEE Proc.-D: CTA*, vol. 143, no. 1, pp. 31-36.

Chen J and Patton R J (editors) (1999), *Robust Model Based Fault Diagnosis for Dynamic Systems*, Kluwer Academic Publishers ISBN 0-7923-841-3.

Chen J and Patton R J (2001), Fault-Tolerant Control systems Design using the Linear Matrix Inequality Method, *ECC'01*, , Porto, September 4-7.

Chen J, Patton R J and Chen Z (1999), Active fault-tolerant flight control systems design using the linear matrix inequality method, *Trans. Inst MC*, vol. 21, no. 2/3, pp. 77-84.

Chen J, Patton R J and Liu G P, (1996), Optimal residual design for fault diagnosis using multi-objective optimisation and genetic algorithms, *Int. J. Sys. Sci*., vol. 27, no. 6, pp. 567-576.

Chisti A (1986), *Dateline Bhopal Concept Publishing Company*, New Delhi, India.

Chow E Y and Willsky A (1984), Analytical Redundancy and the Design of Robust Failure Detection Systems, *IEEE Trans. Automat. Contr*., vol. 29, no. 7, pp. 603-614.

Chow E Y and Willsky A S (1980), Issues in the development of a general algolitm for reliable failure detection, *19th Conf. on Decision & Control*, Albuquerque, NM.

Cieslak J, Henry D and Zolghadri A (2009), Design of Fault Tolerant Control Systems: a Flight Simulator Experiment, *7th IFAC Symposium on Fault Detection, Supervision and Safety of Technical Processes*, June 30th - July 3rd, 2009, Barcelona, Spain.

Clark R N (1978), Instrument Fault Detection, *IEEE Trans. Aero & Electron. Syst*. AES, vol. 14, pp. 456-465.

Clark R N, Fosth D C and Walton V M (1975), Detecting instrument malfunctions in control systems, *IEEE Trans. Aero & Electron. Syst*. AES, vol. 114, pp. 465-473.

DeCarlo R A, Zak S H, and Matthew G P (1988), Variable structure control of nonlinear multivariable systems: a tutorial, *Proceedings of IEEE*, vol. 76, pp. 212-232.

Delgado A, Kambhampati C and Warwick K (1996), Input/output linearization using dynamic recurrent neural networks, *Mathematics and Computers in Simulation*, vol. 41, no. 5-6, pp. 451- 460.

Demetriou M A and Polycarpou M M (1998), Incipient fault diagnosis of dynamical systems using online approximators, *IEEE Transactions of Automatic Control*, vol. 43, pp.1612-1617.

Derkert J C, Desai M N, Deyst J J and Willsky A S (1977), F-8 DFBW sensor failure identification using analytic redundancy, *IEEE Trans. Automat. Contr*. AC, vol. 22, no. 5, pp. 795-803.

Diao Y and Passino K M (2001), Stable fault-tolerant adaptive fuzzy/neural control for turbine engine, *IEEE Transactions on Control Systems Technology*, vol. 9, no. 3, pp. 494–509.

Ding (editor) (2007), *Model-Based Fault Diagnosis Techniques*: Design Schemes, Algorithms, and Tools, Springer, ISBN: 3540763031

Dorling C M and Zinober A S I (1986), Two approaches to hyperplane design of multivariable structure control systems, *Int. J. Control*, vo. 44, pp. 65-82.

Dorling C M and Zinober A S I (1988), Robust hyperplane design in multivariable variable structure control systems, *International Journal of Control*, vol. 48, pp. 2043 - 2054.

Draženović, B (1969), The invariance conditions in variable structure systems, *Automatica*, vol. 5, pp. 287-295.

Edwards C (2004), A practical method for the design of sliding mode controllers using linear matrix inequalities, *Automatica*, vol. 33, pp. 1761–1769.

Edwards C and S Spurgeon K (editors) (1998), *Sliding Mode Control: Theory and Applications*, Taylor and Francis, London, UK.

Edwards C and Spurgeon S K and Patton R J (2000), Sliding mode observers for fault detection and isolation, *Automatica*, vol. 36, pp.541-553.

El-Ghezawi O M E, Zinober A S I and Billings S A (1983), Analysis and design of variable structure systems using a geometric approach, *Int. J. Cont*., pp. 657-671.

Eterno J S, Weiss J L, Looze D P and Willsky A S (1985), Design issues for fault tolerant-restructurable aircraft control, *24th IEEE conference on decision and control*, pp. 900-905.

Ferrari, R M G, Parisini, T, and Polycarpou, MM (2007), Distributed fault diagnosis with overlapping decompositions and consensus filters, *American Control Conference*, pp. 693 – 698.

Frank P M (1990), Fault diagnosis in dynamic systems using analytical and knowledge-based redundancy-a survey and some new results, *Automatica*, vol, 26, no. 3, pp. 459 – 474.

Frank P M and Ding X (1997), Survey of Robust residual generation and evaluation methods in observer-based fault detection systems, *J. of Process Control*, vol. 7, no. 2, pp. 403-424.

Franklin G F, Powell J D, and Emami-Naeini A (editors) (2002), *Feedback Control of Dynamic Systems*, Prentice Hall International Edition, (4th Edit).

Gahinet P and Apkarian P (1994), A linear matrix inequality approach to H_∞ control. *Int. J. Robust and Nonlinear Control*, vol. 4, pp. 421-448.

Ganguli S A, Marcos A, and Balas G J (2002), Reconfigurable LPV control design for Boeing 747-100/200 longitudinal axis, *American Control Conference*, Anchorage, Alaska, May 8-10, pp. 3612–3617.

Gao Z and Antsaklis, P J (1991), Stability of the pseudo-inverse method for reconfigurable control systems, *International Journal of Control*, vol. 53, no. 3, 717–729.

Gao Z and P J Antsaklis (1992), Reconfigurable control systems design via perfect model following, *International Journal of Control*, vol. 56, no. 4, pp. 783–798.

Garces F, Becerra V M, Kambhampati C and Warwick K (editors) (2003), *Strategies for Feedback Linearisation, A Dynamic Neural Network Approach*, Springer-Verlag, ISBN 1852335017.

Gero D, (2006), *Aviation disasters: the world's major civil airliner crashes since 1950*, Sparkford: Patrick Stephens.

Gertler J (1991), Analytical redundancy methods in failure detection and isolation. *IFAC/IMACS Symposium, Safeprocess'91*, Baden-Baden, vol. 1, pp. 9-21.

Gertler J (editor) (1998), *Fault Detection and Diagnosis in Engineering Systems*. Marcel Dekker, New York.

Gertler J, Janos J (1988), Survey of Model-based Failure Detection and Isolation in Complex Plants, *IEEE Control Systems Magazine*, vol. 8, no.6, pp.3-11.

Goodwin G C, Haimovich H, Quevedo D E and Welsh J S (2004), A moving horizon approach to networked control system design, Special Issue: *IEEE Trans. on Aut. Control on*: *Networked Control Systems*, vol. 49, no. 9, pp. 1427-1445.

Grimble M J (editor) (2001), *Industrial Control Systems design*, John Wiley, Chichester, ISBN 0 471492256.

Hassen S, Crusca F and Abachi H (2000), Modelling system for control studies – An overview, *ISCA 15th International conference on Computer and their Application*, March 11-13, 1992, Orlando, Florida, USA.

Haykin S (editor) (1994), *Neural Networks: A Comprehensive Foundation*, Macmillan, ISBN 0-02-352761-7.

Henry D, (2008), Fault Diagnosis of the Microscope Satellite Thrusters using Hinf/H- Filters, *AIAA Journal of Guidance, Control, and Dynamics*, vol. 31, no. 3, pp. 699-711.

Henry D, Falcoz, A and Zolghadri, A, (2009), Structured Hinfinity / H LPV Filters for Fault Diagnosis: Some New Results (I), *7th IFAC Symposium on Fault Detection, Supervision and Safety of Technical Processes*, June 30 - July 3, 2009, Barcelona, Spain.

Henry D, Zolghadri A, (2004), Robust fault diagnosis in uncertain Linear Parameter-Varying systems, *Proceedings of SMC'2004*, The Hague, NL.

Hermans F J and Zarrop M B (1996), Sliding mode observers for robust sensor monitoring. *13th IFAC world congress*, San Fran Cisco, pp. 211–216.

Hess R A and Wells S R (2003), Sliding mode control applied to reconfigurable flight control design, *Journal of Guidance, Control and Dynamics*, vol. 26, pp. 452–462.

Himmelblau D M (1978). *Fault Detection and Diagnosis in Chemical and Petrochemical Process*, Elsevier, Amsterdam.

Huang C Y and Stengel R F (1990), Restructurable control using proportional integral implicit model following, *Journal of Guidance, Control, and Dynamics*, vol. 13, no. 2, pp. 303–309.

Huzmezan M, and Maciejowski J M (1998), Reconfiguration and scheduling in flight using quasi-LPV high-fidelity models and MBPC control, *In Proceedings of the American control conference*, pp. 3649–3653.

Ioannou P, Gousman K and Rooney R (1989), Surface Failure Detection and Evaluation of Control Law for Reconfiguration of Flight Control System, *Proc. AIAA Fuidance & Navigation Control Conf*, pp. 733-740, Boston, USA.

Isermann R (1994). Integration of Fault Detection and Diagnosis Methods. R*eprints of IFAC Sympo. on Fault Detection, Supervision and Safety for Technical Processes*, Espoo, Finland, no. 2, pp. 575-590.

Isermann R (editor) (2006), *Fault-diagnosis systems: An introduction from fault detection to fault tolerance*. Berlin, Germany: Springer.

Isermann R and Ballé P (1997), Trends in the application of model-based fault detection and diagnosis of technical processes. *Control Engineering Practice*, vol. 5, no. 5, pp. 709-719.

Isermann R (1984), Process Fault Detection Based on Modeling and Estimation Methods, *Automatica*, no. 20, pp. 387-404.

Issury I and Henry D, (2009), Multiple and Simultaneous Fault Isolation with Minimal Fault Indicating Signals: A Case Study, *7th IFAC Symposium on Fault Detection, Supervision and Safety of Technical Processes*, June 30 - July 3, 2009, Barcelona, Spain.

Jacobson C A and Nett C N (1991), An integrated approach to controls and dianostics using the four parameter control, *IEEE Contr. Syst. Magazine*, vol. 11, no. 6, pp. 22-29.

Jean-Jacques E. Slotine and Weiping Li (editors) (1991), *Applied Nonlinear Control*, Prentice Hall, Upper Saddle River, NJ.

Jiang B and Straroswiecki (2002), Adaptive Observer Design for Robust Fault Estimation, *Int. J. of System Science*, vol. 33, no. 9, pp. 767-775.

Jiang B, Staroswiecki M and Cocquempot V (2004), Fault estimation in nonlinear uncertain systems using robust sliding–mode observers, *IEE Proceedings: Control Theory & Applications*, vol. 151, no.29-37.

Jiang J (1994), Design of reconfigurable control systems using eigenstructure assignment, *International Journal of Control*, vol. 59, no. 2, pp. 395–410.

Jones C N (2005), *Reconfigurable flight control*: First year report. Technical report, Cambridge University Engineering Department.

Joosten D A, and Maciejowski J M (2009), Fault Tolerant Control of a Civil Aircraft Using MPC, *7th IFAC Symposium on Fault Detection, Supervision and Safety of Technical Processes*.

Kale M M and Chipperfield, A J (2005), Stabilized MPC formulations for robust reconfigurable flight control, *Control Engineering Practic*e, vol. 13, no. 6, pp.771–788.

Kambhampati C and Rajasekharan S (2003), Multiple manipulator control from a human motor-control perspective, *IEEE Trans. on Robotics & Automation*, vol. 19, no. 3, pp. 433-442.

Kambhampati C, Delgado A and Mason J D (1997), Stable receding horizon control based on recurrent networks, *IEE Proceedings CTA*, vol. 144, no. 3, pp. 249-254.

Kambhampati C, Mason J D and Warwick K (2000), A stable one-step-ahead predictive control of nonlinear systems, *Automatica*, vol. 36, no. 4, pp. 485-495.

Kambhampati C, Perkgoz C, Patton R J, and Ahamed W (2007), An interaction predictive approach to fault-tolerant control in network control systems, *Proc. IMechE*, Part I: J. Systems and Control Engineering, vol. 221, pp. 885-894.

Katsuhiko O, (1997), *Modern Control Engineering* (3rd ed.). Upper Saddle River, NJ: Prentice-Hall, ISBN 0-13-227307-1

Keerthi S S and Gilbert E G (1988), Optimal Infinite-horizon feedback laws for general class of constrained discrete-time-systems-stability and moving horizon approximations, *Journal of Optimization Theory and Application*, vol. 57, no. 2, pp. 265-293.

Kim J (1997), *Project Report: LMI optimization of Two-link Manipulator using Polytopic model and State feedback*, Department of Aerospace Engineering, Inha University, South Korea.

Kim K S, Lee K J and Kim Y, (2003), Reconfigurable flight control system design using direct adaptive method, *Journal of Guidance, Control, and Dynamics*, vol. 26, no. 4, pp. 543–550.

Klinkhieo S, Patton R J and Kambhampati C (2008), Robust FDI for FTC Coordination in a Distributed Network System, *18th IFAC World Congress*, July 6-11, Seoul.

Leith D J and Leithead W E (2000), Survey of gain–scheduling analysis and design. *International Journal of Control*, vol. 73, pp. 1001–1025.

Leveson N G (2002), A New Approach To System Safety Engineering: Back to the Future, Aeronautics and Astronautics Massachusetts Institute of Technology.

Liu G P and Patton R J (1996), Robust control design using eigenstructure assignment and multi-objective optimization, *Int. J. Sys. Sci*., vol. 27, no. 9, pp.871-879.

Lombaerts T J J, Chu Q P, Mulder J A, and Joosten D A (2009), Flight Control Reconfiguration Based on a Modular Approach, *7th IFAC Symposium on Fault Detection, Supervision and Safety of Technical Processes*.

Maciejowski J M and Jones C N (2003), MPC fault-tolerant control case study: flight 1862, *In Proceedings of the IFAC Symposium SAFEPROCESS '03*, Washington.

Mahmoud M, Jiang J and Zhang Y (editors) (2003), *Active Fault Tolerant Control Systems Stochastic Analysis and Synthesis*, Springer.

Mahmoud M.S (2004), New results on linear parameter-varying time-delay systems. *Journal of the Franklin Institute*, vol. 341, pp. 675-703.

Marcos A, Ganguli S, and Balas G J (2005), An application of H_α fault detection and isolation to a transport aircraft. *Control Engineering Practice*, vol. 13, pp. 105–

119.

Maturana F P, Tichy P, Slechta P, Staron R J, Discenzo F M and Hall K (2003), A Highly distributed intelligent multi-agent architecture for industrial automation, Multi-agent systems and applications III, *Proceedings Lecture Notes in Artificial Intelligence 2691*, pp 522-532.

Maybeck P S (1999), Multiple model adaptive algorithms for detecting and compensating sensor and actuator/surface failures in aircraft flight control systems, *International Journal of Robust and Nonlinear Control*, vol. 9, no. 14, pp. 1051–1070.

Maybeck P S and Stevens R D (1991), Reconfigurable flight control via multiple model adaptive control methods, *IEEE Transactions on Aerospace and Electronic Systems*, vol. 27, no. 3, pp. 470–479.

Mayne D Q and Michalska H (1990), Receding Horizon Control of Nonlinear-Systems, *IEEE Trans. on Automatic Control*, vol. 35, no. 7, pp. 814-824.

MacFarlance A G J and Karcanias N, (1976), Poles and Zeros of linear Multivariable Systems: A survey of the Algebraic, Geometric and Complex Variable Theory, *Int. J. Control*, vol. 24, pp. 33-74.

McKerrow P J (1991), *Introduction to robotics*, Addison-Wesley Publishing Company, Inc.

Mesarovic M D, Macko D and Takahara Y (editor) (1970), Theory of Hierarchical Multilevel Systems, *Academic Press*, New-York.

Mohammadpour, J and K M Grigoriadis (2006), Delay-dependent H_∞ filtering for a class of time-delay LPV systems, *Proc of the 2006 American Control Conference*, Minnesota, USA, pp. 1523-1528.

Monaco J, Ward D, Barron R and Bird R (1997), Implementation and flight test assessment of an adaptive, reconfigurable flight control system, *In Proceedings of 1997 AIAA guidance, navigation, and control conference*, pp. 1443–1454.

Montoya R J, Howell W E, Bundick W T, Ostroff A J, Hueschen R M and Belcastro C M (1983), Restructurable controls, *Tech. Rep. NASA CP-2277* and *Proceedings of a workshop*, NASA Langley Research Center, Hampton, VA, USA, pp. 21–22.

Morari M, and Zafiriou E (editors) (1989), *Robust Process Control*, Prentice Hall: Hemel Hemstead.

Napolitano M R, Neppach C, Casdorph V and Naylor S (1995), Neural network-based scheme for sensor failure detection, identification, and accommodation, *Journal*

of Guidance, Control, and Dynamics, vol. 18, no.6, pp.1280–1286.

Nelles, (editor) (2001), *Nonlinear system identification: From classical approaches to neural networks and fuzzy models*, Springer, New York.

Niemann H and Stoustrup J (1997), Integration of control and fault detection: Nominal and robust design, *In Proceedings of IFAC symposium on fault detection, supervision and safety for technical processes*, pp. 341–346.

Noura H, Theilliol D and Sauter D (2000), Actuator fault-tolerant control design: Demonstration on a three-tank-system, *International Journal of Systems Science*, vol. 31, no. 9, pp. 1143–1155.

Olsson H, Aström K J, Canudas de Wit C,Gäfvert M and Lischinsky M (1998), Friction models and friction compensation, *European Journal of Control*, vol. 4, pp.176-195.

Pachter M, Chandler P R and Mears, M (1995), Reconfigurable tracking control with saturation, *Journal of Guidance, Control, and Dynamics*, vol. 18, no. 5, pp. 1016–1022.

Packard A and Kantner M (1992), Gain scheduling the LPV way, *Proc. of the Conf. on Decision and Control*, pp. 1997-2001.

Patek S N (2001), Spiny lobsters stick and slip to make sound, *Nature 411*: pp. 153–154.

Patton R J (1994), Robust model-based fault diagnosis: The state of the art, Plenary paper, Proc. of the IFAC Symposium on Fault Detection, Supervision and Safety for Technical Processes: *SAFEPROCESS'94*, pp. 1-24, Finland.

Patton R J (1997), Fault-tolerant control: The 1997 situation (survey), *IFAC SAFEPROCESS'97*, Hull, UK, August 26-28, vol. 2, pp. 1033-1055.

Patton R J and Chen (1997), Observer-based fault detection and isolation: Robust and applications, *Contr. Eng. Practice*, vol. 5, no. 5, pp. 671-682.

Patton R J and Chen J (1991a), A review of parity space approaches to fault diagnosis, *Proceedings of IFAC/IMACS Symposium SAFEPROCESS'91*, Baden-Baden, pp. 239-255.

Patton R J and Chen J (1991b), A parity space approach to robust fault diagnosis using eigenstructure assignment, *Proc. First European Control Conf.* Grenoble, France, pp. 1419-1424.

Patton R J and Chen J (1997), Observer-based fault detection and isolation: robustness and applications, *IFAC Journal: Control Engineering Practice*, vol. 5, no. 5, pp. 671-682.

Patton R J and Chen J, (2000), On eigenstructure assignment for robust fault diagnosis, *Int. J. of Robust & Nonlinear Control*, Special Issue on Fault Detection and Isolation, vol. 10, no. 9, pp. 1193 – 1208.

Patton R J, Chen J and Benkhedda H A (2000b), The study on neuro-fuzzy systems for fault diagnosis, *International Journal of Systems Science*, no. 31, no. 11, pp: 1441-1448.

Patton R J, Frank P M and Clark R N (editors) (2000a), *Issue of Fault Diagnosis for Dynamic Systems*, Springer-Verlag, London, ISBN 3-540-19968-3.

Patton R J, Frank P M and Clark R N. (editors) (1989). *Fault diagnosis in dynamic System*, Theory and Application, Control Engineering Series (New York: Prentice Hall).

Patton R J, Kambhampati C, Casavola A and Franze G (2006), Fault-tolerance as a key Requirement for the Control of Modern Systems, Invited Plenary Paper, 6th IFAC Symposium on Fault Detection, Supervision and Safety of Technical Processes, *SAFEPROCESS 2006*, pp 26-35, Beijing, P.R. China.

Patton R J, Kambhampati C, Casavola A, Zhang P, Ding S and Sauter D (2007), A Generic Strategy for Fault-Tolerance in Control Systems Distributed over a Network, *Invited Special Issue Paper, European Journal of Control*, vol. 13, pp. 280-296.

Patton R J, Lopez-Toribio C J and Uppal F J (1999), Artificial Intelligence Approaches to Fault Diagnosis, *J. Applied Mathematics and Computer Science*, vol. 9, no. 3, pp. 471-518.

Patton R J, Putra D and Klinkhieo S, (2008b), Friction Compensation as a Fault-Tolerant Control Problem, Semi-Plenary Paper, *23rd IAR Workshop on Advanced Control and Diagnosis*, November 27-28, Coventry University, UK.

Patton R J, Uppal F J, Simani S and Polle B (2008a), Reliable fault diagnosis scheme for a spacecraft attitude control system, *IMechE Proc*. Part O, vol. 222, no. 2, pp. 139-152.

Patton, R. J. Uppal, S. Simani, and B. Polle (2009), Robust FDI applied to thruster faults of a satellite system, *Control Engineering Practice, ACA'07 – 17th IFAC Symposium on Automatic Control in Aerospace Special Issue*.

Peng Y, Youssouf A, Arte Ph and Kinnaert M (1997), A complete procedure for residual generation and evaluation with application to heat exchanger, *IEEE transaction on Control System and Technology*, vol. 5, no. 6, pp. 542-555.

Polycarpou M M, Helmicki A J (1995), Automated Fault Detection and Accommodation: A Learning Systems Approach, *IEEE Tr. Sys. Man & Cyb*, vol. 25, no. 11, pp 1447-1458.

Polycarpou, M M and Vemuri A T (1995), Learning methodology for failure detection and accommodation, IEEE Control Systems Magazine, vol. 15, no. 3, pp. 16–24.

Putra D, Moreau L and Nijmeijer H (2004), Observer-Based Compensation of Discontinuous Friction, *Proceedings of the 43rd IEEE Conference on Decision and Control*, the Bahamas. pp. 4940-4945

Rauch H E (1995), Autonomous Control Reconfiguration, *IEEE Con. Sys. Mag*, vol. 15, no. 6, pp. 37-48.

Rodrigues M, Theilliol D, Aberkane S and Sauter D (2007), Fault tolerant control design for polytopic LPV systems. *International Journal of Applied Mathematics and Computer Science*, vol. 17, pp. 27–37.

Rodrigues M, Theilliol D, and Sauter D (2005), Design of an Active Fault-Tolerant control Polytopic Unknown Input Observer described by a Multi-model Representation, *CDC and ECC' 05*, pp. 3815–3820, Spain.

Rugh W (1991), Analytical framework for gain scheduling, *IEEE Cont. Syst. Mag*, vol. 11, no. 1, pp. 79–84.

Rugh W J and Shamma J S (2000), Research on gain scheduling, *Automatica*, vol. 36, pp. 1401–1425.

Ryan E P and Corless M (1984), Ultimate boundedness and asymptotic stability of a class of uncertain dynamical systems via continuous and discontinuous control, *IMA Journal of Mathematical Control and Information*, vol. 1, pp. 223–242.

Sadati N and Moment A R, (2005), Nonlinear Optimal Control of Two-Level Large-Scale Systems; Part I - Interaction Prediction Principle, *Industrial Electronics and Control Applications*, ICIECA 2005.

Sauter D, Boukhobza T and Hamelin F (2005), Decentralized and Autonomous Design for FDI/FTC of Networked Control Systems, *NeCST Workshop*, Ajaccio.

Shamma J and Athans M (1992), Gain scheduling: potential hazards and possible remedies, *IEEE Cont. Syst. Mag*, vol. 12, no. 3, pp. 101–107.

Sharif M A and Grosvenor R I (1998), Process Plant Condition Monitoring and Fault Diagnosis, *Proceedings of the Institute of Mechanical Engineers*, vol. 212, part E, pp. 13-30

Shin J and Belcastro C M (2006), Performance analysis on fault tolerant control system.

IEEE Transactions on Control Systems Technology, vol.14, pp. 920–925.

Simani S, Fantuzzi C and Patton R J (editors) (2003), *Model-Based Fault Diagnosis in Dynamic Systems Using Identification Techniques, Advances in Industrial Control*, Springer.

Singh M G and Titli A (1978), *Systems Decomposition, Optimisation and Control*, Pergamon Press, Oxford, ISBN 0-08-022150-5.

Singh M G, Hassan M F, Chen Y L, Li D S and Pan Q R (1983), New approach to failure detection in large-scale systems, *IEE Proceedings, Control Theory & Applications*, vol. 130D, no. 5, pp. 243-249.

Slotine J E and Li W (editors) (1991), *Applied nonlinear control*, Prentice Hall.

Smaili M H and Mulder J A (2000), Flight data reconstruction and simulation of the 1992 Amsterdam Bijlmermeer airplane accident, *AIAA Modeling and Simulation Technologies Conferenc*.

Spurgeon S K (1991), Choice of discontinuous control components for robust sliding mode performance, *Int. J. Control*, vol. 53, pp. 163-179.

Spurgeon S K and Davies R (1993), A nonlinear control strategy for robust sliding mode performance in the presence of unmatched uncertainty, *Int. J. Control*, vol. 57, pp. 1107-1123.

Sreedhar R, Fernandez B and Masada G (1993), Robust fault detection in nonlinear systems using sliding mode observers, *IEEE Conference on Control Applications*, pp. 715-721.

Staroswiecki M and Gehin A L (2000), From control to supervision, *IFAC Safeprocess*, Budapest, pp. 312-323.

Staroswiecki, M and Gehin, A L (2001), From control to supervision. *Annual Reviews in Control*, vol. 25, pp. 1–11.

Steele, JM (editor) (2004), *The Cauchy–Schwarz Master Class*, Cambridge University Press, ISBN 052154677X.

Steinberg M (2005), Historical overview of research in reconfigurable flight control. Proceedings of IMechE, Part G: *Journal of Aerospace Engineering*, no. 219, pp. 263–275.

Stoustrup J, Grimble M J and Neimann H H (1997), Design of integrated systems for control and detection of actuator/sensor faults, *Sensor Review*, no. 17, pp. 157-168.

Sun M, Jia Y, Du J and Yuan S (2007), Delay-dependent H∞ control for LPV systems with time delays, *46th IEEE Conference on Decision and Control*, New Orleans, USA, pp. 2089-2093.

Takahara Y, (1965), *A multi-level structure for a class of dynamical optimization problems*, MS Thesis, Case Western Reserve University, Cleveland, USA.

Tan C P and Edwards C (2002), Sliding mode observers for detection and reconstruction of sensor faults. *Automatica*, vol. 38, pp. 1815–1821.

Tan C P and Edwards C (2003), Sliding mode observers for robust detection and reconstruction of actuator and sensor faults. *International Journal of Robust and Nonlinear Control*, vol. 13, pp. 443–463.

Tan C P and Edwards C (2006), Fault reconstruction/estimation using a sliding mode observer, *Proceeding of the 45th IEEE Conference on Decision & Control*, December 13-15, San Diego, USA.

Tanaka S and Müller P C (1993), Fault-detection in linear discrete dynamic systems by reduced order generalized-likelihood –ratio method, *Int. J. System and Science*, vol. 24, no. 4, pp. 721-732.

Tao G, Chen S and Joshi S M (2002), An adaptive actuator failure compensation controller using output feedback, *IEEE Transactions on Automatic Control*, vol. 47, no. 3, pp. 506–511.

Tao G, Chen S, Joshi S M and Tang X (editors) (2004), *Adaptive control of systems with actuator failures*, Berlin, Springer.

Tao G, Joshi S M and Ma X (2001), Adaptive state feedback and tracking control of systems with actuator failures, *IEEE Transactions on Automatic Control*, vol. 46, no. 1, pp. 78–95.

Theilliol D, Ponsart J and Noura H (2000), Sensor fault diagnosis and accommodation based on analytical redundancy: application to a three-tank system, *IFAC Safeprocess*, Budapest, pp. 542-547.

Theilliol, D, Noura H and Ponsart, J C (2002), Fault diagnosis and accommodation of a three-tank system based on analytical redundancy, *ISA Transactions*, vol. 41, no. (3), pp. 365–382.

Uppal F J and Patton R J (2005), Neuro-fuzzy uncertainty de-coupling: A multiple-model paradigm for fault detection and isolation, Special Issue on Condition Monitoring in Process Control, *J. of Adaptive Control and Signal Processing*, vol. 19, no. 4, pp. 281-304.

Utkin V I (1971), Equation of slipping regime in discontinuous systems: I, *Autom.*

Remote Control, vol. 32, pp. 1897-1907

Utkin V I (1977), Variable structure system with sliding modes: A survey, *IEEE Trans. AC*, no. 22, pp. 212-222.

Utkin V I (editor) (1992), *Sliding Modes in Control Optimization*, Springer-Verlag, Berlin.

Utkin V I and Young K D (1978), Methods for constructing discontinuity planes in multidimensional variable structure systems, *Automation and Remote Control*, vol. 39, pp. 1466 –1470.

Veillette R J (1995), Reliable linear-quadratic state-feedback control, *Automatica*, vol. 31, no. 1, pp. 137–143.

Veillette R J, Medanic J V and Perkins W R (1992), Design of reliable control systems, *IEEE Transactions on Automatic Control*, vol. 37, no.3, pp. 290–300.

Vetter T K, Wells S R, and Hess R A (2003), Designing for damage–robust flight control design using sliding mode techniques. *Proceedings of the Institution of Mechanical Engineers, Part G: Journal of Aerospace Engineering*, no. 217:pp. 245–261.

Walcott B L and Zak S H (1987), State observation of nonlinear uncertain dynamical systems, *IEEE Transaction on Automatic Control*, vol. 32, pp.166–170.

Walcott B L and Zak S H (1988), Combined observer–controller synthesis for uncertain dynamical systems with applications, *IEEE Transactions on Systems, Man and Cybernetics*, vol. 18, pp. 88–104.

Wang H, and Daley S (1996), Actuator fault diagnosis: an adaptive observer-based technique, *IEEE Transactions of Automatic Control*, vol. 41, pp. 1073-1078.

Wang S H, Davison E J, and Dorato P, (1975), Observing the states of systems with unmeasurable disturbance, IEEE *Trans. Automat. Contr*. AC-20, pp. 716-717.

Wang, H, Huang Z J and Daley S (1997), On the use of adaptive updating rules for actuator and sensor fault diagnosis, *Automatica*, vol. 33, pp. 217-225.

Watanabe K and Himmelblau D M (1982), Instrument fault detection in systems with uncertainies, *Int. J. Syst. Sci*., vol. 13, no. 2. pp. 137-158.

Weng Z, Patton R J and Cui P (2008), Integrated design of robust controller and fault estimator for linear parameter varying systems, *Proc. 17th World Congress of IFAC*, Seoul, Korea, pp. 4535-4539.

Weng Z, Patton R J and Cui P (2007), Active fault-tolerant control of a double inverted pendulum, *J. of Systems and Control Engineering*, vol. 221, no. I6, pp. 895-904.

Wikipidia, Adaptive Control, The free encyclopedia, http://en.wikipedia.org/wiki/Adaptive control.

Willsky A S (1976), A survey of design methods for failure detection in dynamic systems, *Automatica*, vol. 12, pp. 601-611.

Willsky A S and Jones H L (1974), A generalized likelihood approach to state estimation in the linear systems subjected to abrupt changes, *Proc. IEEE Conference on Control and Decision*, Arizona.

Wise K A, Brinker J S, Calise A J, Enns D F, Elgersma M R and Voulgaris P (1999), Direct adaptive reconfigurable flight control for a tailless advanced fighter aircraft, *International Journal of Robust and Nonlinear Control*, vol. 9, no. 14, pp.999–1012.

Wu F and Grigoriadis K M (2001), LPV systems with parameter-varying time delays: analysis and control. *Automatica*, vol. 37, pp. 221-229.

Wu F (2001), A generalized LPV system analysis and control synthesis framework. *International Journal Control*, no. 74, pp. 745–759.

Wu N E (1992), Failure sensitizing reconfigurable control design, *Proc. of the 31st IEEE Conference on Control & Decision*, Tucson, AZ, pp. 44-49.

Wu N E, Zhang Y and Zhou K (2000), Detection, estimation, and accommodation of loss of control effectiveness, *International Journal of Adaptive Control and Signal Processing*, vol. 14, pp. 775–95.

Yan G X and Edwards C (2008), Robust decentralized actuator fault detection and estimation for large-scale systems using a sliding mode observer, *International Journal of Control*, vol. 81, no. 4, pp. 591–606.

Yan G X, Edwards C and Spurgeon S K (2004), Decentralised robust sliding mode control for a class of nonlinear interconnected systems by static output feedback, *Automatica*, vol. 40, pp. 613-620.

Yan G X, Spurgeon S K and Edwards C (2003), Decentralized Output Feedback Sliding Mode Control f Nonlinear Large-Scale Systems with Uncertainties, *J. of Optimization theory and applications*, vol. 119, no. 3, pp. 597-614.

Yan G X, Spurgeon S K and Edwards C (2006), Decentralised sliding mode control for nonminimum phase interconnected systems based on a reduced-order compensator, *Automatica*, vol. 42, pp. 1821-1828.

Yang G H, Wang J L and Soh Y C (2001), Reliable H_∞ controller design for linear systems, *Automatica*, vol. 37, no. 5, pp. 717–725.

Yang H and Saif M (1995), Fault detection in a class of nonlinear systems via adaptive

sliding observer, *Proceedings of the IEEE International Conference on Systems, Man and Cybernetics*, pp. 2199–2204.

Yang Z and Stoustrup J (2000), Robust reconfigurable control for parametric and additive faults with FDI uncertainties, *In Proceedings of the 39th IEEE conference on decision and control*, pp. 4132–4137.

Yen G G and Ho L W (2003), Online multiple-model-based fault diagnosis and accommodation, *IEEE Transactions on Industrial Electronics*, vol. 50, no. 2, 296–312.

Zhang K, Jiang B and Cocquempot V (2002), Adaptive observer –based Fast fault Estimation, *Int. J. of System Science*, vol. 33, no. 9, pp. 767-775.

Zhang P, Ding S X, Wang G Z and Zhou D Z (2002), Fault detection for multirate sampled-data systems with time delay, *Int. J. Control*, vol. 75, no. 18, pp. 1457-1471.

Zhang Y and Jiang J (1999), Design of integrated fault detection, diagnosis and reconfigurable control systems, *In Proceedings of the IEEE Conference on Decision and Control*, pp. 3587–3592.

Zhang Y and Jiang J (2002), Active fault-tolerant control system against partial actuator failures, *IEE Proceedings: Control Theory & Applications*, vol. 149, pp. 95–104.

Zhang Y and Jiang J (2003), Bibliographical review on reconfigurable fault tolerant control systems, *IFAC Symposium SAFEPROCESS '03*, Washington, pp. 265–276.

Zhang Y and Jiang J (2006), Issues on integration of fault diagnosis and reconfigurable control in active fault-tolerant control systems, *IFAC Symposium AFEPROCESS '06*, Beijing.

Zhong M, Ding S X, Lam J and Zhang C (2003), Fault detection filter design for LTI system with time delays, *Proc. of the 42nd IEEE Conference on Decision & Control*, Manui, Hawaii, pp. 1467-1472.

Zhong M, Ye H, Ding S X, Wang G and Zhou D (2005), Fault detection filter for linear time-delay systems, *Nonlinear Dynamics and Systems Theory*, vol. 5, no. 3, pp. 273-284.

Zhou K and Doyle J C (editors) (1997), *Essentials of robust control*, Prentice Hall, New Jersey.

Zinober A S I (1990), *An introduction to variable structure control*, in Zinober, A S I (ed.), *Deterministic Control of Uncertain Systems*, Peter Peregrinus, Stevenage,

UK, pp. 1-26.

Zolghadri A, Henry D, Grenaille S (2008), Fault diagnosis for LPV systems, *16th IEEE Mediterranean Conference on Control and Automation*, Ajaccio, Corsica.